Identification of biomarkers associated with aortic valve stenosis in humans through untargeted metabolomic profiling of biofluids

Cynthia Al Hageh

Université de Paris

ED Médicament, Toxicologie, Chimie, Imageries (563)

Centre de recherche des Cordeliers INSERM UMR 1124

Identification of biomarkers associated with aortic valve stenosis in humans through untargeted metabolomic profiling of biofluids

Cynthia AL HAGEH

Thèse de doctorat de Biochimie

Dirigée par Dominique Gauguier
Et Rony Khnayzer

Présentée et soutenue publiquement le 25 mars 2021

Devant un jury composé de:

David TOUBOUL, DR, ICSN CNRS UPR2301, Gif sur Yvette, Rapporteur

James C. ENGERT, PU, McGill University, Montreal, Canada, Rapporteur

Jomana ELARIDI, PU, Lebanese American University, Examinateur

Christophe MAGNAN, PU, Université de Paris, Examinateur

Dominique GAUGUIER, DR, Université de Paris, Directeur

Rony KHNAYZER, PU, Lebanese American University, Co-directeur

Université de Paris

LISTE DES ÉLÉMENTS SOUS DROITS

Liste de **tous les éléments retirés** de la version complète de la thèse
faute d'en détenir les droits

Articles, chapitres, entretiens cliniques…

Titre du document	N° (si numéroté)	Page(s) dans la thèse
1H NMR Metabolomics Identifies Association between Urinary Trigonelline and Hippurate and Aortic Valve Stenosis. Submitted in the *Journal of Proteome Research* on February 18, 2021.	Chapter III. 3	114 – 186

Table of contents

Résumé

Titre : Profilage métabolomique dans la sténose de la valve aortique

Contexte. La sténose de la valve aortique (SVA) est la maladie cardiaque valvulaire fréquente. Elle se produit chez des personnes souvent âgées lorsque les feuillets de la valve deviennent épais, calcifiés et rétrécis, ce qui réduit le flux sanguin du ventricule gauche vers l'aorte. La prévalence de la SVA augmente avec l'âge. Elle touche 0,2% des personnes âgées de 50 à 59 ans, 1,3% de celles âgées de 60 à 69 ans, 3,9% âgées entre 70 et 79 ans et les plus touchées (9,8%) sont entre 80 et 89 ans.

LA SVA est une maladie à progression lente, et dans de nombreux cas, la maladie reste asymptomatique et aucune intervention médicale n'est nécessaire. Les symptômes de la SVA sont très variables d'un patient à l'autre. Chez certains patients, les symptômes apparaissent comme une diminution de la tolérance à une activité physique. La SVA se caractérise par trois symptômes classiques tels que l'angine (douleur thoracique), la syncope (évanouissement) et l'insuffisance cardiaque. Après l'apparition de ces symptômes, la survie moyenne est de cinq ans après l'angine, trois ans après l'apparition de la syncope et deux ans après l'insuffisance cardiaque. Une fois que les symptômes apparaissent, ils indiquent que le travail supplémentaire nécessaire à l'ouverture de la valve affecte l'organisme. Dans ce cas, il est urgent de poser un diagnostic et d'envisager un traitement approprié.

Le SVA est mortel puisque la survie moyenne est de trois ans maximum en l'absence de traitement. La SVA est souvent diagnostiquée tardivement, après le développement des symptômes et lorsque la maladie devient sévère. Aucun traitement pharmacologique n’est efficace pour arrêter ou retarder sa progression. Le seul traitement disponible est le remplacement de la valve sténosée par une intervention chirurgicale ou par un cathéter.

SVA nécessite le remplacement de la valve aortique chez plus de 2 % des personnes de plus de 65 ans. Ces méthodes sont invasives, coûteuses et présentent des complications.

La plupart des décès d'origine cardiovasculaire surviennent chez des personnes qui ne connaissent pas leur état de santé sous-jacent et le décès est probablement dû à l'absence de traitement à temps. Le défi pour la détection précoce et la prévention de la SAV réside dans le fait qu'il n'existe actuellement aucun biomarqueur fiable. Il est important de comprendre l'étiologie et la pathogenèse de la SVA pour développer des solutions thérapeutiques et de diagnostic précoce efficaces. L'objectif de ma recherche a consisté dans l'identification de modifications métaboliques chez des patients atteints de SVA en utilisant des technologies complémentaires de profilage du métabolome.

Méthodes. Dans ce travail, nous avons effectué des analyses métaboliques globales dans une seule population d'étude en utilisant des outils analytiques distincts pour détecter et quantifier les variations du métabolome dans deux biofluides humains, l'urine et le plasma, afin d'identifier les métabolites associés à la sténose valvulaire aortique calcifié.

Dans cette étude, les techniques de spectroscopie de résonance magnétique nucléaire du proton (RMN ^{1}H) et de spectrométrie de masse (SM) ont été appliquées. Ces deux techniques sont complémentaires, et possèdent leurs avantages et leurs inconvénients. Ainsi, chaque approche peut détecter et quantifier un ensemble spécifique de métabolites et la combinaison des deux techniques permet d'augmenter la gamme des métabolites capturés.

Des échantillons de 46 cas atteints de SVA et 46 sujets contrôles ont été utilisés. Les technologies d'analyse du métabolome utilisées ont été basées sur un profilage (1) non ciblé par chromatographie en phase gazeuse et la spectrométrie de masse (GC/MS) sur des échantillons d'urine et de plasma

et (2) non ciblé et ciblé par spectroscopie de résonance magnétique nucléaire du proton (RMN ^{1}H) sur des échantillons d'urine. De plus, une approche lipidomique non ciblée basée sur la spectrométrie de masse à temps de vol avec ionisation par désorption laser assistée par matrice (MALDI-TOF/MS) a été appliquée sur des échantillons de plasma pour analyser les lipides.

Des analyses de données multivariées ont été effectuées sur les données prétraitées afin de détecter les biomarqueurs potentiels liés à la SVA. La détection de différences quantitatives de métabolites entre cas et contrôles a été effectuée par analyses de régression.

Après la détection des métabolites significativement régulés de manière différentielle entre les cas et les contrôles, des expériences de validation *in vivo* ont été réalisées en utilisant des modèles de souris, suivies d'analyses de l'expression cardiaque des gènes candidats par RT-qPCR dans ces modèles. Des échantillons cardiaques de souris traités chroniquement par des métabolites candidats (hippurate et benzoate) ont été utilisés pour tester leurs effets sur l'expression de gènes liés aux maladies cardiovasculaires.

Les mêmes échantillons d'urine ont été analysés par GC/MS et RMN ^{1}H. Afin d'améliorer l'annotation des signaux métabolomiques urinaires dérivés de la RMN ^{1}H, des coefficients de corrélation entre les signaux de la RMN ^{1}H et les caractéristiques métaboliques urinaires dérivées de la GC/MS ont été calculés.

Résultats. La combinaison de plusieurs stratégies de profilage métabolomique a permis d'obtenir 159 éléments métaboliques qui caractérisent la SVA calcifié dans les deux biofluides. 105 ont été identifiés dans l'urine par RMN ^{1}H et GC/MS et 54 ont été identifiés dans le plasma par GC/MS et MALDI-TOF/MS. La SM et la RMN ^{1}H ont permis de différencier

les cas des témoins, ce qui démontre que la SVA calcifié entraîne des changements dans les métabolites des biofluides.

1. La métabolomique basée sur le GC/MS a fourni un ensemble de traits métaboliques connues et inconnues qui caractérisent la SVA calcifiée dans les deux biofluides. Certains de ces métabolites connus étaient couramment retrouvés dans les deux biofluides, mais pas toujours avec la même direction de régulation. Seuls le 2,4-di-tert-butylphénol et l'acide trans-aconitique présentaient le même sens de régulation dans les deux biofluides. Des rapports publiés ont montré que plusieurs des métabolites candidates identifiés dans notre étude sont impliqués dans les maladies cardiaques, ce qui pourrait expliquer leur association avec la SVA. La glycine, le myo-inositol et l'acide méthylmalonique ont été trouvés associés à l'insuffisance cardiaque. L'acide élaïdique, l'acide dodécanoïque, l'acide myristique et l'acide palmitique ont été associés aux maladies coronariennes. L'acide aconitique a été associé à des lésions myocardiques et son isomère l'acide cis-aconitique a été associé à des maladies coronariennes. Le 2,4-di-tert-butylphénol a été suggéré pour prévenir l'athérosclérose grâce à ses propriétés antioxydantes.

   Les métabolites connus capturés par l'approche de profilage GC/MS a permis d'analyser la pertinence biologique de ces métabolites. L'une des voies perturbées chez les patients AVS était le métabolisme des acides gras. Le cœur a besoin d'un taux élevé d'énergie pour maintenir sa fonction contractile. En général, le cœur obtient la majeure partie de son énergie par la β-oxydation des acides gras. Les acides gras perturbés peuvent provenir de la biosynthèse des acides gras dans le foie, des graisses alimentaires, de la β-oxydation et de l'élongation des acides gras. Ainsi, toute perturbation de l'oxydation des acides gras peut introduire des conséquences énergétiques et fonctionnelles sur le cœur.

2. La discrimination entre les AVS et les contrôles a été détectée par la métabolomique non ciblée et ciblée basée sur la RMN 1H. La métabolomique non ciblée a permis d'identifier une association entre la SVA et 27 métabolites urinaires inconnus et des signaux correspondant à l'hippurate, avec une régulation principalement positive chez les patients AVS. Les associations étaient indépendantes de la présence de covariantes de la maladie telles que l'âge, le sexe, l'indice de masse corporelle (IMC), l'hyperlipidémie, l'hypertension et le diabète. En outre, les métabolites associés à la SVA n'étaient pas associés aux niveaux de cholestérol, LDL ou HDL.

   Des analyses complémentaires utilisant la métabolomique ciblée basée sur la RMN ^{1}H ont identifié des associations significatives entre la SVA et des niveaux élevés de trigonelline, d'hippurate et de benzoate. Plusieurs études ont mis en évidence une implication directe ou indirecte de la trigonelline dans les maladies cardiovasculaires. L'acide hippurique et son précurseur, l'acide benzoïque, ont été des découvertes nouvelles dans le contexte de la SVA et plus généralement des maladies cardiaques. Ces métabolites sont des produits du métabolisme des bactéries intestinales, suggérant ainsi un lien entre le risque de la SVA et les changements fonctionnels et/ou architecturaux du microbiote intestinal.

   Les métabolites candidats identifiés dans cette étude sont associés à la SVA calcifié indépendamment de la présence de facteurs de risque cardiovasculaire communs. Ils sont associés à la SVA indépendamment des différences de sexe, de la tranche d'âge, des taux de cholestérol LDL et HDL, de l'indice de masse corporelle (IMC) et de la présence de diabète, d'hypertension ou d'hyperlipidémie.

Des expériences de validation ont été réalisées dans un modèle préclinique d'obésité chez des souris nourries avec un régime riche en graisses et perfusées de façon chronique avec de l'hippurate ou du benzoate. Ce modèle développe un large champ d'anomalies pertinentes pour la résistance à l'insuline, l'obésité, le diabète de type 2, les maladies cardiovasculaires ainsi que l'épaississement et la calcification de la valve aortique. Les résultats de l'expression des gènes cardiaques dans ce modèle suggèrent que l'administration chronique sous-cutanée d'hippurate et de benzoate pourrait augmenter la calcification via *NF-κB*, puisque l'inhibition de *NF-κB*, une méthode pour traiter l'ostéoporose, inhibe la calcification vasculaire. En outre, l'hippurate et le benzoate peuvent activer la différenciation des myofibroblastes par l'intermédiaire de *CXCL9* et de *BMP6*. Leurs effets sur l'induction de l'inflammation restent peu clairs car ils favorisent l'expression de certains gènes impliqués dans l'inflammation tout en inhibant d'autres.

Les analyses de corrélation entre les données RMN 1H et GC/MS nous a permis de découvrir la corrélation entre les deux ensembles de données. Cette corrélation a amélioré l'annotation des métabolites et a suggéré l'implication de métabolites co-régulés dans la SVA.

3. L'étude du lipidome a identifié des différences entre cas et contrôles pour 22 ions connus et inconnus. Parmi les lipides connus, les lysophosphatidylcholines, la lysophosphatidylcholine oxydée et les phosphatidylcholines ont été capables de distinguer les cas d'AVS des contrôles. Cette association a confirmé l'association des métabolites de la voie de la choline avec le risque de maladies cardiovasculaires.

Conclusions. Mes résultats ont permis d'identifier des modifications significatives dans la régulation de métabolites plasmatiques et urinaires de patients atteints de SVA, qui peuvent servir d'outils moléculaires dans le

diagnostic et le traitement de la maladie. En outre, ils soulignent l'importance de combiner plusieurs technologies complémentaires pour le profilage du métabolome d'échantillons humains et identifier de biomarqueurs candidats de la maladie. L'un des points forts de notre étude est la détection de biomarqueurs potentiels de la SVA, tels que l'hippurate et le benzoate, qui ne sont pas connus pour participer à des voies déjà associées aux maladies cardiovasculaires. Nos résultats suggèrent que la métabolomique peut identifier un métabotype de biofluide qui caractérise la SVA et ainsi mettre en lumière des traitements ciblés.

Mots clefs : Biomarqueur ; Spectrométrie de masse ; RMN ; Métabolites ; Cœur ; Maladies cardiovasculaires

Abstract

Title : Metabolomic profiling in Aortic Valve Stenosis

***Background*.** Calcific aortic valve stenosis is the most common valvular heart disease. Aortic valve stenosis (AVS) occurs when the valve leaflets become thick, calcific and narrow, obstructing the blood flow from left ventricle to the aorta. AVS is often diagnosed late after the development of symptoms and when the disease becomes severe. The disease progression is rapid and if left untreated it results in heart failure and death. There are no effective pharmacological therapies to stop or delay its progression. The only available treatment is the replacement of the stenotic valve with surgery or via catheter, which are invasive and expensive procedure with risk of complications, thus calling for novel effective therapeutic agents and early diagnostic tools. It is important to understand the etiology and pathogenesis of AVS in order to develop tools for effective therapeutic and early diagnostic solutions. The central objective of this research was to identify metabolic changes in AVS patients using complementary metabolome profiling technologies.

Methods. Samples from 46 AVS cases and 46 control subjects were used. Metabolome analyses were based on (1) untargeted metabolomic profiling using gas chromatography and mass spectrometry (GC/MS) in urine and plasma samples and (2) untargeted and targeted profiling using proton nuclear magnetic resonance spectroscopy (^{1}H NMR) in urine samples. In addition, untargeted lipidomics based on time-of-flight mass spectrometry with matrix-assisted laser desorption ionization (MALDI-TOF/MS) was applied to plasma samples for lipid analysis. The detection of quantitative differences in metabolites between cases and controls was performed by regression analyses. Cardiac samples from mice chronically treated with candidate metabolites were used to test their effects on the expression of genes related to cardiovascular diseases.

Results. Significant associations were identified between AVS and 21 plasma metabolites by GC/MS, and 22 and 21 urinary metabolites by GC/MS and NMR, respectively. Approximately 50% of the associations were significant in both biofluids. Targeted NMR analyses allowed the identification of associations between AVS and six known metabolites, including hippurate and trigonelline. Lipidome analysis identified differences between cases and controls for 22 ions, several of which corresponding to lysophosphatidylcholines, oxidized lysophosphatidylcholine and phosphatidylcholines. Treatment of mice with hippurate and its precursor benzoate led to significant alterations in the cardiac expression of *Bmp6*, *Cxcl9* and *Mcp1*.

Conclusions. Significant changes were identified in the regulation of plasma and urinary metabolites in AVS patients. These metabolites may be used as molecular tools in the diagnosis and treatment of the disease. In addition, they underline the importance of combining complementary technologies for metabolome profiling of human biospecimens, in order to maximize the identification of candidate biomarkers of the disease.

Keywords : Biomarker; Mass Spectrometry; NMR; Metabolites; Heart; Cardiovascular diseases

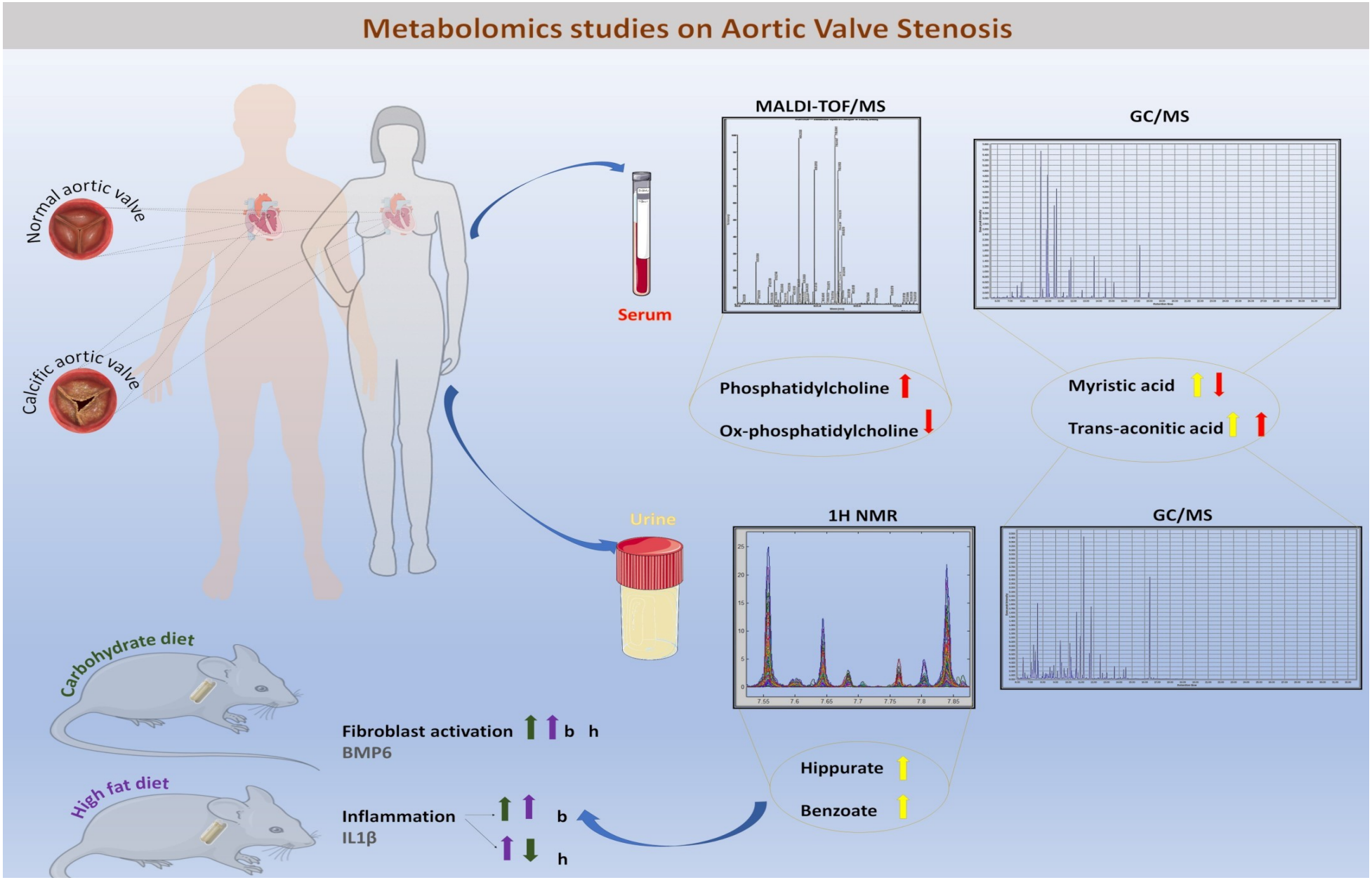

Graphical Abstract. Biomarker discovery based on untargeted metabolomic profile analyses of Human urine and plasma and exploration in preclinical models.

Human biofluids from calcific aortic valve stenosis (AVS) patients and controls were used to study the metabolic differences between these groups. Gas chromatography mass spectrometry (GC/MS) was applied on both urine (yellow) and serum samples (red) of the same subjects. Myristic acid was found upregulated in the urine (yellow arrow) and downregulated in the serum (red arrow) of AVS subjects; Trans-aconitic acid was found upregulated in both urine (yellow arrow) and serum (red arrow) of AVS. Matrix-assisted laser desorption ionization-time of flight mass spectrometry (MALDI-TOF/MS) was applied on the serum samples (red arrow). Phosphatidylcholines were found upregulated while Oxidized-phosphatidylcholine (ox-phosphatidylcholine) was downregulated. Proton nuclear magnetic resonance (^{1}H NMR) was applied on the urine samples. Hippurate and its precursor benzoate were found upregulated in urine of AVS (yellow arrow). A validation approach was performed on mice to test the effect of hippurate (h) and benzoate (b) on the gene expression of genes associated with fibroblast activation and inflammation under high fat diet (purple) and control carbohydrate diet (green). Under benzoate (b) or hippurate (h) treatment, the expression of gene associated to fibroblast activation was upregulated in both mice-fed carbohydrate (green arrow) and high fat (purple arrow) diets. Under benzoate (b) treatment, the expression of gene associated to inflammation was upregulated in both mice-fed carbohydrate (green arrow) and high fat (purple arrow) diets; while under hippurate (h) treatment, the expression of gene associated to inflammation was upregulated in mice-fed high fat diet (purple arrow) and downregulated in mice-fed carbohydrate diet (green arrow).

Acknowledgement

I would like to sincerely thank my thesis directors, Dr. Dominique Gauguier and Dr. Rony Khnayzer. Thank you for giving me the opportunity to be here today, for supporting and trusting me through this thesis. Thank you also for the help that you have given me and for the patience and encouragement. I truly appreciate what you both have done for me. Also, a very special thanks to Dr. Pierre Zalloua for his help and support while working in Lebanon.

I would like to take this opportunity to thank the Paris Descartes University and the Lebanese American university for welcoming me as PhD student.

I would also like to thank the members of the jury: Dr. David Touboul from ICSN CNRS UPR2301 and Dr. James C. Engert from McGill University, rapporteurs for this work, and Dr. Jomana Elaridi from the Lebanese American University and Dr. Christophe Magnan from the university of Paris, examiners, for giving me the honor of evaluating my work.

I would like to express my gratitude to Francois Brial. Thank you for your friendship, your support and for the precious help you have given me throughout the work I have done in the laboratory in France.

I also thank the Lebanese National Council for Scientific Research (CNRS) for granting me the scholarship to accomplish this PhD.

I also would like to thank the team of Imperial College, Marc Dumas and Michael Olanipekun who collaborated with this work. I also thank all the people that contributed directly or indirectly to the success of this thesis. For Robert Barouki, the director of the research Unit T3S (Environmental Toxicity, Therapeutic Targets, Cellular Signaling and Biomarkers). Thank you for welcoming me into the research unit.

Finally, more personally, I thank my father and mother. Without them, I definitely would not have made it here. Thank you for always believing in me and for your support. I also thank my husband. Thank you for helping me improve my computer skills and build my programming skills to work on some research tasks, especially at the beginning when I needed help. Thank you for your support and encouragement. I also thank my brothers and sister and all my loved relatives and friends for the support they keep giving me.

List of main abbreviations

^{1}H NMR	Proton nuclear magnetic resonance
2,5-DHB	2,5- dihydroxybenzoic acid
9-AA	9-aminoacridine
apo(a)	Apolipoprotein(a)
apoB100	Apolipoprotein b100
ATX	Autotaxin
AUC	Area under the curve
AUROC	Area under roc curve
AV	Aortic valve
AVA	Aortic valve area
AVC	Aortic valve calcification
AVCS	Aortic valve calcium scores
AVR	Aortic valve replacement
AVS	Aortic valve stenosis
AVSc	Aortic valve sclerosis
BAV	Bicuspid aortic valve
BAVS	Bicuspid aortic valve stenosis
BMP-2	Bone morphogenic protein-2
BMP-6	Bone morphogenic protein-6
BSTFA	N,o-bis(trimethylsilyl)trifluoroacetamide
CACNA1C	Calcium channel, voltage-dependent, L type, alfa 1c subunit
CAVD	Calcific aortic valve disease
cDNA	Complementary DNA

CEs	Cholesteryl esters
$CHCl_3$	Chloroform
CID	Collision-induced dissociation
CNV	Copy number variation
CTGF	Connective tissue growth factor
CVD	Cardiovascular disease
CXCL9	C-X-C Motif Chemokine Ligand 9
DCM	Dilated cardiomyopathy
DM	Diabetes mellitus
ECM	Extracellular matrix
FADS1/2	Fatty acid desaturase 1 and 2
FDR	False discovery rate
GC/MS	Gas chromatography mass spectrometry
GC	Gas chromatography
GDF15	Growth differential factor15
GERA	Genetic epidemiology research on adult health and aging
GWAS	Genome-wide association study
HCM	Hypertrophic cardiomyopathy
HIF1α	Hypoxia-inducible factor1alfa
HMDB	Human metabolome database
HR	Hazardous ratio
hsCRP	High sensitivity c-reaction protein
HTN	Hypertension
IDT	Integrated dna technologies
IFN-γ	Interferon gamma

IL-1β	Interleukin-1 beta
IL-6	Interleukin-6
IP-TFA	Industrially produced-trans fatty acid
KEGG	Kyoto encyclopedia of genes and genomes
KIV	Kringle iv
LC	Liquid chromatography
LDHB	L-lactate dehydrogenase b chain
LDLR	Low-density-lipoprotein receptor
LPA	Lipoprotein(a)
LPAR	Lysophosphatidic receptor
LysoPC	Lysophosphatidylcholine
Lp-PLA2	Lipoprotein-associated phospholipase a
Lrp5	Low-density-lipoprotein (LDL) Receptor Related Protein 5
LV	Left ventricle
LVEF	Left ventricle ejection fraction
LVH	Left ventricle hypertrophy
LysoPA	Lysophosphatidic acid
LysoPLs	Lysophosphospholipids
MALDI-TOF/MS	Matrix-assisted laser desorption/ionization-time of flight mass spectrometry
MCP1	Monocyte chemoattractant protein 1
MeOH	Methanol
MPG	Mean pressure gradient
MR	Mendelian randomized
MS	Mass spectrometry

MYH6	Myosin heavy chain 6
NF-kB	Nuclear factor -kb
NMR	Nuclear magnetic resonance
NO	Nitric oxide
OPG	Osteoprotegerin
OPLS-DA	Orthogonal pls-da
OR	Odd ratio
OxPLs	Oxidized phospholipids
PAR	Population -attributed risk
PC	Phosphatidylcholine
PCA	Principle component analysis
PCSK9	Protein convertase subtilisin/kexin type 9
PCSK9	Proprotein convertase subtilisin/kexin type 9
PE	Phosphatidylethanolamine
PI	Phosphatidylinositol
PLs	Phospholipids
PLS-DA	Partial least-squares discriminant analysis
PPP	Pentose phosphate pathway
PS	Phosphatidylserine
RAAS	Renin-angiotensin-aldosterone system
RANK	Receptor activator of nuclear factor kappa b
RANKL	Rank ligand
ROC	Receiver operator characteristic
RT	Retention time
Runx-2	Runt-related transcription factor 2

SCD	Sudden cardiac death
SLs	Sphingolipids
SMs	Sphingomyelins
SNP	Single nucleotide polymorphism
TAVI	Transcatheter av implantation
TCA	Tricarboxylic acid cycle
TDA	Topological data analysis
TERA	Transitional endoplasmic reticulum ATPase
TEX41	Testis expressed 41
TFA	Trifluoroacetic acid
TFAs	Trans fatty acids
TGF-β	Transforming growth factor-beta
TGF-β1	Transforming growth factor-beta 1
TGs	Triglycerides
TMA	Trimethylamine
TMCS	Trimethylchlorosilane
TNF- γ	Tumor necrosis factor-gamma
TNF-α	Tumor necrosis factor-alfa
TOF	Time-of-light
TPM-1	Tropomyosin α-1 chain
TR	Transferrin receptor protein 1
TWAS	Transcriptome-wide association study
UBE2C	Ubiquitin e2 ligase-c
VHL	Von hippel-lindau
VICs	Valve interstitial cells

vWf	Von willebrand factor
α-CHCA	Alfa-cyano-4-hydroxycinnamic acid
αMHC	Alpha myosin heavy chain subunit

Chapter I: Introduction

I.1. Heart anatomy and role

The heart pumps blood to the body using a circulation system that supplies the body tissues and organs with oxygen and nutrients while also removing carbon dioxide. The heart also provides itself with oxygen and nutrients via the coronary arteries so that it could function much like the rest of the body's organs and tissue. It is a muscular organ that beats about 100,000 times a day and consists of four chambers: two atria chambers that receive venous blood and two ventricles chambers that pump the blood from the heart (Shaffer, McCraty and Zerr, 2014). The heart is separated into left and right sides, the right side consists of the right atrium and ventricle, and the left side consists of the left atrium and ventricle with the septum separating the two sides (**Figure 1**).

Figure 1: Heart chambers and valves. The heart has four chambers: two atria and two ventricles. Four valves regulate the blood flow: mitral, aortic, tricuspid, and pulmonary valves.

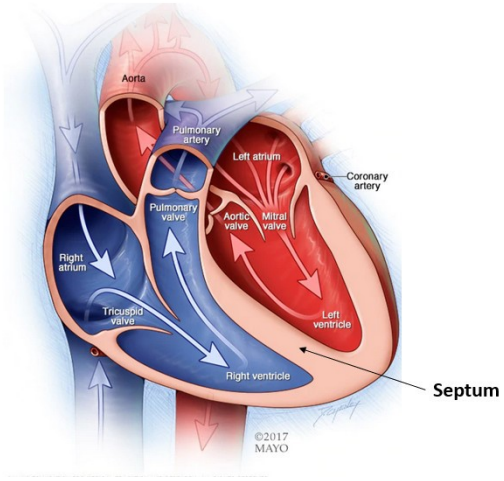

(From Aortic valve stenosis - Symptoms and causes -Mayo Clinic. Available at : https://www.mayoclinic.org/diseases-conditions/aortic-stenosis/symptoms-causes/syc-20353139)

The heart circulates blood through the pulmonary and systemic circulations. The pulmonary circuit transports blood between the lungs and the heart, while the systemic circuit circulates blood between the heart and the body. Therefore, blood low in oxygen (deoxygenated) returns

from the body, enters the right atrium via the venae cava, then flows to the right ventricle and via pulmonary arteries to the lungs to receive oxygen. The oxygenated blood is transported from the lungs to the left atrium via the pulmonary veins, then to the left ventricle and when the left ventricle contracts, the blood is pumped out to the body through the aorta (Shaffer, McCraty and Zerr, 2014) (**Figure 2**).

Figure 2 : The blood flow in the heart. Blood enters the heart through vena cava to the right atrium, and through pulmonary veins to the left atrium. It flows to the right and left ventricles, then the blood is pumped out through pulmonary artery and aorta.

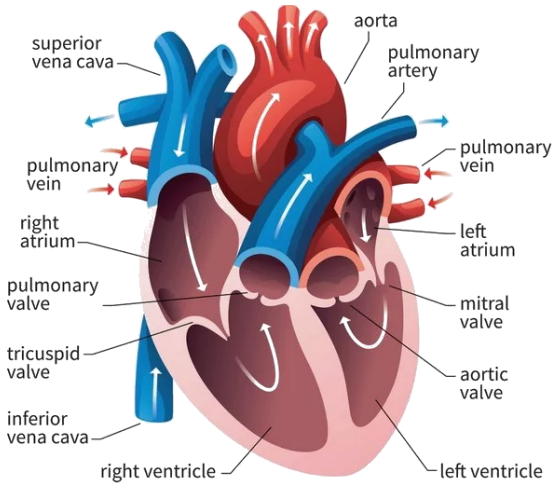

(From How the Human Heart Evolved Four Chambers – ThoughtCo. Available at : https://www.thoughtco.com/evolution-of-the-human-heart-1224781)

As the heart beats, it pumps blood through a sequence of events called the cardiac cycle. The cardiac cycle consists of systole during which the ventricles contract and pump the blood to the lungs and the body, and diastole during which the ventricles are relaxed and refilled with blood from the atria. During systole, blood pressure (BP), referred to as systolic BP, is the highest due to the contraction and blood ejection from the heart. During diastole, the diastolic BP is the lowest due to ventricle relaxation (Shaffer, McCraty and Zerr, 2014) (**Figure 3**).

Figure 3 : Heart cycle ventricular systole and diastole. During diastole, the left and right atria contract and pump the blood to the ventricles. During systole, the ventricles contract and eject the blood out of the heart.

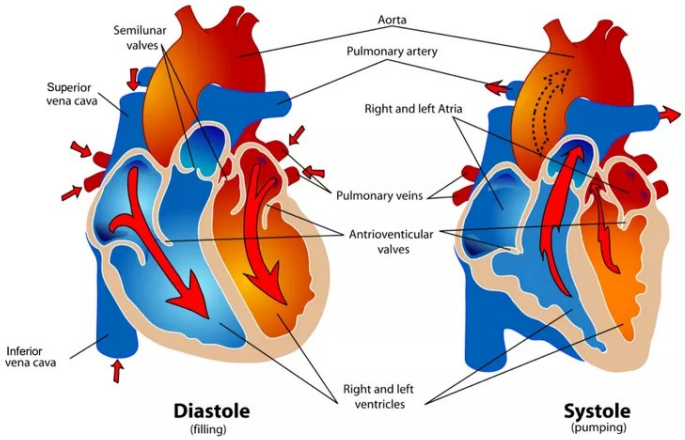

(From Learn How the Heart Beats in the Phases of the Cardiac Cycle – ThoughtCo. Available at : https://www.thoughtco.com/phases-of-the-cardiac-cycle-anatomy-373240)

The four heart valves are unidirectional allowing the blood to flow only in one direction and preventing the blood from flowing back. There is a different structure of heart valves in different locations. Two valves allow the blood to enter the ventricles: the tricuspid valve lies between the right atrium and ventricle while the mitral valve is between the left atrium and ventricle. The other two valves allow the blood to leave the ventricles: the aortic valve is located between the left ventricle and the aorta while the pulmonary valve is located between the right ventricle and the pulmonary artery are located between the atria and the ventricles (Misfeld and Sievers, 2007) (**Figure 1 and 2**). The aortic, pulmonary, and tricuspid valves have three cusps, meaning they contain three leaflets, while the mitral valve has two cusps.

I.2. Pathogenesis of cardiovascular diseases

Cardiovascular disease (CVD) is the most common cause of death worldwide. According to the Global Burden of Disease (GBD) 2019 study, CVD affected nearly 523 million people and caused an estimated 18.6 million deaths in 2019. The 2019 GBD study reported a higher percentage of deaths than previously reported in 1990. In 2019, the disability-adjusted life years (DALYs), which represent the years lost due to disability caused by CVD, are higher in men

than women before reaching the age of 80 years and the number of total deaths due to CVD is higher among men than women (Roth *et al.*, 2020).

Based on epidemiological studies (Townsend *et al.*, 2015; Nichols *et al.*, 2013) , over 30% of all deaths are caused by CVD, which is more than double that of cancer; 4 million European people die every year from CVD of which 1.4 million die before reaching the age of 75. CVD accounts for 45% of all deaths in Europe . Among females almost half of the death (49%) is caused by CVD, while among males only 40% of all death is caused by CVD. In both females and males, coronary heart disease is responsible for the most CVD deaths (**Figure 4**) (Townsend *et al.*, 2016).

Figure 4 : Percentage of deaths in Europe among men (A) and women (B) caused by the major death causes. Among men (A) 40% of all death is due to cardiovascular disease and almost half of these deaths are caused by coronary heart disease (19%). Among females (B) 49% of all death is caused by cardiovascular disease and coronary heart disease causes most of these deaths.

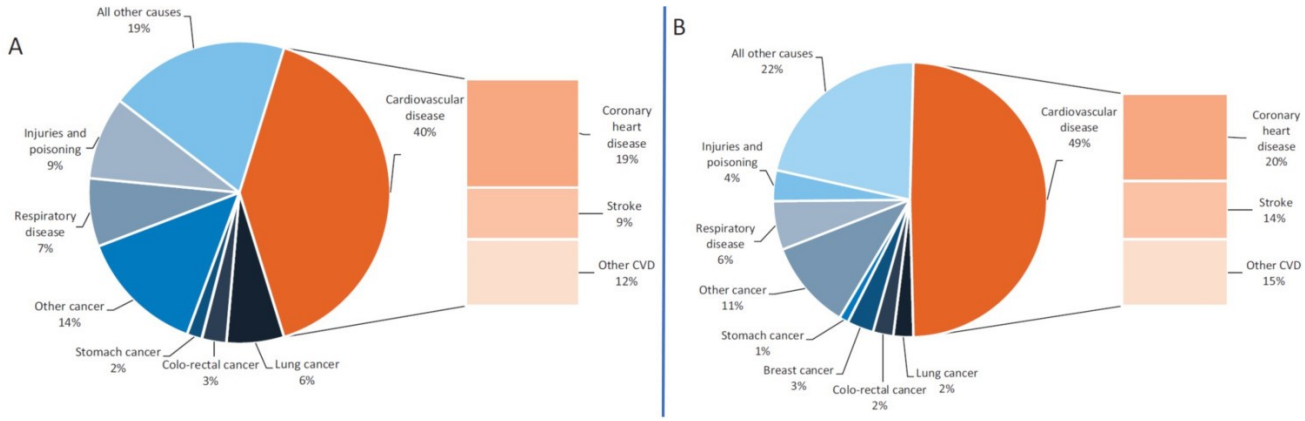

(From Townsend, N. et al. European Heart Journal. 2016. 37(42):3232-3245)

I.2.1. Atherosclerotic cardiovascular disease

Atherosclerotic cardiovascular disease (ACVD) is a chronic disorder that progresses during aging. Atherosclerosis is caused by the accumulation of fatty lipids in the arteries, the build-up of plaques, and arterial hardening and narrowing leading subsequently to coronary artery stenosis (McLaughlin and Fuster, 1995). ACVD, and especially coronary artery disease (CAD), is the most common cause of premature death globally and is considered a pandemic. High levels of LDL-cholesterol are associated with CAD (Wilson *et al.*, 1998), while a high level of HDL-cholesterol is suggested as protective against CAD (Gordon *et al.*, 1977). There is a

correlation between ACVD and unhealthy habits such as smoking, unhealthy diets (high level of saturated fats, trans-unsaturated fats, salt, alcohol, and low consumption of fish, vegetables, fruits, and fibers), lack of exercise and psychosocial problems. Many risk factors for CAD have been identified such as elevated blood pressure, smoking, diabetes, plasma lipid, and markers for inflammation. Over 75% of all ACVD mortalities may be prevented with a healthy lifestyle, as stated by the World Health Organization (WHO) (Perk *et al.*, 2012).

I.2.2. Myocardial infraction

Myocardial infraction (MI) manifests itself through chest pain, usually described as stabbing, burning, or substantial pain. It is mainly due to thrombus formation in the coronary artery. Thus, a reduction in myocardial perfusion (blood flow through the heart muscle) occurs, which eventually causes cell necrosis. Thrombus formation starts with a rupture of a lipid-rich core plaque in the coronary artery. This rupture leads eventually to the formation of occlusive clots result in complete block of the blood supply to an area of myocardium (**Figure 5**). Risk factors (RFs) of MI are classified as (**a**) non-modifiable RFs which are uncontrollable such as age, gender, and family history; (**b**) modifiable RFs such as smoking, alcohol intake, lack of exercise, the presence of hypertension, diabetes, dyslipidemia, and metabolic syndrome; and (**c**) emerging RFs such as fibrinogen, high-sensitivity c-reactive protein (hs-CRP), coronary artery calcification, lipoprotein(a) (LPA), LDL-cholesterol, and homocysteine. MI prevention can be achieved by reducing modifiable risk factors and regulating blood pressure and cholesterol by taking medications (Boateng and Sanborn, 2013).

Figure 5 : Myocardial Infraction. Cell necrosis in the myocardium occurs due to plaque rupture and thrombus formation.

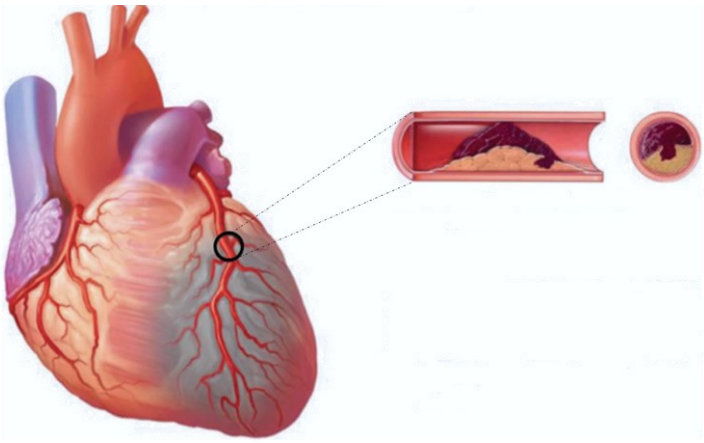

(Adapted from Thygesen Kristianet al. Circulation. 2018. 138(20): e618-e651)

I.2.3. Heart Failure

Heart failure (HF) is the most common cause of illness and mortality. HF means that the heart is unable to pump enough blood to the body. Some of its symptoms are fatigue, dyspnea, tiredness, and ankle swelling. HF affects nearly 2.1% of people aged >65 years and causes around 30% mortality per year (Chang Patricia *et al.*, 2018). The major risk factors of HF are hypertension, coronary heart disease, myocardial infraction, valvular heart disease, and diabetes. HF is a common cause for ischemic stroke (cardioembolic stroke), and approximately 10 to 24% of all stroke patients have HF. Therefore, HF is associated with high risks of thrombus formation and a stroke. Both ischemic stroke and HF have similar risk factors, such as hypertension and diabetes (Haeusler Karl, Laufs and Endres, 2011).

I.2.4. Cardiomyopathies

Hypertrophic cardiomyopathy (HCM) and dilated cardiomyopathy (DCM) are two morbid cardiomyopathies. They are characterized by an enlargement of the heart and reduced cardiac performance (**Figure 6**). HCM is characterized by ventricle wall and septa thickening, while DCM is depicted by reduced wall thickness and enlarged cardiac chambers. Mechanical stress (exercise) and hypertension stimulate the enlargement of the heart. Both HCM and DCM cause sudden cardiac death (SCD). Cardiac hypertrophy (CH) and heart failure (HF) are the leading causes of morbidity and mortality globally (Raghow, 2016).

Figure 6 : Normal heart versus cardiomyopathy. Cardiomyopathy is presented as hypertrophic cardiomyopathy or dilated cardiomyopathy and it is characterized by an enlargement of the heart.

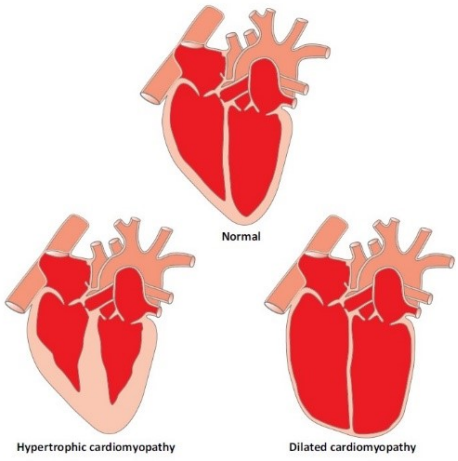

(From Raghow, R. Trends Mol Med. 2016. 22(9):813-827)

I.2.5. Valvular heart disease

Aortic valve stenosis (AVS), known as degenerative valve disease, has become the leading cause of valvular heart disease (Nazarzadeh *et al.*, 2020). AVS is characterized by the narrowing of the aortic valve (**Figure 7**), which blocks the delivery of blood from the heart's left ventricle to the aorta and subsequently to the body and makes the heart work harder. The prevalence of degenerative AVS increases with age (Lindman *et al.*, 2016). It affects 0.2% of people aged between 50 and 59 years, 1.3% of those between 60 and 69 years, 3.9% of people with an age range between 70 and 79 years and the most affected (9.8%) are between 80 and 89 years old (Eveborn *et al.*, 2013).

Figure 7 : Illustration of healthy and stenotic aortic valves

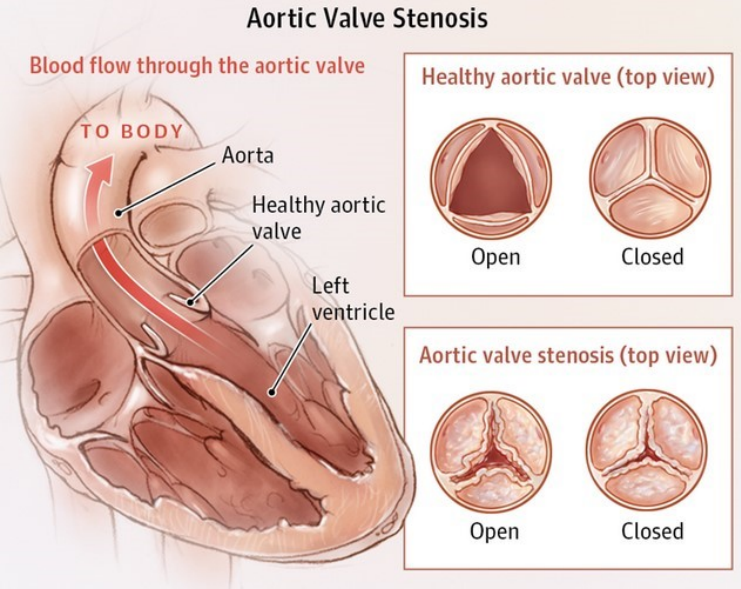

(From Patel, A., and Kirtane, A.J. JAMA Cardiology. 2016. 1(5):623-623)

A healthy aortic valve (AV) is avascular and contains three distinct layers: (**a**) the fibrosa layer which faces the aorta and is rich in oriented collagen fibers that provide strength to the leaflets; (**b**) the spongiosa layer, the middle valve layer, which is rich in proteoglycans; and (**c**) the ventricularis layer that faces the left ventricle and is rich in oriented elastin fibers which contribute to the flexibility of the valve. The three layers are covered with endothelium on both the ventricle and aorta sides (**Figure 8**) (Czarny and Resar, 2014). In all three layers, fibroblast-like cells known as valve interstitial cells (VICs) are found which regulate homeostasis in the leaflets (Dweck, Boon and Newby, 2012). AV consists mainly of endothelial cells (ECs), VICs, and leukocytes.

Figure 8 : Aortic valve layers. From the aorta side to the ventricle side, the multilayered aortic valve is composed of the ventricularis, the spongiosa and the fibrosa layers. Endothelial cells are present around the valve layers.

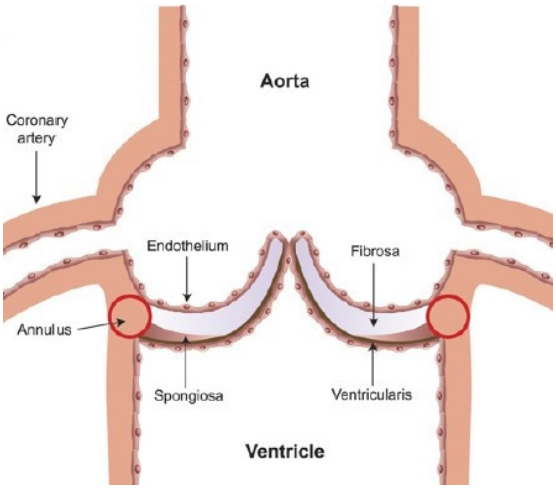

(From Dweck, M.R. et al. Journal of the American College of Cardiology. 2012. 60(19):1854-1863)

Mild valve changes are associated with an increased risk for myocardial infraction and death after five years (Otto, 2008). Usually the area of the valve is 3-4 cm^2 and when the symptoms of AVS appear, the aortic valve area (AVA) becomes ≤ 1cm^2 (Czarny and Resar, 2014). The obstacle to the left ventricle ejection creates a gradient of pressure between the left ventricle (LV) and the aorta. According to Ohm's law (V=IR), to maintain the same blood flow (I) when the resistance to flow (R) increases (due to the narrowing in the valve area), the pressure (V) must increase (Czarny and Resar, 2014). AVS causes the development of left ventricular hypertrophy (LVH) in response to the narrowing of the AV, which therefore increases the pressure on the LV and stimulates the hypertrophy of the myocardium (Dweck, Boon and Newby, 2012). According to Laplace's law ($\delta = (Pr)/(2t)$) (r = left ventricle radius), as the left ventricular pressure (P) increases to maintain the same blood flow in the face of valve obstruction, the wall thickness of the left ventricle (t) increases to reduce the change in wall stress (δ). While AVS progresses, the aortic valve area will decrease and subsequently the left ventricle hypertrophy (LVH) develops. Then, LVH leads to myocyte disarray and dysregulation, thus failure in left ventricle contraction occurs. Following LVH, the ventricle is no longer able to pump the blood and inadequate cardiac output and low exercise capacity occur leading subsequently to heart failure and death (Czarny and Resar, 2014). AVS is characterized by a variation in hypertrophic response, and it is weakly related to the severity of valve

narrowing. Therefore, AVS severity is determined by both the valve narrowing and the myocardial hypertrophy (Dweck, Boon and Newby, 2012).

I.2.5.1. Aortic valve stenosis pathophysiological development

AVS can occur due to several conditions, including rheumatic heart disease which is rare, abnormal congenital bicuspid valve or age-related calcification of a normal valve. Abnormal congenital bicuspid AV and rheumatic heart disease make the AV prone to calcification and stenosis. Yet, the senile aortic valve calcification is a frequent cause of AVS (Czarny and Resar, 2014).

I.2.5.1.1. Rheumatic heart disease

Rheumatic heart disease is a rare disease but still an important cause of developing AVS in developing countries. Rheumatic heart disease affects mostly the mitral valve, thus rheumatic AVS almost always co-occurs with rheumatic mitral stenosis. Rheumatic AVS is characterized by the fusion of the valve cusps due to the chronic inflammation, which subsequently predispose the valve to injury, fibrosis and calcification (Czarny and Resar, 2014).

I.2.5.1.2. Congenital bicuspid aortic valve

Congenital bicuspid aortic valve (BAV) is the most congenital heart disease and it affects 1-2% of general population (Czarny and Resar, 2014). BAV is when the AV has two leaflets instead of three (**Figure 9**). BAV is commonly asymptomatic in children and symptoms typically manifest in adults. The development of AVS is often due, similar to tri-leaflet valves, to the calcification of the bicuspid valves (Siu and Silversides, 2010). Yet, this malformation makes the development of AVS decades earlier (Helgadottir *et al.*, 2018). Calcific aortic valve stenosis of tricuspid AV appears at the age of > 70 years. Yet, when the AVS appears at a younger age, it is commonly caused by the calcification of bicuspid valve (Argulian, Windecker and Messerli, 2017). Though the congenital BAV affects about 2 % of general population, it is the cause of half the cases with severe AVS (Siu and Silversides, 2010).

Figure 9 : Bicuspid aortic valve. Bicuspid aortic valve stenosis is due to the calcification of the congenital abnormal bicuspid valve. Tricuspid aortic valve stenosis is due to the calcium deposition on the normal tri-leaflets valve.

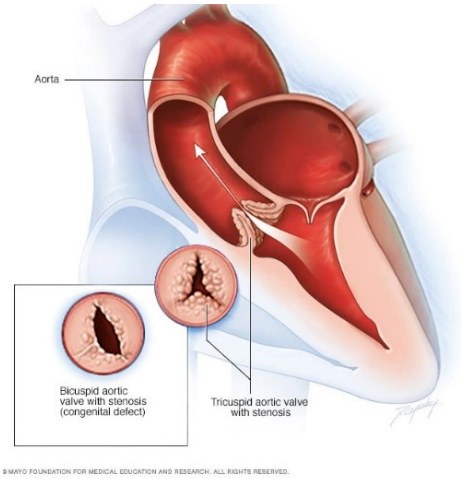

(From Aortic valve stenosis - Symptoms and causes -Mayo Clinic. Available at : https://www.mayoclinic.org/diseases-conditions/aortic-stenosis/symptoms-causes/syc-20353139#dialogId46146375)

I.2.5.1.3. Calcium build-up on the aortic valve

One of the causes of AVS is the idiopathic calcification of the normal tri-leaflet valves (Shipton and Wahba, 2001; Joseph *et al.*, 2016) that causes degeneration of the aortic leaflets (Shipton and Wahba, 2001). The calcium deposits increase the leaflets stiffness, thus making the aortic valve orifice narrower (Joseph *et al.*, 2016; Carabello and Paulus, 2009). Calcific AVS is the third cause of cardiovascular disease (Nkomo *et al.*, 2006).

Mechanisms leading to calcific AVS remain poorly documented, but many factors have been suggested such as aging, inflammation and atherosclerosis (Lindman *et al.*, 2016). Until recently, AVS was believed to be a passive disease, but currently it is widely acknowledged as active and characterized by inflammation, extracellular matrix (ECM) remodeling, and subsequently bone formation (Lindman *et al.*, 2016).

This thesis project focuses on determining the metabotype linked to the senile calcification of aortic valve stenosis. The following pages focus on the senile calcium build-up on AV, its clinical manifestations, diagnosis and treatments; In addition to the pathological processes, clinical factors, and genes, transcripts and proteins risk factors linked to AVS.

I.3. Calcific aortic valve disease

Calcific aortic valve disease (CAVD) is the leading cause of valve disorder (Coffey, Cox and Williams, 2014) and it includes aortic valve sclerosis (AVSc) and aortic valve stenosis (AVS). AVSc arises when the valve is calcified without the obstruction of blood flow and without a transvalvular pressure gradient, whereas in AVS, a significant narrowing in the outflow occurs (**Figure 10**) (Czarny and Resar, 2014). The prolonged subclinical period of AVSc precedes the AVS stage (Joseph *et al.*, 2016). Coffey et al. showed in a meta-analysis study that the frequency of AVSc increases with age from 9% at the age of 54 years to 42% by the age of 81 years (Coffey, Cox and Williams, 2014).

Figure 10 : Depict of a healthy and calcific aortic valve when the valve is open. Aortic sclerosis occurs when the valve is calcified without the obstruction of blood flow. Aortic stenosis comes after aortic sclerosis and it is characterized by the narrowing in the blood flow.

(FromOtto, C.M. New England Journal of Medicine. 2008. 359(13):1395-1398)

I.3.1. Clinical manifestations of aortic valve stenosis

AVS is a slowly progressive disease, and in many cases the disease remains asymptomatic and no medical intervention is needed (Patel and Kirtane, 2016). Once the symptoms appear they indicate that the extra work required to open the valve is affecting the body (Patel and Kirtane, 2016). In this case diagnosis and consideration of appropriate treatment are urgently required (Patel and Kirtane, 2016). AVS is fatal since the average survival is maximum three years if left untreated (Shipton and Wahba, 2001; Joseph *et al.*, 2016).

AVS symptoms and their onset are highly variable among patients. In some patients the symptoms appear as a decrease in exercise tolerance. AVS is characterized by three classical symptoms such as exertional angina (chest pain), syncope (fainting), and heart failure. After the appearance of these symptoms, the mean survival is five years after angina, three years after

the onset of syncope and two years after heart failure (Czarny and Resar, 2014). Angina results from insufficient oxygen supply to the heart. Angina may happen in patients with AVS in concomitant with CAD but also it can happen in patients with only AVS. The demand of myocardial oxygen increases due to LVH and to the increased afterload (which is an increase in the pressure that the left ventricle must overcome to eject the blood during systole) on the left ventricle after the valve obstruction. Myocardial oxygen supply is based on the coronary blood flow. The obstruction of the aortic valve increases the systolic ejection period and decreases the diastolic period. Thus, this leads to a decrease in coronary heart flow since coronary blood supply occurs primarily during diastole (Czarny and Resar, 2014). Syncope is a result of the incapability of the heart to meet the demands of the body. The limit blood flow to the body results in cerebral hypoperfusion (decrease of blood supply to the brain) and syncope. Heart failure manifestation is associated with a poor assessment of the AVS. As the disease progresses and worsens, the increased pressure in left ventricle is transmitted to the left atrium, then to the pulmonary blood vessels, and finally to the right side of the heart. Clinically, these are revealed by dyspnea (Czarny and Resar, 2014).

I.3.2. Aortic valve stenosis diagnosis

AVS can be diagnosed by (**1**) a physical assignment through a stethoscope of a heart murmur which is an abnormal heart sound produced when the blood flows through the valve; (**2**) with echocardiography to image the structure and the function of the heart and to measure the speed of blood through the valve; (**3**) with cardiac catheterization in which a tube is inserted and passed across the valve to determine its tightness; and (**4**) imaging tests such as magnetic resonance imaging (MRI) or computed tomography (CT) (Patel and Kirtane, 2016).

Echocardiography is the standard tool to detect and asses the severity of AVS (Lancellotti, 2012). The assessment relies on the following parameters: peak aortic jet velocity measured in meter per second (m/s), mean pressure gradient measured in millimeter of mercury (mmHg) and aortic valve area measured in square centimeter (cm^2) (Baumgartner *et al.*, 2009). Jet velocity is the measurement of the highest velocity signal (Vmax) through the stenotic valve. It increases as stenosis severity increases. Mean pressure gradient (MPG) or transvalvular aortic gradient is the pressure difference between the left ventricle and the aorta during systole. Aortic valve area (AVA) measures the effective orifice area (Baumgartner *et al.*, 2009). AVS is classified regarding the severity as mild, moderate, and severe (**Table 1**) (Baumgartner *et al.*, 2009). Severe AVS is usually characterized by a MPG>40 mmHg, AVA <1 cm^2 and peak aortic

jet velocity >4 m/s (Baumgartner *et al.*, 2009; Lancellotti, 2012). Mild calcific AVS is characterized by the absence of hypertrophy or left ventricle systolic dysfunction, while severe AVS is accompanied by hypertrophy and impaired systolic function (Mourino-Alvarez *et al.*, 2018).

Table 1 : Criteria for grading the severity of aortic valve stenosis

	Peak aortic jet velocity (m/s)	Mean pressure gradient (mmHg)	Aortic valve area (cm^2)
Mild AVS	2-2.9	< 20	> 1.5
Moderate AVS	3-3.9	20-39	1-1.5
Severe AVS	≥ 4	≥ 40	≤ 1

(Adapted from Czarny, M.J., and Resar, J.R. Clinical Medicine Insights: Cardiology. 2014. 8S1:15–24)

I.3.2.1. Low gradient aortic stenosis

All the parameter gradings should be concordant. Yet, discordant grading is common. Low gradient aortic stenosis is characterized by a discordant between transaortic velocity/pressure gradient and AVA. Thus up to 40% of AVS patients have aortic velocity <4 m/s, transvalvular MPG <40 mmHg and AVA ≤1 cm^2 (Argulian, Windecker and Messerli, 2017). Therefore, to determine the actual severity of AVS, calcium deposits should be measured with CT. AVS calcium scoring is a quantitative method to verify AS severity (Otto and Prendergast, 2014).

I.3.2.2. Low gradient aortic stenosis with low left ventricular ejection fraction

In low gradient aortic stenosis, the low velocity/pressure gradient and the low valve area are sometimes accompanied by low ventricle ejection fraction. In these patients, it is critical to distinguish the truly severe AVS patients from the patients with pseudo-stenosis characterized by moderate AVS. The true severe low-gradient low-flow AVS patients are characterized by severe stenotic lesion which increases the LV afterload and reduces left ventricle ejection fraction (LVEF), this causes a decreased in stroke volume (which is the blood volume ejected from the left ventricle per beat) and low transvalvular pressure gradient. While the low-gradient low-flow in pseudo-stenotic patients are characterized by moderate AVS and low cardiac output. Thus, the low cardiac output causes limited mobility of the moderate stenotic valve. In this case the AVS is not severe and no aortic valve replacement (AVR) is needed. Therefore,

distinguishing between the two cases is crucial to identify the patients that truly require AVR. To determine which case is behind the low flow rate and to better understand if the valve needs replacement, a dobutamine stress echocardiography is applied (dobutamine infusion). Dobutamine increases stroke volume and flow rate. Thus, in patients with impaired LV contractility, the pressure gradient will increase while the AVA remains ≤1 cm^2 due to the severity of the stenosis of AV, whereas in patients with moderately stenosed AV, the valve area will increase with dobutamine (Argulian, Windecker and Messerli, 2017).

I.3.2.3. Low gradient aortic stenosis with preserved left ventricular ejection fraction

Patients with discordant aortic stenosis and preserved LVEF are separated into two groups, some of them have truly severe AVS and need AVR while others have non-severe AVS and should not undergo AVR. Unfortunately, there are no effective tools to separate these two subgroups (Argulian, Windecker and Messerli, 2017).

I.3.3. AVS stages

AVS severity can be assessed using valve anatomy information, hemodynamics, symptoms, and the response of left ventricle to pressure overload. Commonly AVS severity is assessed using transvalvular jet velocity and mean pressure gradient. There are seven stages in AVS (**Table 2**): (**1**) stage A which is at risk stage characterized by the presence of congenital abnormal bicuspid valve or aortic valve sclerosis of the normal tricuspid valve; (**2**) stage B where AVS is progressive and characterized by mild to moderate calcification of the valve leaflets; stage C with severe and asymptomatic AVS characterized by two substages: (**3**) stage C1 where the left ventricle ejection fraction (LVEF) is normal, and (**4**) stage C2 with low LVEF; stage D with symptomatic severe AVS, with three substages: (**5**) stage D1 is characterized by high transaortic MPG, (**6**) stage D2 is characterized by low transaortic MPG and low LVEF and (**7**) stage D3 is characterized by low MPG, low-flow but normal LVEF (Otto and Prendergast, 2014).

Table 2 : Aortic valve stenosis stages

Stage	Description
A	At risk
B	Progressive
C1	Asymptomatic, severe aortic valve stenosis with normal left ventricular function
C2	Asymptomatic, severe aortic valve stenosis with low ejection fraction <50%
D1	Symptomatic, severe, high-gradient aortic valve stenosis
D2	Symptomatic, severe, low-gradient aortic stenosis with low ejection fraction <50%
D3	Symptomatic, severe, low-flow, low-gradient aortic valve stenosis with normal ejection fraction ≥50%

(Adapted from Otto, C.M., and Prendergast, B. New England Journal of Medicine. 2014. 371(8): 744-756)

I.3.4. Risk factors and co-morbidities linked to calcific aortic valve disease

AVS is not a passive age-related disease, but instead an active multifactorial disease (Otto, 2008) involving anatomical anomalies and clinical factors. Anatomical factor includes congenital bicuspid valve which affects between 40 to 60% of patients with severe AVS. AVS clinical factors are often shared with coronary atherosclerosis and coronary artery disease. In addition, AVS risk increases in individuals with renal failure, familial hyperlipidemia or calcium metabolism disorders (Kurtz and Otto, 2010).

I.3.4.1. Clinical factors

In the last decades, many studies have reported an association between risk factors for atherosclerotic cardiovascular disease and AV calcification, such as age, male gender, smoking, hypertension, LDL-cholesterol, diabetes mellitus. In 1997, Stewart BF et al showed that degenerative AV was associated with age, which increases the risk of calcific aortic valve disease (CAVD) by 2-fold for each 10-year of increased age, male gender with also 2-fold increased risk, hypertension with 20% increased risk, hypercholesterolemia, diabetes and smoking with 35% increased risk; In addition, LPA and LDL-cholesterol were found associated with CAVD (Stewart *et al.*, 1997). Yet, Awan et al did not find an association between hypercholesterolemia and AV calcification (Awan *et al.*, 2011), nor between aortic calcification score and cholesterol (Awan *et al.*, 2008). Elevated LPA level (≥48 mg/dL) was associated with a high risk of AVS (Glader *et al.*, 2003) and LPA lowering in 20% of the population (which have LPA ≥ 50mg/dL) could prevent one in fourteen AVS cases. Thus,

elevated serum LPA is a risk factor for AVS and other heart diseases such as CAD, ischemic stroke, peripheral artery disease, myocardia infraction (MI) (Baumgartner *et al.*, 2009).

An association was identified between the number and duration of the conventional cardiovascular risk factors and the development of AVS in a large study including elderly population (Yan *et al.*, 2017). Therefore, hypertension had the strongest effect for developing AVS with a hazard risk (HR) of 1.71. Diabetes had a HR of 1.49 and dyslipidemia had the lowest effect on increasing the hazard of AVS with a HR of 1.17 (**Figure 11A**). The low HR of dyslipidemia for AVS is consistent with previous randomized controlled trials in which statins (lipid-lowering drugs) could not decrease the calcification of AV or stop the need for AV replacement (Cowell *et al.*, 2005; Rossebø *et al.*, 2008; Teo *et al.*, 2011). The combination of the three risk factors increases the HR from 1.73 to 2.77 (**Figure 11B**); and these risk factors increase the HR of AVS in older people since the duration of risk factor increases the HR (**Figure 11C**). The population-attributed risk (PAR) was calculated, and the three risk factors combined represented 34% of the PAR of AVS of which hypertension had the highest risk 23.4%. These data suggest that the prevention of AV sclerosis and stenosis progression can be achieved by reducing risk factors (Yan *et al.*, 2017).

Figure 11 : Hazard Risk of cardiovascular risk factors on developing aortic valve stenosis. High hazard risk (HR) indicates high hazard for development AVS. HRs are presented with their 95% confidence interval (95% CI) and p-values. Hypertension has the highest HR (1.71) of developing AVS, then diabetes with HR 1.49 and dyslipidemia with HR 1.17 (A); combining the three risk factors increases the HR of developing AVS from HR 1.73 for 1 risk factor to HR 2.77 for 3 risk factors combined (B); having these risk factors for more than 5 years increases the HR of having AVS (C).

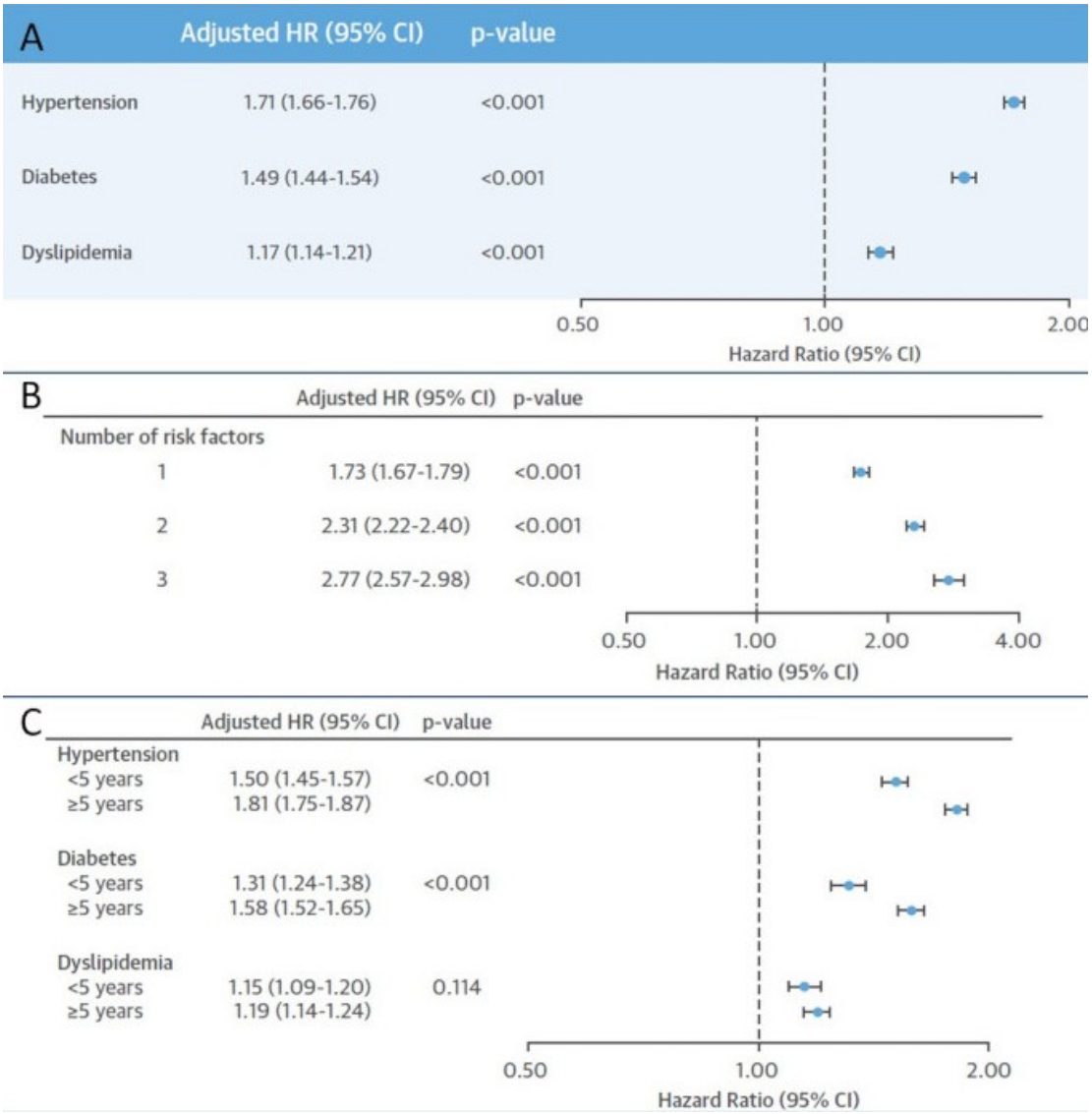

(From Yan, A.T. et al. Journal of the American College of Cardiology. 2017. 69(12): 1523-1532)

I.3.4.1.1. Dyslipidemia

The association between dyslipidemia and AVS is debated. A Mendelian randomized (MR) study performed to assess the association between the risk of AVS and dyslipidemia showed that high levels of LDL-cholesterol, total-cholesterol and triglycerides increase the risk of AVS (Nazarzadeh *et al.*, 2020). Despite the association between elevated plasma level of lipoprotein(a) and AVS (Thanassoulis *et al.*, 2013), the MR study confirmed the association between AVS and LDL-cholesterol after adjustment for LPA. This MR study suggested a causal relationship between elevated LDL-cholesterol and AVS risk. Regarding the suggested beneficial effects of HDL-cholesterol on AVS, Gebhard et al found no association between the HDL-cholesterol level and AVS (Gebhard *et al.*, 2018). In contrast, Nazarzadeh et al provided evidence that lipids may be risk factors for AVS (Nazarzadeh *et al.*, 2020).

I.3.4.1.2. Obesity

The association between BMI/obesity and AVS also remains debated (Lindroos *et al.*, 1994; Messika-Zeitoun *et al.*, 2007; Thanassoulis *et al.*, 2010; Eveborn *et al.*, 2013; Dumesnil and Pibarot, 2013). A recent large observational study showed an association between high BMI and AVS risk (Larsson *et al.*, 2017). Therefore, obesity may promote the formation of AVS either directly through structural changes of the heart or indirectly through metabolic changes. Structural changes can be caused by the higher blood pressure in obese patients, which increases the stress on the heart and results in changes in AV (Pawade, Newby and Dweck, 2015). Metabolic changes in obese subjects may result in the deposition of high level of lipoproteins on the wall of AV (Pawade, Newby and Dweck, 2015; Varbo *et al.*, 2015). Most recently, a MR study designed to assess the association of obesity with AVS showed that elevated BMI is a causal risk for AVS and AVR (Kaltoft, Langsted and Nordestgaard, 2020). In this study, an increase of 1 Kg/m^2 in BMI was associated with AVS with causal risk ratio of 1.52 (95% CI 1.23-1.87) and with AVR with a causal risk ratio of 1.49 (95% CI 1.07- 2.08).

I.3.4.1.3. Bicuspid aortic valve

Bicuspid aortic valve is the major risk factor to AVS. It is the cause of half the cases of severe AVS (Siu and Silversides, 2010). Therefore, it was suggested that the congenital abnormality of aortic valve is implicated in the pathogenesis of AVS due to the fact of the association of AVS genetic variants with BAV (Helgadottir *et al.*, 2018).

I.3.4.1.4. Aortic valve sclerosis

AVSc is a risk factor for AVS because approximately 1.9% of AVSc patients progress to AVS per year (Coffey, Cox and Williams, 2014). In the elderly population, AVSc is associated with an increased risk of death by cardiovascular causes and an increased risk of myocardial infarction (Otto *et al.*, 1999). Although only 1.9% of patients with AVSc progress to AVS, AVSc is associated with an increased risk of coronary events by 68% (Hazardous Ratio 1.68), stroke by 27% (HR 1.27), and cardiovascular mortality by 69% (HR 1.69) (Coffey, Cox and Williams, 2014).

I.3.5. Cellular mechanisms involved in aortic valve stenosis development and progression

Calcified aortic valves share with atherosclerosis many features such as endothelial damage, lipid deposition, inflammation and calcification (**Table 3**) (Dweck, Boon and Newby, 2012). Although AVS and atherosclerosis share many common pathological features, there are differences in disease pathogenesis, since lipid-lowering drugs fail to halt or delay the progression of AVS (Czarny and Resar, 2014).

Table 3 : Aortic valve stenosis and atherosclerosis pathological processes

	Aortic valve stenosis	**Atherosclerosis**
Initiating event	Increased mechanical stress and reduced shear stress causing endothelial damage	Increased mechanical stress and reduced shear stress causing endothelial damage
Early pathology	Oxidized lipid deposition	Oxidized lipid deposition
	Inflammation	Inflammation
Later pathology	Calcification and fibrosis predominant	Lipid deposition and pools, and calcification
	Neovascularization and hemorrhage	Neovascularization and hemorrhage
Disease progression	Fibrosis, calcification, and hemorrhage	Lipid deposition and pools, inflammation, plaque rupture and thrombosis
Mechanism	Progressive valve rigidity due to calcification and fibrosis	Plaque rupture due to lipid-rich pool. Intravascular thrombosis

(Adapted from Dweck, M.R. et al. Journal of the American College of Cardiology. 2012. 60(19):1854-1863)

Calcific AVS development is a dynamic process involving valvular endothelial cells, VICs, inflammatory cells, and extracellular matrix (ECM) (Czarny and Resar, 2014). Calcification often starts when lipids infiltrate in the fibrosa layer and accumulate in aortic valves (Mathieu *et al.*, 2017). Lipid deposit process occurs in mineralized AV and could take part in promoting inflammation and the formation of osteogenic VICs (O'Brien Kevin *et al.*, 1996). VICs are the most abundant cells in the aortic valve and are found in all three valve layers (Liu, Joag and Gotlieb, 2007). They are usually formed of quiescent fibroblasts, which are activated to myofibroblasts and osteoblasts upon mechanical stimuli and biochemical changes. Myofibrogenesis drives cardiac ECM remodeling, fibrosis and stiffening of valve leaflets (Schlotter *et al.*, 2018). Yutzey et al suggested the occurrence of osteogenic processes as additional mechanisms for calcific AVS (Yutzey *et al.*, 2014). Thus, it was suggested that Wnt signaling pathways may be responsible for osteoblast differentiation in AV, thus promoting AV calcification (Johnson and Rajamannan, 2006).

AVS is initiated by factors such as mechanical stress and bicuspid valves (**Figure 12**). AVS is the result of inflammation caused by mechanical stress and lipid penetration. It progresses through fibrosis and valve thickening and results in valve calcification and stenosis. Then, the leaflets become rigid and less mobile and the blood outflow is progressively obstructed which subsequently leads to heart failure. The mechanical stress induces endothelial damage, which allows the penetration of lipids and inflammatory cells to the valvular endothelium. Both LDL-cholesterol and LPA are implicated in atherogenesis and are present in AV lesions. These lipids undergo oxidative modification (oxidized-lipids), which are cytotoxic and increase the inflammation and mineralization. In addition, the inflammatory cells contribute to AV lesions through (**a**) differentiation of monocytes to macrophages which secrete calcium and (**b**) release of proinflammatory cytokines by T cells, including tumor necrosis factor alfa (TNF-α), Transforming growth factor-beta (TGF-β) and interleukin 1-beta (IL-1β). Altogether, this will subsequently induce the transformation of fibroblasts to myofibroblasts. Calcification starts in the early stages due to the secretion of calcium by macrophages, and the subsequent rate of calcification increases after the differentiation of myofibroblasts into osteoblasts through Wnt3-Lrp5-βcatenin signaling pathway. Then the osteoblasts induce the calcification, remodeling, and bone formation. The calcification occurs under the influence of mediators such as osteocalcin, alkaline phosphatase and bone morphogenic protein (BMP-2). At the end of this stage small calcific accumulation appears, which progresses to bone formation in the end-stage (Otto, 2008).

Figure 12 : Pathological process in the valve during aortic valve stenosis. The early lesion causes the penetration of lipids such as LDL and inflammatory cells (T cell and monocyte) to the fibrosa. This induces the secretion of calcium (Ca^{2+}), angiotensin II, tumor necrosis factor alfa (TNF-α), Transforming growth factor beta (TGF-β) and interleukin 1 beta (IL-1β). These products induce the transformation of fibroblasts to myofibroblasts. Then these cells are activated to osteoblasts under the effect of Wnt3, Lrp5 and βcatenin pathway. The calcification occurs after the production of osteocalcin, alkaline phosphatase, and bone morphogenic protein (BMP-2).

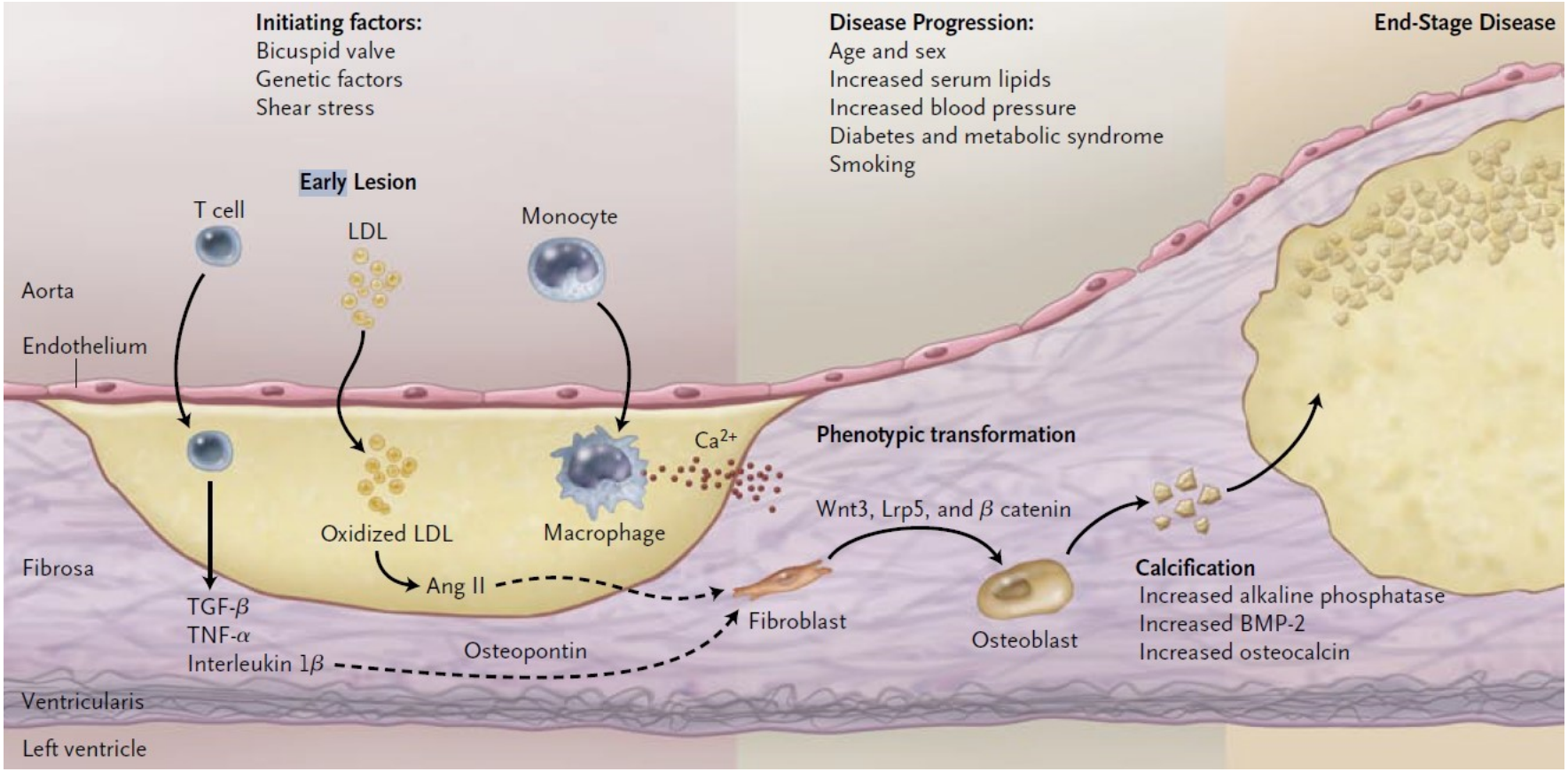

(From Otto, C.M. New England Journal of Medicine. 2008. 359(13):1395-1398)

I.3.5.1. Mineralization transition of aortic valves mediated by autotaxin

The role of LPA on VICs mineralization and oxidant formation was recently investigated. Using proteomic and lipidomic approaches, the impact of LPA on superior stimulation of calcium deposition than LDL, and increased concentration of proteins involved in calcium deposition and ROS formation was demonstrated suggesting, that LPA induces oxidative stress changes that lead to inflammations in AVS (Yu *et al.*, 2018).

Oxidized phospholipids (OxPLs) are covalently bound to apo(a)/LPA in humans and they are carried with LPA in plasma (Leibundgut *et al.*, 2013). Thus, LPA is a carrier of OxPLs which promote inflammation. LPA contains also lipoprotein-associated phospholipase A (Lp-PLA2). Mahmut et al showed that Lp-PLA2 is highly expressed in mineralized aortic valve (Mahmut *et al.*, 2014). Lp-PLA2 enzyme transforms OxPLs/LPA into lysophosphatidylcholine (lysoPC) (Tellis and Tselepis, 2009). LysoPC promotes inflammation and is a substrate to autotaxin (ATX) which is a lysophospholipase D enzyme highly abundant in the isolated LPA fraction and may be carried by LPA into the aortic valve (**Figure 13**). ATX uses LysoPC as substrate to produce choline and lysophosphatidic acid (LysoPA), which has potent inflammatory properties. Thus, in isolated VICs, LysoPA promoted_via LPAR (lysophosphatidic receptor) signaling_ the activation of NF-kB (nuclear factor -kB) and subsequently the production of IL-6 which increases the expression of BMP2 promoting by that inflammation, mineralization and osteogenic transition. The activity of ATX is enhanced in mineralized aortic valve. Hence, ATX is a mediator between OxPL/LPA and mineralized aortic valve (Bouchareb *et al.*, 2015) and it promotes this aortic valve remodeling via LysoPA production. In conclusion, LPA is associated to CAVD and it enhances inflammation and mineralization via, in part, ATX activity and lysoPA production which could represent a novel therapeutic approach (Mathieu and Ruohola-Baker, 2017).

Figure 13 : Autotaxin implication in calcific AVS. (1) Autotaxin (ATX) is transported to the aortic valve by LP(a); (3) ATX transforms lysophosphatidylcholine (LysoPC) to lysophosphatidic acid (LysoPA); LysoPA binds to LPAR (lysophosphatidic receptor) in valve interstitial cells (VICs) which (4) activates NF-κB (nuclear factor-κB) and (5) induces the production of interleukin 6 (IL-6) and (2) the production of ATX. (6) IL-6 promotes the production of osteogenic genes such as bone morphogenetic protein 2 (BMP-2). High level of IL-6 and BMP-2 promotes mineralization and osteogenic transition.

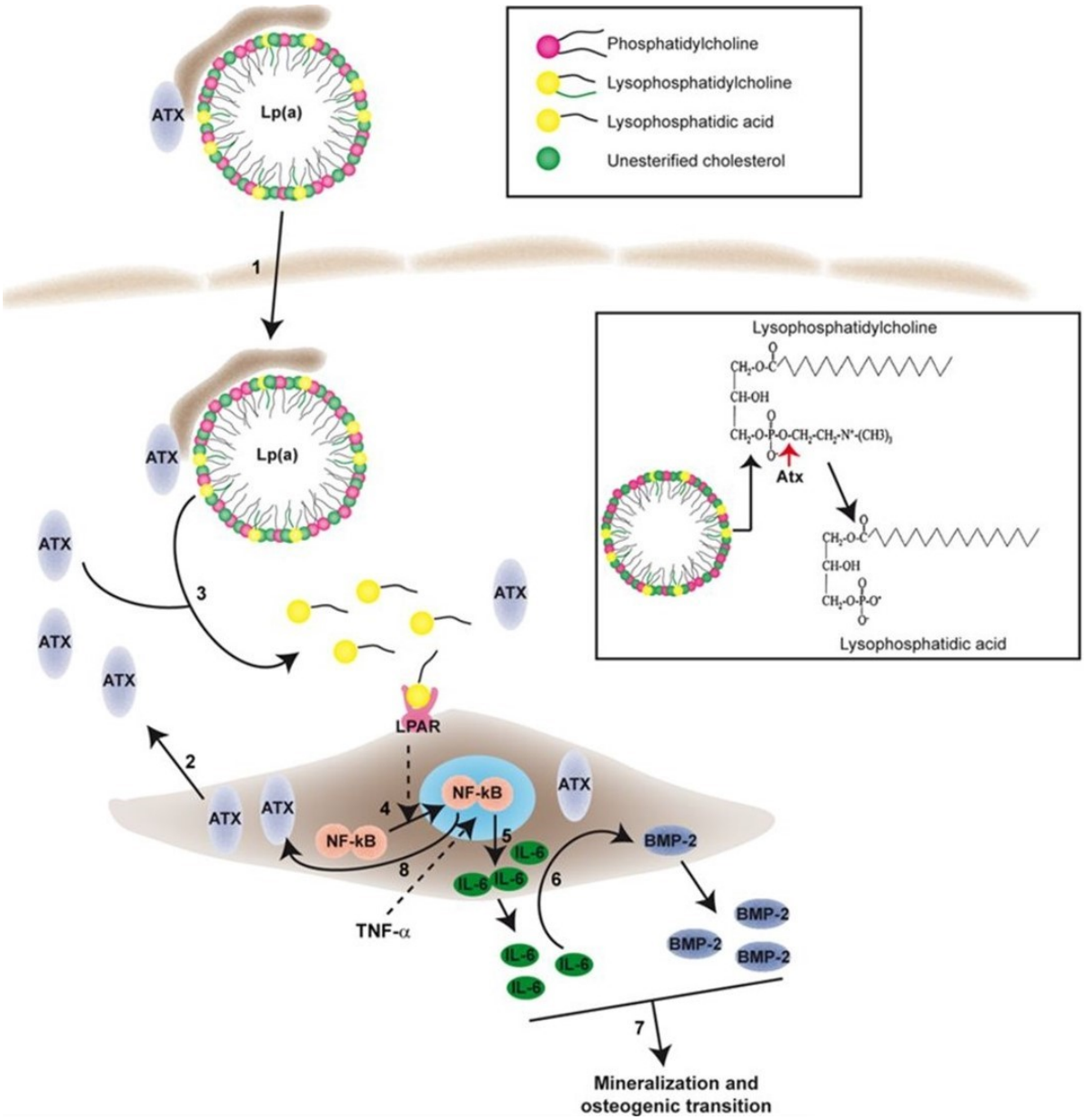

(From Bouchareb, R. et al. Circulation. 2015. 132(8): 677-690)

I.3.6. Aortic valve stenosis treatment

AVS therapeutic solutions include drug treatment, valve repairing and valve replacement. Pharmacologic treatments are ineffective, limited and not sufficient (Shipton and Wahba, 2001; Dharmarajan *et al.*, 2017; Joseph *et al.*, 2016; Bashir *et al.*, 2017) in a way that the valve would eventually be repaired or replaced (Baumgartner *et al.*, 2009). In 2010, 65,000 aortic valve replacements (AVRs) were conducted in the United States commonly due to AVS and 70% of these patients are above 65 years old (Otto and Prendergast, 2014).

I.3.6.1. Pharmacological treatments

Severe AVS is only treated with AVR. The available pharmacological treatments have failed so far to convincingly halt AVS progression or to improve prognosis. Therefore, there is no evidence that lipid-lowering statins, blood-pressure-lowering drugs, and phosphate-calcium-targeting drugs have beneficial effects in subclinical AVS (Marquis-Gravel *et al.*, 2016).

I.3.6.1.1. Lipid-lowering drugs

Owing to similarities between atherosclerosis and AVS, drugs designed to treat atherosclerosis have been tested on AVS. Statin drugs have been the most studied in AVS. Statin is a lipid-lowering drug able to experimentally reduce cholesterol deposition in the leaflets and osteoblast activity. Unfortunately, none of the observational studies have provided evidence that statin is effective to reduce AV calcification and AVS progression (Cowell *et al.*, 2005; Rossebø *et al.*, 2008; Chan *et al.*, 2010). This could be due to the late medical intervention since the disease manifests itself only after a long asymptomatic period or due to a short follow-up time (Trenkwalder *et al.*, 2019). In addition, statin has been found to increase the LPA level in serum, which may explain its ineffectiveness to halt the progression of AVS. For this reason, many none-statin lipid-lowering drugs have been developed such as inhibitors of PCSK9 (protein convertase subtilisin/kexin type 9) (Goemann, Londero and Dora, 2015) and antisense oligonucleotides (Viney *et al.*, 2016), both have been found to decrease the plasma LPA levels. A recent study showed that LPA lowering in 20% of the population (which have LPA ≥ 50mg/dL) could prevent one in seven AVS cases (Afshar *et al.*, 2016).

I.3.6.1.2. Antihypertensive drugs in AVS

The pathogenesis of calcific AVS includes lipid infiltration into the valve leaflets and lipid oxidation. This will trigger inflammation and oxidative stress. It has been shown that diet rich in cholesterol and high plasma levels of LDL-cholesterol and oxidized-LDL-cholesterol increase the deposition of oxidized-LDL-cholesterol in the valve leaflets, leading to macrophage infiltration and calcification. The narrowing of aortic valve and the sclerosis of the leaflets cause an increase in left ventricle (LV) afterload which is the resistance that the LV must work against to outflow the blood. This leads to LV remodeling, fibrosis and diastolic dysfunction (the heart can't relax between heart contractions). Then with the progression of AVS, systolic dysfunction occurs where the heart is not able to contract and pump the blood out. High blood pressure increases cardiac afterload in AVS patients and accelerates LV hypertrophy. Therefore, the American and European cardiology guidelines recommend treating the hypertension in AVS patients with emphasis on blood pressure monitoring (Marquis-Gravel *et al.*, 2016).

Nitrate derivatives drugs have been studied as antihypertensive drugs. They reduce LV afterload and preload (pressure left at the end of diastole) in AVS patients and have been suggested to treat hypertension without affecting the cardiac output (Eleid Mackram *et al.*, 2013; Khot *et al.*, 2003). Yet, there are not enough data to determine the long-term effect of nitrate treatment for patients with stable AVS. Thus, nitrate drugs are not recommended for severe AVS patients (Nishimura *et al.*, 2014).

The RAAS (renin-angiotensin-aldosterone system) promotes the penetration of inflammatory cells (monocytes), the release of proinflammatory cytokines, and the transformation of valve cells into osteoblasts. Thus, RAAS inhibition (**Figure 14**) in AVS patients prevents the mineralization and the osteogenic transition in the valve, reduces blood pressure and LV hypertrophy and improves survival. Moreover, the use of such drugs is recommended because they are effective in slowing down the progression of AVS and in attenuating myocardial remodeling that follow the increase LV afterload. In addition, Angiotensin II, which stimulates the expression of pro-inflammatory cytokine in monocytes (Kranzhöfer *et al.*, 1999), is overexpressed in stenotic valves (Helske *et al.*, 2004). Thus, RAAS blocking in animal models and in humans results in reducing the effect of angiotensin II on monocytes in the AV leaflets,

preventing valve calcification and slowing down the progression of AVS (Marquis-Gravel *et al.*, 2016).

Figure 14 : RAAS (renin-angiotensin-aldosterone system) inhibition in aortic valve stenosis. RAAS inhibition improves the heart function on three levels: valve, systemic and vascular, and myocardial levels. On the valve level, it inhibits monocyte infiltration and mineralization, reduces endothelial mechanical stress, acts as antioxidant, and it slows the progression of AS. On the systemic and vascular level, it reduces afterload, improves endothelial function and inhibit the expression of pro-inflammatory cytokines. On the myocardial level, it improves reverse myocardial remodeling before and after aortic valve replacement, inhibits hypertrophy, diastolic dysfunction, and the fibrosis of myocardial interstitial. AS: aortic valve stenosis; AVR: aortic valve replacement.

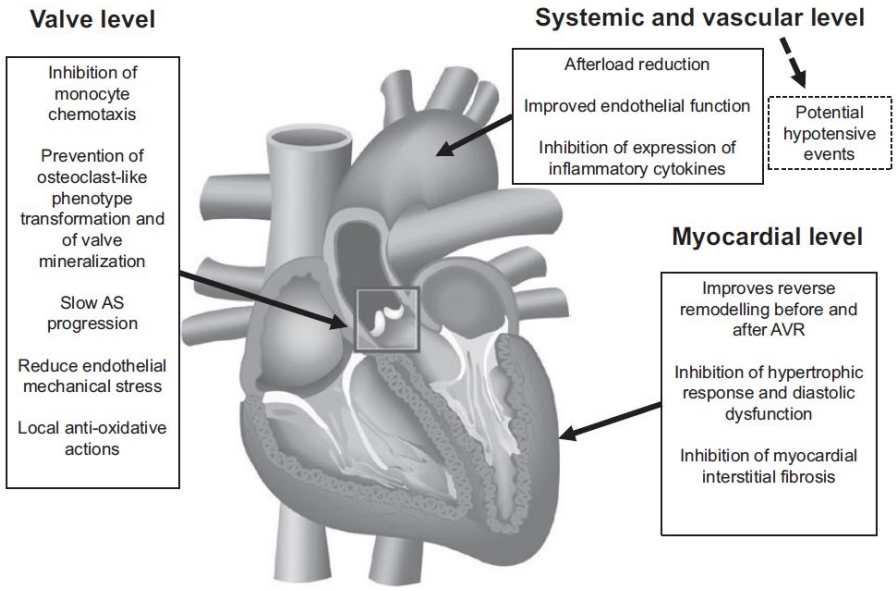

(From Marquis-Gravel, G. et al.Circulation. 2016.134(22):1766-1784)

I.3.6.1.3. Calcium and phosphate targeting drugs

Patients with calcium metabolism disorder have a high risk for developing AVS (Kurtz and Otto, 2010). One of the studies on the differences in calcium metabolism showed an association between serum phosphate levels and CAVD (Linefsky *et al.*, 2011). In addition, low bone density was associated with vascular calcification (Hyder *et al.*, 2007). Thus, treatment of osteoporosis may prevent AV calcification. Hence, reduced vascular calcification can be achieved through denosumab, a monoclonal antibody used to treat osteoporosis that inhibits

the receptor activator of nuclear factor-κB ligand (RANKL) and thereby prevents the activation of osteoclasts and the bone resorption and reduces the availability of calcium (Helas *et al.*, 2009); and through bisphosphonates, drugs used also to treat osteoporosis and strengthening bones which prevent bone resorption and reduce the calcium particles released from the bones and inhibit the differentiation of myofibroblasts into osteogenic phenotype preventing by that the deposition of calcium in the valve (Marquis-Gravel *et al.*, 2016) (**Figure 15**). Yet, bisphosphonates have no effect on AVA, transvalvular MPG, or clinical outcomes, calling for specific studies to test their effects in AVS patients with no concomitant osteoporosis (Aksoy *et al.*, 2012).

Figure 15 : Drugs targeting phospho-calcific metabolism. Biphosphate can be used to: treat osteoporosis by increasing bone mineral density; prevent vascular calcification, the differentiation of myofibroblast and the mineralization of aortic valve; decrease the inflammatory cytokines and LDL level; and increase HDL level. HDL: high-density lipoprotein; LDL: low-density lipoprotein

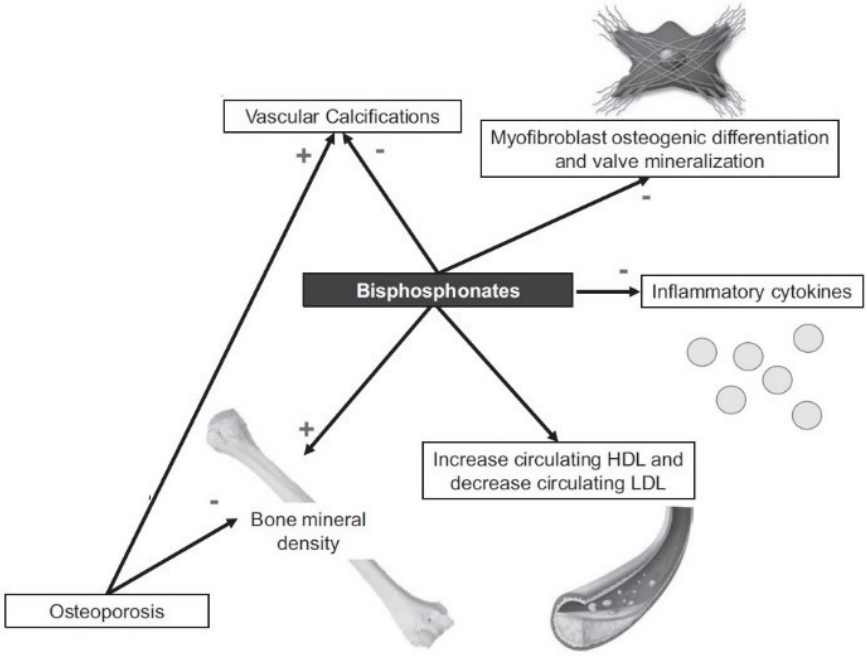

(Adapted from Marquis-Gravel, G. et al.Circulation. 2016.134(22):1766-1784)

I.3.6.2. Valve repairing

Valve repairing with catheter coupled to a balloon procedure, known as balloon valvuloplasty, is used to widen the narrowed valve (**Figure 16**) but it has a short recovery time (Bashir *et al.*, 2017).

Figure 16 : Balloon valvuloplasty. Stenotic aortic valve repairing with a balloon valvuloplasty to stretch the valve

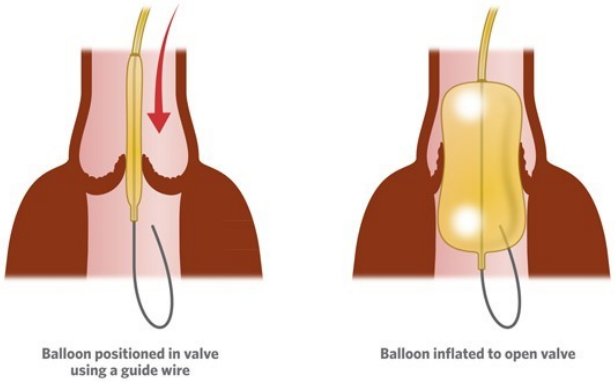

(From Cardiology : Aortic Stenosis AS - RCH. Available at : https://www.rch.org.au/cardiology/heart_defects/aortic_stenosis_as/)

I.3.6.3. Valve replacement

Eventually, AVR is needed and it can be performed with surgery (open heart surgery) or with a less invasive procedure using catheter (**Figure 17**). Thus, AVR remains the gold standard treatment and it is considered safe and effective to remove the obstruction (Shipton and Wahba, 2001; Sherwood and Kiefer, 2017). Surgical aortic valve replacement (SAVR) is an effective treatment due to its benefits regarding symptoms improvement and survival and because of the low complications and durable late outcome (Bashir *et al.*, 2017). SAVR is usually performed with mechanical or bioprosthetic valves. For the latter, either bovine or porcine valves can be used, thus preventing prolonged anticoagulant treatments. Yet, their long-term efficacy is poorly documented compared to mechanical valves (Elmariah *et al.*, 2016). Recently, transcatheter aortic valve replacement (TAVR) was used to replace the faulty aortic valve (Bashir *et al.*, 2017; Catalano *et al.*, 2019). TAVR consists in the replacement of the stenotic AV through blood vessels instead of open-heart surgery. TAVR commonly includes three different ways transfemoral, transapical or transaortic (**Figure 17**) (Joseph *et al.*, 2016). Balloon valvuloplasty can be performed in patients who cannot be subjected to AVR because of comorbid conditions and it can be used before the SAVR in unstable patients with high surgical risk (Elmariah *et al.*, 2016; Catalano *et al.*, 2019). TAVR is usually performed in elderly patients and is being used for patients with severe AVS (Leon *et al.*, 2010; Smith *et al.*, 2011; Popma *et al.*, 2014; Adams *et al.*, 2014). TAVR is associated with a lower risk of post-procedure mortality through acute kidney injury (AKI) than SAVR (Catalano *et al.*, 2019).

Figure 17: Stenotic aortic valve replacement with transcatheter or open-heart surgery. Three common ways of transcatheter aortic valve replacement (TAVR) are used: transfemoral, transapical or transaortic.

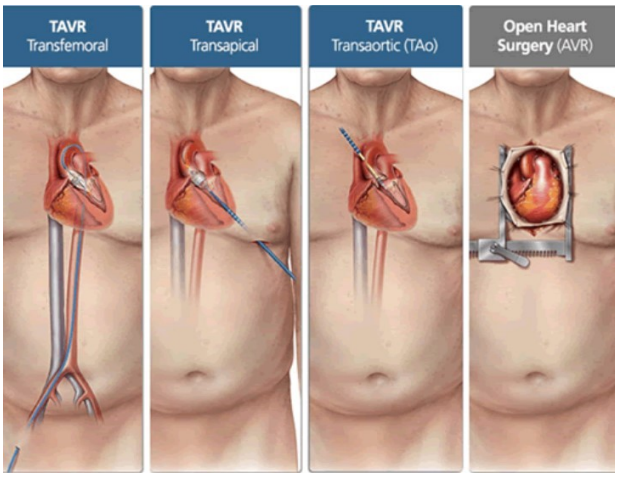

(From CVT Surgical Center Transcatheter Aortic Valve Replacement. Available at : http://www.cvtsc.com/index.php/transcatheter-aortic-valve-replacement/)

I.3.7. Genetic etiology of AVS.

Genome-wide association studies (GWAS) have identified genetic risk variants contributing to AVS that can be potentially used in AVS early diagnosis and the elaboration of novel therapeutic solutions. Many genetics studies have been performed so far in which genetic variants associated with AVS were discovered as described in this section.

I.3.7.1. ApoE4

An apolipoprotein E allele (apoE4) was found an independent predictor of AVS. Based on genotyping distribution in a study population of 802 patients undergoing transthoracic echocardiography, the prevalence of apoE4 is higher in patients with AVS when compared to control individuals. In fact, apoE4 allele was found associated with high LDL-cholesterol and total-cholesterol levels and low HDL-cholesterol level. In addition, apoE4 allele was also found associated with an increased risk for CAD (Novaro Gian *et al.*, 2003).

I.3.7.2. NOTCH1

A genome-wide scan of a large family with 11 cases of congenital heart disease was performed to seek the mechanism behind the development of congenital heart disease and valve

calcification (Garg *et al.*, 2005). Mutations in the gene encoding NOTCH1 on chromosome 9 was associated with AV anomalies and valve calcification. One of the proposed mechanisms behind valvular calcification is the activation of osteoblast-specific gene expression, such as osteopontin and osteocalcin. These genes are regulated by Runx2 which was previously found highly expressed in models with valvular calcification. NOTCH1 was found to repress the activity of Runx2. Altogether, the mutations in NOTCH1 may underlie the development of congenital valve disease and valve calcification via de-repressing Runx2.

I.3.7.3. LPA

LPA is an LDL-like molecule formed with cholesteryl esters and triglycerides, surrounded by phospholipids, cholesterol and apolipoprotein B100 (apoB100). An apolipoprotein(a) (apo(a)) molecule is bound to apoB100 molecule via one disulfide bridge (Yu *et al.*, 2018). Apo(a) is a highly polymorphic molecule, in which Kringle IV (KIV) domain has 10 types (KIV 1-10) and KIV-2 exist in many repeats (**Figure 18**). The copy number variation (CNV) of KIV-2 affects the level of LPA. Thus, the number of KIV-2 repeats is negatively associated to LPA plasma level. Yet, the level of LPA is not quite explained by KIV-2 copy number (Mathieu *et al.*, 2017).

Figure 18 : Lipoprotein(a) structure. Lipoprotein(a) is surrounded by apolipoprotein B100 (apoB) which is bound to apolipoprotein(a). Apolipoprotein(a) contains 10 types of kringle IV (KIV) in which KIV type 2 exists in many repeats. P. Protease domain

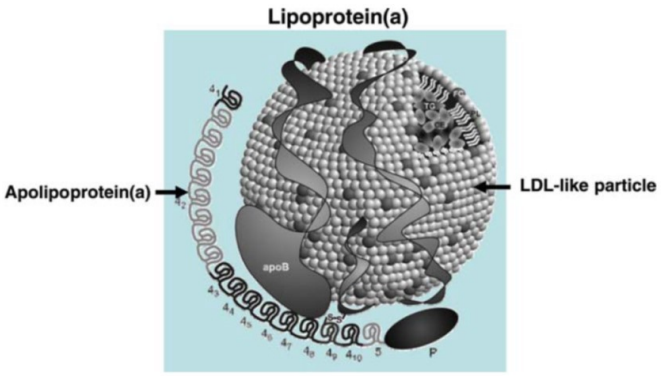

(From Nordestgaard, B.G., et al. European Heart Journal. 2010. 31(23): 2844-2853)

The first genetic study regarding LPA in AVS was a GWAS, where the SNP (single nucleotide polymorphism) "rs1333049" at the LPA locus on chromosome 6 encoding apo(a) of LPA was

associated with AV calcification (Thanassoulis *et al.*, 2013). This study provided evidence of the causal role of LPA in promoting and progression of CAVD. This finding was subsequently confirmed in two studies the following year using a Mendelian randomization design (Kamstrup, Tybjærg-Hansen and Nordestgaard, 2014; Arsenault *et al.*, 2014). Also, another SNP "rs10455872" at the LPA locus was associated with aortic stenosis using a meta-analysis (Cairns *et al.*, 2017) . Emdin and colleagues showed that low LPA level was associated with lower risk of AVS (Emdin *et al.*, 2016). Furthermore, plasma levels of LPA and oxidized phospholipids bound to apolipoprotein B-100 (OxPL-apoB) of LPA were associated with AVS progression, and this association was prominent in younger patients (Capoulade *et al.*, 2015). Finally, Kamstrup et al showed that oxidized phospholipids on -apoB or -apo(a) of LPA were associated with the risk of AVS (Kamstrup *et al.*, 2017).

I.3.7.4. PALMD

Genetic association between the gene palmdelphin PALMD on chromosome 1p2.2 and AVS was demonstrated through a GWAS carried out in 1009 AVS cases and 1017 controls and replicated in 1391 cases and 352,195 controls of UK Biobank (Thériault *et al.*, 2018). In the same study, a transcriptome-wide association study (TWAS) in 233 samples from human aortic valve revealed that low expression of PALMD was associated with high disease severity and with AVS risk alleles. The SNP rs6702619 of PALMD was strongly associated with the expression level of PALMD and showed the strongest evidence of association with AVS. The "G" allele at rs6702619 was the risk allele for AVS (Thériault *et al.*, 2018). Genetic association between the SNP rs7543130 near PALMD and AVS was confirmed in a GWAS study of 2,457 cases in Icelandic population and 349,342 controls with a follow-up in 4,850 cases and 451,731 controls of European ancestry (Helgadottir *et al.*, 2018). In this study, this SNP also showed evidence of association with BAV, a major risk factor for AVS.

The relevance of PALMD in the etiopathogenesis of heart diseases and AVS is supported by functional studies which showed that it is highly expressed in cardiac and skeletal muscle (Andreu *et al.*, 2001), promotes myoblast differentiation and muscle regeneration (Nie *et al.*, 2017) and is a target of p53 that control apoptosis in response to DNA damage in osteosarcoma cell lines (Dashzeveg *et al.*, 2014).

I.3.7.5. TEX41

The above mentioned GWAS performed in the Icelandic population also identified a significant association between AVS and the SNP rs1830321 in the gene encoding testis expressed 41 (TEX41) (Helgadottir *et al.*, 2018). TEX41 is a non-protein coding gene located on chromosome 2q22. The associated SNP contributed to 15% higher odds for AVS. In addition, TEX41 showed evidence of significant association with CAD and BAV in the same study.

I.3.7.6. MYH6

A genetic study showed an association between AVS and the MYH6 missense variant rs387906656 leading to the rare missense mutation p.Arg721Trp in MYH6 (Helgadottir *et al.*, 2018). MYH6 (myosin heavy chain 6) encodes for an essential sarcomere protein, the alpha myosin heavy chain subunit (αMHC), expressed in cardiac muscle. This genetic variant was also associated with BAV (Helgadottir *et al.*, 2018).

I.3.7.7. CFDP1

The GWAS in Icelandic subjects identified a significant association between the SNP rs17696696 intronic in CFDP1 and aortic root diameter and both AVS (OR = 1.07; 95% CI 1.03-1.11, p-value = 0.00013) and CAD (Helgadottir *et al.*, 2018).

I.3.7.8. FADS1/2

A large GWAS conducted in 44 703 participants, including 3469 AVS cases, and replicated in 7 other cohorts totaling 256 926 participants and 5926 AVS, identified a significant association between AV calcification (AVC) and stenosis and the intronic SNP rs1745747 in the gene encoding the fatty acid desaturase 1 and 2 (FADS1/2) located on chromosome 11 (Chen *et al.*, 2020). This SNP was associated with 12% lower odds for AVS. In addition, a significant association between AV calcification and rs1745747 was found with an OR 0.91 (95% CI 0.83-0.99). A mendelian randomization analysis showed that AVS and AVC were significantly associated with high FADS1 expression level in the liver with an OR 1.31 (95% CI 1.17-1.48) and OR 1.25 (95% CI 1.02-1.52), respectively. This data suggested a causal relationship between elevated FADS1 expression and both AVS and AVC. Moreover, due to the role of FADS1/2 in omega-6 and omega-3 fatty acid biosynthesis, the association of several omega-3

and omega-6 fatty acids with AVS was tested. FADS1 and 2 have key functions in the desaturation steps of the conversation of dietary linolenic acids (omega-6) into arachidonic and α-linolenic acid (omega-3) into eicosapentaenoic acid. AV stenosis and calcification was found significantly associated with a high level of plasma arachidonic acid, the product of omega-6 pathway which reflects omega-6 desaturation. Thus, an increase of 5% in the plasma level of arachidonic acid increases the odds for AVS by 8% (OR 1.08) and the odds for AVC by 23% (OR 1.23). This suggested that increased omega-6 fatty acid synthesis may be a causal pathway for AVS. In addition, AVC was significantly associated with a high ratio of arachidonic acid to linoleic acid with an OR 1.19 (95% CI 1.09-1.30), which indicates that the increased conversation of linoleic acid to arachidonic acid is associated with 19% increased odds of AVS. Therefore, fatty acid desaturase 1 and 2 and omega-6 fatty acid biosynthesis, which is catalyzed by FADS1/2, were suggested as potential therapeutic targets in AVS.

I.3.7.9. LDLR

Investigations designed to test the role of hypercholesterolemia in calcific aortic valve stenosis applied computed topography calcium measures in hypercholesterolemic patients, which determined aortic valve calcium deposition scores (AVCS) and their association with LDLR (low-density-lipoprotein receptor) gene mutation, which can cause high cholesterol levels (Gałąska *et al.*, 2018). In the study, two groups of patients were enrolled: hypercholesterolemic with or without LDLR mutation. AVCS was found significantly higher in the group with LDLR mutation. AVCS and LDLR mutation were shown to be dependable. LDLR mutation was found associated with a high AVCS with an odd ratio 7.89 (95%CI 2.08-29.50) even after adjustment for cholesterol levels. This suggests that LDLR plays a role in calcification independent to lipid levels and can be considered as an independent risk factor of high AVCS. These results confirm previous findings that showed that calcific AVS is a multifactorial disease and cannot be explained based only on cholesterol levels but also on non-lipid mechanisms. Thus, the progression of calcific AV in hypercholesterolemia patients seems to be cholesterol-independent. This was consistent with a study that showed that lipid-lowering drug such as statin did not stop or reduce the progression of AVS despite the reduction of LDL-cholesterol levels (Teo *et al.*, 2011).

I.3.7.10. Genetic risk shared in AVS and CAD

AVS and CAD are both age-related diseases, which co-exist in most cases and share common risk factors (Yan *et al.*, 2017; Stewart *et al.*, 1997). Accordingly, any analysis of genetic determinants of AVS should take into consideration CAD to exclude the possibility that the finding is due to the presence of CAD (Trenkwalder *et al.*, 2019). Considering this requirement, variants in LPA and TEX41 were found associated with both AVS and CAD in the Icelandic population. On the other hand, AVS risk variants in MYH6 and PALMD failed to show evidence of significant association with CAD (Helgadottir *et al.*, 2018). In addition, when 71 CAD genetic variants were tested for their association with AVS, only six were significantly associated with AVS, including rs10455872 and rs3798220 in LPA, rs1830321 in TEX41, rs116843064 in ANGPTL4, rs646776 in CELSR2/PSRC1, and rs3184504 in SH2B3 (Helgadottir *et al.*, 2018). Subsequently, Trenkwalder investigated the possible implication of the SNPs rs10455872 and rs1333049 at the two strongest CAD risk loci (LPA and 9p21) in AVS (Trenkwalder *et al.*, 2019). Results showed that the SNP rs10455872 in apo(a) of LPA was significantly associated with AVS with an odd ratio OR 1.37 (95% CI 1.31-1.79) and this risk increases in patients without CAD. On the other hand, the SNP rs1333049 was not associated with AVS risk. In addition, it was demonstrated that the high level of LPA in AVS patients in the absence of concomitant CAD makes AVS progression faster and undergoing AVR earlier. These findings give more evidence on the importance of LPA as therapeutic target for AVS.

I.3.8. Contribution of functional genomics to the definition of altered molecular mechanisms in AVS.

High density genomic data generation technologies designed to document the control of gene transcription (transcriptomics), protein abundance and activity (proteomic) and small metabolite regulation (metabolomics) provide opportunities to interrogate genome-wide gene expression. They have been used to generate powerful information regarding the function of the aortic valve in physiological conditions and in situations of disease recovery following surgical procedures. They can also point to biological pathways underlying increased disease risk through analysis of changes in whole genome gene expression regulation in biospecimens from AVS patients and healthy controls, as well as samples from animal models.

I.3.8.1. Alteration in proteins and pathways after transcatheter aortic valve replacement

The mechanical and hemodynamic stresses in AVS patients increase myofibroblast activation in cardiac tissues (Ozkan *et al.*, 2011). Molecular changes underlying the cellular response to valve replacement have been characterized through proteomic profiling of serum samples from patients before and after TAVR procedure (Aguado *et al.*, 2019). Results from this study identified adhesion of proinflammatory cells to the implant and suggested changes in myofibroblast activation and changes in fibrosis regulating after TAVR, which confirm a previous report of changes in serum macrophage factors (Yahagi *et al.*, 2018).

The proinflammatory cytokines TNF-α and IL-1β were more abundant in post-TAVR sera, suggesting release inflammatory factors in the circulation by these macrophages once on the implanted valve thus promoting antifibrosis. TNF-α and IL-1β may be implicated in myofibroblast deactivation. In the sera of pre-TAVR, proteins upstream of the MAPK pathway which mediate myofibroblast activation, such as IFN-γ (Interferon gamma), BMP-6 (Bone morphogenic protein-6) and CXCL9, were found abundant. Transcriptomics revealed activation of the p38 MAPK signaling pathway in pre-TAVR, suggesting myofibroblast activation. Collectively, this study showed that TAVR induces changes in inflammatory factors that help in reversing myofibroblast activation, suggesting that early TAVR may help reverse the fibrosis state of the valve and prevent further disease progression (Aguado *et al.*, 2019).

I.3.8.2. Identification of proteins and biological pathways linked to calcific tissues and diseased fibrosis

Valve mineralization mainly starts in the fibrosa side and at the base of the attachment of the valve to the aortic wall of the valve and progresses toward the tip. Transcriptome and proteome analyses carried out in samples from three layers (fibrosa, ventricularis and spongiosa) of severe AVS patients allowed disentangling molecular mechanisms underlying disease progression (non-diseased, fibrotic and calcific tissues) (Schlotter *et al.*, 2018). (**a**) In the non-diseased tissues of AV, proteins with homeostatic collagens properties were over-presented; (**b**) in fibrotic tissues of AV, proteins involved in myofibrogenic differentiation and oxidative stress, an inhibitor of calcification and other proteins related to the fibrotic phenotype were abundant; (**c**) in calcific tissues of the AV, proteins related to calcification and inflammation were abundant. Proteomic analysis in the three valvular layers identified distinct changes in the three layers in both valve types. In general, in the diseased valves, a higher proportion of

apolipoproteins was found in the fibrosa while a higher proportion of proteins involved in myofibroblast activation was observed in the ventricularis. Further biological pathway analysis identified enriched processed in the calcific stage relevant to the immune system, lipids and MAPK signaling. In fibrosa of the diseased valves, pathways related to fibrosis and calcification were enriched. In general, inflammatory signals were detected in both calcific tissues and diseased fibrosa (Schlotter *et al.*, 2018).

I.3.8.3. Protein biomarkers linked to AVS in a rabbit model

Investigations in a rabbit model of AVS showed that in the stenotic aortic valves calcium deposits, macrophage and myofibroblast were more abundant than in normal valves (Mourino-Alvarez *et al.*, 2018). Analysis of human plasma samples revealed changes in the regulation of proteins involved in osteoblastic differentiation, including downregulation of TPM-1 (tropomyosin α-1 chain) and LDHB (L-lactate dehydrogenase B chain) and upregulation of TERA (transitional endoplasmic reticulum ATPase) in AVS patients. The overexpression of TERA and the downregulation of TPM-1 point to the differentiation of VICs to osteoblasts (Park *et al.*, 2009; Cai *et al.*, 2013; Lei *et al.*, 2014). LDHB is heart specific isoform of L-lactate dehydrogenase and it was found downregulated in oxygen deprivation conditions (Rossignol *et al.*, 2003; Kay, Zhu and Tsoi, 2007).

I.3.8.4. Proteomic profiling of 92 cardiovascular candidate proteins

In a study of 92 cardiovascular candidate proteins in plasma samples from AVS patients who later underwent AVR and control subjects, the expression of five proteins (growth differential factor15 (GDF15), galectin4, transferrin receptor protein 1 (TR), proprotein convertase subtilisin/kexin type 9 (PCSK9) and von Willebrand factor (vWf)) was altered in AVS patients before the AVR requirement (Ljungberg *et al.*, 2018). Yet, this study did not provide evidence of a predictive role of these proteins to AVS pathogenesis. Indeed, PCSK9, TR and vWF may contribute to AVS through their prevalence in CAD (Ljungberg *et al.*, 2018). Nevertheless, these results confirm previously reported association between GDF15 and AVS (Krau *et al.*, 2015). In addition, association between a protein functionally related to galectin 4 (galectin 3) and AVS has been reported (Sádaba *et al.*, 2016).

I.3.8.5. miR-483 mimic and HIF1α pathway inhibitors as potential therapeutic targets of AVS

MicroRNA (miRNAs) are short single-stranded non coding RNAs that contribute to genome expression control through binding with mRNA targets. Their implication in AVS pathogenesis was tested through analysis of miR-483, which is able to suppress endothelial-to-mesenchymal transition (He *et al.*, 2017), and may protect AV endothelial cells against inflammation, proliferation and endothelial-to-mesenchymal transition (EndMT).

Under disturbed flow (d-flow) exposure, miR-483 expression was downregulated, EndMT markers were significantly highly expressed, and the pro-inflammatory markers were upregulated (Fernandez Esmerats *et al.*, 2019). Reduced miR-483 level led to endothelial inflammation and endothelial-to-mesenchymal-transition, which are critical for CAVD pathogenesis. The low level of miR-483 in the fibrosa-side in response to the d-flow, increased the expression of UBE2C, which binds and ubiquitinates pVHL (von Hippel-Lindau) and mediates its degradation. This in turn increases the level of HIF1α (hypoxia-inducible factor1alfa), which mediates endothelial inflammation, endothelial-mesenchymal-transition and ultimately leading to AV calcification.

I.3.9. Metabolomics

In contrast to transcriptomics and proteomics, which have been considerably used to profile gene expression in health and AVS, metabolomics was only applied lately in this disease context.

Metabolomics is the study of low molecular weight molecules (metabolites) and allows the detection and quantification of any changes in the endogenous and exogenous metabolites in the biospecimens (Fanos *et al.*, 2014). The metabolic phenotype (i.e. metabotype) is affected by genetics, nutrition, pharmacology, and environment (Monteiro *et al.*, 2013). Therefore, metabolomics enables the study of metabolites or small molecules in the body. These molecules are the end products of the interaction of gene/protein expression with their surroundings (Chen and Kim, 2016). This makes the metabolomics an important tool to study the environment-gene interactions, and to discover biomarkers and drugs (Bouatra et al., 2013).

Recently, a comprehensive metabolomics study identified a bunch of metabolites and lipids associated with the severity of human stenotic aortic valves tissues. Lysophosphatidic acid (LysoPA) was found strongly associated with calcific aortic valve stenosis (CAVS) severity

(Surendran *et al.*, 2020). LysoPA was previously implicated in the pathobiology of CAVD (Bouchareb *et al.*, 2015) (**Figure 13**), it is the product of Autotaxin activity and it promotes inflammation and mineralization. Yet, this metabolomics study of stenotic biopsies is limited for diagnosing the severity of the disease, only biofluid-related metabolomics can offer potential biomarkers for clinical diagnosis.

I.3.9.1. Metabolome profiling strategies

Metabolomics is a powerful tool to identify changes in the body metabolism that accompany a certain disease and treatment with drugs (Ser *et al.*, 2015). **Targeted metabolomics** focuses on a defined set of metabolites to determine their presence and abundance (Rhee and Gerszten, 2012), whereas **untargeted metabolomics** (Rhee and Gerszten, 2012) is a global profiling method (Nagana Gowda and Raftery, 2013) or metabolite fingerprint (Nishiumi *et al.*, 2010) designed to exploit spectral signals of metabolomic profiles regardless of their metabolite annotation. Analysis of metabotype variations between groups of individuals has many applications, e.g., in the prediction of risk disease, in diagnosis, assessment of drug efficacy, the influence of the environment and our lifestyle (Dunn *et al.*, 2015).

Statistical tools applied to metabolomic datasets are used to identify the metabolites that are important and that change in response to various stimuli or disease conditions (Nishiumi *et al.*, 2010). Metabolic differences between normal and diseased samples could provide information about the disease pathology (Chen and Kim, 2016) and help discover biomarkers required for an early detection of a disease, or its progression (Nishiumi *et al.*, 2010). Metabolomic studies can be applied to: (1) understanding and identification altered metabolic pathways (Nagana Gowda and Raftery, 2013; Sana, Waddell and Fischer, 2008), (2) identifying metabolic biomarkers (Nagana Gowda and Raftery, 2013; Sana, Waddell and Fischer, 2008), (3) translating a diagnostic biomarker to the clinic (Nagana Gowda and Raftery, 2013).

Lipidomics is the analysis of lipids, particularly the lipids of human serum lipoproteins and cell membranes (Hidaka *et al.*, 2007). Blood lipids are dynamic because of their transfer between serum/plasma lipoproteins and peripheral cell membranes. Phospholipids (PLs) are the major constituents of cell membranes. Cellular lipids are highly dynamic, they change with physiology, pathology, and environmental conditions (Yang and Han, 2016). PLs in

lipoproteins are classified structurally as either glycerophosphatides or sphingolipids (SLs) (**Figure 21**). Phosphatidyl choline (PC), phosphatidylserine (PS), phosphatidylethanolamine (PE), phosphatidyl inositol (PI), and lysophospholipids are included in glycerophosphatides. PLs contain hydrophilic bases and hydrophobic fatty acid residues (**Figure 19**). Since the physical chemical property of lipid is affected by its fatty acid groups, any degradation or transfer of the fatty acids groups of cell surface lipids can affect the metabolism of serum/plasma lipoproteins (Hidaka *et al.*, 2007).

Figure 19 :Phospholipids in cell membrane. (A) Phospholipid has a phosphate group on the "head" and two chains of fatty acids making up the lipid "tails"; (B) Phospholipids are classified into sphingomyelin and glycerophospholipids such as phosphatidylethanolamine, Phosphatidyl choline, phosphatidylserine, phosphatidyl inositol, and lysophospholipids; Sphingolipids include mainly sphingomyelin

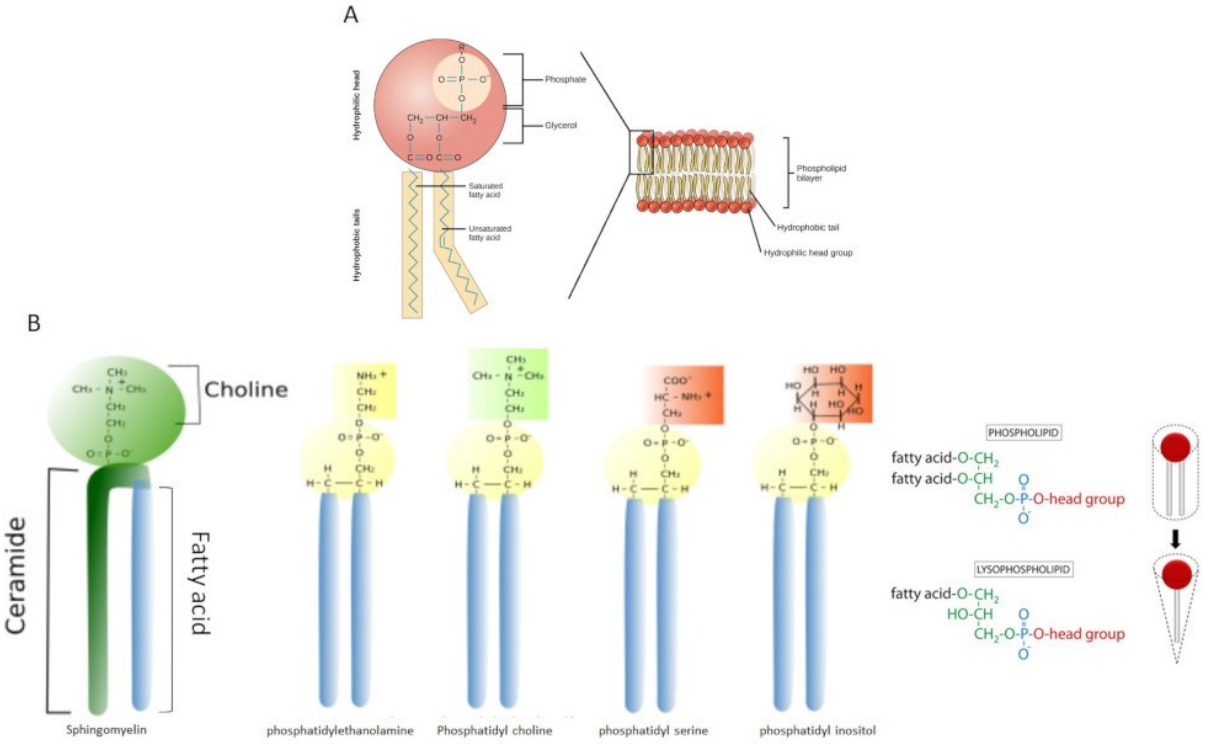

(Adapted from https://courses.lumenlearning.com/ap1/chapter/the-cell-membrane/ and https://mmegias.webs.uvigo.es/02-english/5-celulas/imagenes/membrana-lipidos.png)

I.3.9.2. Metabolomic profiling technologies

Endogenous metabolites vary in polarity, size and concentrations, thus requiring various methods to extract the largest number of metabolites. (Patti, Yanes and Siuzdak, 2012; Buchholz *et al.*, 2002; Monteiro *et al.*, 2013) and to allow the profiling of the whole metabolome in a biospecimen. The choice of the analytical tool for metabolomic data acquisition depends on the resources of the laboratory, the nature of investigated compounds, the nature of the sample, and the purpose of the study (Monteiro *et al.*, 2013). Thus, using different instruments, and different analytical tools can enhance the coverage of the metabolite profile (Ren *et al.*, 2015; Chen and Kim, 2016).

Mass spectrometry (MS) is always coupled to separation techniques; liquid chromatography (LC) and gas chromatography (GC) are the most popular since they can detect the metabolites with low concentration and can decrease the spectrum complexity (Nagana Gowda and Raftery, 2013; Ren *et al.*, 2015). In MS, the metabolites are ionized, fragmented and separated according to their mass-to-charge ratios (m/z). MS-based metabolomics is sensitive and cost-efficient (Chen and Kim, 2016), The drawback of MS-based techniques is the variation between instruments and alteration in metabolite composition due to sample preparation (Monteiro *et al.*, 2013).

Nuclear magnetic resonance (NMR) spectrometry is reproducible, requires minimal sample handling, has quantitative ability and gives structural information. Yet, NMR has low sensitivity and limited identification methods.

I.3.10. Biomarkers

Metabolic differences between normal and diseased samples provide information about the disease pathology in numerous diseases (Bujak *et al.*, 2015; Troisi *et al.*, 2018). Metabolomics has been applied to biomarkers discovery (Rhee and Gerszten, 2012), which provide opportunities to uncover compounds and pathways for early disease diagnosis (Nagana Gowda *et al.*, 2008; Troisi *et al.*, 2018). Many metabolomics studies have identified candidate biomarkers in cardiovascular field such as: plasma 4-hydroxyproline identified with GC/MS in patients with acute coronary syndrome (Vallejo *et al.*, 2009); 17 urinary polypeptides with fragments of collagen α1 (I and III) identified with capillary electrophoresis directly coupled with mass spectrometer in CAD patients (von zur Muhlen *et al.*, 2009); Aconitic acid,

hypoxanthine, trimethylamine N-oxide, threonine identified in plasma with LC/MS in MI patients (Lewis *et al.*, 2008); 24 differential metabolites identified in plasma of atherosclerosis patients using NMR and GC/MS (Teul *et al.*, 2009); plasma Dicarboxyl acylcarnitines in CAD patients with GC/MS (Shah Svati *et al.*, 2010), etc. Usually a biomarker follows the following criteria: (i) it should be readily available biofluids such as blood and urine; (ii) it should be sufficiently sensitive so it contributes to early detection and specific so it stays unaffected by the external conditions; (iii) it should response to treatment approach and disease progression; (iv) it should help to better understand the disease mechanisms; and (v) it should be used for risk assessment and disease prediction (Monteiro *et al.*, 2013). Many biomarkers have been identified and incorporated into cardiology practices, including for example troponin I and troponin T for MI, B-type natriuretic peptide (BNP) for decompensated heart failure, and LDL cholesterol for adverse cardiovascular outcomes (Rhee and Gerszten, 2012).

Hypotheses and Aims

Aortic valve stenosis (AVS) is a severe condition that is increasingly prevalent among the elderly population and the number of patients may increase in the next decades due to the lack of early detection and treatment. Aortic valve replacement through open-heart surgery or trans-catheter is required in > 2% of patients over the age of 65. Though the aortic valve can be replaced, the procedure is expensive and is associated with complications and substantial morbidity or mortality because AVS affects mostly the aged population. This situation rationalizes the dire need to develop early detection and preventive therapies for AVS. Most cardiovascular deaths occur in individuals with late prognosis, or those who are not aware of their underlying medical condition, and death is likely due to lack of in-time treatment. The challenge for early detection and prevention of AVS lies in the fact that currently there are no reliable predictive biomarkers. Metabolomics is a powerful technique that can be applied to discover biomarkers and affected pathways linked to AVS using samples collected through non-invasive techniques.

We hypothesized that there are metabolic differences in biofluids between AVS cases and control individuals. The differential signals can be used as potential biomarkers associated with the disease. As such, we combined metabolomic profiling of urine and plasma, which may unveil new biological pathways that contribute to AVS.

Our study aimed to identify potential biomarkers linked to AVS. Biomarkers may likely ameliorate the diagnosis and prognosis of this disease in the near future. To fulfill these aims, we adopted complementary metabolomic profiling strategies to identify metabolites that distinguish AVS cases from healthy controls. We have also tested the effects of candidate metabolites on the expression of selected genes.

- Aim 1: apply untargeted metabolomic profiling based on gas chromatography-mass spectrometry (GC/MS) to differentially identify regulated metabolites and discover potential biomarkers linked to AVS. Plasma and urine samples of 46 AVS patients and 46 healthy controls were used to study the association to AVS in the two biofluids.
- Aim 2: Perform proton nuclear magnetic resonance (^{1}H NMR) spectroscopy-based metabolic profiling using urine samples of 36 AVS patients and 40 controls. Both

untargeted and targeted ^{1}H NMR-based metabolomics was applied to identify metabolites associated with AVS.

- Aim 3: Use untargeted lipidomics based on matrix-assisted laser desorption ionization-time of flight mass spectrometry (MALDI-TOF/MS) to identify possible lipid profile alterations using 92 plasma samples segregated between cases and controls.
- Aim 4: Test the effects of candidate metabolites on the transcription of specific genes related to cardiovascular diseases using heart samples of mice treated chronically with theses metabolites.

Chapter II: Metabolomics based on GC/MS

II.1: Introduction

The application of metabolite profiling strategies to biomarker discovery projects in human population studies remains a technical challenge. Mass spectrometry-based techniques have the following advantages: high sensitivity as well as improved metabolites identification and discrimination capacity. It can be used to perform targeted and untargeted metabolomics (Rhee and Gerszten, 2012). In gas chromatography mass spectrometry (GC/MS), the derivatized metabolites are introduced into a heated injector, vaporized, and mixed with the carrier gas. The mixture enters the chromatographic column, typically a fused silica capillary column, where the metabolites are separated and then reaches the MS detection system where the metabolites are characterized. The signals are detected and presented in a chromatogram illustrating the variation of these detected metabolites with time (**Figure 20).**

GC/MS is ideal for analysis of volatile non-polar analytes and to those that can be volatilized. Thus, the non-volatile and thermolabile compounds cannot be directly analyzed using GC-MS. However, derivatization methods can cover a significant proportion of the metabolome. For example, polar metabolites such as sugars, nucleotides, and amino acids are not volatile and can not be detected directly with GC/MS. Their derivatization requires a 2-stage process of oximation followed by trimethylsilylation. The purpose of the oximation step using methoxylamine is to protect aldehyde and ketones groups (Lee and Fiehn, 2008) by converting the functional group (C=O) to oximes (R=NOH). Then the hydrogen of the functional groups in compounds such as carboxylic acids, alcohol, thiols, and amines (-COOH, -OH, -SH, and -NH) are blocked by alkylation, acylation or silylation. Silylation is the most commonly used reaction and it can be performed using MSTFA (N-(trimethylsilyl)trifluoroacetamide) (Lee and Fiehn, 2008) and BSTFA (N,O-bis(trimethylsilyl)trifluoroacetamide) (Cheng *et al.*, 2012) as derivatization agents. For the silylation reaction, trimethylsilyl groups (TMS) replace the active hydrogens (Lee and Fiehn, 2008). On the one hand, derivatization increases the

volatility, decreases polarity, improves the peaks shape and chromatographic resolution, and increases the thermal stability of some compounds. On the other hand, the time-consuming derivatization may increase the probability of metabolites loss, cause artifacts, lead to a complex spectra, and lead to the formation of multiple products from a single metabolite (Monteiro, Carvalho and Pinho, 2012).

Figure 20 :Gas Chromatography/Mass Spectrometry (GC/MS). The mixture is carried with a carrier gas, enters the chromatogram column where the carried mixture is separated and then reaches the MS detection system.

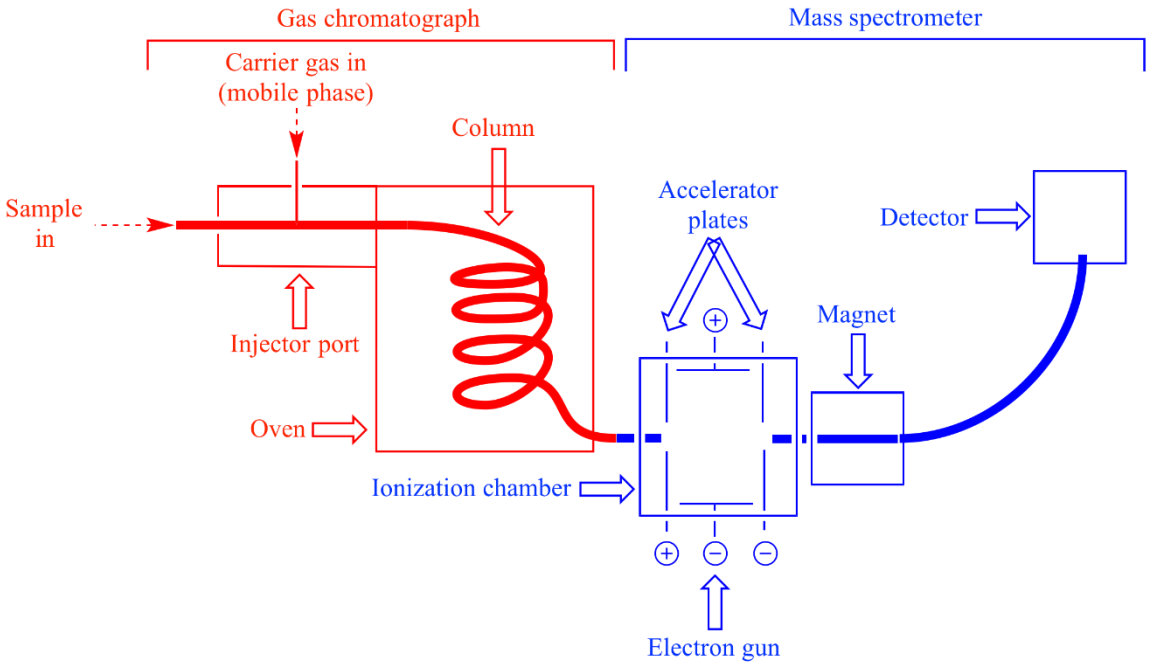

(From Illustrated Glossary of Organic Chemistry - Gas chromatography-mass spectrometry (GC-MS). [online] Chem.ucla.edu. Available at: https://www.chem.ucla.edu/~harding/IGOC/G/gc_ms.html)

The main drawback of GC/MS in metabolomic studies of epidemiological scale lies in the variability of results during runs and between runs when the same equipment is used, and between experiments when different equipments are used. The purpose of this part of the work was to take advantage of the sensitivity of the GC/MS technology to identify potential metabolite biomarkers in both urine and plasma samples in a population study of relatively modest size (92 samples), with the objective to propose hypotheses to be tested in future large scale epidemiological studies.

II.2: Plasma and urinary GC/MS metabolomics reveals potential biomarkers of aortic valve stenosis

Plasma and urine metabolomic analyses in aortic valve stenosis reveal shared and biofluid-specific changes in metabolite levels. Published in the journal PLOS ONE on the 25th of November 2020.

Cynthia Al Hageh, Ryan Rahy, Georges Khazen, Francois Brial, Rony S. Khnayzer, Dominique Gauguier, Pierre A. Zalloua.

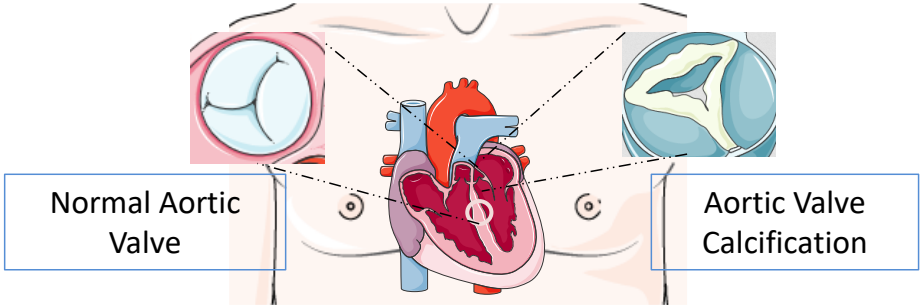
Normal Aortic Valve
Aortic Valve Calcification

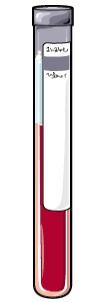

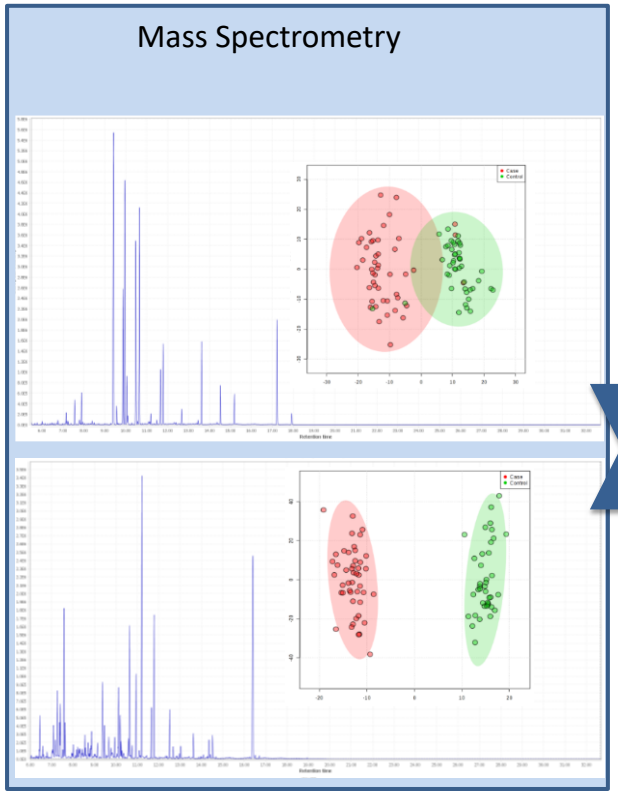
Mass Spectrometry


Generalized Linear Model

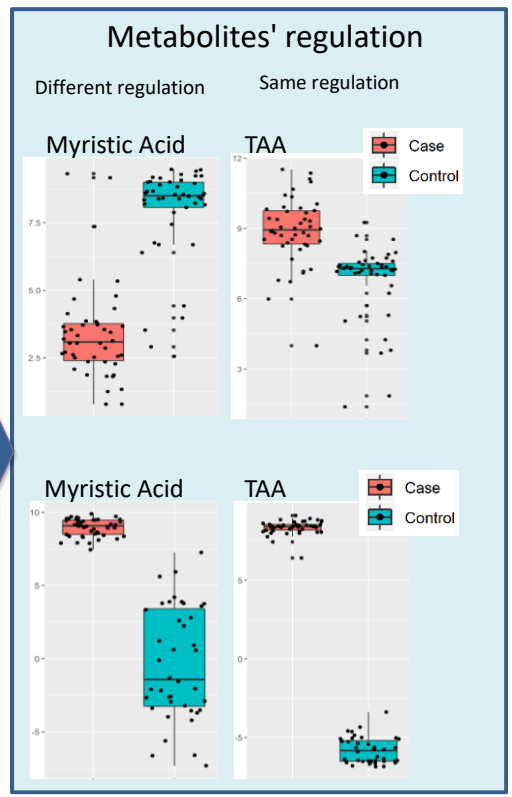
Metabolites' regulation
Different regulation
Same regulation
Myristic Acid
TAA
Case
Control
Myristic Acid
TAA
Case
Control

PLOS ONE

RESEARCH ARTICLE

Plasma and urine metabolomic analyses in aortic valve stenosis reveal shared and biofluid-specific changes in metabolite levels

Cynthia Al Hageh[1,2], Ryan Rahy[2], Georges Khazen[2], Francois Brial[1], Rony S. Khnayzer[2☯]*, Dominique Gauguier[1,3☯]*, Pierre A. Zalloua[4☯]*

1 Université de Paris, INSERM UMRS 1124, Paris, France, **2** Department of Natural Sciences, School of Arts and Sciences, Lebanese American University, Beirut, Lebanon, **3** McGill University and Genome Quebec Innovation Centre, Montreal, QC, Canada, **4** School of Medicine, University of Balamand, Amioun, Lebanon

☯ These authors contributed equally to this work.
* dominique.gauguier@inserm.fr (DG); rony.khnayzer@lau.edu.lb (RSK); pierre.zalloua@balamand.edu.lb (PAZ)

Citation: Al Hageh C, Rahy R, Khazen G, Brial F, Khnayzer RS, Gauguier D, et al. (2020) Plasma and urine metabolomic analyses in aortic valve stenosis reveal shared and biofluid-specific changes in metabolite levels. PLoS ONE 15(11): e0242019. https://doi.org/10.1371/journal.pone.0242019

Editor: Harald Mischak, University of Glasgow, UNITED KINGDOM

Received: August 10, 2020

Accepted: October 24, 2020

Published: November 25, 2020

Peer Review History: PLOS recognizes the benefits of transparency in the peer review process; therefore, we enable the publication of all of the content of peer review and author responses alongside final, published articles. The editorial history of this article is available here: https://doi.org/10.1371/journal.pone.0242019

Data Availability Statement: The data underlying the results presented in the study are available in S4 and S5 Tables.

Abstract

Aortic valve stenosis (AVS) is a prevalent condition among the elderly population that eventually requires aortic valve replacement. The lack of reliable biomarkers for AVS poses a challenge for its early diagnosis and the application of preventive measures. Untargeted gas chromatography mass spectrometry (GC-MS) metabolomics was applied in 46 AVS cases and 46 controls to identify plasma and urine metabolites underlying AVS risk. Multivariate data analyses were performed on pre-processed data (e.g. spectral peak alignment), in order to detect changes in metabolite levels in AVS patients and to evaluate their performance in group separation and sensitivity of AVS prediction, followed by regression analyses to test for their association with AVS. Through untargeted analysis of 190 urine and 130 plasma features that could be detected and quantified in the GC-MS spectra, we identified contrasting levels of 22 urine and 21 plasma features between AVS patients and control subjects. Following metabolite assignment, we observed significant changes in the concentration of known metabolites in urine (n = 14) and plasma (n = 15) that distinguish the metabolomic profiles of AVS patients from healthy controls. Associations with AVS were replicated in both plasma and urine for about half of these metabolites. Among these, 2-Oxovaleric acid, elaidic acid, myristic acid, palmitic acid, estrone, myo-inositol showed contrasting trends of regulation in the two biofluids. Only trans-Aconitic acid and 2,4-Di-tert-butylphenol showed consistent patterns of regulation in both plasma and urine. These results illustrate the power of metabolomics in identifying potential disease-associated biomarkers and provide a foundation for further studies towards early diagnostic applications in severe heart conditions that may prevent surgery in the elderly.

Funding: C Al Hageg is funded by a PhD studentship of the Lebanese National Center for Scientific Research. R Khnayzer acknowledges support from the School Research and Development Council at the Lebanese American University (srdc-r-2017-20). The patient cohort was collected by P Zalloua with the financial support from the European Commission (FGENTCARD, LSHGCT-2006-037683). The funders had no role in study design, data collection and analysis, decision to publish, or preparation of the manuscript.

Competing interests: The authors have declared that no competing interests exist.

Introduction

Aortic valve stenosis (AVS) results from inflammation caused by mechanical stress, lipid infiltration leading to fibrosis, leaflet thickening, and eventually calcification [1, 2]. The risk of AVS increases with age with 10% of AVS patients being above the age of 80 [3]. Pharmacologic treatments of AVS are often ineffective [4] and surgical valve repair or replacement is eventually needed in the elderly when surgery is often problematic [5]. Elevated concentration of plasma lipopotein(a) remains the most robust marker for AVS that may account for disease pathophysiology and valve molecular anomalies described in AVS [6]. Nevertheless, early diagnosis and prognosis of AVS can be greatly improved by the high-throughput measurement of reliable molecular biomarkers in easily accessible biospecimens.

Metabolomics provides a platform for biomedical discovery, as well as clinical and pharmaceutical applications, which has been extensively used for biomarker discovery, drug response ascertainment and disease pathway identification [7]. It relies on the qualitative and quantitative analysis of small molecular weight metabolites, which are end products of genome expression while integrating consequences of environmental exposures [8]. It has been successfully used for in depth characterisation of metabolic changes in health and disease [9] and particularly powerful to identify metabolites associated with increased risk of metabolic and vascular diseases [10–12]. The application of metabolomics to test associations between AVS and many metabolites simultaneously represents a prospect of significant advances for early disease diagnosis and improved treatment efficacy.

Here, we applied highly sensitive untargeted metabolomics based on gas chromatography mass spectrometry to identify metabolites associated with AVS. Through plasma and urine paralleled metabolomic profiling of AVS patients and control subjects, we sought to identify a series of metabolic features associated with the disease. We also investigated the existence of metabolites showing either shared or biofluid-specific association with AVS. These results underline the power of metabolomics to identify potential biomarkers for early AVS diagnosis and targets for therapeutic applications that may prevent or anticipate the need for cardiac surgery in the elderly.

Material and methods

Study subjects and AVS diagnosis

Subjects were recruited as part of a comprehensive study on coronary artery disease between 2007 and 2009 [13]. They were selected based on the presence (cases) or absence (controls) of AVS as clinically determined by the occurrence of a systolic murmur in the aortic valve area, which was subsequently confirmed in cases by echocardiography. Urine and plasma samples from 46 AVS patients and 46 healthy controls (matched for sex and age ± 5 years) were used in this study. About 30 ml of urine and 20 ml of arterial blood were collected in subjects after 12 hours fasting. Blood was collected on EDTA and plasma was separated by centrifugation at room temperature. Urine samples were centrifuged at room temperature. Plasma and urine aliquots were stored at -80˚C until metabolomic analysis.

All subjects provided a written informed consent, and the study protocol was approved by the International Review Board (IRB) at the Lebanese American University. All protocols were performed according to the Helsinki Declaration of 1975.

Gas chromatography coupled with mass spectrometry

Samples were prepared for metabolite extraction using methods optimized for urine [14] and plasma [15]. The internal standard 2-isopropylmalic acid was used for quality control.

Trimethylsilylation was applied in sample preparation of urine and plasma extracts for gas chromatography mass spectrometry (GC-MS) acquisition. Samples were subjected to GC-MS HP6890 (Agilent Technologies, Santa Clara, CA) equipped with a capillary column HP-5MS 5% phenyl methyl siloxane of 30m nominal length, 250μm nominal diameter and 0.25μm nominal film thickness (Agilent Technologies, Santa Clara, CA). A 1μL aliquot of the derivatized solution was injected under split mode with a ratio 3:1 using Helium gas. GC-MS raw chromatograms were exported in CDF format for data pre-processing, and CSV files were obtained which included peak retention time, peak height, peak area and metabolites identification using the NIST08 library (https://chemdata.nist.gov/). Metabolite annotation was manually checked using a similarity criterion of ≥80%. Data from negative controls (same reagents and conditions excluding sample) were acquired with GC-MS in order to remove artifact peaks from the solvents used in extraction and derivatization.

Metabolomic data pre-processing

GC-MS raw data were pre-processed to generate a comprehensive peak table that included all detected peaks characterized by a specific retention time (RT), mass to charge ratio (m/z) and the intensity of each peak across multiple samples from multiple sample groups. The XCMS (v 3.6.1) tool in R statistical language (through Bioconductor v 1.30.4) was used for GC-MS data pre-processing where RT were aligned, and signal drift and batch effect were corrected. XCMS uses CDF format as input, and gives a data Matrix table as output. Using XCMS, peak detection was performed while the peak width parameter was set visually after assessing the chromatographic peaks belonging to the internal standard. Thus, based on the internal standard, the range of RT values was set between 450 and 460 seconds, the m/z range was between 275 and 278 and the value of maximum expected deviation of m/z values was set to 3ppm. Then, peak alignment was performed so that all RTs can be adjusted to match across all samples.

Metabolomic data processing

The MetaboAnalyst tool (v 2.0.1) in R package was used for statistical analysis. Each spectral feature was normalized to the internal standard 2-isopropylmalic acid. In a separate analysis, data generated from urine samples were normalized to creatinine, which is proposed as an alternative method to internal standard to account for urine dilution [16]. A generalized logarithm transformation was subsequently applied for data transformation. Then univariate analysis using volcano plot and multivariate analysis using principle component analysis (PCA), Partial Least Squares-Discriminant Analysis (PLS-DA) and Orthogonal PLS-DA (OPLS-DA) [17] were performed. Volcano plot showed the combination between the fold-change (log 2 (FC)) of the relative abundance of each spectral feature in AVS cases and controls and the statistical significance of the FC. Model cross validation with R^2 and Q^2 was used to assess the goodness of fit and predictability of the OPLS-DA model respectively. The index of Variable Importance in Projection (VIP), which measures the importance of individual metabolite features in the PLS-DA model, was used to weigh their contribution to the separation between cases and controls. Since OPLS-DA tends to over fit data a permutation test with 1,000 iterations was performed to validate the model and understand the significance of class discrimination. To decrease the rate of false positives in the selection, q-values were calculated using Benjamini-Hochberg method [18] and the threshold was set at 0.05. Metabolites were selected as candidates when VIP>1, False Discovery Rate (FDR) <0.05 and q-values <0.05. Receiver operating characteristic (ROC) analysis was developed using the Biomarker Analysis tool in MetaboAnalyst (www.metaboanalyst.ca) to evaluate the performance of each candidate metabolite to separate cases and controls. Area under the ROC curve (AUC) for each metabolite, as

well as their 95% confidence intervals, were used to assess the utility of the candidate metabolites according to criteria [19] designed to rank candidate biomarkers as excellent (AUC = 0.9–1.0), good (AUC = 0.8–0.9), fair (AUC = 0.7–0.8), poor (AUC = 0.6–0.7) or failed (AUC = 0.5–0.6).

Generalized linear models (GLMs) were used to determine the metabolomic peaks significantly associated with AVS. After adjusting for age, sex, body mass index (BMI), hyperlipidemia and diabetes, logistic regression was used to assess the association of the metabolite peaks with AVS. The p-values obtained corresponded to the p-value of the peak in each model. These values were then corrected using the Benjamini-Hochberg method [18]. Peaks were considered to be statistically significant when their adjusted p-values (q-values) were less than 0.05.

Biological pathway analysis

Analysis of the biological pathways in the Kyoto Encyclopedia of Genes and Genomes (KEGG, www.genome.jp/kegg) underlying AVS risk was carried out with data from urine and plasma metabolites that were significantly associated with AVS using the web-tool MetaboAnalyst (www.metaboanalyst.ca). Both over-representation of significantly altered metabolites within pathways (P-values based on hypergeometric test) and the impact of metabolite changes on the function of the pathway through alterations in critical junction points of the pathway (relative betweenness centrality) were assessed.

Results

Clinical and biochemical features of AVS patients and control individuals

The 92 subjects were phenotypically well characterized with a mean age of 59.1 (±1.3) years, a mean body weight of 81.9 kg (±1.7), a mean BMI of 30.8 kg/m^2 (±0.5), a mean blood glucose 112.3 mg/dL (±5.3), a mean triglyceride of 186.5 mg/dL (±9.0), a mean HDL-cholesterol of 40.1 mg/dL (±1.4), a mean of LDL-cholesterol of 115.0 mg/dL (±4.3) and mean of total cholesterol of 188.3 mg/dL (±5.1) (**Table 1**). A total of 63 subjects were hypertensive (68.5%), 68 had family history of hypertension (73.9%), 18 were diagnosed with diabetes (19.6%), 40 were hyperlipidemic (43.5%), 52 had family history of diabetes (56.5%) and 37 had family history of hyperlipidemia (40.2%). There were no significant differences between AVS patients and control individuals for biochemical variables. Markedly reduced serum LDL-cholesterol in AVS subjects when compared to controls was not statistically significant (p = 0.215). There were no significant differences between males and females in any of these variables (**S1 Table**).

General features of metabolomic profiling data

Using a signal to noise ratio of 6 applied to peak detection on the GC-MS chromatograms, a total of 190 and 130 peaks have been confidently detected in urine and plasma, respectively. Using the NIST08 library, a total of 112 and 70 metabolites possessing a similarity index $\geq$ 80% were detected with GC-MS in urine and plasma extracts respectively (**S2 Table**). The intensity of each peak was measured and normalized to the internal standard (2-isopropylmalic acid).

Metabolomic analysis of urine and plasma samples in AVS patients

Using volcano plots, we identified 30 features showing evidence of difference in urine levels (nominal p<0.05) between AVS patients and controls, including 21 features which were more abundant in AVS patients than in controls (**Fig 1A**; **S3 Table**). In the PCA score plots derived

Table 1. Clinical and biochemical features of the 92 subjects selected for presence or absence of aortic valve stenosis.

	Total (92)	Controls (46)	Cases (46)	p-value
Age	59.1 ± 1.3	59.5 ± 1.9	58.8 ± 1.9	0.81
Body weight (Kg)	81.9 ± 1.7	82.2 ± 2.4	81.6 ± 2.3	0.86
Body mass index (Kg/m^2)	30.8 ± 0.5	30.9 ± 0.8	30.8 ± 0.7	0.93
Plasma glucose (mg/dL)	112.3 ± 5.3 (49)	112.2 ± 6.6 (36)	112.6 ± 7.5 (13)	0.97
Triglycerides (mg/dL)	186.5 ± 9.0 (80)	186.6 ± 13.2 (42)	186.4 ± 12.2 (38)	0.99
HDL cholesterol (mg/dL)	40.1 ± 1.4 (82)	40.1 ± 1.9 (43)	40.0 ± 2.1 (39)	0.98
LDL cholesterol (mg/dL)	115.0 ± 4.3 (80)	120.0 ± 6.2 (42)	109.4 ± 5.7 (38)	0.22
Total cholesterol (mg/dL)	188.3 ± 5.1 (82)	191.0 ± 8.0 (43)	185.3 ± 6.3 (39)	0.58
Diagnosed diabetic (%)	18 (19.6%)	7 (15.2%)	11 (23.9%)	
Diagnosed hypertensive (%)	63 (68.5%)	27 (58.7%)	36 (78.3%)	
Diagnosed hyperlipidemic (%)	40 (43.5%)	12 (26.1%)	28 (60.9%)	
FH diabetes (%)	52 (56.5%)	29 (63.0%)	23 (50.0%)	
FH hypertension (%)	68 (73.9%)	34 (73.9%)	34 (73.9%)	
FH hyperlipidemia (%)	37 (40.2%)	16 (34.8%)	21 (45.7%)	

FH, Family History. Data are means ± SEM.

https://doi.org/10.1371/journal.pone.0242019.t001

from GC-MS spectra, a clear separation was obtained to differentiate metabolome profiles of AVS patients and controls (Fig 1B). The principal components PC1, PC2, and PC3 described 26.8%, 16.6% and 9.2% of the variation, respectively. The OPLS-DA score plot also provided a clear separation of AVS patients and controls (Fig 1C). The goodness of fit values of the OPLS-DA model were 0.113 (R^2X) and 0.76 (R^2Y), with a predictive ability value of 0.735 (Q^2) (S1A Fig). This model explained 11.3% of the variation in metabolites levels and 76.0% of the variation between the groups, and the average prediction capability was 73.5%. The difference between R^2Y and Q^2 was less than 0.2 and the Q^2 value was greater than 50%, revealing an

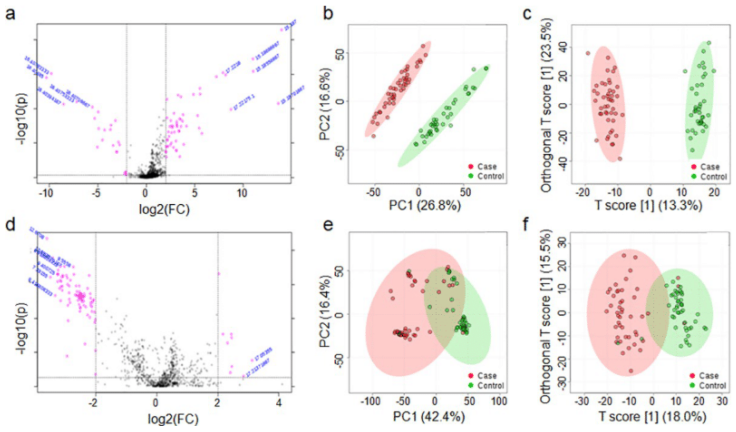

Fig 1. Discrimination analysis of AVS patients and control individuals through metabolomic profiling of biofluids. Metabolomic data were derived from GC-MS spectra of urine (a-c) and plasma (d-f) samples from AVS patients (n = 46) and healthy controls (n = 46). Univariate analysis of GC-MS spectral data in the 92 samples was performed to identify metabolomic features significantly separating cases and controls (nominal $p<0.05$), which are plotted in pink dots in the upper part of the volcano plots (a, d). Multivariate statistics were applied to perform principle component analysis (PCA) (b, e) and orthogonal partial least squares-discriminant analysis (OPLS-DA) (c, f) and assess sample classification in cases and controls. The 95% confidence regions are displayed by shaded ellipses in AVS patients (red) and controls (green).

https://doi.org/10.1371/journal.pone.0242019.g001

excellent predictive capability. Permutation tests were performed (1000 iterations) to verify that this OPLS-DA model was not random or due to over fitting ($p<0.001$) (S1B Fig).

To improve the metabolic profile of AVS patients, we complemented urine metabolic analyses with GC-MS metabolomic profiling of plasma samples from the same panel of AVS and control subjects. As previously observed with urine metabolic features, volcano plot analysis identified 23 significantly contributing features (nominal $p<0.05$), including 10 features that were more abundant in AVS patients than in controls (Fig 1D; S3 Table). The PCA score plots of plasma metabolomics provided some evidence of clustering of AVS and control groups that was however inferior to that achieved with urine data (Fig 1E). The PC1, PC2 and PC3 described 42.4%, 16.4%, and 7.7% of the variation, respectively. The OPLS-DA plot also indicated that the two groups are well separated into 2 clusters (Fig 1F). OPLS-DA showed significantly good predictability ($Q^2 = 0.649$), and good capability to explain the metabolic variation between AVS patients and controls ($R^2Y = 0.684$), with goodness of fit values of 0.180 (R^2X) and 0.684 (R^2Y) (S1C Fig). The model explained 18.0% of the variation in metabolite levels and 68.4% of the variation between the groups, and a higher average prediction capability (94.9%) than urine data (73.5%). The difference between R^2Y and Q^2 (<0.2) and the Q^2 value (>50%) confirmed the excellent predictive capability of the model (0.684). The permutation test indicated that AVS had significant impacts on the plasma metabolic profiling ($p<0.001$; 1,000 iterations) (S1D Fig).

Urine and plasma metabolomic profiling in AVS underlines biofluid-specific changes in metabolite abundance

We used the index of Variable Importance in Projection (VIP) derived from the PLS-DA models of urine and plasma metabolomic datasets to weigh the impact of each individual metabolite feature to separate AVS cases and controls (Fig 2). Following feature annotations using the NIST08 library, we identified a total of 16 known urine metabolites significantly contributing to the separation between AVS and controls (VIP>1, nominal $p<0.05$, $q<0.05$). These include

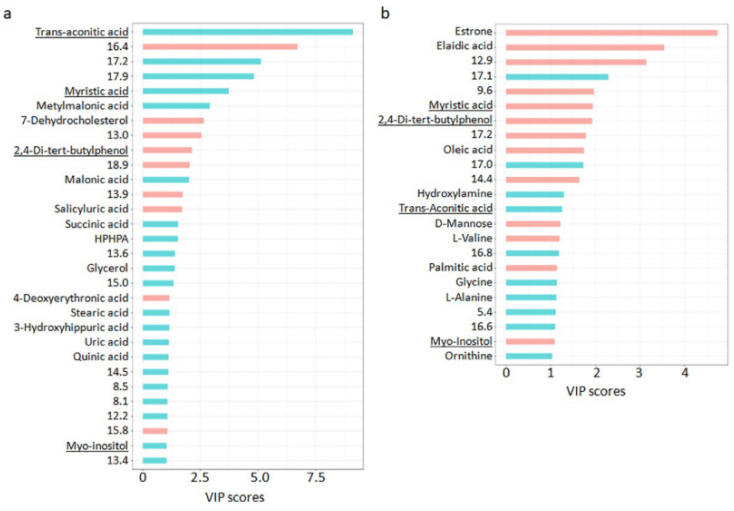

Fig 2. Contribution of metabolites in the separation of AVS cases and controls. The Variable Importance in Projection (VIP) was used to weigh the contribution of urine (a) and plasma (b) metabolomic features to the separation between cases and controls in the PLS-DA model. Data were normalized to the internal standard 2-isopropylmalic acid. Upregulated (blue bars) and downregulated (red bars) features are shown. Metabolites found associated with AVS in both urine and plasma are underlined. Details of metabolite features are given in S3 Table.

https://doi.org/10.1371/journal.pone.0242019.g002

trans-Aconitic acid, myristic acid, methylmalonic acid, 7-Dehydrocholesterol, 2,4-Di-tert-butylphenol, malonic acid, 2-Hydroxyhippuric acid, 3-Hydroxyhippuric acid, succinic acid, glycerol, quinic acid, uric acid, stearic acid, 4-Deoxyerythronic acid, 3-(3-Hydroxyphenyl)-3-Hydroxypropanoic acid (HPHPA) and myo-inositol (**Fig 2A**, **S3 Table**). We included elaidic acid in the list of annotated metabolites even though it is not reported as yet in human urine in the Human Metabolome Database (HMDB).

Results from association analysis to AVS were generally conserved when urine metabolomic data were normalized to creatinine (**S4 Table**). The metabolites salicyluric acid (2-Hydroxyhippuric acid), myo-inositol, glycerol, 4-Deoxyerythronic acid, uric acid and two unknown metabolites at RT 8.1 and 15.8mins were associated to AVS only following normalization to the internal standard. On the other hand, associations between AVS and the metabolites p-Hydroxyphenylacetic acid, palmitic acid, oxoadipic acid, hypoxanthine, estrone, D-Glucose and two unknown metabolites at RT 13.3 and 13.5mins were significant only when data were normalized to creatinine. The remaining metabolites consistently associated to AVS using the two normalization procedures showed similar VIP, similar magnitude and direction of changes between AVS and controls and consistent magnitude statistical significance of association. Strong conservation of our results derived through two different normalization methods underlines the robustness of our findings.

Among the plasma metabolic features significantly contributing to the separation between AVS and controls, 14 could be attributed to known metabolites (elaidic acid, palmitic acid, oleic acid, myristic acid, trans-Aconitic acid, D-Mannose, estrone, L-Alanine, L-Valine, myo-inositol, ornithine, hydroxylamine, 2,4-Di-tert-butylphenol, glycine) (**Fig 2B**, **S3 Table**). According to HMDB, 2,4-Di-tert-butylphenol has not been previously reported in human plasma.

In the urine dataset normalized to the internal standard, levels of myristic acid, trans-Aconitic acid, myo-inositol and 2,4-Di-tert-butylphenol were different between AVS patients and controls in both plasma and urine, but myristic acid and myo-inositol showed discordant direction of changes in the two biofluids. In addition when urine metabolomic data were normalized to creatinine, estrone and palmitic acid also showed opposite direction of changes in AVS in plasma and urine.

Biofluid metabolomic profiling data suggest novel candidate metabolite biomarkers for AVS

The performance of each urine and plasma candidate metabolite to separate AVS cases and controls was evaluated by ROC curve analysis (**S2 and S3 Figs**). AUC values with their p-values and FC for each urine and plasma metabolite associated with AVS are summarized in **S3 Table**. The majority of potential metabolite biomarkers showed good to excellent (AUC>0.8) discriminant capability. In urine, trans-Aconitic acid, myristic acid, methylmalonic acid, 7-Dehydrocholesterol, 2,4-Di-tert-butylphenol, succinic acid, malonic acid were excellent potential biomarkers (AUC = 0.90–1.00). The known metabolites 3-(3-Hydroxyphenyl)-3-Hydroxypropanoic acid (HPHPA), quinic acid, 4-Deoxyerythronic acid and uric acid were good potential biomarkers (AUC = 0.80–0.90). The remaining candidates (2-Hydroxyhippuric acid, 3-Hydroxyhippuric acid, stearic acid, glycerol, and myo-inositol) were fair biomarkers (AUC = 0.7–0.8) (**S3 Table**).

Excellent potential plasma biomarkers showing AUC above 0.90 include elaidic acid, estrone, palmitic acid, myristic acid, 2,4-Di-tert-butylphenol, oleic acid and myo-inositol. Glycine, hydroxylamine, trans-Aconitic acid, L-Alanine and L-Valine were good biomarkers (AUC = 0.80–0.90), whereas ornithine and D-Mannose were not considered as good biomarkers (**S3 Table**).

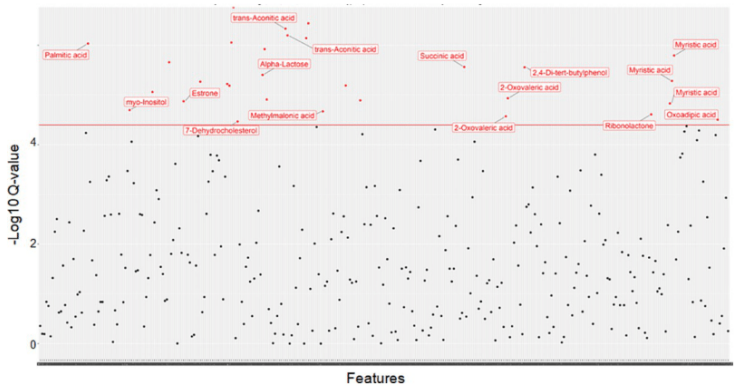

Fig 3. Association analysis of urine GC-MS spectral data in AVS patients and control individuals. Data were derived by GC-MS analysis of urine samples from 46 patients and 46 controls. Generalized linear models were used to determine significant associations between metabolomic peaks and AVS after adjusting for age, sex, body mass index, hyperlipidemia and diabetes, and correcting for multiple testing. Signal intensities normalized to the internal standard 2-isopropylmalic acid are plotted against the Q-values. Features showing evidence of statistically significant association with AVS (q values<0.05) are shown with red dots.

https://doi.org/10.1371/journal.pone.0242019.g003

These analyses also pointed to GC-MS signals associated with AVS that correspond to unknown metabolites in urine (n = 9) and plasma (n = 9) and show fair to excellent capacity to separate AVS patients to control individuals.

Statistical association of urine and plasma GC-MS features identifies metabolites underlying AVS risk

Following adjustment for age, sex, BMI, hyperlipidemia and diabetes, we identified statistically significant associations between AVS and 30 features in urine (Fig 3) and 35 features in plasma (Fig 4). In several instances, several independent features were attributed to a single metabolite. Among these features, 14 urine metabolites and 15 plasma metabolites could be identified based on available information in the NIST08 data repository (**Tables 2 and 3**). Urine

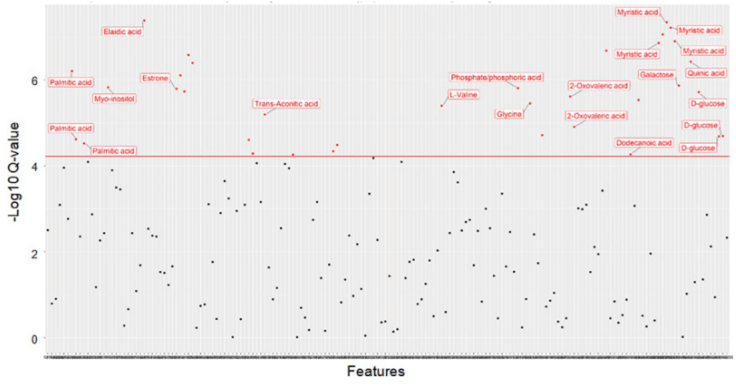

Fig 4. Association analysis of plasma GC-MS spectral data in AVS patients and control individuals. Data were derived by GC-MS analysis of plasma samples from 46 patients and 46 controls. Generalized linear models were used to determine significant associations between metabolomic peaks and AVS after adjusting for age, sex, body mass index, hyperlipidemia and diabetes, and correcting for multiple testing. Signal intensities normalized to the internal standard 2-isopropylmalic acid are plotted against the Q-values. Features showing evidence of statistically significant association with AVS (q values<0.05) are shown with red dots.

https://doi.org/10.1371/journal.pone.0242019.g004

Table 2. Urinary metabolites contributing to the separation between the AVS patients and healthy controls.

		Normalization internal standard				Normalization creatinine				Regulation
Metabolite	**RT**	**q-value**	**RC**	**CI 2.5**	**CI 97.5**	**q-value**	**RC**	**CI 2.5**	**CI 97.5**	**in AVS**
Methylmalonic acid	2.7	0.0301	4.78	2.78	7.24	NS	-	-	-	Positive
Unknown	3.4	0.0183	4.98	3.10	7.66	0.0099	9.95	6.25	15.1	Positive
Unknown	3.5	NS	-	-	-	0.0291	5.41	3.20	8.24	Positive
Succinic acid	5.5	0.0040	4.82	3.02	7.10	0.0273	6.88	4.06	10.44	Positive
4-Deoxyerythronic acid	6.3	NS	-	-	-	0.0384	4.15	2.41	6.35	Positive
2-Oxovaleric acid	6.8	0.0376	3.83	2.22	5.82	0.0131	7.50	4.51	11.21	Positive
Unknown	7.1	NS	-	-	-	0.0382	6.94	4.05	10.63	Positive
2,4-Di-tert-butylphenol	7.3	0.0041	-2.15	-3.27	-1.41	0.0009	-5.52	-8.02	-3.61	Negative
Erythronic acid	7.4	NS	-	-	-	0.0372	3.29	1.90	5.02	Positive
Unknown	7.9	NS	-	-	-	0.0388	4.07	2.36	6.23	Positive
2-Deoxypentonic acid	8.2	NS	-	-	-	0.0346	5.61	3.30	8.58	Positive
D-Fructose	8.3	NS	-	-	-	0.0342	5.07	2.98	7.75	Positive
Unknown	8.5	NS	-	-	-	0.0291	6.46	3.78	9.79	Positive
Ribonolactone	9.1	0.0343	1.40	0.82	2.13	0.0289	8.84	5.34	13.62	Positive
Myristic acid	9.4	0.0209	3.91	2.41	6.01	0.0111	4.69	2.97	7.16	Positive
HPHPA	9.5	NS	-	-	-	0.0153	5.84	3.58	8.88	Positive
Quinic acid	9.7	NS	-	-	-	0.008	3.94	2.40	5.83	Positive
Oxoadipic acid	9.84	0.0439	5.42	3.11	8.27	0.0468	7.37	4.22	11.28	Positive
Palmitic acid	10.6	0.0014	5.88	3.84	8.64	0.0048	8.07	5.04	11.93	Positive
Myo-inositol	11.1	0.0284	7.57	4.53	11.59	NS	-	-	-	Positive
Elaidic acid	11.7	0.0125	7.24	4.44	10.92	0.0251	7.36	4.33	11.13	Positive
Stearic acid	11.8	NS	-	-	-	0.048	8.32	4.82	12.80	Positive
Unknown	12.2	0.0032	3.24	2.07	4.80	NS	-	-	-	Positive
D-Glucose	12.4	NS	-	-	-	0.0186	4.86	2.93	7.37	Positive
Unknown	12.5	NS	-	-	-	0.0206	5.38	3.18	8.10	Positive
Estrone	12.7	0.0190	3.40	2.11	5.22	0.0234	8.55	5.13	13.03	Positive
Unknown	13	0.0079	-1.58	-2.44	-1.02	0.0109	-4.47	-6.79	-2.78	Negative
Unknown	13.3	NS	-	-	-	0.0057	4.83	2.98	7.13	Positive
Unknown	13.4	NS	-	-	-	0.031	4.29	2.54	6.57	Positive
Unknown	13.5	0.0087	1.74	1.05	2.58	0.01	6.10	3.72	9.12	Positive
Unknown	13.6	0.0094	5.02	3.23	7.75	0.006	6.75	4.29	10.17	Positive
7-Dehydrocholesterol	14	0.0475	-0.77	-1.17	-0.43	NS	-	-	-	Negative
Unknown	14.1	NS	-	-	-	0.031	5.89	3.50	9.02	Positive
Alpha-Lactose	14.4	0.0058	4.21	2.69	6.35	0.0224	11.95	7.44	18.58	Positive
Unknown	14.5	0.0018	4.16	2.67	6.08	0.0074	6.48	4.03	9.68	Positive
Trans-Aconitic acid	15.2	0.0007	1.57	1.05	2.30	0.0015	3.28	2.15	4.86	Positive
Unknown	16.4	0.0011	-1.23	-1.85	-0.83	0.0012	-4.11	-6.13	-2.74	Negative
Unknown	20.3	0.0094	-2.00	-2.98	-1.22	NS	-	-	-	Negative

Data were derived by GC-MS analysis of urine samples from 46 patients and 46 controls. P-values were adjusted for age, sex, body mass index, hyperlipidemia and diabetes. Data are shown for urine metabolomic signals normalized to either the internal standard 2-isopropylmalic acid or creatinine. The regression coefficient (RC) illustrates the magnitude of the statistical effect on the increased or decreased concentration of the metabolites in AVS patients. RT, Retention Time; CI, Confidence Interval. Positive and negative regulation indicates up- and down-regulation of the metabolic features in AVS patients, respectively. HPHPA, 3-(3-Hydroxyphenyl)-3-hydroxypropanoic acid.

https://doi.org/10.1371/journal.pone.0242019.t002

Table 3. Plasma metabolites contributing to the separation between the AVS patients and healthy controls.

Metabolite	RT	q-value	Regression coefficient	CI 2.5	CI 97.5	Regulation in AVS
L-Valine	4.4	0.0035	-0.77	-1.14	-0.48	Negative
Phosphate/phosphoric acid	5.1	0.0014	-1.81	-2.64	-1.14	Negative
Glycine	5.2	0.0031	0.91	0.56	1.34	Positive
Unknown	5.4	0.0167	2.08	1.27	3.21	Positive
2-Oxovaleric acid	6.8	0.0021	-1.86	-2.74	-1.17	Negative
2,4-Di-tert-butylphenol	7.3	0.0002	-0.98	-1.40	-0.65	Negative
Dodecanoic acid	8.0	0.0452	-1.12	-1.71	-0.61	Negative
Unknown	8.4	0.0026	-1.37	-2.01	-0.85	Negative
Myristic acid	9.4	0.0001	-0.80	-1.13	-0.53	Negative
Galactose	9.5	0.0012	-0.82	-1.20	-0.52	Negative
Quinic acid	9.7	0.0004	-0.89	-1.30	-0.59	Negative
D-Glucose	9.9	0.0176	4.62	2.73	7.03	Positive
Palmitic acid	10.6	0.0006	-1.71	-2.50	-1.13	Negative
Myo-inositol	11.1	0.0013	-1.22	-1.78	-0.78	Negative
Elaidic acid	11.7	<0.001	-0.93	-1.30	-0.63	Negative
Estrone	12.7	0.0014	-0.66	-1.01	-0.44	Negative
Unknown	12.9	0.0007	-0.68	-1.00	-0.44	Negative
Unknown	14.5	0.0211	-0.48	-0.74	-0.28	Negative
Trans-Aconitic acid	15.2	0.0056	0.90	0.55	1.34	Positive
Unknown	16.9	0.0455	0.63	0.35	0.97	Positive
Unknown	17.2	0.0382	-0.33	-0.50	-0.18	Negative

Data were derived by GC-MS analysis of plasma samples from 46 patients and 46 controls. P-values were adjusted for age, sex, body mass index, hyperlipidemia and diabetes. The regression coefficient illustrates the magnitude of the statistical effect on the increased or decreased concentration of the metabolites in AVS patients. RT, Retention Time; CI, Confidence Interval. Positive and negative regulation indicates up- and down-regulation of the metabolic features in AVS patients, respectively.

https://doi.org/10.1371/journal.pone.0242019.t003

metabolites significantly associated with AVS included myristic acid, palmitic acid, methylmalonic acid, succinic acid, 2-Oxovaleric acid, elaidic acid, ribonolactone, oxoadipic acid, myo-inositol, estrone, α-lactose, trans-Aconitic acid, 7-Dehydrocholesterol and 2,4-Di-tert-butylphenol (Table 2). With the exception of methylmalonic acid, myo-inositol, 7-Dehydrocholesterol and two unknown metabolites at RT 12.2 and 20.3mins, statistically significant associations between AVS and urine metabolites were replicated when metabolomic data normalized to creatinine were used for statistical analysis (Table 2). Normalization of urine data to creatinine allowed the identification of several additional associations between AVS and metabolites, including 4-Deoxyerythronic acid, erythronic acid, 2-Deoxypentonic acid, D-Fructose, HPHPA, quinic acid, stearic acid, D-Glucose, 7-Dehydrocholesterol and nine unknown metabolites (Table 2).

We identified statistically significant associations between plasma features and AVS for glycine, D-Glucose, trans-Aconitic acid, myristic acid, palmitic acid, elaidic acid, L-Valine, 2,4-Di-tert-butylphenol, phosphoric acid, 2-Oxovaleric acid, dodecanoic acid, quinic acid, galactose, myo-inositol and estrone (Table 3).

AVS patients showed significantly elevated urinary concentrations of myristic acid, trans-Aconitic acid, methylmalonic acid, 2-Oxovaleric acid, oxoadipic acid, palmitic acid, elaidic acid, α-lactose, estrone, ribonolactone, succinic acid and myo-inositol (Fig 5, Table 2). By contrast, urine concentration of the remaining metabolites (2,4-Di-tert-butylphenol and 7-Dehydrocholesterol) were lower in AVS patients than in controls. Plasma concentration of the saturated fatty acids myristic acid and palmitic acid, dodecanoic acid, the unsaturated fatty

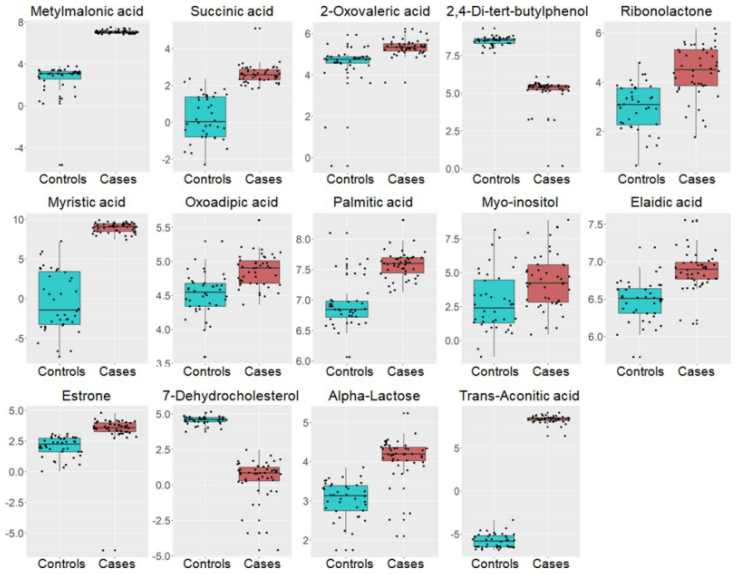

Fig 5. Regulatory pattern of urine metabolites associated with AVS in patients and control individuals. Data from urine candidate metabolites in the 46 AVS cases (orange boxes) and 46 controls (blue boxes) are shown. Data are normalized to the internal standard (2-isopropylmalic acid) and log transformed. The boxplots show the median and the inter-quartile range for each metabolite in the two groups.

https://doi.org/10.1371/journal.pone.0242019.g005

acid elaidic acid, the essential amino acid L-Valine, estrone, phosphoric acid, 2-Oxovaleric acid, quinic acid, 2,4-Di-tert-butylphenol, myo-inositol and galactose were significantly lower in AVS patients than in controls (Fig 6, Table 3). In contrast, plasma concentration of the

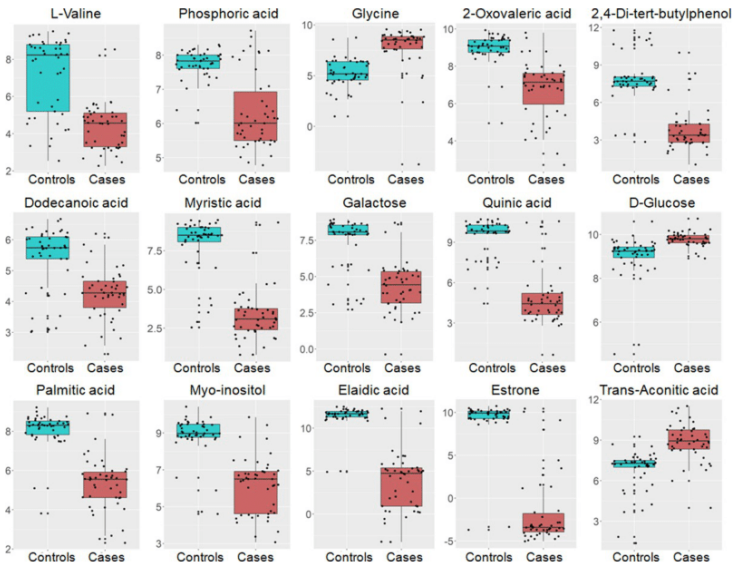

Fig 6. Regulatory pattern of plasma metabolites associated with AVS in patients and control individuals. Data from plasma candidate metabolites in the 46 AVS cases (orange boxes) and 46 controls (blue boxes) are shown. Data are normalized to the internal standard (2-isopropylmalic acid) and log transformed. The boxplots show the median and the inter-quartile range for each metabolite in the two groups.

https://doi.org/10.1371/journal.pone.0242019.g006

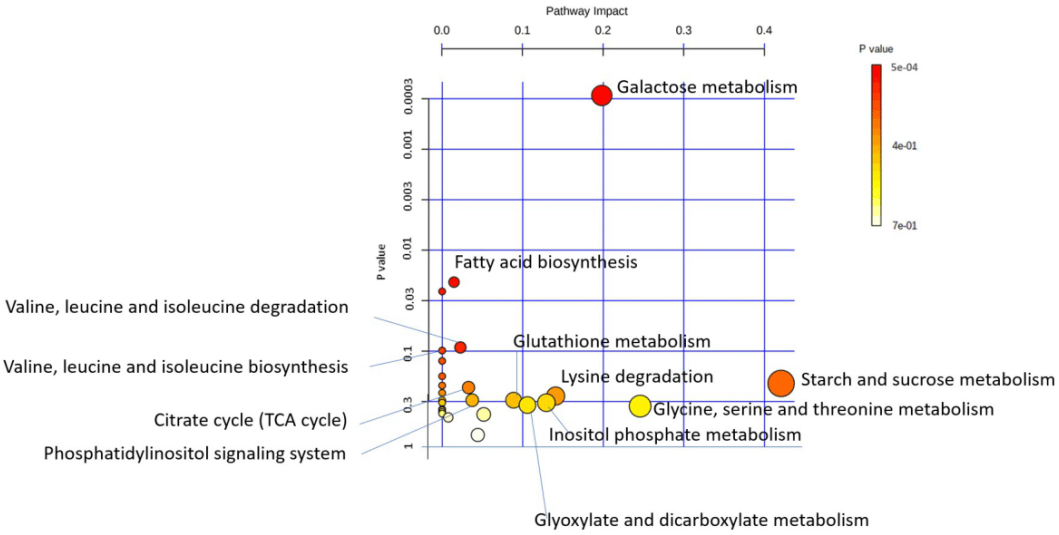

Fig 7. Pathway analysis of metabolites associated with AVS. Outputs of urine and plasma metabolomic profiling in AVS patients and control subjects were used to identify changes in biological pathways in the human Kyoto Encyclopedia of Genes and Genomes (KEGG, www.genome.jp/kegg) using the MetaboAnalyst web-tool (www.metaboanalyst.ca). Data are plotted to illustrate the most significantly altered pathways in terms of p-values derived from hypergeometric test on the vertical axis and impact on the horizontal axis.

https://doi.org/10.1371/journal.pone.0242019.g007

amino acid glycine, D-Glucose and trans-Aconitic acid were higher in AVS patients than in controls (Fig 6, Table 3). Interestingly, evidence of replicated association to AVS in both urine and plasma was observed for a series of 9 metabolites (myristic acid, trans-Aconitic acid, palmitic acid, estrone, 2-Oxovaleric acid, elaidic acid, 2,4-Di-tert-butylphenol, myo-inositol, quinic acid and an unknown metabolite at RT 14.5mins) (**Tables 2 and 3**). However, only 2,4-Di-tert-butylphenol and trans-Aconitic acid displayed concordant pattern of up- or down-regulation in the two biofluids in AVS patients.

Fatty acid biosynthesis and galactose metabolism are altered in AVS

To elucidate the biological relevance of metabolites associated with AVS, we carried out pathway analysis using data from urine and plasma metabolites associated with AVS. These metabolites are involved in 28 pathways in KEGG. The most significant pathways underlying AVS risk were the metabolism of galactose (α-lactose, galactose, glucose, myo-inositol) ($p = 0.0003$; FDR $p = 0.025$), the biosynthesis of fatty acids and, to a lesser extent, the metabolism of branched chain amino acids (valine, leucine, isoleucine) (Fig 7). The metabolism of starch and sucrose and the metabolism of glycine, serine and threonine were also detected.

Discussion

We report results from paralleled untargeted metabolomic profile analyses of urine and plasma in a cohort of patients with AVS and control subjects that identified individual metabolites, metabolite patterns and biological pathways underlying disease risk. Known and unknown metabolites showed biofluid-specific changes between AVS and control individuals or either conserved or discordant regulation patterns in the two biofluids. Our data provide a solid foundation for the definition of metabolites and biological pathways that may be used as potential biomarkers for AVS diagnosis and prevention, as well as targets for therapeutic applications.

Metabolomic profiling is a powerful hypothesis-free strategy that we applied to the identification of a repository of unknown and known urine and plasma metabolites associated with AVS. Several of these associations concern individual metabolites that show evidence of pathophysiological relevance to heart diseases and therefore potentially to AVS. Metabolomic studies have shown that plasma levels of glycine and myo-inositol are increased in patients with heart failure [20]. Elevated plasma myo-inositol was also reported in primary dilated cardiomyopathy [21] and in a preclinical model of myocardial infarction [22]. Elaidic acid is an unsaturated trans-fatty acid, which was found elevated in the serum of patients with coronary artery disease and positively associated with LDL-cholesterol and triglyceride [23, 24].

Biological pathway analysis pointed to fatty acid metabolism as a prominent mechanism associated with AVS in our study. The underlying metabolites that are the most relevant to cardiovascular diseases were the saturated fatty acids dodecanoic, myristic, stearic and palmitic acids and the unsaturated trans fatty acid elaidic acid. Examples of dietary sources of these fatty acids are hydrogenated vegetable oils (elaidic acid), palm oil, meats, cheeses, butter and dairy products (palmitic acid), animal and vegetable fats, coconut and nutmeg oils (myristic acid). Palmitic acid can also be synthesized in the liver through fatty acid biosynthesis or elongation from myristic acid in the mitochondria. Fatty acids are central to the function of the heart since 50 to 70% of its energy is produced by mitochondrial fatty acid β-oxidation [25]. Epidemiological studies and clinical trials have suggested an association between the intake of saturated fatty acids and the risk of coronary heart disease (CHD) [26–28], even though this link remains contested [29]. For instance, the intake of palmitic, stearic and elaidic acids was correlated to the progression of CHD [30] and was associated with a 9–24% increased risk of CHD [31]. Reducing the dietary palmitic and myristic acid decreased the risk for CHD [32], whereas high consumption of myristic acid was correlated with high mortality due to CHD [33], presumably through the effect of myristic, palmitic and stearic acids on increased platelet aggregation [34]. Palmitic, dodecanoic and myristic acids are the major cholesterol-raising saturated fatty acids [35] and diets rich in these metabolites result in high LDL-cholesterol level and low HDL/LDL cholesterol [36]. Plasma levels of myristic acid are negatively associated with HDL-cholesterol in a population characterized with obesity and metabolic syndrome [37]. These fatty acids may therefore contribute to AVS in our study through their role in lowering HDL and increasing LDL-cholesterol levels [38]. The lack of association between AVS and fatty acids despite non-significant differences in lipoprotein levels between cases and controls may be explained by the treatment of many patients with lipid lowering medications (statins).

Paralleled metabolomic analysis of plasma and urine samples provides information about biofluid-specific changes in AVS. It also identifies conserved associations of metabolites to AVS in the two biofluids, which may suggest dysregulation in relevant biological pathways and allows prediction of the level of plasma metabolites based on their urine concentration in patients. Intriguingly, over 75% of GC-MS features and over 80% of known metabolites associated with AVS were up-regulated in urine and downregulated in plasma. In addition, even though the level of half of these known metabolites was different between patients and controls in both plasma and urine, they were almost all upregulated in urine and downregulated in plasma in the AVS group, suggesting a stimulation of their elimination in urine of patients. Only 2,4-Di-tert-butylphenol and trans-Aconitic acid (TAA) displayed consistent trend of regulation in the two biofluids.

2,4-Di-tert-butylphenol is a lipophilic phenol present in the environment and a product of bacterial metabolism [39]. It shows antioxidant properties against LDL-oxidation [40], thus potentially preventing atherosclerosis, and anti-inflammatory properties by decreasing the expression of TNF-α, interleukins *IL-6* and *IL-1b* in a mouse macrophage cell line [41]. TAA is

an unsaturated tricarboxylic acid and an isomer of the tricarboxylic acid cycle intermediate cis-Aconitic acid. TAA is mainly obtained from the sugar cane molasses [42] and is also metabolized by bacteria [43]. Metabolomic studies in humans indicated that the isomer cis-Aconitic acid is downregulated in the plasma of patients with CHD [44] and that aconitic acid is a marker of myocardial injury [45]. These data support a role of 2,4-Di-tert-butylphenol and TAA in AVS, which requires experimental validation.

Conclusions

Our findings provide initial evidence of candidate metabolite biomarkers of AVS and raise novel hypotheses regarding their contribution to the disease and the relevant pathophysiological mechanisms involved. Many metabolites associated with AVS in our study are involved in biological pathways that do not have obvious relevance to heart diseases, and therefore open new research avenues to test their implication in AVS etiopathogenesis. In addition, several urine and plasma metabolomic features associated with AVS remain unknown and require chemical attribution for unambiguous identification of the underlying metabolites. Further investigations are warranted to replicate association between metabolites and AVS in larger population studies. In addition, future work is required to determine whether the candidate metabolites identified affect aortic valve either directly or indirectly through factors known to contribute to AVS risk, including for example cholesterol metabolism and Lpa. We have verified that metabolites associated with AVS do not show evidence of significant association with plasma LDL and HDL (**S4 Fig**). Along the same line, changes in these metabolites may be reactive to AVS pathology and drug treatments. Assessment of causal relationships between the candidate metabolites that we have identified and AVS can be tested through extended genetic association analyses and application of Mendelian randomization methods in large genetic studies.

Supporting information

S1 Table. Clinical and biochemical features in males and females selected for presence or absence of aortic valve stenosis. Data are means ± SEM.
(DOCX)

S2 Table. Metabolites identified using the NIST08 library (https://chemdata.nist.gov/) after analysis of gas chromatography mass spectrometry (GC-MS) of urine and plasma samples of patients with aortic valve stenosis and controls. RT, Retention Time; HMDB, Human Metabolome Database; KEGG, Kyoto Encyclopedia of Genes and Genomes.
(XLSX)

S3 Table. Urinary and plasma metabolites contributing to the separation between the AVS patients and healthy controls. Data were derived by GC-MS analysis of urine and plasma samples from 46 patients and 46 controls. Data were normalized to the internal standard 2-isopropylmalic acid. Variable importance in the projection (VIP) was obtained from PLS-DA with a threshold of 1.0; p-values are calculated from a volcano plot; q-values are the adjusted p-value with Benjamini-Hochberg method. Area Under the Curve (AUC) was calculated using the online tool MetaboAnalyst to determine biomarker utility. Regulation gives information on up- or down-regulation of the features in AVS patients. RT, Retention time; FDR, False Discovery Rate.
(XLSX)

S4 Table. Urinary metabolites contributing to the separation between the AVS patients and controls. Data were derived by GC-MS analysis of urine samples from 46 patients and 46

controls. Data were normalized to creatinine and logTranformed. Variable importance in the projection (VIP) was obtained from PLS-DA with a threshold of 1.0; q-values are the adjusted p-value with Benjamini-Hochberg method. Regulation gives information on up- or down-regulation of the features in AVS patients. RT, Retention time; FDR, False Discovery Rate.
(XLSX)

S5 Table. Urine metabolic fingerprint of AVS patients and healthy controls. Intensity values derived by GC-MS analysis of urine samples in AVS cases and controls were normalized to the internal standard 2-isopropylmalic acid.
(XLSX)

S6 Table. Plasma metabolic fingerprint of AVS patients and healthy controls. Intensity values derived by GC-MS analysis of plasma samples in AVS cases and controls were normalized to the internal standard 2-isopropylmalic acid.
(XLSX)

S1 Fig. Validation of the OPLS-DA model of biofluid metabolomic data from patients with aortic valve stenosis (AVS) and control individuals. Data were derived from GC-MS spectra of urine (a, b) and plasma (c, d) samples from AVS patients (n = 46) and control individuals (n = 46). Model validation was performed using permutation test with 1000 iterations on the OPLS-DA model. Empirical p-values Q2: $p<0.001$ and R2Y: $p<0.001$.
(TIF)

S2 Fig. ROC analysis of candidate urine metabolites separating AVS patients and control individuals. Each of the 16 candidate metabolites (VIP>1, nominal $p<0.05$, $q<0.05$) has a ROC curve where the sensitivity is on the y-axis and the specificity is on the x-axis. The AUROC is shown in blue and the AUC values with their 95% confidence intervals are presented in the curves.
(TIF)

S3 Fig. ROC analysis of candidate plasma metabolites separating AVS patients and control individuals. Each of the 14 candidate metabolites (VIP>1, nominal $p<0.05$, $q<0.05$) has a ROC curve where the sensitivity is on the y-axis and the specificity is on the x-axis. The AUROC is shown in blue and the AUC values with their 95% confidence intervals are presented in the curves.
(TIF)

S4 Fig. Association analysis of plasma GC-MS spectral data with HDL and LDL in patients and controls. Data were derived by GC-MS analysis of plasma samples from 46 AVS patients and 46 control individuals. Generalized linear models were used to determine significant associations between metabolomic peaks and HDL (a) and LDL (b) and correcting for multiple testing. Signal intensities normalized to the internal standard are plotted against the Q-values.
(TIF)

Author Contributions

Conceptualization: Rony S. Khnayzer, Dominique Gauguier, Pierre A. Zalloua.

Data curation: Georges Khazen, Dominique Gauguier.

Formal analysis: Cynthia Al Hageh, Ryan Rahy, Georges Khazen, Francois Brial.

Funding acquisition: Rony S. Khnayzer, Dominique Gauguier, Pierre A. Zalloua.

Investigation: Cynthia Al Hageh, Francois Brial.

Methodology: Dominique Gauguier.

Resources: Rony S. Khnayzer, Pierre A. Zalloua.

Supervision: Rony S. Khnayzer, Dominique Gauguier, Pierre A. Zalloua.

Writing – original draft: Dominique Gauguier, Pierre A. Zalloua.

References

1. Sherwood MW, Kiefer TL. Challenges in Aortic Valve Stenosis: Low-Flow States Diagnosis, Management, and a Review of the Current Literature. Curr Cardiol Rep. 2017; 19(12):130. Epub 2017/10/30. https://doi.org/10.1007/s11886-017-0941-z PMID: 29086035.
2. Otto CM, Prendergast B. Aortic-valve stenosis—from patients at risk to severe valve obstruction. N Engl J Med. 2014; 371(8):744–56. https://doi.org/10.1056/NEJMra1313875 PMID: 25140960.
3. Nkomo VT, Gardin JM, Skelton TN, Gottdiener JS, Scott CG, Enriquez-Sarano M. Burden of valvular heart diseases: a population-based study. Lancet. 2006; 368(9540):1005–11. https://doi.org/10.1016/S0140-6736(06)69208-8 PMID: 16980116.
4. Marquis-Gravel G, Redfors B, Leon MB, Généreux P. Medical Treatment of Aortic Stenosis. Circulation. 2016; 134(22):1766–84. https://doi.org/10.1161/CIRCULATIONAHA.116.023997 PMID: 27895025.
5. Joseph J, Naqvi SY, Giri J, Goldberg S. Aortic Stenosis: Pathophysiology, Diagnosis, and Therapy. Am J Med. 2017; 130(3):253–63. Epub 2016/11/01. https://doi.org/10.1016/j.amjmed.2016.10.005 PMID: 27810479.
6. Yu B, Khan K, Hamid Q, Mardini A, Siddique A, Aguilar-Gonzalez LP, et al. Pathological significance of lipoprotein(a) in aortic valve stenosis. Atherosclerosis. 2018; 272:168–74. Epub 2018/03/15. https://doi.org/10.1016/j.atherosclerosis.2018.03.025 PMID: 29614432.
7. Nicholson JK, Connelly J, Lindon JC, Holmes E. Metabonomics: a platform for studying drug toxicity and gene function. Nat Rev Drug Discov. 2002; 1(2):153–61. https://doi.org/10.1038/nrd728 PMID: 12120097.
8. Barouki R, Audouze K, Coumoul X, Demenais F, Gauguier D. Integration of the human exposome with the human genome to advance medicine. Biochimie. 2018; 152:155–8. Epub 2018/06/28. https://doi.org/10.1016/j.biochi.2018.06.023 PMID: 29960033.
9. Holmes E, Wilson ID, Nicholson JK. Metabolic phenotyping in health and disease. Cell. 2008; 134(5):714–7. https://doi.org/10.1016/j.cell.2008.08.026 PMID: 18775301.
10. Holmes E, Loo RL, Stamler J, Bictash M, Yap IK, Chan Q, et al. Human metabolic phenotype diversity and its association with diet and blood pressure. Nature. 2008; 453(7193):396–400. https://doi.org/10.1038/nature06882 PMID: 18425110.
11. Elliott P, Posma JM, Chan Q, Garcia-Perez I, Wijeyesekera A, Bictash M, et al. Urinary metabolic signatures of human adiposity. Sci Transl Med. 2015; 7(285):285ra62. https://doi.org/10.1126/scitranslmed.aaa5680 PMID: 25925681.
12. Wang Z, Klipfell E, Bennett BJ, Koeth R, Levison BS, Dugar B, et al. Gut flora metabolism of phosphatidylcholine promotes cardiovascular disease. Nature. 2011; 472(7341):57–63. https://doi.org/10.1038/nature09922 PMID: 21475195; PubMed Central PMCID: PMC3086762.
13. Hager J, Kamatani Y, Cazier JB, Youhanna S, Ghassibe-Sabbagh M, Platt DE, et al. Genome-wide association study in a Lebanese cohort confirms PHACTR1 as a major determinant of coronary artery stenosis. PLoS One. 2012; 7(6):e38663. https://doi.org/10.1371/journal.pone.0038663 PMID: 22745674; PubMed Central PMCID: PMC3380020.
14. Cheng Y, Xie G, Chen T, Qiu Y, Zou X, Zheng M, et al. Distinct urinary metabolic profile of human colorectal cancer. J Proteome Res. 2012; 11(2):1354–63. Epub 2011/12/28. https://doi.org/10.1021/pr201001a PMID: 22148915.
15. Ikeda A, Nishiumi S, Shinohara M, Yoshie T, Hatano N, Okuno T, et al. Serum metabolomics as a novel diagnostic approach for gastrointestinal cancer. Biomed Chromatogr. 2012; 26(5):548–58. Epub 2011/07/20. https://doi.org/10.1002/bmc.1671 PMID: 21773981.
16. Fiehn O. Metabolomics by Gas Chromatography-Mass Spectrometry: Combined Targeted and Untargeted Profiling. Curr Protoc Mol Biol. 2016; 114:30.4.1–.4.2. Epub 2016/04/01. https://doi.org/10.1002/0471142727.mb3004s114 PMID: 27038389; PubMed Central PMCID: PMC4829120.

17. Cloarec O, Dumas ME, Craig A, Barton RH, Trygg J, Hudson J, et al. Statistical total correlation spectroscopy: an exploratory approach for latent biomarker identification from metabolic 1H NMR data sets. Anal Chem. 2005; 77(5):1282–9. https://doi.org/10.1021/ac048630x PMID: 15732908.

18. Benjamini Y, Hochberg Y. Controlling the false discovery rate: a practical and powerful approach to multiple testing. J R Stat Soc. 1995; 57(1):289–300.

19. Xia J, Broadhurst DI, Wilson M, Wishart DS. Translational biomarker discovery in clinical metabolomics: an introductory tutorial. Metabolomics. 2013; 9(2):280–99. Epub 2012/12/04. https://doi.org/10.1007/s11306-012-0482-9 PMID: 23543913; PubMed Central PMCID: PMC3608878.

20. Deidda M, Piras C, Dessalvi CC, Locci E, Barberini L, Torri F, et al. Metabolomic approach to profile functional and metabolic changes in heart failure. J Transl Med. 2015; 13:297. Epub 2015/09/12. https://doi.org/10.1186/s12967-015-0661-3 PMID: 26364058; PubMed Central PMCID: PMC4567812.

21. Alexander D, Lombardi R, Rodriguez G, Mitchell MM, Marian AJ. Metabolomic distinction and insights into the pathogenesis of human primary dilated cardiomyopathy. Eur J Clin Invest. 2011; 41(5):527–38. Epub 2010/12/14. https://doi.org/10.1111/j.1365-2362.2010.02441.x PMID: 21155767; PubMed Central PMCID: PMC3071865.

22. McKirnan MD, Ichikawa Y, Zhang Z, Zemljic-Harpf AE, Fan S, Barupal DK, et al. Metabolomic analysis of serum and myocardium in compensated heart failure after myocardial infarction. Life Sci. 2019; 221:212–23. Epub 2019/02/05. https://doi.org/10.1016/j.lfs.2019.01.040 PMID: 30731143; PubMed Central PMCID: PMC6445392.

23. Mori K, Ishida T, Yasuda T, Hasokawa M, Monguchi T, Sasaki M, et al. Serum Trans-Fatty Acid Concentration Is Elevated in Young Patients With Coronary Artery Disease in Japan. Circ J. 2015; 79 (9):2017–25. Epub 2015/07/13. https://doi.org/10.1253/circj.CJ-14-0750 PMID: 26166015.

24. Oshita T, Toh R, Shinohara M, Mori K, Irino Y, Nagao M, et al. Elevated Serum Elaidic Acid Predicts Risk of Repeat Revascularization After Percutaneous Coronary Intervention in Japan. Circ J. 2019; 83 (5):1032–8. Epub 2019/03/13. https://doi.org/10.1253/circj.CJ-18-1175 PMID: 30867359.

25. Lopaschuk GD, Ussher JR, Folmes CD, Jaswal JS, Stanley WC. Myocardial fatty acid metabolism in health and disease. Physiol Rev. 2010; 90(1):207–58. https://doi.org/10.1152/physrev.00015.2009 PMID: 20086077.

26. Virtanen JK, Mursu J, Tuomainen TP, Voutilainen S. Dietary fatty acids and risk of coronary heart disease in men: the Kuopio Ischemic Heart Disease Risk Factor Study. Arterioscler Thromb Vasc Biol. 2014; 34(12):2679–87. Epub 2014/09/25. https://doi.org/10.1161/ATVBAHA.114.304082 PMID: 25256234.

27. Guasch-Ferré M, Babio N, Martínez-González MA, Corella D, Ros E, Martín-Peláez S, et al. Dietary fat intake and risk of cardiovascular disease and all-cause mortality in a population at high risk of cardiovascular disease. Am J Clin Nutr. 2015; 102(6):1563–73. Epub 2015/11/11. https://doi.org/10.3945/ajcn.115.116046 PMID: 26561617.

28. Zhuang P, Zhang Y, He W, Chen X, Chen J, He L, et al. Dietary Fats in Relation to Total and Cause-Specific Mortality in a Prospective Cohort of 521 120 Individuals With 16 Years of Follow-Up. Circ Res. 2019; 124(5):757–68. https://doi.org/10.1161/CIRCRESAHA.118.314038 PMID: 30636521.

29. de Souza RJ, Mente A, Maroleanu A, Cozma AI, Ha V, Kishibe T, et al. Intake of saturated and trans unsaturated fatty acids and risk of all cause mortality, cardiovascular disease, and type 2 diabetes: systematic review and meta-analysis of observational studies. BMJ. 2015; 351:h3978. Epub 2015/08/11. https://doi.org/10.1136/bmj.h3978 PMID: 26268692; PubMed Central PMCID: PMC4532752.

30. Watts GF, Jackson P, Burke V, Lewis B. Dietary fatty acids and progression of coronary artery disease in men. The American Journal of Clinical Nutrition. 1996; 64(2):202–9. https://doi.org/10.1093/ajcn/64.2.202 PMID: 8694021

31. Hu FB, Stampfer MJ, Manson JE, Ascherio A, Colditz GA, Speizer FE, et al. Dietary saturated fats and their food sources in relation to the risk of coronary heart disease in women. The American Journal of Clinical Nutrition. 1999; 70(6):1001–8. https://doi.org/10.1093/ajcn/70.6.1001 PMID: 10584044

32. Ebbesson SOE, Voruganti VS, Higgins PB, Fabsitz RR, Ebbesson LO, Laston S, et al. Fatty acids linked to cardiovascular mortality are associated with risk factors. International Journal of Circumpolar Health. 2015; 74(1):28055. https://doi.org/10.3402/ijch.v74.28055 PMID: 26274054

33. Zong G, Li Y, Wanders AJ, Alssema M, Zock PL, Willett WC, et al. Intake of individual saturated fatty acids and risk of coronary heart disease in US men and women: two prospective longitudinal cohort studies. The BMJ. 2016;355. https://doi.org/10.1136/bmj.i5796 PMID: 27881409

34. Renaud SC. What is the epidemiologic evidence for the thrombogenic potential of dietary long-chain fatty acids? The American Journal of Clinical Nutrition. 1992; 56(4):823S–4S. https://doi.org/10.1093/ajcn/56.4.823s PMID: 1414999

35. Hunter JE, Zhang J, Kris-Etherton PM. Cardiovascular disease risk of dietary stearic acid compared with trans, other saturated, and unsaturated fatty acids: a systematic review. Am J Clin Nutr. 2010; 91 (1):46–63. Epub 2009/11/25. https://doi.org/10.3945/ajcn.2009.27661 PMID: 19939984.

36. Zock PL, de Vries JH, Katan MB. Impact of myristic acid versus palmitic acid on serum lipid and lipoprotein levels in healthy women and men. Arteriosclerosis and Thrombosis: A Journal of Vascular Biology. 1994; 14(4):567–75.

37. Noto D, Fayer F, Cefalù AB, Altieri I, Palesano O, Spina R, et al. Myristic acid is associated to low plasma HDL cholesterol levels in a Mediterranean population and increases HDL catabolism by enhancing HDL particles trapping to cell surface proteoglycans in a liver hepatoma cell model. Atherosclerosis. 2016; 246:50–6. https://doi.org/10.1016/j.atherosclerosis.2015.12.036 PMID: 26756970

38. Siri-Tarino PW, Sun Q, Hu FB, Krauss RM. Saturated fatty acids and risk of coronary heart disease: modulation by replacement nutrients. Current atherosclerosis reports. 2010; 12(6):384–90. https://doi.org/10.1007/s11883-010-0131-6 PMID: 20711693.

39. Zhao F, Wang P, Lucardi RD, Su Z, Li S. Natural Sources and Bioactivities of 2,4-Di-Tert-Butylphenol and Its Analogs. Toxins (Basel). 2020; 12(1). Epub 2020/01/06. https://doi.org/10.3390/toxins12010035 PMID: 31935944; PubMed Central PMCID: PMC7020479.

40. Yoon MA, Jeong TS, Park DS, Xu MZ, Oh HW, Song KB, et al. Antioxidant effects of quinoline alkaloids and 2,4-di-tert-butylphenol isolated from Scolopendra subspinipes. Biol Pharm Bull. 2006; 29(4):735–9. https://doi.org/10.1248/bpb.29.735 PMID: 16595909.

41. Nair RVR, Jayasree DV, Biju PG, Baby S. Anti-inflammatory and anticancer activities of erythrodiol-3-acetate and 2,4-di-tert-butylphenol isolated from Humboldtia unijuga. Nat Prod Res. 2018:1–4. Epub 2018/11/26. https://doi.org/10.1080/14786419.2018.1531406 PMID: 30475646.

42. Montoya G, Londono J, Cortes P, Izquierdo O. Quantitation of trans-Aconitic Acid in Different Stages of the Sugar-Manufacturing Process. Journal of Agricultural and Food Chemistry. 2014; 62(33):8314–8. https://doi.org/10.1021/jf5008874 PMID: 25098840

43. Altekar WW, Rao MRR. MICROBIOLOGICAL DISSIMILATION OF TRICARBALLYLATE AND TRANS-ACONITATE1. Journal of Bacteriology. 1963; 85(3):604–13.

44. Tao T, He T, Wang X, Liu X. Metabolic Profiling Analysis of Patients With Coronary Heart Disease Undergoing Xuefu Zhuyu Decoction Treatment. Frontiers in Pharmacology. 2019;10. https://doi.org/10.3389/fphar.2019.00010 PMID: 30733675

45. Lewis GD, Wei R, Liu E, Yang E, Shi X, Martinovic M, et al. Metabolite profiling of blood from individuals undergoing planned myocardial infarction reveals early markers of myocardial injury. The Journal of Clinical Investigation. 2008; 118(10):3503–12. https://doi.org/10.1172/JCI35111 PMID: 18769631

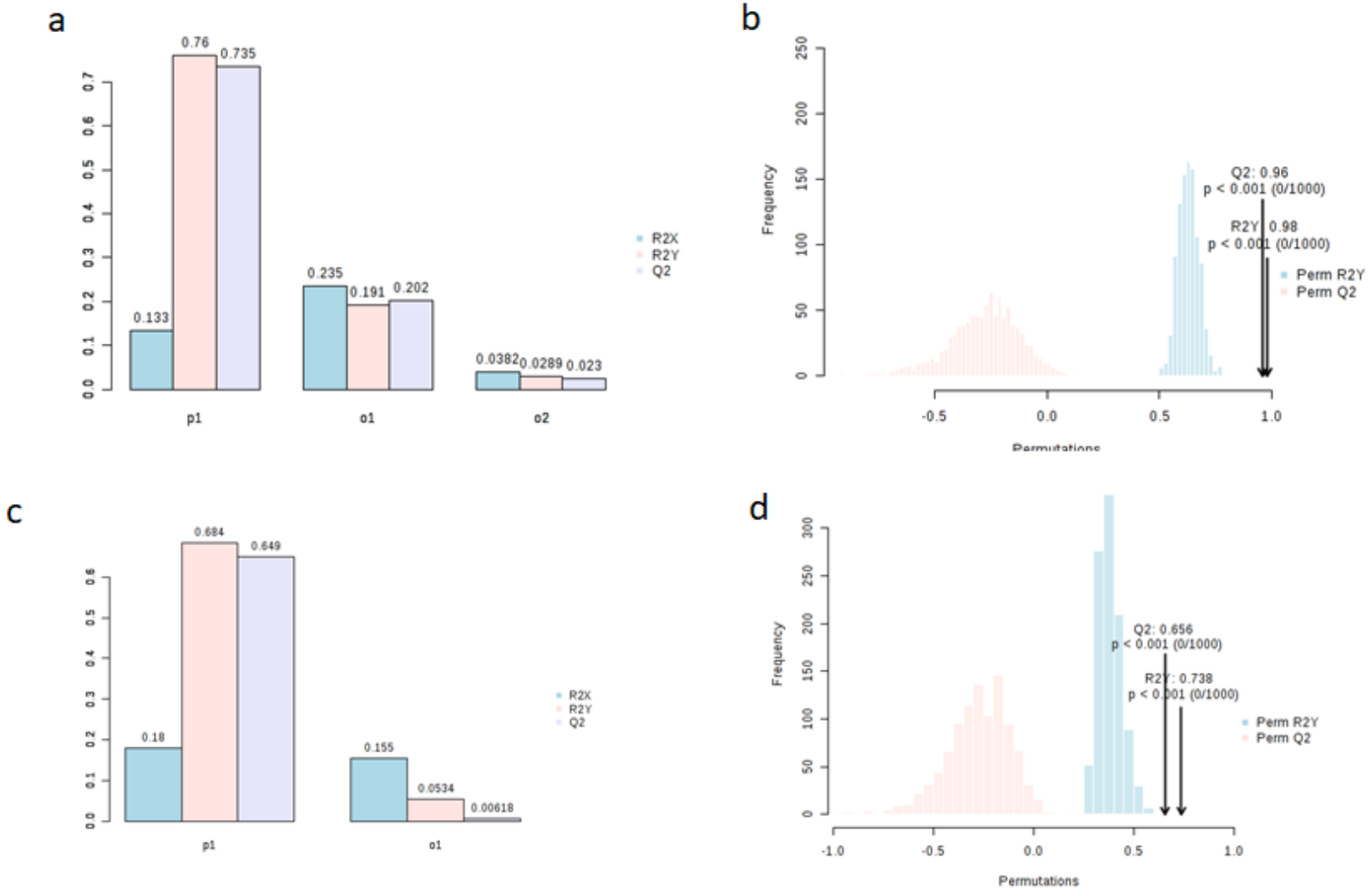

S1 Figure. Validation of the OPLS-DA model of biofluid metabolomic data from patients with aortic valve stenosis (AVS) and control individuals. Data were derived from GC-MS spectra of urine (A,B) and plasma (C,D) samples from AVS patients (n=46) and control individuals (n=46). Model validation was performed using permutation test with 1000 iterations on the OPLS-DA model. Empirical p-values Q2: p<0.001 and R2Y: p<0.001.

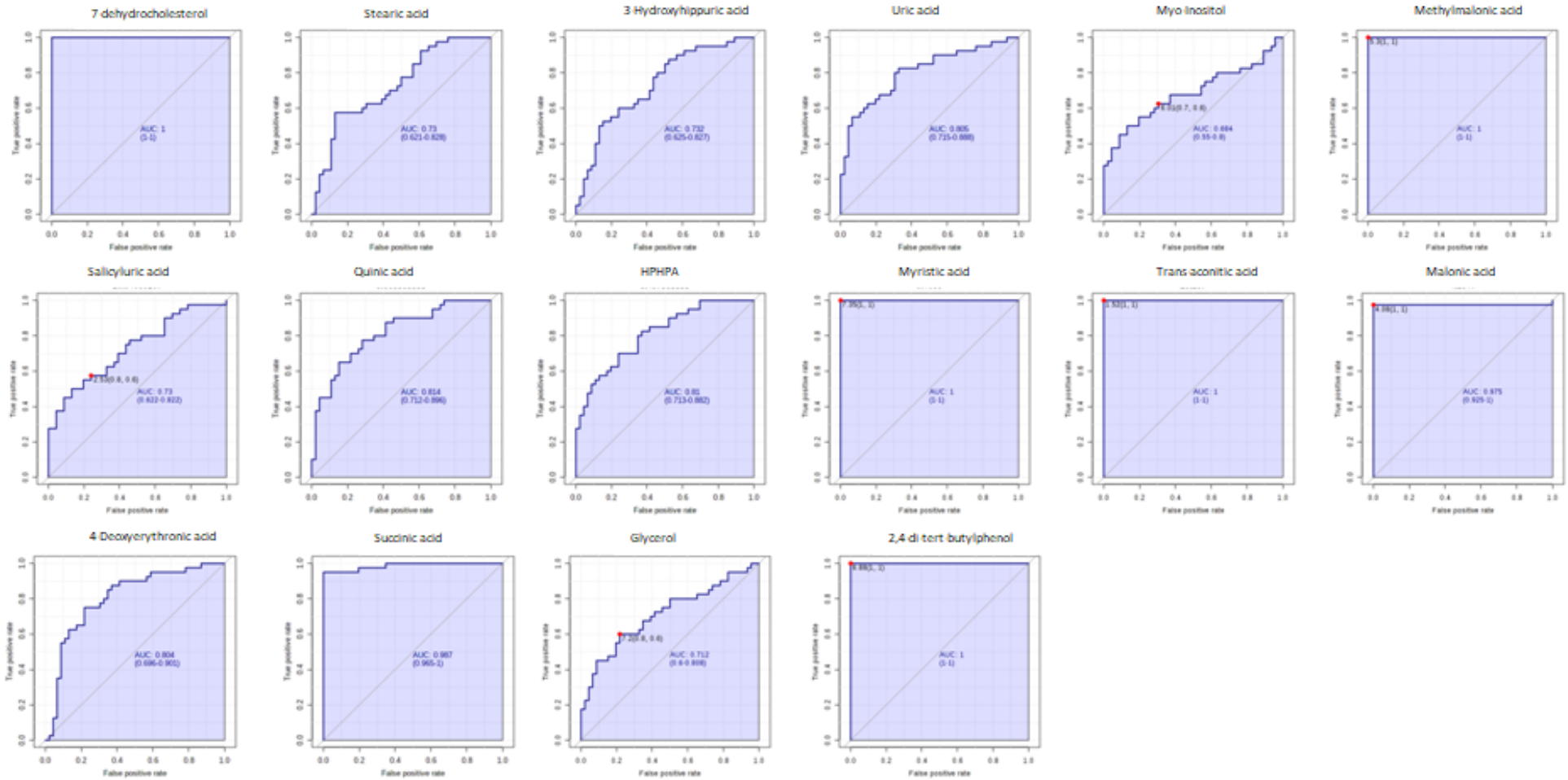

S2 Figure . ROC analysis of candidate urine metabolites separating AVS patients and control individuals. Each of the 16 candidate metabolites (VIP>1, nominal p<0.05, q<0.05) has a ROC curve where the sensitivity is on the y-axis and the specificity is on the x-axis. The AUROC is shown in blue and the AUC values with their 95% confidence intervals are presented in the curves.

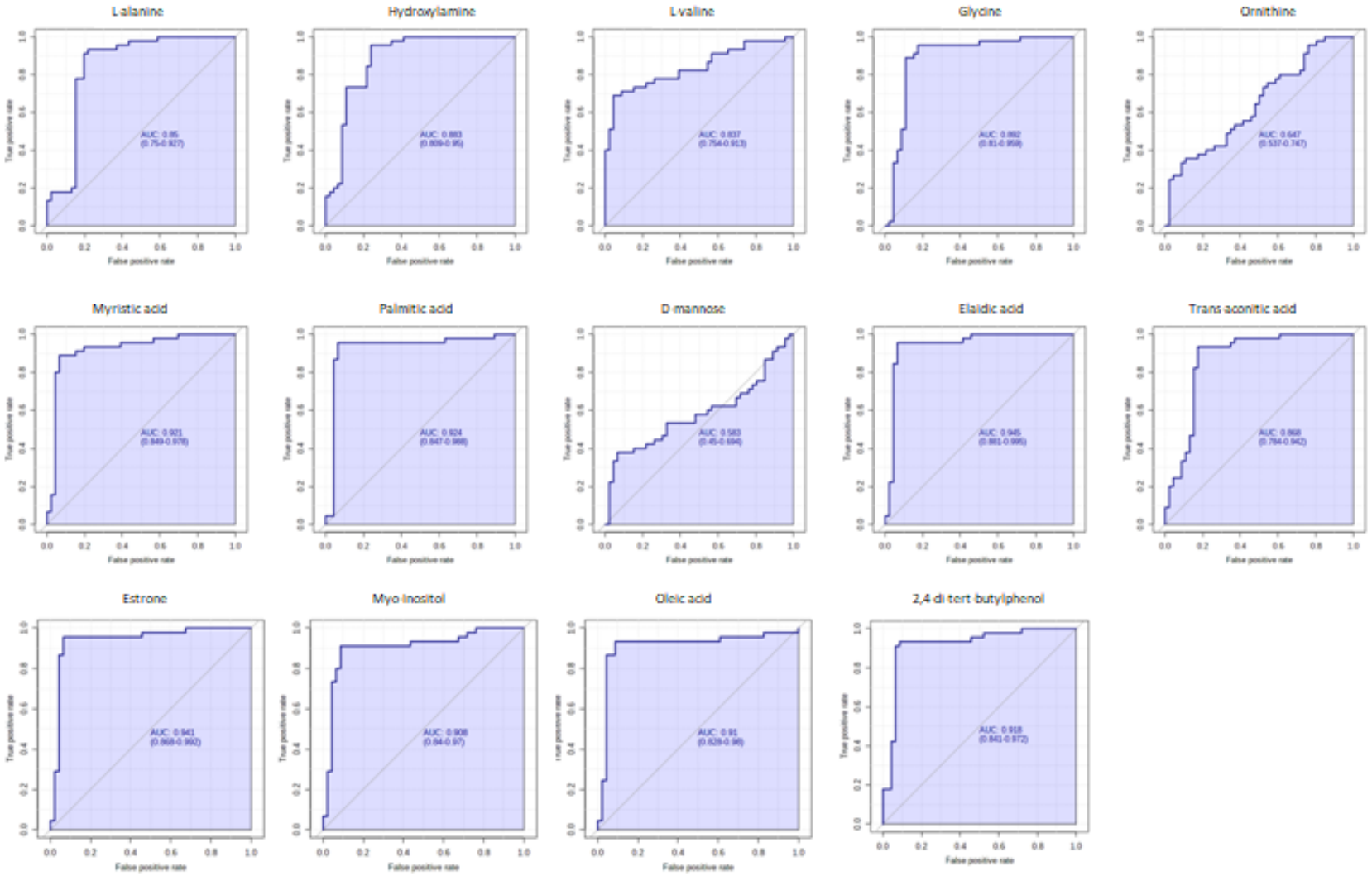

S3 Figure. ROC analysis of candidate plasma metabolites separating AVS patients and control individuals. Each of the 14 candidate metabolites (VIP>1, nominal p<0.05, q<0.05) has a ROC curve where the sensitivity is on the y-axis and the specificity is on the x-axis. The AUROC is shown in blue and the AUC values with their 95% confidence intervals are presented in the curves.

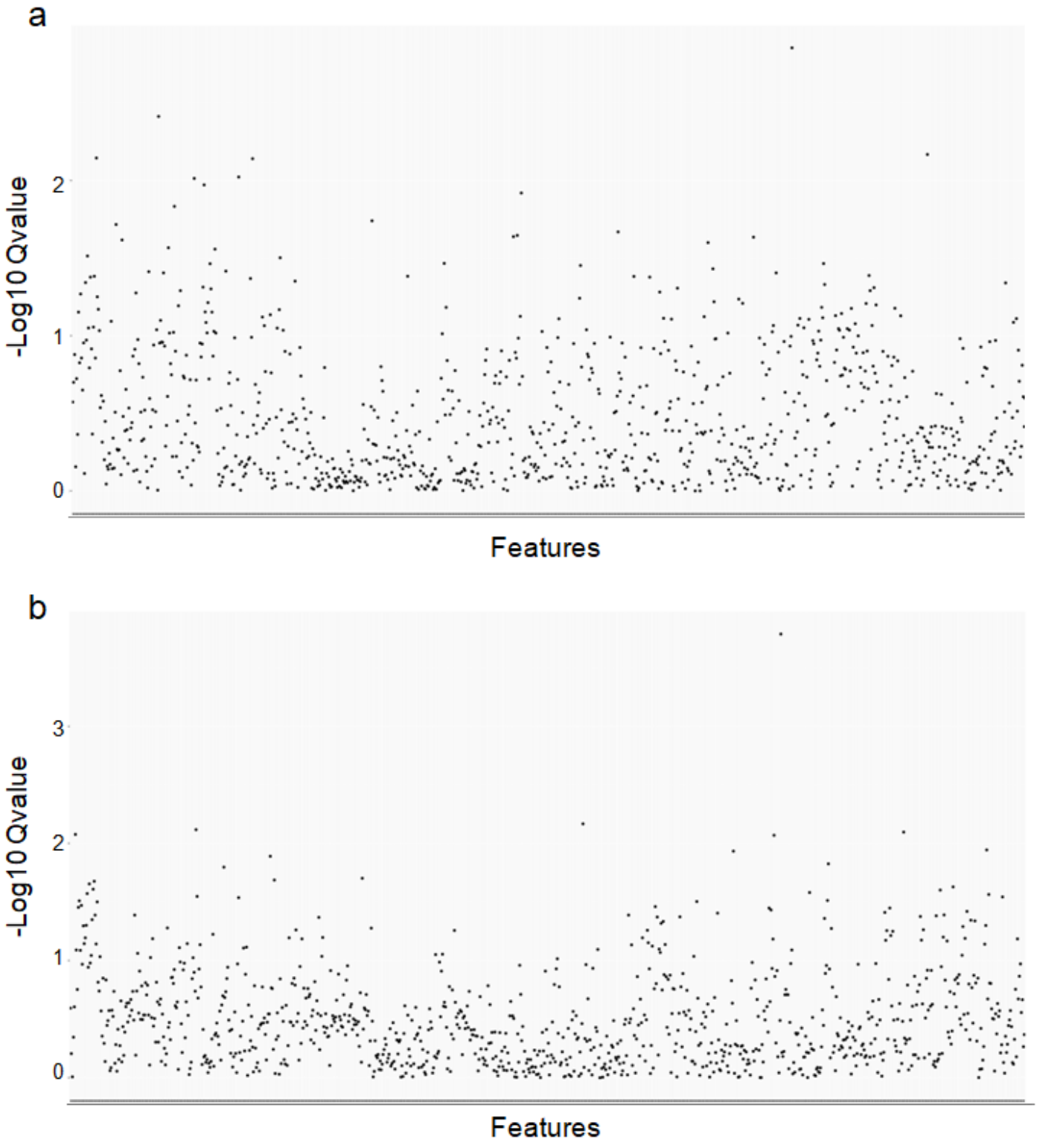

S4 Figure. Association analysis of plasma GC-MS spectral data with HDL and LDL in patients and controls. Data were derived by GC/MS analysis of plasma samples from 46 AVS patients and 46 control individuals. Generalized linear models were used to determine significant associations between metabolomic peaks and HDL (a) and LDL (b) and correcting for multiple testing. Signal intensities normalised to the internal standard are plotted against the Q-values

S1 Table: Clinical and biochemical features in males and females selected for presence or absence of aortic valve stenosis. Data are means ± SEM.

	Females (38)		**Males (54)**	
	Controls (19)	Cases (19)	Controls (27)	Cases (27)
Age	61.8 ± 2.7	61.4 ± 2.6	57.3 ± 2.5	57.0 ± 2.6
Body weight (Kg)	75.2 ± 3.3	73.4 ± 3.0	88.6 ± 3.0	87.4 ± 3.0
Body mass index (Kg/m^2)	31.8 ± 1.3	31.7 ± 1.2	30.0 ± 0.9	30.1 ± 0.9
Plasma glucose (mg/dL)	122.3 ± 12.4 (17)	116.3 ± 23.8 (4)	102.6 ± 5.0 (19)	111.0 ± 5.3 (9)
Triglycerides (mg/dL)	207.4 ± 22.3 (19)	170.5 ± 21.1 (16)	167.6 ± 14.4 (23)	198.0 ± 14.4 (22)
HDL cholesterol (mg/dL)	44.4 ± 3.2 (19)	47.8 ± 3.2 (16)	36.3 ± 1.9 (24)	34.6 ± 2.2 (23)
LDL cholesterol (mg/dL)	126.9 ± 11.3 (19)	109.4 ± 8.0 (15)	114.3 ± 6.4 (23)	109.4 ± 8.0 (23)
Total cholesterol (mg/dL)	199.7 ± 14.6 (19)	184.8 ± 8.3 (16)	183.5 ± 8.0 (24)	185.7 ± 9.1 (23)
Diagnosed diabetic (%)	5 (26.3%)	5 (26.3%)	2 (7.4%)	6 (22.2%)
Diagnosed hypertensive (%)	15 (78.9%)	14 (73.7%)	12 (44.4%)	22 (81.5%)
Diagnosed hyperlipidemic (%)	10 (52.6%)	13 (68.4%)	2 (7.4%)	15 (55.6%)
Family history diabetes (%)	12 (63.2%)	9 (47.4%)	17 (63.0%)	14 (51.9%)
Family history hypertension (%)	15 (78.9%)	15 (78.9%)	19 (70.4%)	19 (70.4%)
Family history hyperlipidemia (%)	11 (57.9%)	9 (47.4%)	5 (18.5%)	12 (44.4%)

S2 Table. Metabolites identified using the NIST08 library (https://chemdata.nist.gov/) after analysis of gas chromatography mass spectrometry (GC/MS) of urine and plasma samples of patients with aortic valve stenosis and controls. RT, Retention Time; HMDB, Human Metabolome Database; KEGG,Kyoto Encyclopedia of Genes and Genomes.

Matrix	RT	Metabolite	Similarity	HMDB	PubChem	KEGG	SMILES	Reference
Urine	2.74	Methylmalonic acid (2TMS)	80	HMDB0000202	487	C02170	CC(C(=O)O)C(=O)O	1,2
Urine	2.82	L-Lactic acid (2TMS)	91	HMDB0000190	107689	C00186	C[C@@H](C(=O)O)O	1,2
Urine	2.94	Glycolic acid (2TMS)	96	HMDB0000115	757	C00160	C(C(=O)O)O	2
Urine	3.07	Succinic acid (2TMS)	86	HMDB0000254	1110	C00042	C(CC(=O)O)C(=O)O	1,2
Urine	3.2	L-Alanine (2TMS)	98	HMDB0000161	5950	C00041	C[C@@H](C(=O)O)N	1,2
Urine	3.29	Hydroxylamine (3TMS)	87	HMDB0003338	787	C00192	NO	
Urine	3.55	Oxalic acid (2TMS)	90	HMDB0002329	971	C00209	C(=O)(C(=O)O)O	2
Urine	3.63	Oxalic acid (2TMS)	93	HMDB0002329	971	C00209	C(=O)(C(=O)O)O	2
Urine	3.69	m-Cresol	93	HMDB0002048	342	C01467	CC1=CC(=CC=C1)O	
Urine	3.81	3-Hydroxybutyric acid	96	HMDB0000357	441	C01089	CC(CC(=O)O)O	
Urine	4.2	Malonic acid (2TMS)	83	HMDB0000691	867	C00383	C(C(=O)O)C(=O)O	2
Urine	4.3	alpha-Ketoisovaleric acid (2TMS)	86	HMDB0000019	49	C00141	CC(C)C(=O)C(=O)O	2
Urine	4.37	3-Hydroxyisovaleric acid (2TMS)	83	HMDB0000754	69362		CC(C)(CC(=O)O)O	
Urine	4.48	2-Ethylhydracrylic acid (2TMS)	95	HMDB0000396	188979		CCC(CO)C(=O)O	1,2
Urine	4.51	Guaiacol (TMS)	86	HMDB0001398	460	C01502	COC1=CC=CC=C1O	
Urine	4.85	Ethanolamine (2TMS)	92	HMDB0000149	700	C00189	C(CO)N	1,2
Urine	5	Glycerol (TMS)	93	HMDB0000131	753	C00116	C(C(CO)O)O	1,2

Urine	5.34	Glycine (3TMS)	90	HMDB0000123	750	C00037	C(C(=O)O)N	
Urine	5.41	Glycine (3TMS)	96	HMDB0000123	750	C00037	C(C(=O)O)N	1,2
Urine	5.47	Succinic acid (2TMS)	97	HMDB0000254	1110	C00042	C(CC(=O)O)C(=O)O	1,2
Urine	5.5	L-Fucose	87	HMDB0000174	17106	C01019	C[C@H]1[C@H]([C@H]([C@@H](C(O1)O)O)O)O	
Urine	5.56	2-Hydroxy-2-methylbutyric acid (TMS)	90	HMDB0001987	95433		CCC(C)(C(=O)O)O	1,2
Urine	5.59	Glyceric acid (3TMS)	94	HMDB0000139	439194	C00258	C([C@H](C(=O)O)O)O	1,2
Urine	5.65	Uracil	90	HMDB0000300	1174	C00106	C1=CNC(=O)NC1=O	
Urine	5.69	4-Deoxyerythronic acid (3TMS)	83	HMDB0000498	13120901		C[C@H]([C@H](C(=O)O)O)O	2
Urine	5.78	4-Deoxyerythronic acid (3TMS)	91	HMDB0000498	13120901		C[C@H]([C@H](C(=O)O)O)O	2
Urine	5.82	L-Serine/ D-Serine (3TMS)	92	HMDB0000187	5951	C00065	C([C@@H](C(=O)O)N)O	1,2
Urine	5.91	gamma-Aminobutyric acid (TMS)	86	HMDB0000112	119	C00334	C(CC(=O)O)CN	1,2
Urine	6.04	L-Threonine (3TMS)	92	HMDB0000167	6288	C00188	C[C@H]([C@@H](C(=O)O)N)O	1,2
Urine	6.15	Glutaric acid	86	HMDB0000661	743	C00489	C(CC(=O)O)CC(=O)O	
Urine	6.26	4-Deoxyerythronic acid (3TMS)	92	HMDB0000498	13120901		C[C@H]([C@H](C(=O)O)O)O	2
Urine	6.3	beta-Alanine (3TMS)	81	HMDB0000056	239	C00099	C(CN)C(=O)O	1,2
Urine	6.43	(S)-3,4-Dihydroxybutyric acid (3TMS)	90	HMDB0000337	150929		C(C(CO)O)C(=O)O	1
Urine	6.58	(S)-b-aminoisobutyric acid (3TMS)	83	HMDB0002166	439434	C03284	C[C@@H](CN)C(=O)O	1,2
Urine	6.74	Citramalic acid (3TMS)	86	HMDB0000426	1081	C00815	CC(CC(=O)O)(C(=O)O)O	2
Urine	6.79	2-Oxovaleric acid (2TMS)	90	HMDB0001865	74563	C06255	CCCC(=O)C(=O)O	

Urine	6.94	Malic acid (3TMS)	94	HMDB0000744	525	C00711	C(C(C(=O)O)O)C(=O)O	2
Urine	7.02	Erythritol (4TMS)	89	HMDB0002994	222285	C00503	C([C@H]([C@H](CO)O)O)O	2
Urine	7.08	Erythritol (4TMS)	91	HMDB0002994	222285	C16884	C([C@H]([C@H](CO)O)O)O	
Urine	7.16	Pyroglutamic acid (2TMS)	93	HMDB0000267	7405	C01879	C1CC(=O)N[C@@H]1C(=O)O	2
Urine	7.26	2,4-Di-tert-butylphenol (TMS)	90	HMDB0013816	NA		[H]OC1=C(C([H])=C(C([H])=C1[H])C(C([H])([H])[H])(C([H])([H])[H])C([H])([H])C([H])([H])[H])C([H])([H])C([H])=C([H])[H]	
Urine	7.35	Threonic acid	83	HMDB0000943	151152	C01620	C([C@H]([C@@H](C(=O)O)O)O)O	
Urine	7.4	Erythronic acid (4TMS)/ 2,3,4-trihydroxybutanoic acid	96	HMDB0000613	2781043		C([C@H]([C@H](C(=O)O)O)O)O	
Urine	7.41	Creatinine (3TMS)	92	HMDB0000562	588	C00791	CN1CC(=O)N=C1N	1,2
Urine	7.52	L-Threonic Acid (4TMS)	99	HMDB0000167	6288	C00188	C[C@H]([C@@H](C(=O)O)N)O	1,2
Urine	7.79	3-Hydroxyphenylacetic acid (3TMS)	87	HMDB0000440	12122	C05593	C1=CC(=CC(=C1)O)CC(=O)O	1,2
Urine	7.98	Acetaminophen (2TMS)	99	HMDB0001859	1983		CC(=O)NC1=CC=C(C=C1)O	
Urine	8.03	p-Hydroxyphenylacetic acid (2TMS)	91	HMDB0000020	127	C00642	C1=CC(=CC=C1CC(=O)O)O	1,2
Urine	8.22	2-Deoxypentonic acid (4TMS)	87	HMDB0000366	11528367		C([C@@H]([C@@H](CO)O)O)C(=O)O	
Urine	8.28	D-Fructose (6TMS)	94	HMDB0000660	439709	C02336	C([C@@H]1[C@H]([C@@H]([C@](O1)(CO)O)O)O)O	1,2
Urine	8.32	D-Xylitol (5TMS)	95	HMDB0002917	6912	C00379	C([C@H](C([C@H](CO)O)O)O)O	2
Urine	8.42	Xylulose (4TMS)	93	HMDB0001644	5289590	C00310	C([C@H]([C@@H](C(=O)CO)O)O)O	1,2
Urine	8.59	Aminoadipic acid (3TMS)	90	HMDB0000510	469	C00956	C(CC(C(=O)O)N)CC(=O)O	1,2
Urine	8.61	D-Xylitol (5TMS)	93	HMDB0002917	6912	C00379	C([C@H](C([C@H](CO)O)O)O)O	2
Urine	8.65	Homoveratric acid (TMS)	93	HMDB0000434	7139		COC1=C(C=C(C=C1)CC(=O)O)OC	1

Urine	8.7	D-Arabitol (5TMS)	86	HMDB00005 68	827	C01904	C(C(C(C(CO)O)O)O)O	1
Urine	8.76	Androstenedione	90	HMDB00000 53	6128	C00280	C[C@]12CCC(=O)C=C1CC[C@@H]3[C@@H]2CC[C@]4([C@H]3CCC 4=O)C	1
Urine	8.83	cis-Aconitic acid (3TMS)	93	HMDB00000 72	643757	C00417	C(/C(=C/C(=O)O)/C(=O)O)C(=O)O	1,2
Urine	8.86	Acetaminophen (TMS)	91	HMDB00018 59	1983		CC(=O)NC1=CC=C(C=C1)O	2
Urine	9	Homovanillic acid (2TMS)	92	HMDB00001 18	1738	C05582	COC1=C(C=CC(=C1)CC(=O)O)O	1,2
Urine	9.01	L-Glutamine (3TMS)	92	HMDB00006 41	5961	C00064	C(CC(=O)N)[C@@H](C(=O)O)N	1,2
Urine	9.14	Ribonolactone (5TMS)	90	HMDB00019 00	111064	C02674	C([C@@H]1[C@H]([C@H](C(=O)O1)O)O)O	
Urine	9.25	Hypoxanthine (2TMS)	91	HMDB00001 57	790	C00262	C1=NC2=C(N1)C(=O)N=CN2	1,2
Urine	9.37	Citric acid (4TMS)	93	HMDB00000 94	311	C00158	C(C(=O)O)C(CC(=O)O)(C(=O)O)O	1,2
Urine	9.44	Myristic acid (TMS)	87	HMDB00008 06	11005	C06424	CCCCCCCCCCCCCC(=O)O	1
Urine	9.53	3-(3-Hydroxyphenyl)-3-hydroxypropanoic acid (HPHPA) (3TMS)	83	HMDB00026 43	102959		C1=CC(=CC(=C1)O)C(CC(=O)O)O	2
Urine	9.62	Oxalic acid (2TBS)	91	HMDB00023 29	971	C00209	C(=O)(C(=O)O)O	2
Urine	9.66	Quinic acid (5TMS)	83	HMDB00030 72	NA	C06746	OC1C[C@@](O)(C[C@@H](O)[C@H]1O)C(O)=O	
Urine	9.73	3,5-Dihydroxybenzoic acid	95	HMDB00136 77	7424	C00180	C1=C(C=C(C=C1O)O)C(=O)O	
Urine	9.77	Vanylglycol (3TMS)	91	HMDB00014 90	10805	C05594	COC1=C(C=CC(=C1)C(CO)O)O	
Urine	9.81	D-Mannose (5TMS)	93	HMDB00001 69	18950	C00159	C([C@@H]1[C@H]([C@@H]([C@@H](C(O1)O)O)O)O)O	1
Urine	9.84	Oxoadipic acid (3TMS)	87	HMDB00002 25	71	C00322	C(CC(=O)C(=O)O)CC(=O)O	2
Urine	9.87	Sorbitol (6TMS)	86	HMDB00002 47	5780	C00794	C([C@H]([C@H]([C@@H]([C@H](CO)O)O)O)O)O	2
Urine	9.94	L-Lysine (4TMS)	87	HMDB00001 82	5962	C00047	C(CCN)C[C@@H](C(=O)O)N	1,2

Urine	9.96	D-Galactose (5TMS)	91	HMDB0000143	439357	C00984	C([C@@H]1[C@@H]([C@@H]([C@H]([C@H](O1)O)O)O)O)O)O	
Urine	10.06	D-Mannose (5TMS)	83	HMDB0000169	18950	C00159	C([C@@H]1[C@H]([C@@H]([C@@H](C(O1)O)O)O)O)O)O	1
Urine	10.12	D-Galactose (5TMS)	97	HMDB0000143	439357	C00984	C([C@@H]1[C@@H]([C@@H]([C@H]([C@H](O1)O)O)O)O)O)O	1,2
Urine	10.2	D-Glucuronic acid (5TMS)	99	HMDB0000127	444791	C00191	[C@@H]1([C@@H]([C@H](O[C@@H]([C@@H]1O)O)C(=O)O)O)O	1,2
Urine	10.28	Galactaric acid (6TMS)	81	HMDB0000639	3037582	C00879	[C@@H]([C@@H]([C@H](C(=O)O)O)O)([C@@H](C(=O)O)O)O	1
Urine	10.36	Galactaric acid (6TMS)	80	HMDB0000639	3037582	C00879	[C@@H]([C@@H]([C@H](C(=O)O)O)O)([C@@H](C(=O)O)O)O	1
Urine	10.46	Pantothenic acid	99	HMDB0000210	6613	C00864	CC(C)(CO)C(C(=O)NCCC(=O)O)O	
Urine	10.50	L-Galactose	91	HMDB0000210	6613	C00864	CC(C)(CO)C(C(=O)NCCC(=O)O)O	
Urine	10.59	Palmitic acid (TMS)	90	HMDB0000220	985	C00249	CCCCCCCCCCCCCCCC(=O)O	
Urine	10.64	Palmitic acid (TMS)	95	HMDB0000220	985	C00249	CCCCCCCCCCCCCCCC(=O)O	1,2
Urine	10.69	Xanthine (2TMS)	95	HMDB0000292	1188	C00385	C1=NC2=C(N1)C(=O)NC(=O)N2	1
Urine	10.75	scyllo-Inositol (6TMS)	92	HMDB0006088	892	C06153	C1(C(C(C(C(C1O)O)O)O)O)O)O	1,2
Urine	10.76	scyllo-Inositol (6TMS)	95	HMDB0006088	892	C06153	C1(C(C(C(C(C1O)O)O)O)O)O)O	1,2
Urine	10.85	7-Methylxanthine (2TMS)	87	HMDB0001991	68374	C16353	CN1C=NC2=C1C(=O)NC(=O)N2	2
Urine	10.86	7-Methylxanthine (2TMS)	94	HMDB0001991	68374	C16353	CN1C=NC2=C1C(=O)NC(=O)N2	2
Urine	10.92	Salicyluric acid/2-Hydroxyhippuric acid (2TMS)	93	HMDB0000840	10253	C07588	C1=CC=C(C(=C1)C(=O)NCC(=O)O)O	2
Urine	10.94	Salicyluric acid/2-Hydroxyhippuric acid (2TMS)	96	HMDB0000840	10253	C07588	C1=CC=C(C(=C1)C(=O)NCC(=O)O)O	2
Urine	11.1	myo-Inositol (6TMS)	83	HMDB0000211	NA	C00137	O[C@H]1[C@H](O)[C@@H](O)[C@H](O)[C@H](O)[C@@H]1O	1
Urine	11.21	Uric acid (4TMS)	97	HMDB0000289	1175	C00366	C12=C(NC(=O)N1)NC(=O)NC2=O	1,2
Urine	11.26	Sorbitol (6TMS)	94	HMDB0000247	5780	C00794	C([C@H]([C@H]([C@@H]([C@H](CO)O)O)O)O)O)O	2

Urine	11.36	3-Hydroxyhippuric acid (TMS)	83	HMDB0006116	450268		C1=CC(=CC(=C1)O)C(=O)NCC(=O)O	1,2
Urine	11.65	Elaidic acid (TMS)/ trans 9 Octadecenoic acid	80	HMDB0000573	445639	C00712	CCCCCCCC/C=C\CCCCCCCC(=O)O	
Urine	11.76	Stearic acid (TMS)	96	HMDB0000827	5281	C01530	CCCCCCCCCCCCCCCCCC(=O)O	
Urine	12.04	Orotic acid	83	HMDB0000226	967	C00295	C1=C(NC(=O)NC1=O)C(=O)O	
Urine	12.4	D-Glucose (5TMS)	87	HMDB0000122	5793	C00031	C([C@@H]1[C@H]([C@@H]([C@H](C(O1)O)O)O)O)O	1,2
Urine	12.67	Estrone (TMS)	89	HMDB0000145	5870	C00468	C[C@]12CC[C@H]3[C@H]([C@@H]1CCC2=O)CCC4=C3C=CC(=C4)O	
Urine	12.82	Arabinofuranose (4TMS)	82	HMDB0012325	440921	C06115	C([C@H]1[C@@H]([C@H](C(O1)O)O)O)O	
Urine	13.79	Oxalic acid (2TBS)	90	HMDB0002329	971	C00209	C(=O)(C(=O)O)O	2
Urine	13.95	7-Dehydrocholesterol	95	HMDB0000032	439423	C01164	C[C@H](CCCC(C)C)[C@H]1CC[C@@H]2[C@@]1(CC[C@H]3C2=CC=C4[C@@]3(CC[C@@H](C4)O)C)C	
Urine	14.27	D-Maltose (TMS)	87	HMDB0000163	10991489	C00208	C([C@@H]1[C@H]([C@@H]([C@H]([C@H](O1)O[C@@H]2[C@H](O[C@@H]([C@H]([C@H]2O)O)O)CO)O)O)O)O	2
Urine	14.35	Alpha-Lactose (TMS)	93	HMDB0000186	84571	C00243	C([C@@H]1[C@@H]([C@@H]([C@H]([C@@H](O1)O[C@@H]2[C@H](O[C@@H]([C@@H]([C@H]2O)O)O)CO)O)O)O)O	
Urine	14.43	Alpha-Lactose (TMS)	93	HMDB0000186	84571	C00243	C([C@@H]1[C@@H]([C@@H]([C@H]([C@@H](O1)O[C@@H]2[C@H](O[C@@H]([C@@H]([C@H]2O)O)O)CO)O)O)O)O	2
Urine	14.59	D-Maltose (TMS)	86	HMDB0000163	10991489	C00208	C([C@@H]1[C@H]([C@@H]([C@H]([C@H](O1)O[C@@H]2[C@H](O[C@@H]([C@H]([C@H]2O)O)O)CO)O)O)O)O	2
Urine	14.67	D-Mannose (5TMS)	93	HMDB0000169	18950	C00159	C([C@@H]1[C@H]([C@@H]([C@@H](C(O1)O)O)O)O)O	1
Urine	14.79	Isomaltose (TMS)	90	HMDB0002923	439193	C00252	C([C@@H]1[C@H]([C@@H]([C@H]([C@H](O1)OC[C@@H]2[C@H]([C@@H]([C@H](C(O2)O)O)O)O)O)O)O)O	
Urine	15.18	trans-Aconitic acid (3TMS)	86	HMDB0000958	444212	C02341	C(/C(=C\C(=O)O)/C(=O)O)C(=O)O	1,2
Urine	16.09	cis-Aconitic acid (3TMS)	90	HMDB0000072	643757	C00417	C(/C(=C/C(=O)O)/C(=O)O)C(=O)O	1,2
Urine	18.75	Arachidonic acid (TMS)	90	HMDB0001043	444899	C00219	CCCCC/C=C\C/C=C\C/C=C\C/C=C\CCCC(=O)O	
Plasma	2.75	2,3-Butanediol (2TMS)	80	HMDB0003156	262	C00265	CC(C(C)O)O	3,4
Plasma	2.81	L-Lactic acid (2TMS)	91	HMDB0000190	107689	C00186	C[C@@H](C(=O)O)O	3,4

Plasma	2.99	L-Valine (TMS)	90	HMDB0000883	6287	C00183	CC(C)[C@@H](C(=O)O)N	3
Plasma	3.01	Caproic acid (TMS)	89	HMDB0000535	8892	C01585	CCCCCC(=O)O	
Plasma	3.1504	L-Alanine (2TMS)	86	HMDB0000161	5950	C00041	C[C@@H](C(=O)O)N	
Plasma	3.24	hydroxylamine (3TMS)	97	HMDB0003338	787	C00192	NO	
Plasma	3.28	L-Alanine (2TMS)	86	HMDB0000161	5950	C00041	C[C@@H](C(=O)O)N	3,4
Plasma	3.35	hydroxylamine (3TMS)	95	HMDB0003338	787	C00192	NO	
Plasma	3.47	3-Hydroxyisovaleric acid (2TMS)	83	HMDB0000754	69362		CC(C)(CC(=O)O)O	3
Plasma	3.55	Oxalic acid (2TMS)	80	HMDB0002329	971	C00209	C(=O)(C(=O)O)O	3
Plasma	3.71	L-Leucine (TMS)	90	HMDB0000687	6106	C00123	CC(C)C[C@@H](C(=O)O)N	3,4
Plasma	3.76	1,3-Butanediol (2TMS)	87	HMDB0031320	7896		CC(CCO)O	
Plasma	3.8	3-Hydroxybutyric acid (2TMS)	95	HMDB0000357	441	C01089	CC(CC(=O)O)O	3
Plasma	4.32	L-Valine (2TMS)	96	HMDB0000883	6287	C00183	CC(C)[C@@H](C(=O)O)N	3,4
Plasma	4.41	L-Valine (2TMS)	80	HMDB0000883	6287	C00183	CC(C)[C@@H](C(=O)O)N	3,4
Plasma	4.5371	Urea (2TMS)	83	HMDB0000883	6287	C00183	CC(C)[C@@H](C(=O)O)N	
Plasma	4.67	Urea (2TMS)	87	HMDB0000294	1176	C00086	C(=O)(N)N	3,4
Plasma	4.71	Urea (2TMS)	93	HMDB0000294	1176	C00086	C(=O)(N)N	3,4
Plasma	4.76	L-Serine	82	HMDB0000187	5951	C00065	C([C@@H](C(=O)O)N)O	3,4
Plasma	4.87	L-Leucine (2TMS)	90	HMDB0000687	6106	C00123	CC(C)C[C@@H](C(=O)O)N	3
Plasma	4.93	Glycerol (TMS)	93	HMDB0000131	753	C00116	C(C(CO)O)O	3,4
Plasma	4.95	Phosphate/phosphoric acid (TMS)	99	HMDB0002142	1004	C00009	OP(=O)(O)O	3
Plasma	5.1378	Phosphate/phosphoric acid (TMS)	98	HMDB0002142	1004	C00009	OP(=O)(O)O	

Plasma	5.18	Glycine/ 2-aminoacetic acid (3TMS)	89	HMDB0000123	750	C00037	C(C(=O)O)N	3,4
Plasma	5.48	Glyceric acid/ 2,3-dihydroxypropanoic acid (3TMS)	80	HMDB0006372	6326776		C([C@@H](C(=O)O)O)O	3
Plasma	5.74	L-Serine/ (2S)-2-amino-3-hydroxypropanoic acid (3TMS)	91	HMDB0000187	5951	C00065	C([C@@H](C(=O)O)N)O	3,4
Plasma	5.98	L-Threonine/ 2-amino-3-hydroxybutanoic acid (3TMS)	90	HMDB0000167	6288	C00188	C[C@H]([C@@H](C(=O)O)N)O	3,4
Plasma	6.79	2-Oxovaleric acid (2TMS)	80	HMDB0001865	74563	C06255	CCCC(=O)C(=O)O	
Plasma	7.13	Pyroglutamic acid/ L-5-oxoproline (2TMS)	93	HMDB0000143	439357	C00984	C([C@@H]1[C@@H]([C@@H]([C@H]([C@H](O1)O)O)O)O)O)O	3
Plasma	7.24	Pyroglutamic acid/ L-5-oxoproline (2TMS)	95	HMDB0000267	7405	C01879	C1CC(=O)N[C@@H]1C(=O)O	
Plasma	7.26	2,4-Di-tert-butylphenol (TMS)	80	HMDB0013816	NA		[H]OC1=C(C([H])=C(C([H])=C1[H])C(C([H])([H])[H])(C([H])([H])[H])C([H])([H])C([H])([H])[H])C([H])([H])C([H])=C([H])[H]	
Plasma	7.37	Creatinine (3TMS)	93	HMDB0000562	588	C00791	CN1CC(=O)N=C1N	
Plasma	7.49	L-Threonic Acid (4TMS)	90	HMDB0000943	151152	C01620	C([C@H]([C@@H](C(=O)O)O)O)O)O	
Plasma	7.77	Pipecolic acid (2TMS)	87	HMDB0000070	849	C00408	C1CCNC(C1)C(=O)O	
Plasma	7.87	Glutamic acid (3TMS)	99	HMDB0000148	33032	C00025	C(CC(=O)O)[C@@H](C(=O)O)N	3
Plasma	7.91	L-Phenylalanine (2TMS)	91	HMDB0000159	6140	C00079	C1=CC=C(C=C1)C[C@@H](C(=O)O)N	3,4
Plasma	8.02	Dodecanoic acid (TMS)	96	HMDB0000638	3893	C02679	CCCCCCCCCCCC(=O)O	
Plasma	8.45	L-Lysine (3TMS)	96	HMDB0000182	5962	C00047	C(CCN)C[C@@H](C(=O)O)N	
Plasma	8.85	Ornithine (3TMS)	99	HMDB0000214	6262	C00077	C(C[C@@H](C(=O)O)N)CN	
Plasma	8.98	L-Glutamine (3TMS)	87	HMDB0000641	5961	C00064	C(CC(=O)N)[C@@H](C(=O)O)N	3,4
Plasma	9.02	Glycerol 3-phosphate	91	NA	NA	NA	NA	

Plasma	9.1	Azelaic acid (2TMS)	91	HMDB0000784	2266	C08261	C(CCCC(=O)O)CCCC(=O)O	
Plasma	9.25	Ornithine (4TMS)	99	HMDB0000214	6262	C00077	C(C[C@@H](C(=O)O)N)CN	
Plasma	9.3469	Citric acid (4TMS)	90	HMDB0000094	311	C00158	C(C(=O)O)C(CC(=O)O)(C(=O)O)O	
Plasma	9.38	Myristic acid (TMS)	97	HMDB0000806	11005	C06424	CCCCCCCCCCCCCC(=O)O	3
Plasma	9.4213	Myristic acid (TMS)	98	HMDB0000806	11005	C06424	CCCCCCCCCCCCCC(=O)O	
Plasma	9.541	Galactose	90	HMDB0000143	439357	C00984	C([C@@H]1[C@@H]([C@@H]([C@H]([C@H](O1)O)O)O)O)O)O	
Plasma	9.66	Quinic acid (5TMS)	86	HMDB0003072	NA	C06746	OC1C[C@@](O)(C[C@@H](O)[C@H]1O)C(O)=O	
Plasma	9.74	L-Tyrosine (2TMS)	94	HMDB0000158	6057	C00082	C1=CC(=CC=C1C[C@@H](C(=O)O)N)O	3,4
Plasma	9.8437	d-glucopyranose (5TMS)/d-glucose	94	HMDB0000158	6057	C00082	C1=CC(=CC=C1C[C@@H](C(=O)O)N)O	
Plasma	9.86	d-glucopyranose (5TMS)/d-glucose	93	HMDB0000122	5793	C00031	C([C@@H]1[C@H]([C@@H]([C@H](C(O1)O)O)O)O)O)O	4
Plasma	9.94	d-glucose (5TMS)	91	HMDB0000122	5793	C00031	C([C@@H]1[C@H]([C@@H]([C@H](C(O1)O)O)O)O)O)O	4
Plasma	10.04	d-mannose (5TMS)	91	HMDB0000169	18950	C00159	C([C@@H]1[C@H]([C@@H]([C@@H](C(O1)O)O)O)O)O)O	
Plasma	10.08	L-Tyrosine (3TMS)	91	HMDB0000158	6057	C00082	C1=CC(=CC=C1C[C@@H](C(=O)O)N)O	3
Plasma	10.38	Pipecolic acid (2TMS)	86	HMDB0000070	849	C00408	C1CCNC(C1)C(=O)O	4
Plasma	10.46	L-Fucose (4TMS)	91	HMDB0000174	17106	C01019	C[C@H]1[C@H]([C@H]([C@@H](C(O1)O)O)O)O	
Plasma	10.50	Palmitoleic acid (TMS)	97	HMDB0003229	445638	C08362	CCCCCC/C=C\CCCCCCCC(=O)O	3
Plasma	10.62	Palmitic acid (TMS)	98	HMDB0000220	985	C00249	CCCCCCCCCCCCCCCC(=O)O	3,4
Plasma	10.67	Palmitic acid (TMS)	98	HMDB0000220	985	C00249	CCCCCCCCCCCCCCCC(=O)O	
Plasma	10.77	d-mannose (5TMS)	81	HMDB0000169	18950	C00159	C([C@@H]1[C@H]([C@@H]([C@@H](C(O1)O)O)O)O)O)O	
Plasma	11.08	myo-Inositol (6TMS)	87	HMDB0000211	NA	C00137	O[C@H]1[C@H](O)[C@@H](O)[C@H](O)[C@H](O)[C@@H]1O	
Plasma	11.19	Uric acid (4TMS)	87	HMDB0000289	1175	C00366	C12=C(NC(=O)N1)NC(=O)NC2=O	3

Plasma	11.62	Oleic acid (TMS)/ cis 9 Octadecenoic acid	99	HMDB0000207	445639	C00712	CCCCCCCC/C=C\CCCCCCCC(=O)O	
Plasma	11.65	Elaidic acid (TMS)/ trans 9 Octadecenoic acid	93	HMDB0000573	445639	C00712	CCCCCCCC/C=C\CCCCCCCC(=O)O	
Plasma	11.76	Stearic acid (TMS)	96	HMDB0000827	5281	C01530	CCCCCCCCCCCCCCCCCC(=O)O	3,4
Plasma	12.67	Estrone (TMS)	80	HMDB0000145	5870	C00468	C[C@]12CC[C@H]3[C@H]([C@@H]1CCC2=O)CCC4=C3C=CC(=C4)O	
Plasma	12.82	Arachidic acid (TMS)	95	HMDB0002212	10467	C06425	CCCCCCCCCCCCCCCCCCCC(=O)O	
Plasma	13.80	Behenic acid (TMS)	92	HMDB0000944	8215	C08281	CCCCCCCCCCCCCCCCCCCCCC(=O)O	
Plasma	15.18	trans-Aconitic acid (3TMS)	80	HMDB0000958	444212	C02341	C(/C(=C\C(=O)O)/C(=O)O)C(=O)O	
Plasma	16.16	Cholesterol (TMS)	99	HMDB0000067	11025495	C00187	C[C@H](CCCC(C)C)[C@H]1CC[C@@H]2[C@@]1(CC[C@H]3[C@H]2CC=C4[C@@]3(CCC(C4)O)C)C	3,4

1. Cheng Y et al., Distinct Urinary Metabolic Profile of Human Colorectal Cancer. Journal of Proteome Research 2012. 11(2):1354-1363 (http://pubs.acs.org/doi/10.1021/pr201001a)

2. Bouatra S et al., The Human Urine Metabolome. PLoS ONE 2013. 8(9):e73076 (http://dx.plos.org/10.1371/journal.pone.0073076)

3. Nishiumi S et al., Serum metabolomics as a novel diagnostic approach for pancreatic cancer. Metabolomics 2010. 6(4):518-528 (http://link.springer.com/10.1007/s11306-010-0224-9)

4. Fan Y et al., Human plasma metabolomics for identifying differential metabolites and predicting molecular subtypes of breast cancer. Oncotarget 2016. 7(9):9925-38 (http://www.oncotarget.com/fulltext/7155)

S3 Table. Urinary and plasma metabolites contributing to the separation between the AVS patients and controls. Data were derived by GC/MS analysis of urine and plasma samples from 46 patients and 46 controls. Data were normalized to the internal standard 2-isopropylmalic acid. Variable importance in the projection (VIP) was obtained from PLS-DA with a threshold of 1.0; p-values are calculated from a volcano plot; q-values are the adjusted p-value with Benjamini-Hochberg method. Area Under the Curve (AUC) was calculated using the online tool MetaboAnalyst to determine biomarker utility. Regulation gives information on up- or down-regulation of the features in AVS patients. RT, Retention time; FDR, False Discovery Rate; AUC, Area under the curve.

Matrix	Metabolite	RT	VIP	p-value	FDR	q-value	AUC	95% CI	Biomarker utility	Regulation
Urine	Trans-Aconitic acid	15.2	9.1	<0.0001	<0.0001	<0.0001	1.00	1_1	Excellent	Up
Urine	Unknown	16.4	6.7	<0.0001	<0.0001	<0.0001	1.00	1_1	Excellent	Down
Urine	Unknown	17.2	5.1	<0.0001	<0.0001	<0.0001	1.00	1_1	Excellent	Up
Urine	Unknown	17.9	4.8	<0.0001	<0.0001	<0.0001	1.00	1_1	Excellent	Up
Urine	Myristic acid	9.4	3.7	<0.0001	<0.0001	<0.0001	1.00	1_1	Excellent	Up
Urine	Metylmalonic acid	2.7	2.9	<0.0001	<0.0001	<0.0001	1.00	1_1	Excellent	Up
Urine	7-Dehydrocholesterol	14	2.6	<0.0001	<0.0001	<0.0001	1.00	1_1	Excellent	Down
Urine	Unknown	13	2.5	<0.0001	<0.0001	<0.0001	1.00	1_1	Excellent	Down
Urine	2,4-Di-tert-butylphenol	7.3	2.1	<0.0001	<0.0001	<0.0001	1.00	1_1	Excellent	Down
Urine	Unknown	13.6	1.4	<0.0001	<0.0001	<0.0001	1.00	1_1	Excellent	Up
Urine	Succinic acid	3.1	1.5	<0.0001	<0.0001	<0.0001	0.99	0.962_1	Excellent	Up
Urine	Malonic acid	4.2	2.0	<0.0001	<0.0001	<0.0001	0.98	0.925-1	Excellent	Up
Urine	Unknown	18.9	2.0	<0.0001	<0.0001	<0.0001	0.97	0.933-0.999	Excellent	Down
Urine	Unknown	12.2	1.1	<0.0001	<0.0001	<0.0001	0.94	0.877-0.984	Excellent	Up
Urine	Unknown	14.5	1.1	<0.0001	<0.0001	<0.0001	0.88	0.803-0.945	Good	Up
Urine	Unknown	13.9	1.7	<0.0001	<0.0001	<0.0001	0.83	0.722-0.91	Good	Down
Urine	Quinic acid	9.7	1.1	<0.0001	<0.0001	<0.0001	0.81	0.712-0.896	Good	Up
Urine	3-(3-Hydroxyphenyl)-3-Hydroxypropanoic acid (HPHPA)	9.5	1.5	<0.0001	<0.0001	<0.0001	0.81	0.713-0.882	Good	Up
Urine	4-Deoxyerythronic acid	5.8	1.2	<0.0001	<0.0001	<0.0001	0.80	0.696-0.901	Good	Down
Urine	Uric acid	11.2	1.1	0.0027	0.0094	0.0258	0.80	0.715-0.888	Good	Up
Urine	Unknown	13.4	1.0	<0.0001	<0.0001	<0.0001	0.77	0.671-0.87	Fair	Up
Urine	Unknown	8.1	1.1	<0.0001	<0.0001	<0.0001	0.76	0.647-0.854	Fair	Up
Urine	Unknown	15	1.3	<0.0001	<0.0001	<0.0001	0.76	0.647-0.857	Fair	Up
Urine	3-Hydroxyhippuric acid	11.4	1.1	0.0001	0.0006	0.0035	0.73	0.625-0.827	Fair	Up

Urine	Salicyluric acid/2-Hydroxyhippuric acid	10.9	1.7	0.0002	0.0006	0.0034	0.73	0.622-0.822	Fair	Down
Urine	Stearic acid	11.8	1.2	0.0003	0.0014	0.0064	0.73	0.621-0.828	Fair	Up
Urine	Unknown	8.5	1.1	<0.0001	0.0003	<0.0001	0.73	0.624-0.824	Fair	Up
Urine	Glycerol	5	1.4	<0.0001	<0.0001	<0.0001	0.71	0.600-0.808	Fair	Up
Urine	Myo-inositol	11.1	1.0	0.0082	0.0039	0.0158	0.70	0.550-0.800	Fair	Up
Urine	Unknown	15.8	1.1	0.0144	0.037	0.0259	0.68	0.567-0.786	Poor	Down
Plasma	Unknown	5.4	1.1	<0.0001	<0.0001	<0.0001	0.96	0.918-0.992	Excellent	Up
Plasma	Elaidic acid	11.7	3.5	<0.0001	<0.0001	<0.0001	0.94	0.881-0.995	Excellent	Down
Plasma	Estrone	12.7	4.7	<0.0001	<0.0001	<0.0001	0.94	0.868-0.992	Excellent	Down
Plasma	Unknown	9.6	2.0	<0.0001	<0.0001	<0.0001	0.93	0.857-0.981	Excellent	Down
Plasma	Palmitic acid	10.6	1.1	<0.0001	<0.0001	<0.0001	0.92	0.847-0.988	Excellent	Down
Plasma	Myristic acid	9.4	1.9	<0.0001	<0.0001	<0.0001	0.92	0.849-0.978	Excellent	Down
Plasma	2,4-Di-tert-butylphenol	7.3	1.9	<0.0001	<0.0001	<0.0001	0.92	0.841-0.972	Excellent	Down
Plasma	Oleic acid	11.6	1.7	<0.0001	<0.0001	<0.0001	0.91	0.828-0.980	Excellent	Down
Plasma	Myo-Inositol	11.1	1.1	<0.0001	<0.0001	<0.0001	0.90	0.840-0.970	Excellent	Down
Plasma	Glycine	5.2	1.1	<0.0001	<0.0001	<0.0001	0.89	0.810-0.959	Good	Up
Plasma	Unknown	12.9	3.1	<0.0001	<0.0001	<0.0001	0.89	0.819-0.954	Good	Down
Plasma	Hydroxylamine	3.4	1.3	<0.0001	<0.0001	<0.0001	0.88	0.809-0.950	Good	Up
Plasma	Trans-Aconitic acid	15.2	1.3	<0.0001	<0.0000	<0.0001	0.87	0.784-0.942	Good	Up
Plasma	L-Alanine	3.3	1.1	0.0001	0.0002	0.0012	0.85	0.750-0.927	Good	Up
Plasma	L-Valine	4.4	1.2	<0.0001	<0.0001	<0.0001	0.84	0.754-0.913	Good	Down
Plasma	Unknown	17.2	1.8	<0.0001	<0.0001	<0.0001	0.83	0.725-0.918	Good	Down
Plasma	Unknown	16.6	1.1	<0.0001	<0.0001	0.0002	0.75	0.637-0.858	Fair	Up
Plasma	Unknown	16.8	1.2	<0.0001	<0.0001	0.0006	0.74	0.616-0.831	Fair	Up
Plasma	Unknown	17	1.7	0.0004	0.0011	0.0056	0.72	0.606-0.833	Fair	Up
Plasma	Unknown	17.1	2.3	<0.0001	0.0001	0.0008	0.71	0.601-0.817	Fair	Up
Plasma	Unknown	14.4	1.6	0.0000	0.0001	0.0006	0.70	0.588-0.799	Fair	Down
Plasma	Ornithine	9.3	1.0	0.0114	0.0227	0.0328	0.65	0.537-0.747	Poor	Up
Plasma	D-Mannose	10.8	1.2	0.0079	0.0165	0.0328	0.58	0.450-0.694	Failed	Down

S4 Table. Urinary metabolites contributing to the separation between the AVS patients and controls. Data were derived by GC-MS analysis of urine samples from 46 patients and 46 controls. Data were normalized to creatinine and logTranformed. Variable importance in the projection (VIP) was obtained from PLS-DA with a threshold of 1.0; q-values are the adjusted p-value with Benjamini-Hochberg method. Regulation gives information on up- or down-regulation of the features in AVS patients. RT, Retention time; FDR, False Discovery Rate.

Metabolite	RT	VIP	p-value	FDR	q-value	Regulation
Trans-Aconitic acid	15.2	8.7061	<0.0001	<0.0001	<0.0001	Up
Unknown	16.4	5.8831	<0.0001	<0.0001	<0.0001	Down
Unknown	17.2	4.8977	<0.0001	<0.0001	<0.0001	Up
Unknown	17.9	4.4808	<0.0001	<0.0001	<0.0001	Up
Myristic acid	9.4	3.4881	<0.0001	<0.0001	<0.0001	Up
Methylmalonic acid	2.7	2.7027	<0.0001	<0.0001	<0.0001	Up
7-Dehydrocholesterol	14	2.2202	<0.0001	<0.0001	<0.0001	Down
Unknown	13	2.1089	<0.0001	<0.0001	<0.0001	Down
Malonic acid	4.2	1.986	<0.0001	<0.0001	<0.0001	Up
2,4-Di-tert-butylphenol	7.3	1.7967	<0.0001	<0.0001	<0.0001	Down
Unknown	18.9	1.6191	<0.0001	<0.0001	<0.0001	Down
Succinic acid	3.1	1.525	<0.0001	<0.0001	<0.0001	Up
Unknown	13.6	1.4475	<0.0001	<0.0001	<0.0001	Up
Unknown	13.9	1.3998	<0.0001	<0.0001	0.02	Down
Unknown	15	1.294	<0.0001	<0.0001	0.0004	Up
Quinic acid	9.7	1.2667	<0.0001	<0.0001	<0.0001	Up
p-Hydroxyphenylacetic acid	8.1	1.2158	<0.0001	<0.0001	<0.0001	Up
Unknown	8.5	1.184	<0.0001	<0.0001	0.0003	Up
Unknown	12.2	1.1538	<0.0001	<0.0001	<0.0001	Up
3-Hydroxyhippuric acid	11.4	1.1346	<0.0001	<0.0001	0.0082	Up
Hypoxanthine	9.2	1.0975	<0.0001	<0.0001	<0.0001	Up
3-(3-Hydroxyphenyl)-3-Hydroxypropanoic acid (HPHPA)	9.5	1.0899	<0.0001	<0.0001	<0.0001	Up
Oxoadipic acid	9.8	1.0817	<0.0001	<0.0001	0.0015	Up
Estrone	12.7	1.0679	<0.0001	<0.0001	<0.0001	Up
Palmitic acid	10.6	1.0483	<0.0001	<0.0001	0.0003	Up
Stearic acid	11.8	1.0464	<0.0001	<0.0001	0.0016	Up
Unknown	13.4	1.0275	<0.0001	<0.0001	<0.0001	Up
Unknown	14.5	1.0235	<0.0001	<0.0001	<0.0001	Up
D-Glucose	12.4	1.0106	<0.0001	<0.0001	<0.0001	Up
Unknown	13.3	1.0067	<0.0001	<0.0001	0.0008	Up
Unknown	13.5	1.0047	<0.0001	<0.0001	<0.0001	Up

II.3: Association of altered urinary features with cholesterol levels and risk factors of heart disease

Linear regression models were applied on the untargeted metabolomic data based on GC/MS using urine biofluids to test the association of each metabolic trait with the continuous values of LDL-cholesterol, HDL-cholesterol and BMI.

After adjusting for age and sex, we demonstrated no association between the metabolic features based on GC/MS metabolic profiling and the continuous phenotypes HDL-cholesterol and LDL-cholesterol in urine biofluid while only one metabolic trait, scyllo-inositol, was found significantly associated with BMI (adjusted p-value <0.05) (**Figure S 1**). The p-value was adjusted with Benjamini-Hochberg method.

Figure S 1 : Untargeted metabolic association between urine GC/MS metabolic features and continuous phenotypes. Data were acquired by GC/MS analysis of urine samples from 46 patients and 46 controls. Linear regression models were used to determine significant associations between metabolomic peaks and (**a**) LDL-cholesterol, (**b**) HDL-cholesterol and (**c**) BMI after adjusting for age and sex and correcting for multiple testing. Features showing evidence of non-significant association with LDL and HDL-cholesterol levels are shown with black dots. Scyllo-inositol (red dot) is significantly (q-value <0.05) associated with BMI levels.

Figure S 1

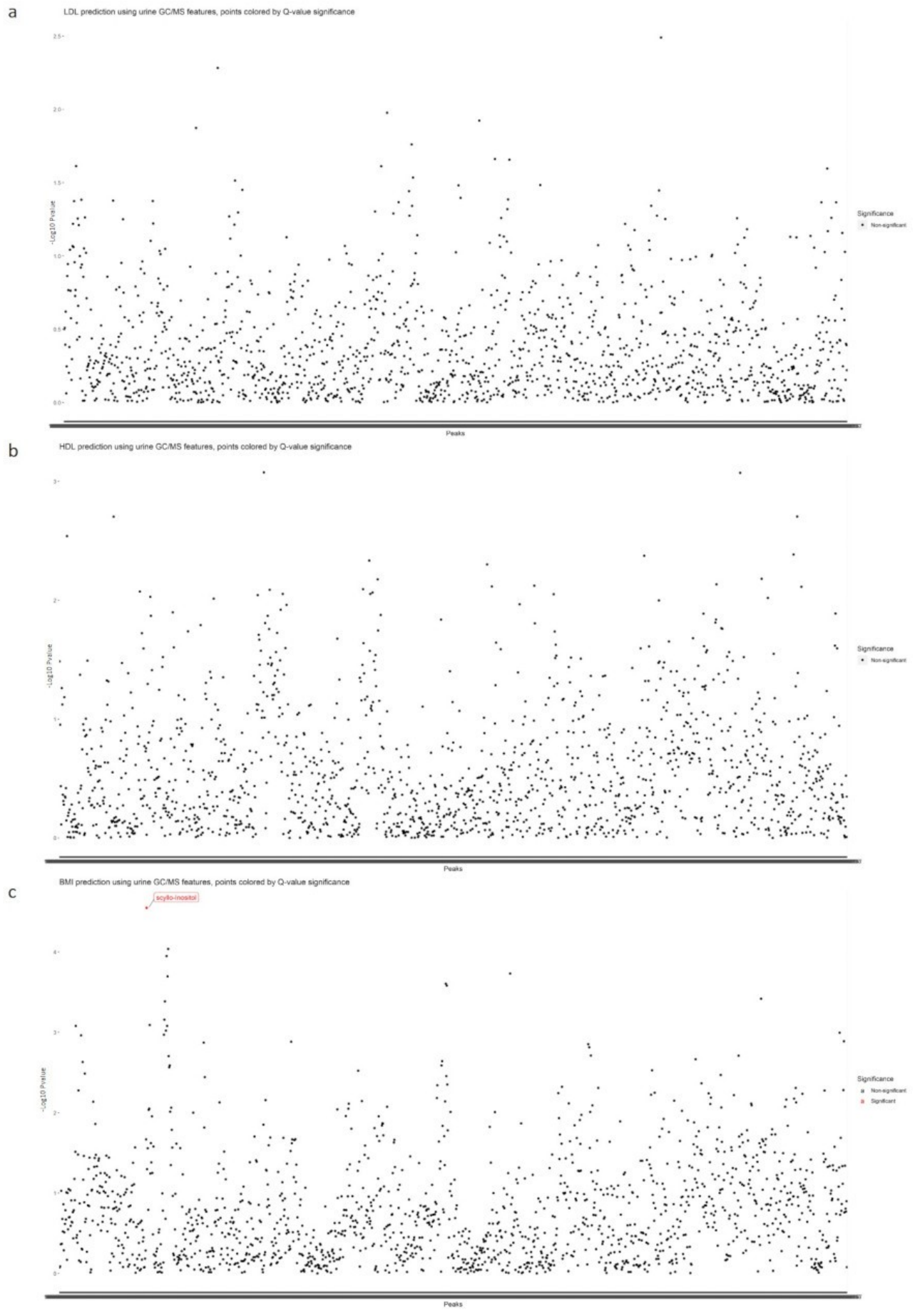
a
LDL prediction using urine GC/MS features, points colored by Q-value significance
-Log10 Pvalue
Peaks
Significance
Non-significant
b
HDL prediction using urine GC/MS features, points colored by Q-value significance
-Log10 Pvalue
Peaks
Significance
Non-significant
c
BMI prediction using urine GC/MS features, points colored by Q-value significance
scyllo-inositol
-Log10 Pvalue
Peaks
Significance
Non-significant
Significant

II.4: Discussion

In this part of the project, we identified differences in the metabolic profiles based on mass spectrometry (GC/MS) of urine and plasma samples of 92 subjects segregated between AVS patients and healthy controls. The PCA score plots of urine and plasma samples using 3 components clearly showed a trend of group clustering between the patient and control groups, which demonstrated that AVS caused changes in the regulation of biofluid metabolites. A set of known and unknown metabolic features that differentiate between cases and controls were provided in this project. The regulation of dietary and circulating metabolites is presented in **Figure S 2**. Some of the known metabolites were commonly found in both biofluids but not always with the same direction of regulation. Only 2,4-di-tert-butylphenol and trans-aconitic acid (TAA) showed the same regulation pattern in the two biofluids.

Figure S 2 : Regulation of dietary and circulating metabolites from urine (yellow arrow) and plasma samples (red arrow). F-6-P. Fructose 6 phosphate; Man-6-P. Mannose 6 phospate

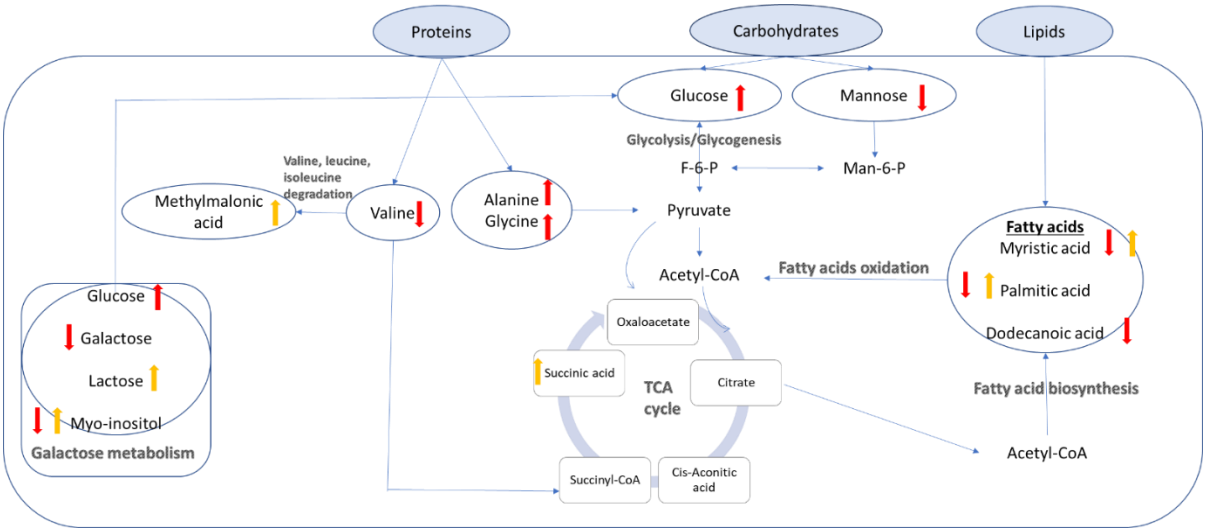

Published reports have shown that several of the differentially regulated metabolites in our case control study are involved in heart diseases which might explain their association with AVS. Glycine, myo-inositol and methylmalonic acid have been found associated with heart failure (HF) (Deidda *et al.*, 2015). Elaidic acid, dodecanoic acid, myristic acid and palmitic acid have been associated with coronary heart disease (Mori *et al.*, 2015; Hu *et al.*, 1999). Aconitic acid

has been associated with myocardial injury (Lewis *et al.*, 2008) and its isomer cis-aconitic acid has been associated with coronary heart disease (Tao *et al.*, 2019). 2,4-di-tert-butylphenol was suggested to prevent atherosclerosis through its antioxidant properties (Yoon *et al.*, 2006).

The extent of known metabolites captured with the GC/MS profiling approach allowed analysis of the association data in the context of biological pathways. One of the perturbed pathways in AVS patients was fatty acid biosynthesis. This finding is in consistent with a recent GWAS study in which fatty acid biosynthesis was causally associated with AVS (Chen *et al.*, 2020). In this study a genetic variant in FADS1/2 and omega-6 fatty acids biosynthesis were found associated with AVS. In my study, the plasma levels of the saturated fatty acids were altered in AVS patients. Which suggests that in addition to the polyunsaturated fatty acid biosynthesis, the saturated fatty acid biosynthesis is an important pathway in AVS patients.

The heart needs high rate of energy to sustain its contractile function. Usually, the heart obtains most of its energy from fatty acid β-oxidation. The perturbed fatty acids can stem from fatty acid biosynthesis in the liver, dietary fats, β-oxidation and fatty acid elongation (**Figure S 3**). Thus, any disruption of fatty acid oxidation can introduce energetic and functional consequences on the heart. Fatty acid biosynthesis was detected among the most significant altered pathways in AVS.

Our findings suggest that the candidate features associated with AVS are not associated to conventional cardiovascular disease risk factors such as hypertension, diabetes, and hyperlipidemia, or age and sex. In addition, the detected features were not associated to AVS through cholesterol levels, such as LDL and HDL-cholesterol, or BMI levels. Yet, urine scyllo-inositol, which was not identified as potential AVS biomarker, was associated with BMI levels. Scyllo-inositol is a product of dietary myo-inositol (Yap *et al.*, 2010) and can be produced by the gut microbiome (Hoffman *et al.*, 2019). Scyllo-inositol blocks Aβ plaques aggregation in the brain and is considered as a therapeutic agent against Alzheimer's disease (Hoffman *et al.*, 2019). Our results underline a potential association between BMI and scyllo-inositol.

Results from this study provide evidence of the application of GC/MS in quantitative analysis of urine and plasma metabolites in the context of a case control study and its power to identify a series of potential biomarkers and biological pathways underlying AVS risk that can be used for diagnostic purposes.

Figure S 3 : Data Dietary fats include (a) trans fats such as Elaidic acid which are unhealthy fats produced by industrially adding hydrogen to vegetable oil so that they can last longer , and it can be found in very small amount in bovine and caprine milk; (b) saturated fats such as (i) Stearic acid (octadecanoic acid C18:0) present in green bell pepper and oregano, (ii) Palmitic acid (hexadecenoic acid C16:0) present in palm oil, meats, cheeses, butter and dairy products, (iii) Myristic acid (tetradecanoic acid C14:0) present in animal and vegetable fats, coconut and nutmeg oils, bovine and breast milks, (iii) Lauric acid (dodecanoic acid) is the main fatty acid in coconut and palm kernel oils; unsaturated fats such as oleic acid present in olive oil, omega-3 and -6 present in fishes and vegetable oils. In the body palmitic acid (P.A.) can be produced in the liver via fatty acid (F.A.) biosynthesis. In addition, P.A. can be produced with F.A. elongation in the mitochondria (from myristic acid) and can be oxidized into myristic acid and then lauric acid with β-oxidation of F.A. in the mitochondria.

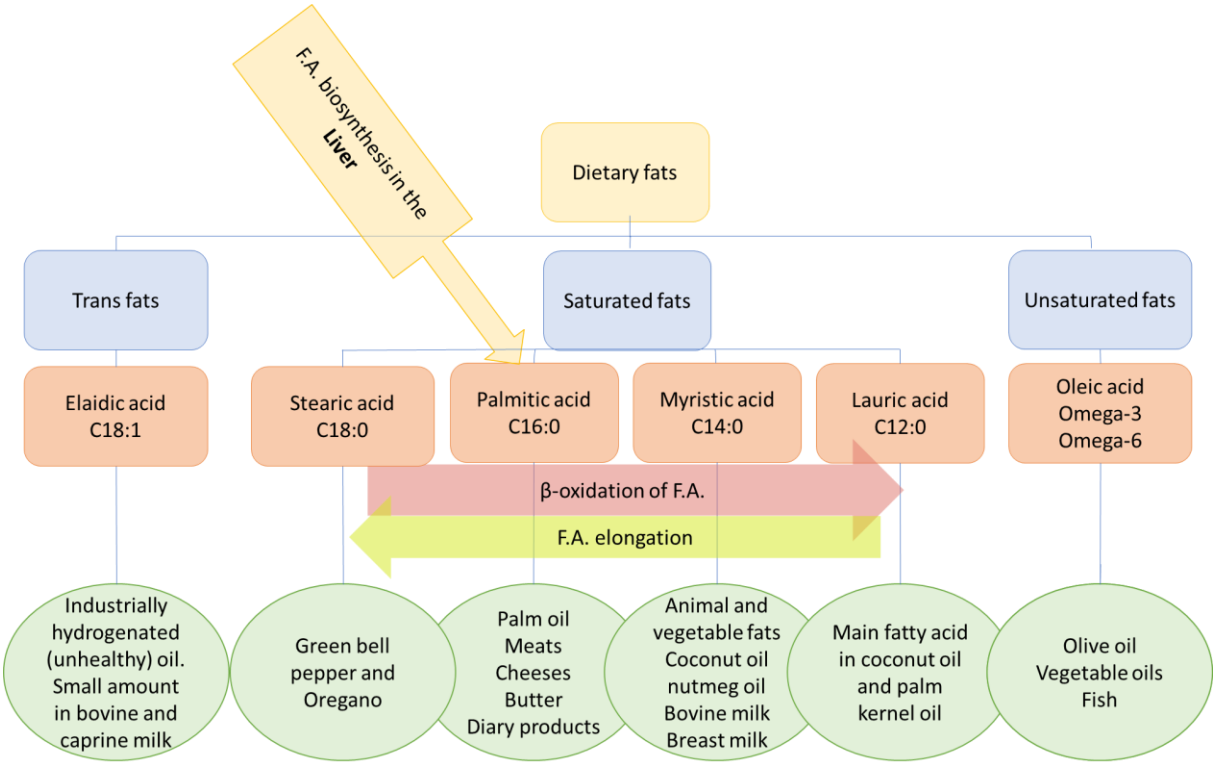

Chapter III: Metabolomic analysis of AVS based on ^{1}H-NMR profiling of urine samples

III.1: Introduction

NMR spectroscopy has been extensively used in metabolome-wide association studies and in the analysis of the genetic control of metabolite abundance in health and disease conditions in human cohorts of epidemiological scale (Suhre, Raffler and Kastenmüller, 2016; K, 2014; Suhre and Gieger, 2012). The technology is based on recording the signal of the interaction of radio frequency radiations with the nuclei of the molecules placed in a strong magnetic field (**Figure 21**). The magnetic field applied to the samples will cause the atoms to possess nuclear spin. Like any spectroscopy that relies on transition between energy states, the radio frequency will promote the transition between different nuclear energy levels. Therefore, after absorption of the radio frequency, the nuclei are promoted from low energy state to a high energy state depending on their environment and overall molecular structure (Ren *et al.*, 2015).

Figure 21 : NMR spectrometer

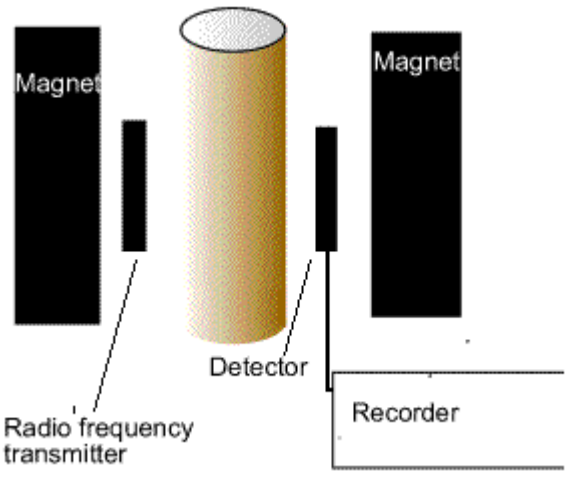

(From Analytical chemsitry-Proton NMR spectra. [online] dynamicscience.com.au. Available at :

http://www.dynamicscience.com.au/tester/solutions1/chemistry/analytical%20chem/nmr3.htm)

Proton nuclear magnetic resonance (^{1}H NMR) spectrometry is the most frequently used technology for large scale metabolome analyses as nearly all known metabolites contain hydrogen atoms, allowing detection of a vast range of metabolites. It is a rapid technique since it does not require derivatization and sample preparation involve only few steps. Also, provided that appropriate standard operating procedures (SOPs) are followed, there are limited variations between outputs from different apparatus since a single company (e.g. Bruker) manufactures NMR equipment and parts, allowing reproducibility of metabolome profiling results between laboratories. Finally, it is non-destructive since the samples do not go in contact with the detector which is the case in mass spectrometry (Ren *et al.*, 2015).

We have applied ^{1}H NMR spectroscopy to urine samples in the case control study already used for GC/MS metabolomics in order to test the capacity of ^{1}H NMR to identifying metabolites associated with AVS and evaluate complementarities of GC/MS and ^{1}H NMR in metabolome wide association studies. This work was submitted for publication in the *Journal of Proteome Research*.

III.2: Metabolic phenotyping of human urine using proton NMR spectroscopy reveals changes in the urinary metabolome caused by aortic valve stenosis.
Chronic administration of myristic and benzoic acids promotes mineralization and osteogenic transition in mouse model of obesity.

1H NMR Metabolomics Identifies Association between Urinary Trigonelline and Hippurate and Aortic Valve Stenosis. Submitted in the *Journal of Proteome Research* on February 18, 2021.

Cynthia Al Hageh, François Brial, Andrée E Gravel, Michael T Olanipekun, Sanjoy, Kumar Das, Rony S Khnayser, Fumihiko Matsuda, Daniel Auld, Marc-Emmanuel, Dumas, Mark Lathrop, Pierre A Zalloua, Dominique Gauguier

III.3: Discussion

The identification of differences in urine metabolites was achieved between 36 AVS cases and 40 controls based on ^{1}H NMR spectroscopy quantitative data. The discrimination between AVS and controls was detected through both untargeted and targeted ^{1}H NMR based metabolomics. Untargeted metabolomics allowed the identification of association between 27 unknown urine metabolites and signals corresponding to hippurate and AVS, with mostly positive regulation in AVS cases. Associations were independent of the presence of disease covariates such as age, sex, BMI, hyperlipidemia, hypertension and diabetes. In addition, the differentially regulated metabolites in AVS were not associated with cholesterol levels, LDL or HDL. Subsequent analyses using targeted metabolomics identified significant associations between AVS and elevated levels of trigonelline, hippurate and benzoate.

The strongest statistical evidence of association with AVS was obtained with trigonelline. Several studies have pointed to a direct or indirect implication of trigonelline in cardiovascular diseases. Trigonelline intake was found to have anti-diabetic effect (Yoshinari, Sato and Igarashi, 2009), to decrease serum levels of total-cholesterol and LDL-cholesterol (Zhang *et al.*, 2015), and to successfully reverse the effect of gut-microbiota choline metabolism on serum lipids (Anwar *et al.*, 2018). Trigonelline was found to reduce cell death and improve antioxidant effect and thus could be used to treat cardiovascular diseases mediated by oxidative stress (Ilavenil *et al.*, 2015) and it was negatively associated with acute coronary syndrome (Wang *et al.*, 2018). To our knowledge, the pathophysiological roles of hippurate and benzoate in cardiovascular diseases and AVS is unknown. Hippuric acid is a gut microbiota co-metabolite and a product of microbial aromatic amino acid, benzoic acid.

An important step in association studies that identified candidates (i.e. sequence variants in genes, transcripts, proteins or metabolites) or biological mechanisms underlying a disease condition lies in experimental validation of the hypotheses raised. In the absence of a robust and accurate rodent model of AVS, we carried out validation experiments of the association of these two metabolites in a mouse preclinical model of obesity induced by high fat diet feeding. This model system develops a wide range of anomalies relevant to insulin resistance, obesity, type 2 diabetes, non-alcoholic fatty liver disease, cardiovascular diseases as well as aortic valve

thickening (Zeng *et al.*, 2017) and calcification (Hofmann *et al.*, 2014). Results from cardiac gene expression in this model suggest that subcutaneous chronic administration of hippurate and benzoate might increase calcification via NF-κB, since the inhibition of NF-κB, a method to treat osteoporosis, inhibits vascular calcification. In addition, hippurate and benzoate may activate myofibroblast differentiation through CXCL9 and BMP-6. Their effects on inducing inflammation remains unclear since they promote the expression of some genes involved in inflammation while inhibiting others.

These results support the use of NMR metabolomics in metabolome-wide association studies carried out in large population studies. They also demonstrate the added value of combining distinct metabolome profiling technologies to increase the coverage of metabolites that can be detected and quantified. Correlation analyses between NMR and GC/MS data collected in the same individuals allowed metabolite annotations of NMR spectral signals. Combining NMR and GC/MS technologies in this case control study identified complementary sets of metabolites associated with AVS and pointed to similar or convergent biological pathways underlying disease risk.

Chapter IV: Lipidomic analysis of plasma in AVS based on MALDI-TOF/MS

IV.1: Introduction

MALDI-TOF/MS (matrix-assisted laser desorption/ionization-time of flight mass spectrometry) is able to analyze large and/or labile molecules such as peptides, lipids, polymers and proteins (Yang and Han, 2016). Although MALDI-TOF/MS is established technique for proteomics, its use in lipidomics has increased and it is now increasingly used for lipid analysis. MALDI-TOF/MS is sensitive, fast, can tolerate impurities (buffers, salts, and detergents), requires small amount of samples and simple procedures for sample preparation, generates very simple mass spectra and can analyze various lipid molecules simultaneously (Hidaka *et al.*, 2007; Fuchs, Süss and Schiller, 2010). MALDI-TOF MS uses matrices that absorb the laser energy and mediate ions generation.

In MALDI-TOF/MS analyte sample is mixed with matrix, then exposed to laser to form gas-phase ions that are measured in time-of-light (TOF) mass analyzers, lighter ions are faster than the heavier ones, so they arrive first at the detector (**Figure 22**) (Kapoor, Ladak and Gomase, 2009). TOF-MS allows high mass accuracy and decrease mass overlapping. The matrix is used to co-crystalize the sample and to absorb the energy emitted by the sample when hit with pulse laser beam, consequently the matrix is vaporized carrying the analyte molecules into the vapor phase. Ions such as H^+ and Na^+ are exchanged in this phase, resulting in the formation of charged analytes called adducts also known as quasimolecular ions. Cations are analyzed in the positive-ion mode while the anions in the negative-ion mode. The m/z of quasimolecular cations or anions is higher or lower respectively (± 1 for H^+ and ± 23 for Na^+) in comparison to the analyte molecule.

The carboxylic acids are used as matrices (such as 2,5-DHB and α-CHCA) because they trigger the formation of H^+ and Na^+ adducts (Fuchs, Süss and Schiller, 2010). After the formation of ions, they are accelerated in an electric field, then separated by their mass. MALDI uses two acquisition modes, the linear mode typically for larger molecules and the reflector mode for smaller ones. In the reflector mode the resolution and peak widths are improved, owing to the longer distance of ions in the flight tube and the reflectron's mass resolving power, allowing the detection of molecule's individual isotopes (**Figure 22**) (Fuchs, Süss and Schiller, 2010).

Figure 22 : MALDI-TOF/MS data acquisition after the separation of analytes based on their m/z via a time a flight measurement

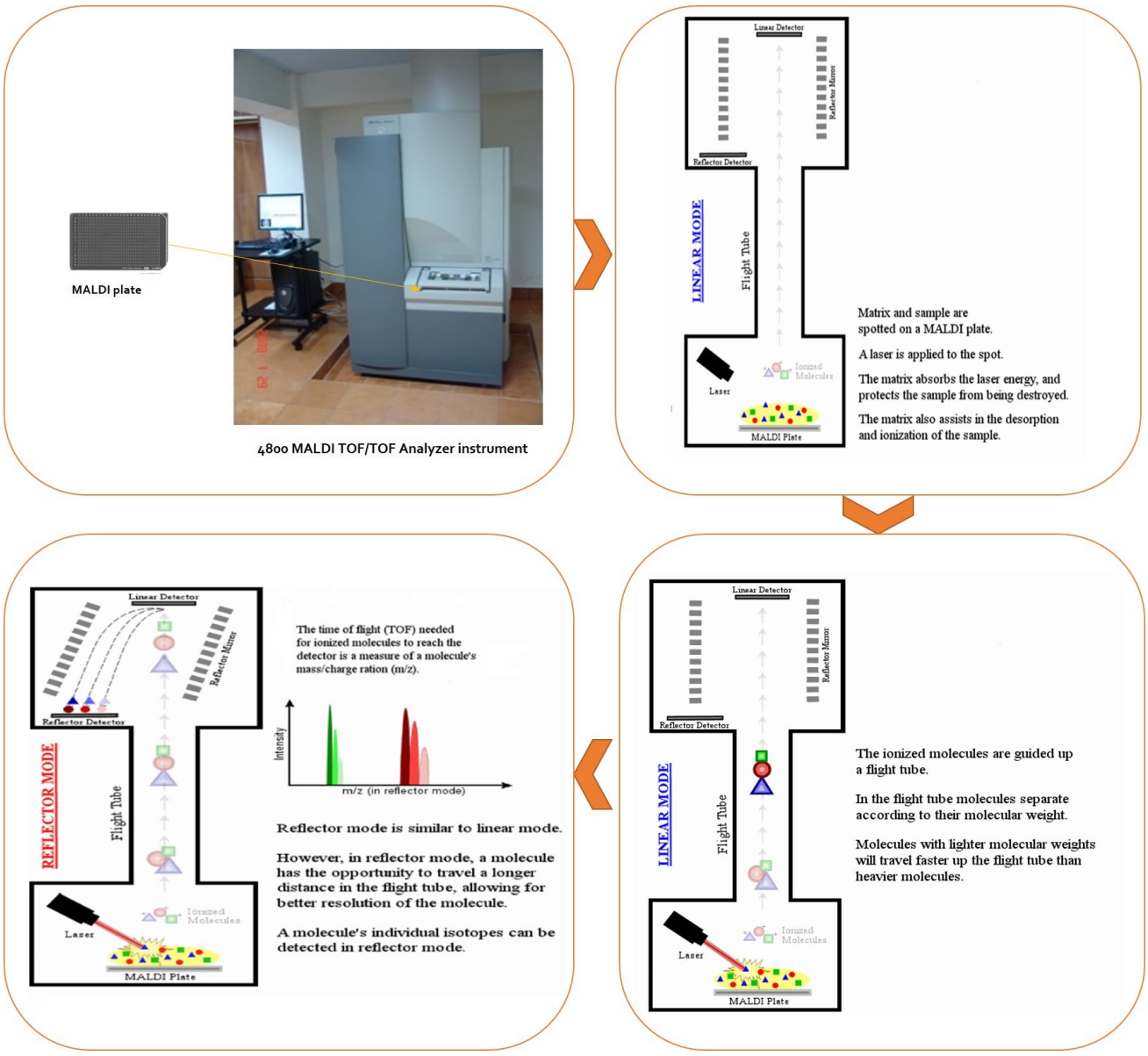

(From Protein and Nucleic Acid (PAN) Facility. [online] csbf.stanford.edu. Available at : https://csbf.stanford.edu/pan/section_html/MS/index.html)

MALDI relies on the co-crystallization of the sample with the matrix, whereas other MS techniques use liquid samples. The homogeneity of these co-crystals is limited because of the solvent mixtures with different volatilities used, making the quantification with MALDI-TOF/MS somewhat difficult. Furthermore, the extraction method, storage and method-inherent parameters can influence the shape of MALDI spectra. In addition, the laser intensity used has an important effect since the absorption of the laser energy depends on the absorption properties of the matrix used and on the matrix/analyte ratio (Zschörnig *et al.*, 2006).

Despite some disadvantages, MALDI-TOF/MS has been increasingly used for lipidomic studies due to its ease to use, sensitivity and high throughput (Serna *et al.*, 2015). Conventional MALDI matrices, such as α-CHCA and 2,5-DHB, produce interfering ions that cluster in the low-mass region (<500 Da), thus masking the detection of small molecules metabolites such as lipids. These limitations restrain the application of MALDI-TOF/MS with conventional matrices in metabolomics (Shroff *et al.*, 2009). The desired features of MALDI-TOF/MS matrix are: (1) ionize/desorb the sample and subsequently yield acceptable signal-to-noise ratio (S/N), (2) absorb laser irradiation (high absorbance at the emission wavelength of the laser in our case at 337 nm, this requires matrix compound with aromatic residues) and minimize or prevent analyte fragmentation , (3) possess low background signal in order to minimize interference between the analyte and matrix ions, and (4) it should provide only single adduct of the analyte without the formation of analyte-matrix clusters (Fuchs, Süss and Schiller, 2010).

Phospholipids (PLs), lysophospholipids (LysoPLs), sphingolipids(SLs), triglycerides (TGs), cholesteryl esters (CEs), and free cholesterol may be identified using MALDI-TOF/MS (Hidaka *et al.*, 2007). Thus MALDI-TOF/MS is able to analyze polar and non-polar lipids, and could detect hydrophobic and non-polar molecules such as cholesterol, CEs and TGs, as well as polar and hydrophilic molecules such as PLs (Hidaka *et al.*, 2007). Phosphatidylcholine (PC), lysophosphatidylcholine (LysoPC) and sphingomyelin (SM) contain a choline group known as quaternary amine group and are therefore always ionized and readily detected in MALDI positive ion mode. Therefore, these phospholipids tend to suppress the detection of the other phospholipid classes such as the non-quaternary ammonia lipids (Berry *et al.*, 2011).

In additional to MS acquisition, structural assignment of certain lipids requires a collisional activation of the sample desorbed ions in both positive and negative ion mode. Using CID (collision-induced dissociation), resulting spectra can be useful for lipid identification. For

instance, the CID of the protonated molecules ($[M+H]^+$) of PC, plasmalogen-PC, and SM lipids ends up with the detection of a phosphocholine ions at m/z 184. The ion m/z 184 is considered as a diagnostic ion of the phosphocholine polar headgroup and reveals that the lipid contains choline (**Figure 23**). To specify whether this phosphocholine ion is derived from PC or SM, one can use the following rule: if the precursor $[M+H]^+$ has an even m/z, it is likely a PC, and if the ion $[M+H]^+$ has an odd m/z, the ion is likely derived from a SM.

Figure 23 : (a) Representative mass spectrum in positive ion mode after data acquisition using MALDI-TOF/MS. Mass-to-charge ratios (x-axis) are plotted against the peak intensity (y-axis). (b) CID spectrum of a precursor ion at m/z 496.3 (Lysophosphatidylcholine 16:0) where the daughter peaks detected at m/z 184 (phosphocholine) and at m/z 104 (choline).

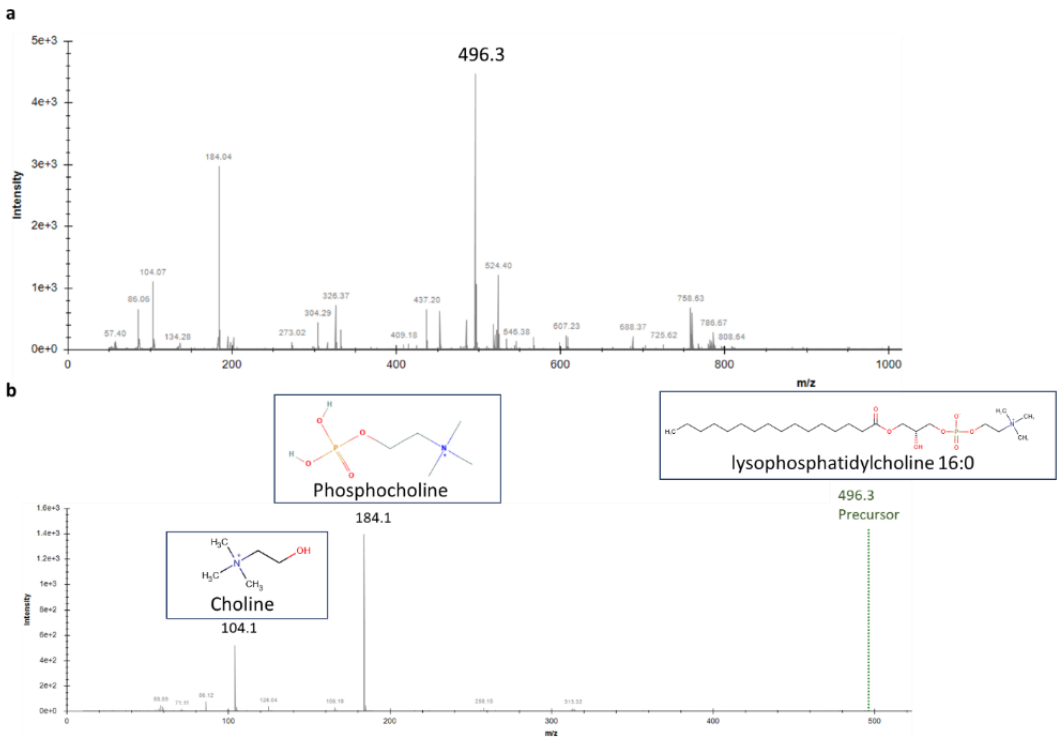

CID of $[M+Na]^+$ and $[M+K]^+$ of PC and SM include neutral loss of trimethylamine (TMA) of 59 Da and neutral loss of phosphocholine of 183 Da (Ho and Huang, 2002). Moreover m/z 147 in the CID spectra of the sodiated PC and SM correspond to [1,2-phosphodiester $+Na]^+$ (Murphy, Hankin and Barkley, 2009; Berry *et al.*, 2011).

It is important to note that CID data do not provide information about the position and the geometry of double bonds in fatty acyl chains of lipids. In addition, the position of unsaturation

is assumed only based on the most common fatty acyls and this uncertain assumption can be problematic since lipids differing only in double-bond position can have different biochemical properties (Berry *et al.*, 2011). Oxidation of GPLs plays an important role in biochemical processes. Thus, several low peaks can be detected that belong to oxidized LysoPCs (e.g. m/z 534, 536, 538, 550, 552, and 554) and PCs (e.g. m/z 772 and 774) (Milman, Lugovkina and Zhurkovich, 2017).

This part of the project aimed at identifying differentially present plasma lipids using MALDI-TOF/MS in the case control study using the same samples used in GC/MS and ^{1}H NMR analyses. Lipidomics is a subset of metabolomics that allow the detection of lipids. This part was performed to get an integrated analysis combining the metabolomics performed in the previous sections and lipidomics which offers a more detailed understanding of complex molecular mechanisms in AVS pathogenesis.

IV.2: MALDI-TOF/MS -based lipidomic: changes in human plasma metabolites in aortic valve stenosis patients involve intermediates of choline pathway

MALDI mass spectrometry was used for lipidomic analysis of 92 plasma samples segregated between AVS patients and healthy controls. MALDI raw data were extracted in the negative and positive MALDI reflector modes and the product ions of lipids were measured using MALDI-TOF MS/MS. The resulting spectra were pre-processed with BioNumerics software where noise filtering, baseline correction, normalization, peak alignment, and peak detection were applied. Reserpine, an internal standard used to evaluate data acquisition with MALDI-TOF MS and to facilitate peak alignment in data pre-processing.

The dataMatrix obtained were normalized to the median. 89 ions and 17 ions were detected in the positive and negative ion modes respectively using 2,4-DHB matrix dissolved in chloroform/methanol/water ($CHCl_3$/MeOH/water) (**Figure 24 A and B**; **Annex Table 1, page 215**); 84 ions and 16 ions were detected in the positive and negative ion modes respectively using 2,4-DHB matrix dissolved in diluted methanol (MeOH/water) (**Figure 24 C and D**; **Annex Table 1**); 33 ions and 7 ions were detected in the positive and negative ion modes respectively using α-CHCA matrix (**Figure 24 E and F**; **Annex Table 1**); 26 ions were detected in the negative ion mode using 9-AA matrix (**Figure 24 G**; **Annex Table 1**). Of all peaks, 29 peaks were successfully identified using the literature and the CID spectrum of each ion (**Table 4**).

Figure 24 : Representative mass spectra acquired in the positive and negative ion modes. Mass spectra obtained in the positive (**A**) and negative (**B**) ion modes using 2,4-DHB matrix dissolved in chloroform/methanol/water; Mass spectra obtained in the positive (**C**) and negative (**D**) ion modes using 2,4-DHB matrix dissolved in diluted methanol; Mass spectra obtained in the positive

(**E**) and negative (**F**) ion modes using α-CHCA matrix; Mass spectrum (**G**) obtained in the negative ion mode using 9-AA matrix.

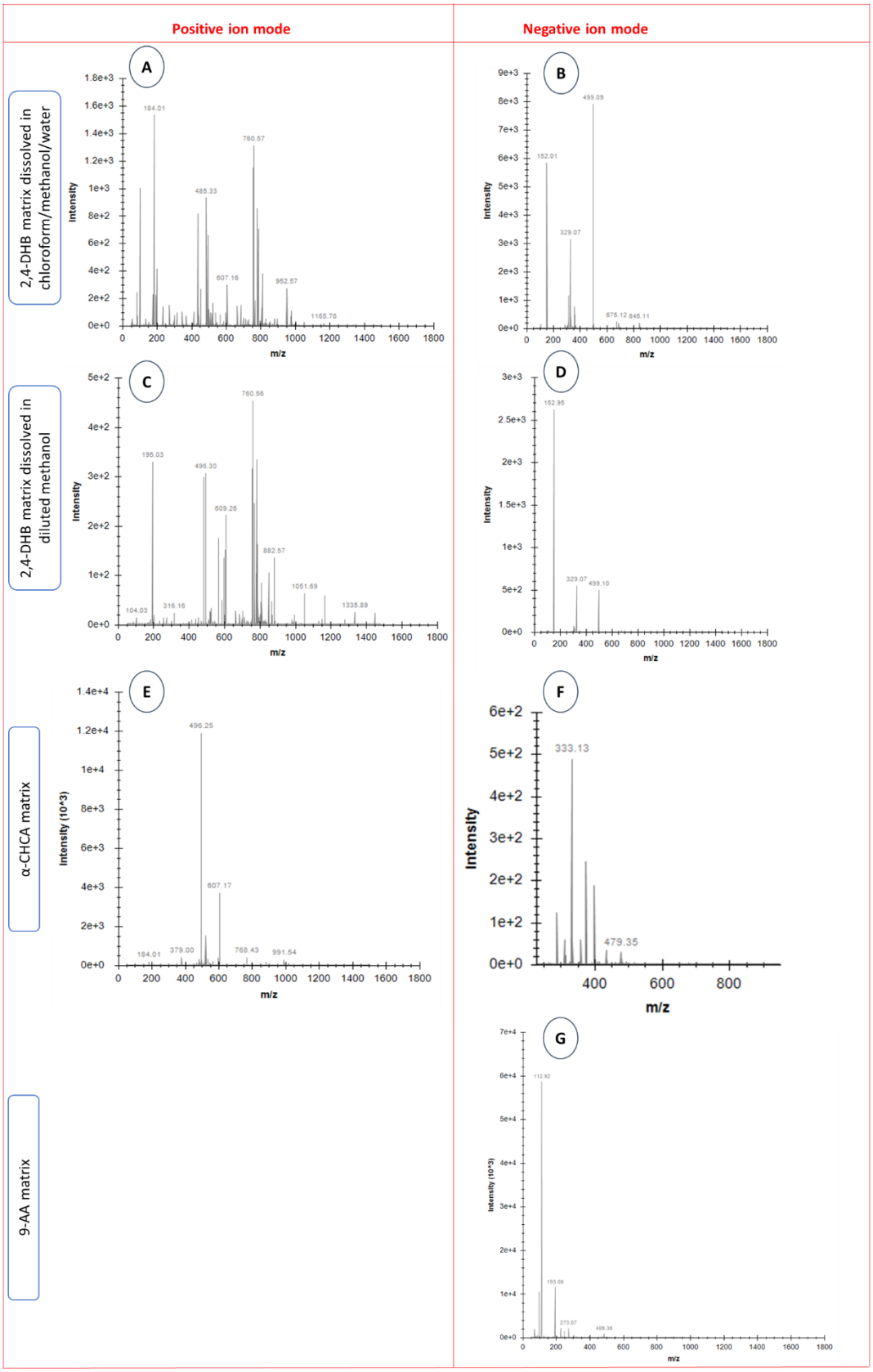

Table 4 : Adduct ions identified based on the literature after MALDI-TOF/MS and MS/MS data acquisition. TMA (trimethylamine); m/z (mass-to-charge ratio).

Group	m/z	Assignment	Adduct ion	Daughter peaks				References
				Choline	Phosphocholine ion	1,2-phosphodiester +Na	Neutral loss of TMA [M+Na-59]+	
	258.1	Glycerophosphocholine	[M+H]+					9
	369.35	Cholesterol	[M+H-H2O]+					1,2,9
Cyclophosphatidic acid	415.21	CPA(16:0)	[M+Na]+					9
Lysophosphatidic acid	485.4	LysoPA(22:4)	[M-H]-					8
Lysophosphatidylcholine	496.3	LysoPC(16:0/0:0)	[M+H]+	104.14	184.12			2,4,5,6,7,11
Lysophosphatidylethanolamine	498.1	LysoPE(20:5)	[M-H]-					8
Lysophosphatidylcholine	518.31	LysoPC(16:0/0:0)	[M+Na]+				459.29	2,4,6,9,11
Lysophosphatidylcholine	518.31	LysoPC(18:3/0:0)	[M+H]+	104.13	184.11			7,11
Lysophosphatidylcholine	520.34	LysoPC(18:2/0:0)	[M+H]+	104.13	184.11			3,5,6,7,11
Lysophosphatidylcholine	522.36	LysoPC(18:1/0:0)	[M+H]+	104.13	184.1			6,7,11
Lysophosphatidylcholine	524.37	LysoPC(18:0/0:0)	[M+H]+	104.14	184.12			2,3,4,5,6,7,9,11
Oxidized-Lysophosphatidylcholine	534.3	LysoPC(ox 18:3)	[M+H]+					11,
Lysophosphatidylcholine	544.34	LysoPC(18:1/0:0)	[M+Na]+					6,9,11
Lysophosphatidylcholine	544.34	LysoPC(20:4/0:0)	[M+H]+	104.13	184.11			3,7,11
Lysophosphatidylcholine	546.35	LysoPC(18:0/0:0)	[M+Na]+				487.29	4,6,9,11
Lysophosphatidylcholine	546.36	LysoPC(20:3/0:0)	[M+H]+	104.12	184.1			3,7,11
Phosphatidylcholine	758.79	PC 34:2	[M+H]+	104.13	184.09			1,5,6,7,10,11
Phosphatidylcholine	760.53	PC 34:1	[M+H]+		184.1			1,4,5,6,7,10,11
phosphatidylcholine plasmalogens	768.55	PC O-36:4	[M+H]+		184.19			7
Phosphatidylcholine	780.57	PC 34:2	[M+Na]+					1,5.6,9,11
Phosphatidylcholine	780.6	PC 36:5	[M+H]+					3,7,11

Sphingomyelin	781.59	SM 38:1	[M+Na]+					7
Phosphatidylcholine	782.59	PC 34:1	[M+Na]+			147		1,5,6,9,11
Phosphatidylcholine	782.6	PC 36:4	[M+H]+		184.1			1,3,7,10,11
Phosphatidylcholine	784.61	PC 36:3	[M+H]+					3,5,6,7,11
Phosphatidylcholine	786.63	PC 36:2	[M+H]+		184.11			1,5,6,7,11
Sphingomyelin	787.64	SM 40:1	[M+H]+					10
Phosphatidylcholine	788.6	PC 36:1	[M+H]+					5,7
phosphatidylcholine plasmalogens	796.58	PC O-38:4	[M+H]+					7
Phosphatidylcholine	796.6	PC 34:2	[M+K]+					5
Phosphatidylcholine	804.58	PC 36:4	[M+Na]+			147.01		1
Phosphatidylcholine	806.6	PC 36:3	[M+Na]+					5,6,9
Phosphatidylcholine	806.6	PC 38:6	[M+H]+					1,3,4,7
Phosphatidylcholine	808.58	PC 36:2	[M+Na]+			147.01		1,6,9
Phosphatidylcholine	808.59	PC 38:5	[M+H]+		184.09			3,7
Phosphatidylcholine	810.6	PC 38:4	[M+H]+		184.07			1,3,4,7
Phosphatidylcholine	812.62	PC 38:3	[M+H]+					7

1. Schiller et al., 2001 ; 2. Hidaka et al., 2007 ; 3. Guerrera et al., 2009; 4. Fuchs et al., 2010 ; 5. Zemski Berry et al., 2011 ; 6. Preianò et al., 2012 ; 7. Serna et al., 2015 ; 8. Wang et al., 2015; 9. Korte et al., 2016 ; 10. Tipthara and Thongboonkerd, 2016 ; 11. Milman et al., 2017

IV.2. 1. 2,4-DHB matrix in $CHCl_3$/MeOH/water using positive ion mode

Univariate data analysis using volcano plot was applied to detect significantly different ions between AVS patients and healthy controls. 9 significant ions (**Table 5**) were detected in the positive ion mode using 2,4-DHB matrix dissolved in $CHCl_3$/MeOH/water. Four ions were downregulated in the plasma of AVS patients and they were detected at mass to charge ratio (m/z) 201.96, m/z 453.16, m/z 453.82, and m/z 534.30 assigned to [Oxidized-lysoPC 18:3 $+H]^+$; five ions were upregulated in AVS patients detected at m/z 782.59 assigned to either [PC 34:1 $+Na]^+$ or [PC 36:4 $+H]^+$, m/z 783.57, m/z 808.56 assigned to [PC 36:2 $+Na]^+$ or [PC 38:5 $+H]^+$, m/z 810.56 assigned to [PC 36:1 $+Na]^+$ or [PC 38:4 $+H]^+$, and m/z 811.43 (**Figure 25**).

Figure 25 : MALDI data acquired in the positive ion mode using 2,4-DHB matrix dissolved in $CHCl_3$/MeOH/water. (A) Volcano plot showing the significant ions (red dots); (B) Boxplot of the significant peaks detected at m/z 201.96, 453.16 , 453.82, 534.30, 782.59, 783.57, 808.56, 810.56 and 811.43

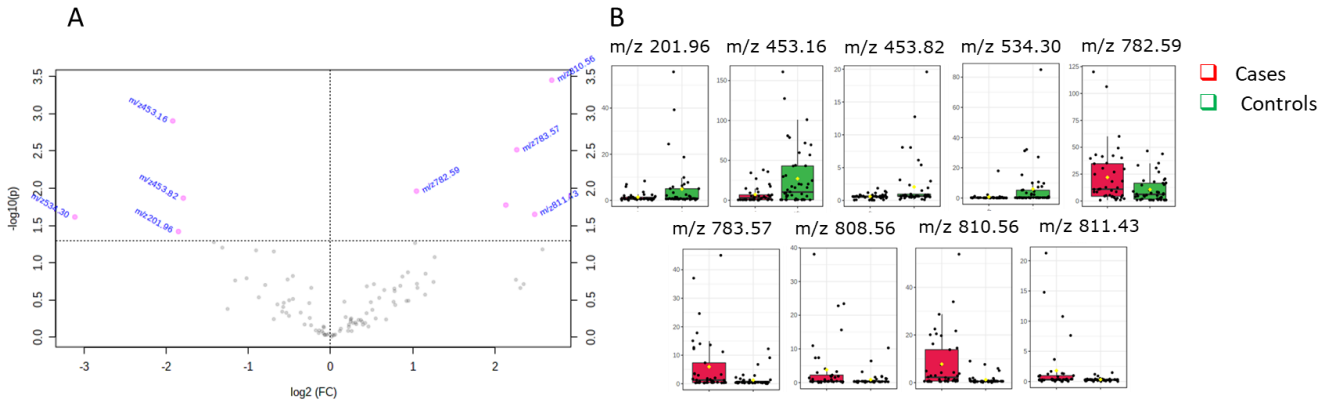

IV.2. 2. 2,4-DHB matrix in MeOH/water in positive ion mode

Based on volcano plot, 11 significant ions (**Table 5**) were detected in the positive ion mode using 2,4-DHB matrix dissolved in MeOH/water. Six ions m/z 155.84, m/z 298.37, m/z 319.75, m/z 360.82, m/z 361.81 and m/z 534.29 assigned to [oxidized-LysoPC 18:3 $+H]^+$were downregulated in AVS patients; while five ions were upregulated in AVS patients detected at m/z 541.63, m/z544.37 assigned to [LysoPC 20:4 $+H]^+$, m/z782.53 assigned to [PC 34:1 $+Na]^+$ or [PC 36:4 $+H]^+$, m/z785.60, m/z806.48 assigned to either [PC 36:3 $+Na]^+$ or [PC 38:6 $+H]^+$ (**Figure 26**).

Figure 26: MALDI data acquired in the positive ion mode using 2,4-DHB matrix dissolved in MeOH/Water. (A) Volcano plot showing the significant ions (red dots); (B) Boxplot of the significant peaks detected at m/z 155.84, 298.37, 319.75, 360.82, 361.81, 534.29, 541.63, 544.37, 782.53, 785.60 and 806.48

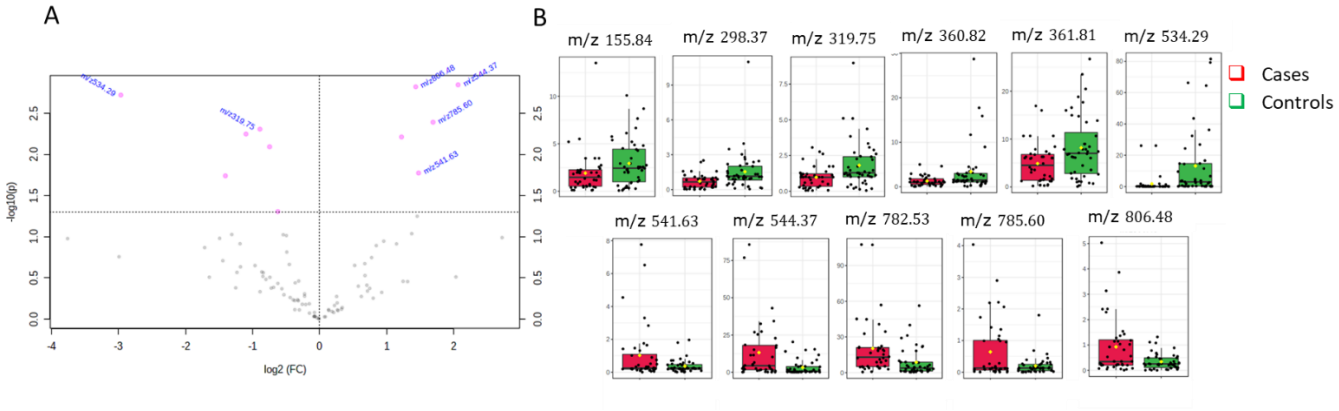

IV.2. 3. Alfa-CHCA matrix in positive ion mode

Two significant ions (**Table 5**) were detected in the positive ion mode using α-CHCA matrix. m/z 534.3 assigned to [oxidized-LysoPC 18:3 +H]$^+$ which was downregulated in AVS patients and m/z 544.3 [LysoPC 20:4 +H]+ which was upregulated in AVS (**Figure 27**).

Figure 27: MALDI data acquired in the positive ion mode using α-CHCA matrix. (A) Volcano plot showing the significant ions (red dots); (B) Boxplot of the significant peaks detected at m/z 534.3 and 544.3

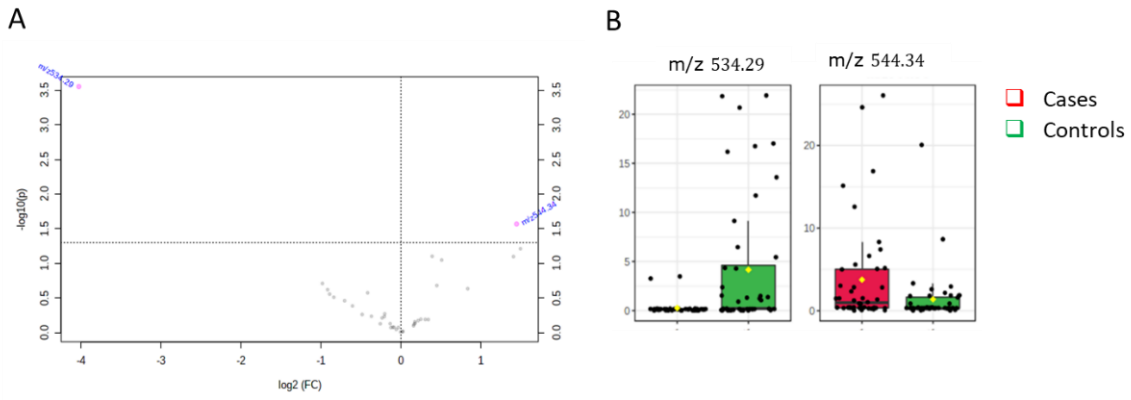

IV.2. 4. 9-AA matrix in negative ion mode

Using 9-AA matrix in the negative ion mode, the ion at m/z 353.04 was downregulated while that at m/z 97.12 was upregulate in AVS cases when compared to healthy controls (**Figure 28 and Table 5**).

Figure 28: MALDI data acquired in the negative ion mode using 9-AA matrix. (A) Volcano plot showing the significant ions (red dots); (B) Boxplot of the significant peaks detected at m/z 97.12 and 353.04

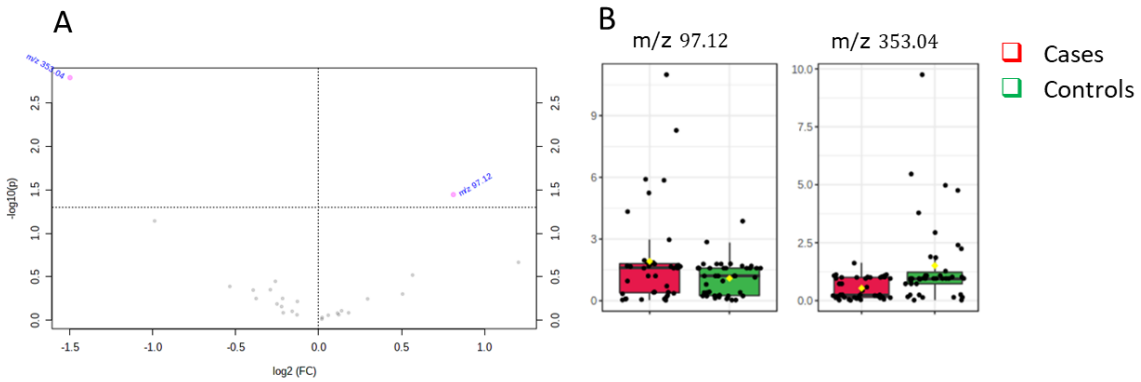

IV.2. 5. 2,4-DHB matrix in $CHCl_3$/MeOH/water, negative ion mode

Only one peak detected at m/z 345.06 was found significantly different between cases and controls when the data were acquired in the negative ion mode with 2,4-DHB matrix dissolved in $CHCl_3$/MeOH/water (**Figure 29 and Table 5**).

Figure 29: MALDI data acquired in the negative ion mode using 2,4-DHB matrix dissolved in $CHCl_3$/MeOH/water. (A) Volcano plot showing the significant ion (red dot); (B) Boxplot of the significant peak detected at 345.06

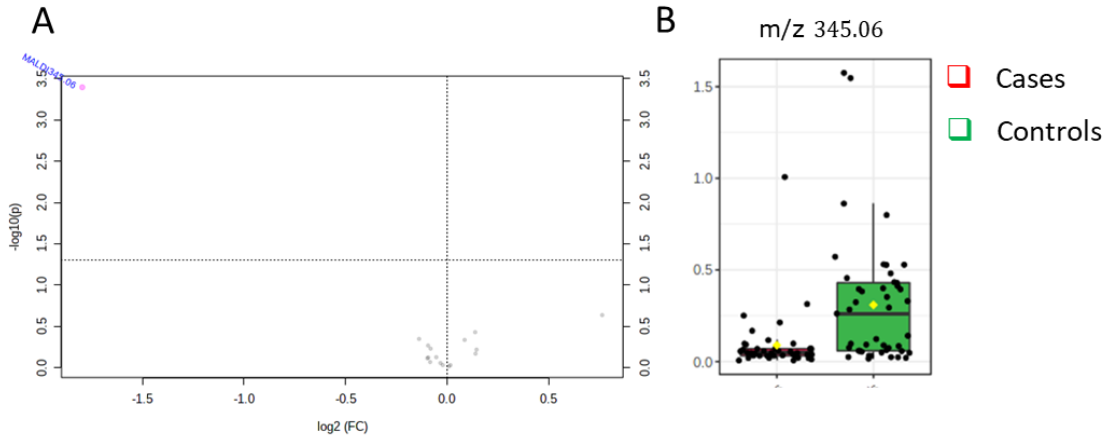

IV.2. 6. 2,4-DHB matrix in MeOH/water, negative ion mode

In the negative ion mode and using 2,4-DHB dissolved in MeOH/water as matrix, one ion at m/z 345.16 was found significantly different between AVS and controls (**Figure 30 and Table 5**).

Figure 30: MALDI data acquired in the negative ion mode using 2,4-DHB matrix dissolved in MeOH/Water. (A) Volcano plot showing the significant ion (red dot); (B) Boxplot of the significant peak detected at m/z 345.16

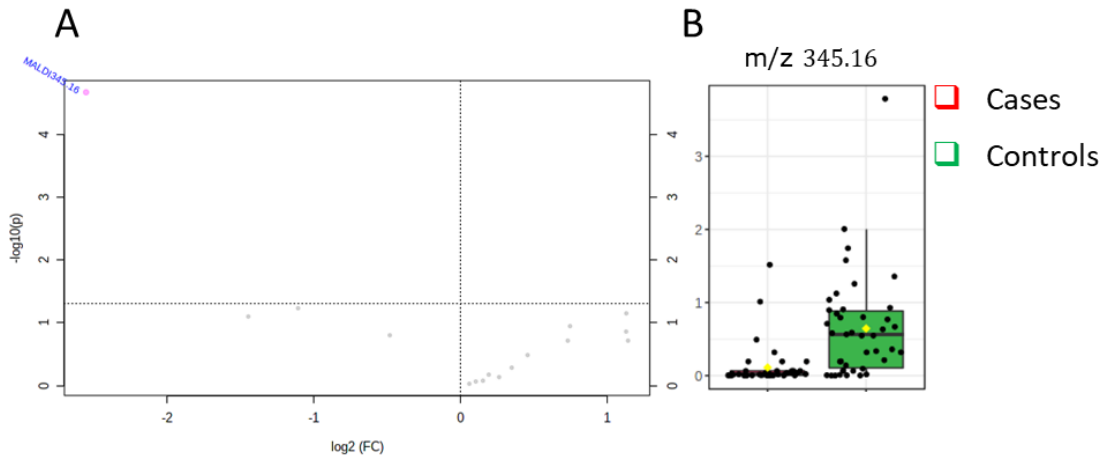

Table 5 : **Plasma ions contributing to the separation between the AVS patients and healthy controls detected using MALDI-TOF/MS in the positive and negative ion modes.** p-values are calculated from a volcano plot; $[M+Na]^+$ are the sodiated adducts; $[M+H]^+$ are the protonated adducts; CHCA (alfa-cyano-4-hydroxycinnamic acid matrix); DHB CMW (2,5- Dihydroxybenzoic acid matrix dissolved in chloroform/methanol/water); DHB MeOH (DHB matrix dissolved in diluted methanol); 9-AA (9-aminoacridine matrix)

Ion mode	Matrix	m/z	Cases/Controls	P-value	$[M+Na]^+$	$[M+H]^+$
Positive	CHCA	534.29	Down	0.000281		lysoPC(ox 18:3)
	CHCA	544.34	Up	0.027015		lysoPC(20:4)
Positive	DHB CMW	201.96	Down	0.038133		
	DHB CMW	453.16	Down	0.001246		
	DHB CMW	453.82	Down	0.013552		
	DHB CMW	534.30	Down	0.024324		lysoPC(ox 18:3)
	DHB CMW	782.59	Up	0.010923	PC 34:1	PC 36:4
	DHB CMW	783.57	Up	0.003042		
	DHB CMW	808.56	Up	0.016811	PC 36:2	PC 38:5
	DHB CMW	810.56	Up	0.000353	PC 36:1	PC 38:4
	DHB CMW	811.43	Up	0.022411		
Positive	DHB MeOH	155.84	Down	0.049335		
	DHB MeOH	298.37	Down	0.005634		
	DHB MeOH	319.75	Down	0.004914		
	DHB MeOH	360.82	Down	0.018153		
	DHB MeOH	361.81	Down	0.008047		
	DHB MeOH	534.29	Down	0.001893		lysoPC(ox 18:3)
	DHB MeOH	541.63	Up	0.016763		
	DHB MeOH	544.37	Up	0.001422		lysoPC(20:4)
	DHB MeOH	782.53	Up	0.006116	PC 34:1	PC 36:4
	DHB MeOH	785.60	Up	0.004045		
	DHB MeOH	806.48	Up	0.001502	PC 36:3	PC 38:6
Negative	9-AA	353.04	Down	0.001621		
	9-AA	97.12	Up	0.035859		
Negative	DHB CMW	345.06	Down	0.000405		
Negative	DHB MeOH	345.16	Down	2.11E-05		

IV.3: Discussion

In this part of the work, lipidomic analysis based on MALDI-TOF/MS was applied on plasma samples of AVS patents and healthy controls in order to detect differential features between the two groups. Different matrices were used to cover as many lipids as possible in the extracted samples. Usually, the matrix co-crystalizes with the samples and mediates ions generation. In our data, cholesterol, lysophosphatidylcholines (lysoPCs), phosphatidylcholine (PCs), sphingomyelins (SMs), lysophosphatidic acid (lysoPAs) and lysophosphatidylethanolamine (lysoPEs) were successfully annotated and detected as $[M+H]^+$, $[M+K]^+$, $[M+Na]^+$, $[M+H-H_2O]^+$ and $[M-H]^-$ ion adducts in plasma samples.

After median normalization of the MALDI data, 22 known and unknown ions were found significantly different between AVS patients and controls. Among the known lipids, lysoPC, oxidized-lysoPC and PCs were able to distinguish AVS cases from controls. Data were replicated using different matrices. The protonated ion of oxidized-lysoPC 18:3 was found significantly downregulated in AVS patients using the three matrices in the positive ion mode; the protonated lysoPC 20:4 was found upregulated when the data were acquired with both matrices α-CHCA and 2,4-DHB dissolved in MeOH/Water; and the ion detected at 782.53 (attributed to sodiated PC 34:1 or protonated PC 36:4) was found also upregulated when using 2,4-DHB dissolved in MeOH/Water and in $CHCl_3$/MeOH/water. At m/z 806.48, 808.56 and 810.56 the ions could be from either sodiated PC (PC 36:3, PC 36:2, PC 36:1 respectively) or protonated PC (PC 38:6, PC 38:5, PC 38:4 respectively). All these lipids followed the same regulation pattern, they were systematically upregulated in AVS when compared to controls. The univariate analysis also pointed to 15 significantly differential ions that correspond to unknown lipids where 10 of them where downregulated in plasma of AVS patients. This ambiguous metabolite annotation should be improved in addition to the chemical attribution of the remain unknown ions. In Guasch-Ferré et al 2017, an evaluation of the association between choline pathway metabolites and risk for cardiovascular disease was made. It was found that plasma metabolites from choline pathway were associated with an increased risk of cardiovascular disease (Guasch-Ferré *et al.*, 2017).

These results support the added value of lipidome analysis using MALDI-TOF/MS and the power of the integration of metabolome and lipidome in the analysis. This integrated analysis

enables a complete view of the metabolic profile and a comprehensive study of the biological pathways that combine lipids and other metabolites linked to AVS development and progression.

Chapter V: Conclusion

Researchers working on the identification of molecular biomarkers underlying the etiopathogenesis of chronic diseases have considerably progressed given all the advances in metabolomic profiling technologies (Rhee and Gerszten, 2012). The latter can also assist in understanding biological pathways involved in these diseases (Sana, Waddell and Fischer, 2008). In this work, we performed comprehensive metabolic analyses in a single study population using distinct analytical tools to detect and quantify variations in the metabolome in two human biofluids, urine and plasma, to identify the metabolites associated with calcific aortic valve stenosis (AVS).

Metabolic Profiling using Human Biofluids

Although any human biospecimen is amenable to metabolic profiling, analysis of human biofluids has advantages over tissue and cell analyses, such as ease of sample acquisition and minimal sample preparation (Oakman *et al.*, 2011). Unlike heart tissue, which can only be extracted during aortic valve replacement or from post-mortem cases, biofluids such as plasma and urine can be readily extracted from living subjects. In the context of clinical applications of improved methods for systematic diagnostic screening in large populations, biofluids are the biological matrices where disease associated biomarkers should be investigated. Therefore, the potential ability of metabolomic tools to extract information from biofluids may help in early diagnosis of AVS and improve prognosis. Both urine and plasma are rich sources of metabolomic information. Urine is an ideal biofluid for disease studies because it is easy to obtain with non-invasive technique in large quantities, and provides a global overview of metabolic regulation over long periods of time, whereas plasma or serum provide a snapshot of the metabolism at the time of sample collection (Bouatra *et al.*, 2013; Zhang *et al.*, 2012). All urine metabolites should be present in the blood since the kidneys extract the soluble wastes from the blood to form urine. However, there are more and unique metabolites in urine than in blood, due to the fact that the kidney concentrates certain metabolites from the blood, so the metabolites that are in very low concentration in blood are more abundant and well identified in urine (Bouatra *et al.*, 2013).

Multiple Analytical Tools to Cover the Human Metabolome

Metabolites have specific features of concentration, size, polarity, and biological location. For this reason, the application of several analytical tools is required to fully cover the metabolome of a biospecimen. Most metabolomic studies in the past have been performed using a single analytical tool. The work presented in this thesis demonstrates the added value of using several metabolomic data acquisition technologies and complementary analytical techniques to maximize the coverage of the metabolome. In this study, both NMR and MS techniques were applied. These two techniques are complementary, and they have their specific strengths and weaknesses. Thus, each approach can detect and quantify a specific set of metabolites and combining the two techniques results in increasing the range of captured metabolites. In general, NMR is characterized by the detection of the most-concentrated metabolites, while MS is characterized by the discovery of readily ionized metabolites (Bhinderwala *et al.*, 2018). NMR is reproducible, requires minimal sample preparation, and gives quantitative and structural information. Yet, NMR has low sensitivity and has fewer identification methods, while MS tools are more sensitive and have better coverage of metabolites than NMR (Chen and Kim, 2016). In the present study, we applied ^{1}H NMR spectroscopy to detect urinary metabolome because it has been proven to be particularly useful to analyze urine metabolomics (Chen and Kim, 2016). GC/MS was applied to detect both urinary and plasma metabolomes. MALDI-TOF/MS was applied to study the lipidome of plasma samples since urine biofluidis more hydrophilic and subsequently is not a good matrix for lipidomics.

The same urine samples were analyzed using GC/MS and NMR. This analysis led us to discover the correlation between the two datasets, which allowed the identification of numerous features. Also, this correlation can provide insights into common biological processes and pathways since it identified many GC/MS features associated with the same NMR feature. This should contribute to improve our understanding of how metabolites are related to each other. In the human body, there is an estimated 15,000 metabolites. Yet, metabolomics approaches allow the unambiguous identification of only a few hundred metabolites. Therefore, peak assignment remains underdeveloped in both NMR and MS-based techniques, which is due to the limitations in reference spectra, metabolite databases, and analytical softwares. Thus, in every metabolomic study, there are misidentified and/or unidentified metabolites that require specialized time consuming analyses for annotations (Bhinderwala *et al.*, 2018). The ongoing advances in

analytical tools and computing power will certainly improve metabolite annotation and in turn biomarker discovery.

Metabolites Associated with Aortic Valve Stenosis

The combination of several metabolomic profiling technologies in a single study population provided a rich series of 159 metabolic features associated with AVS, which were identified in urine (n=105) through ^{1}H NMR and GC/MS and plasma (n=54) through GC/MS and MALDI-TOF/MS, as summarized in **Table 6**. Both GC/MS and ^{1}H NMR were able to differentiate between cases and controls, which demonstrates that calcific AVS results in changes in biofluid metabolites. GC/MS-based metabolomics provided a set of known and unknown metabolic features that characterize calcific AVS in both biofluids. Several of the identified candidate metabolites in AVS have been associated with heart diseases, such as glycine, myo-inositol, methylmalonic acid (Deidda *et al.*, 2015), elaidic acid, dodecanoic acid, myristic acid, and palmitic acid (Mori *et al.*, 2015; Hu *et al.*, 1999). Aconitic acid and 2,4-di-tert-butylphenol were suggested to be associated with myocardial injury (Lewis *et al.*, 2008) and atherosclerosis (Yoon *et al.*, 2006), respectively.

Furthermore, among the metabolites showing evidence of difference in their concentrations between cases and controls through NMR-based metabolomics, hippuric acid and its precursor benzoic acid were novel findings in the context of AVS and more generally in heart diseases. These metabolites are products of gut bacterial metabolism, thus suggesting a link between AVS risk and functional and/or architectural changes of the gut microbiota. Validation experiments in high fat diet fed mice chronically infused with hippurate or benzoate suggest that these metabolites contribute to changes in the cardiac expression of genes involved in calcification and myofibroblast activation.

Finally, a set of plasma lipids listed in **Table 6** were detected by MALDI-TOF/MS and were significantly associated with AVS. Among these lipids, lysophosphatidylcholines, oxidized-lysophosphatidylcholine, and phosphatidylcholines were identified. This association confirmed the association of metabolites from the choline pathway with the risk of cardiovascular disease (Guasch-Ferré *et al.*, 2017).

Table 5 :Urinary and plasma metabolites contributing to the separation between the AVS patients and healthy controls. Data were derived by GC/MS, ^{1}H NMR and MALDI-TOF/MS analyses of urine and/or plasma samples from 46 patients and 46 controls. $[M+Na]^{+}$ are the sodiated adducts; $[M+H]^{+}$ are the protonated adducts; lysoPC, Lysophosphatidylcholine; PC, phosphatidylcholine; d, doublet; dd, doublet of doublets; q, quintet; m, multiplet; s, singlet; t, triplet; RT, Retention time; min, minutes; ppm, parts per million; m/z, mass-to-charge ratio.

Metabolite	Matrix	Analytical technique	Regulation in AVS	Statistics
$[lysoPC(20:4) + H]^{+}$	plasma	MALDI-TOF/MS	Up	0.027
$[lysoPC(ox\ 18:3) + H]^{+}$	plasma	MALDI-TOF/MS	Down	0.024
[PC 34:1 + Na]+ or $[PC\ 36:4 + H]^{+}$	plasma	MALDI-TOF/MS	Up	0.011
[PC 36:1 + Na]+ or $[PC\ 38:4 + H]^{+}$	plasma	MALDI-TOF/MS	Up	<0.001
[PC 36:2 + Na]+ or $[PC\ 38:5 + H]^{+}$	plasma	MALDI-TOF/MS	Up	0.017
[PC 36:3 + Na]+ or $[PC\ 38:6 + H]^{+}$	plasma	MALDI-TOF/MS	Up	0.002
2,4-Di-tert-butylphenol	urine	GC/MS	Down	0.004
2,4-Di-tert-butylphenol	Plasma	GC/MS	Down	<0.001
2-Deoxypentonic acid	urine	GC/MS	Up	0.035
2-Furoylglycine	urine	^{1}H NMR targeted	Up	0.03
2-hydroxyisoburyrate	urine	^{1}H NMR	Up	0.003
2-hydroxyisoburyrate	urine	^{1}H NMR	Up	0.044
2-Oxovaleric acid	urine	GC/MS	Up	0.038
2-Oxovaleric acid	Plasma	GC/MS	Down	0.002
3-Hydroxyhippuric acid	urine	GC/MS	Up	0.004
4-aminohippurate (d)	urine	^{1}H NMR	Up	0.036
4-cresol glucuronide (d) / indoxyl sulphate	urine	^{1}H NMR	Up	0.047
4-Deoxyerythronic acid	urine	GC/MS	Up	0.038
4-hydroxyhippurate (d)	urine	1H NMR	Down	0.048
7-Dehydrocholesterol	urine	GC/MS	Down	0.048
Alanine	urine	1H NMR targeted	Up	0.03
Alpha-Lactose	urine	GC/MS	Up	0.006
Benzoate	urine	^{1}H NMR targeted	Up	0.03
Benzoate (t) or indole-acetate (d)	urine	^{1}H NMR	Down	0.032
Deoxycholate (m)	urine	^{1}H NMR	Up	0.035
D-Fructose	urine	GC/MS	Up	0.034

D-Glucose	Plasma	GC/MS	Up	0.018
D-Glucose	urine	GC/MS	Up	0.019
Dimethylamine	urine	^{1}H NMR targeted	Up	0.1
D-Mannose	Plasma	GC/MS	Down	0.033
Dodecanoic acid	Plasma	GC/MS	Down	0.045
Elaidic acid	urine	GC/MS	Up	0.013
Elaidic acid	Plasma	GC/MS	Down	<0.001
Erythronic acid	urine	GC/MS	Up	0.037
Estrone	Plasma	GC/MS	Down	0.001
Estrone	urine	GC/MS	Up	0.019
Galactose	Plasma	GC/MS	Down	0.001
Glycerol	urine	GC/MS	Up	<0.001
Glycine	Plasma	GC/MS	Up	0.003
Hippurate	urine	^{1}H NMR	Up	0.049
Hippurate	urine	^{1}H NMR	Up	0.049
Hippurate	urine	^{1}H NMR targeted	Up	0.01
Hippurate (d)	urine	^{1}H NMR	Up	0.038
Hippurate (d)	urine	^{1}H NMR	Up	0.043
Hippurate (d)	urine	^{1}H NMR	Up	0.041
Hippurate (t)	urine	^{1}H NMR	Up	0.037
Homoarginine (m) or citrulline (m)	urine	^{1}H NMR	Up	0.009
HPHPA	urine	GC/MS	Up	0.015
Hydroxylamine	Plasma	GC/MS	Up	<0.001
L-Alanine	Plasma	GC/MS	Up	0.001
L-Valine	Plasma	GC/MS	Down	0.004
Malonic acid	urine	GC/MS	Up	<0.001
Methylmalonic acid	urine	GC/MS	Up	0.03
Myo-inositol	Plasma	GC/MS	Down	0.001
Myo-inositol	urine	GC/MS	Up	0.028
Myristic acid	urine	GC/MS	Up	0.021
Myristic acid	Plasma	GC/MS	Down	<0.001
N-acetyl-L-aspartate (NAA) (m) or N-acetylcysteine (m)	urine	^{1}H NMR	Up	0.026
NAD+ (d)	urine	^{1}H NMR	Up	0.008
N-methylnicotinate (Trigonelline) (s)	urine	^{1}H NMR	Up	0.005
Oleic acid	Plasma	GC/MS	Down	<0.001
Ornithine	Plasma	GC/MS	Up	0.033
Oxoadipic acid	urine	GC/MS	Up	0.044
Palmitic acid	urine	GC/MS	Up	0.001
Palmitic acid	Plasma	GC/MS	Down	<0.001
Phenylalanine (m)	urine	^{1}H NMR	Up	0.038
Phosphate/phosphoric acid	Plasma	GC/MS	Down	0.001

Phospho(enol)pyruvate (t) or allantoin (s)	urine	^{1}H NMR	Up	0.049
Quinic acid	Plasma	GC/MS	Down	<0.001
Quinic acid	urine	GC/MS	Up	0.008
Raffinose (d) or 3-(3-hydroxyphenyl)-3-hydroxypropionic acid (dd)	urine	^{1}H NMR	Up	0.043
Ribonolactone	urine	GC/MS	Up	0.034
Salicyluric acid/2-Hydroxyhippuric acid	urine	GC/MS	Down	0.003
Sarcosine	urine	^{1}H NMR targeted	Down	0.07
Stearic acid	urine	GC/MS	Up	0.048
Succinate (s)	urine	^{1}H NMR	Up	0.03
Succinic acid	urine	GC/MS	Up	0.004
Tartrate	urine	^{1}H NMR targeted	Up	0.02
Tiglate (q) or mesaconate (s) or 3-hydroxycinnamate	urine	^{1}H NMR	Up	0.042
Trans-Aconitic acid	Plasma	GC/MS	Up	0.006
Trans-Aconitic acid	urine	GC/MS	Up	0.0007
Trigonelline	urine	^{1}H NMR targeted	Up	0.0002
Uracil (d) or uridine (s)	urine	^{1}H NMR	Up	0.04
Uric acid	urine	GC/MS	Up	0.026
Unknown (1.2342 ppm)	urine	^{1}H NMR	Down	0.049
Unknown (1.5692 ppm)	urine	^{1}H NMR	Up	0.049
Unknown (1.7039 ppm)	urine	^{1}H NMR	Down	0.049
Unknown (1.7782 ppm)	urine	^{1}H NMR	Up	0.049
Unknown (1.8013 ppm)	urine	^{1}H NMR	Up	0.049
Unknown (2.3246 ppm)	urine	^{1}H NMR	Up	0.049
Unknown (2.7580 ppm)	urine	^{1}H NMR	Up	0.049
Unknown (2.7940 ppm)	urine	^{1}H NMR	Up	0.049
Unknown (2.8226 ppm)	urine	^{1}H NMR	Up	0.049
Unknown (3.7936 ppm)	urine	^{1}H NMR	Down	0.049
Unknown (4.0694 ppm)	urine	^{1}H NMR	Down	0.049
Unknown (5.1994 ppm)	urine	^{1}H NMR	Down	0.032
Unknown (6.8500 ppm)	urine	^{1}H NMR	Up	0.049
Unknown (7.2817 ppm)	urine	^{1}H NMR	Up	0.046
Unknown (7.2974 ppm)	urine	^{1}H NMR	Up	0.049
Unknown (7.4148 ppm)	urine	^{1}H NMR	Up	0.049
Unknown (7.4277 ppm)	urine	^{1}H NMR	Up	0.049
Unknown (7.6070 ppm)	urine	^{1}H NMR	Up	0.049
Unknown (7.6307 ppm)	urine	^{1}H NMR	Up	0.049
Unknown (8.3914 ppm)	urine	^{1}H NMR	Down	0.049
Unknown (8.5091 ppm)	urine	^{1}H NMR	Up	0.041
Unknown (8.6804 ppm)	urine	^{1}H NMR	Down	0.023
Unknown (8.8272 ppm)	urine	^{1}H NMR	Up	0.017

Unknown (8.9130 ppm)	urine	^{1}H NMR	Down	0.044
Unknown (9.1242 ppm)	urine	^{1}H NMR	Up	0.014
Unknown (m/z=155.84)	plasma	MALDI-TOF/MS	Down	0.049
Unknown (m/z=201.96)	plasma	MALDI-TOF/MS	Down	0.038
Unknown (m/z=298.37)	plasma	MALDI-TOF/MS	Down	0.006
Unknown (m/z=319.75)	plasma	MALDI-TOF/MS	Down	0.005
Unknown (m/z=345.06)	plasma	MALDI-TOF/MS	Down	<0.001
Unknown (m/z=345.16)	plasma	MALDI-TOF/MS	Down	<0.001
Unknown (m/z=353.04)	plasma	MALDI-TOF/MS	Down	0.002
Unknown (m/z=360.82)	plasma	MALDI-TOF/MS	Down	0.018
Unknown (m/z=361.81)	plasma	MALDI-TOF/MS	Down	0.008
Unknown (m/z=453.16)	plasma	MALDI-TOF/MS	Down	0.001
Unknown (m/z=453.82)	plasma	MALDI-TOF/MS	Down	0.014
Unknown (m/z=541.63)	plasma	MALDI-TOF/MS	Up	0.017
Unknown (m/z=783.57)	plasma	MALDI-TOF/MS	Up	0.003
Unknown (m/z=785.60)	plasma	MALDI-TOF/MS	Up	0.004
Unknown (m/z=811.43)	plasma	MALDI-TOF/MS	Up	0.022
Unknown (m/z=97.12)	plasma	MALDI-TOF/MS	Up	0.036
Unknown (RT=12.2 min)	urine	GC/MS	Up	0.003
Unknown (RT=12.5 min)	urine	GC/MS	Up	0.021
Unknown (RT=12.9 min)	Plasma	GC/MS	Down	<0.001
Unknown (RT=13.0 min)	urine	GC/MS	Down	0.008
Unknown (RT=13.3 min)	urine	GC/MS	Up	0.006
Unknown (RT=13.4 min)	urine	GC/MS	Up	0.031
Unknown (RT=13.5 min)	urine	GC/MS	Up	0.009
Unknown (RT=13.6 min)	urine	GC/MS	Up	0.009
Unknown (RT=13.9 min)	urine	GC/MS	Down	<0.001
Unknown (RT=14.1 min)	urine	GC/MS	Up	0.031
Unknown (RT=14.4 min)	Plasma	GC/MS	Down	<0.001
Unknown (RT=14.5 min)	urine	GC/MS	Up	0.002
Unknown (RT=14.5 min)	Plasma	GC/MS	Down	0.021
Unknown (RT=14.8 min)	urine	GC/MS	Down	0.026
Unknown (RT=15.0 min)	urine	GC/MS	Up	<0.001
Unknown (RT=16.4 min)	urine	GC/MS	Down	0.001
Unknown (RT=16.6 min)	Plasma	GC/MS	Up	<0.001
Unknown (RT=16.8 min)	Plasma	GC/MS	Up	<0.001
Unknown (RT=16.9 min)	Plasma	GC/MS	Up	0.046
Unknown (RT=17.0 min)	Plasma	GC/MS	Up	0.006
Unknown (RT=17.1 min)	Plasma	GC/MS	Up	0.0008
Unknown (RT=17.2 min)	Plasma	GC/MS	Down	0.038
Unknown (RT=17.9 min)	urine	GC/MS	Up	<0.001
Unknown (RT=18.9 min)	urine	GC/MS	Down	<0.001
Unknown (RT=20.3 min)	urine	GC/MS	Down	0.009
Unknown (RT=3.4 min)	urine	GC/MS	Up	0.018

Unknown (RT=3.5 min)	urine	GC/MS	Up	0.029
Unknown (RT=5.4 min)	Plasma	GC/MS	Up	0.017
Unknown (RT=7.1 min)	urine	GC/MS	Up	0.038
Unknown (RT=7.9 min)	urine	GC/MS	Up	0.039
Unknown (RT=8.1 min)	urine	GC/MS	Up	<0.001
Unknown (RT=8.4 min)	Plasma	GC/MS	Down	0.003
Unknown (RT=8.5 min)	urine	GC/MS	Up	0.029
Unknown (RT=9.6 min)	Plasma	GC/MS	Down	<0.001

Potential biomarkers and different cofounders

The candidate metabolites identified in this study are associated with calcific AVS independently of the presence of common cardiovascular risk factors. They are associated with AVS independently on the sex differences, age range, LDL- and HDL-cholesterol levels, BMI, and presence or family history of diabetes, hypertension, or hyperlipidemia. Even though clinical and biochemical data were available in AVS patients and controls, which allowed statistical adjustment for several potential confounders, the involvement of other variables that were not considered in the study cannot be ruled out. Future work is required to determine if the potential biomarkers detected are linked to AVS through other risk factors, such as lipoprotein(a) (LPA), which has been consistently found associated with the pathogenesis of AVS.

LPA concentrations are significantly increased in patients with AVS (Yu *et al.*, 2018). Measure of plasma LPA concentrations in the study population would be useful to test a possible association of the candidate metabolites reported in this work with AVS either directly or through LPA. This can also be addressed *in vitro*. It was found that lipids such as LDL and mainly LPA increase calcium deposition in human aortic valve interstitial cells (HAVICs), which were isolated from standard aortic valves, when cultured in osteogenic medium (Yu *et al.*, 2018). Therefore, one could study the effect of the metabolites detected in our project on calcium deposition in HAVICs. Also, incubation with LPA and LDL could determine whether these metabolites are associated with AVS calcification via LPA and LDL metabolism and provide novel insights into mechanisms through which LPA induces the progression of AVS (Yu *et al.*, 2018). In the absence of preclinical models reproducing the exact pathological features of AVS, mice fed high-fat diet are a useful model to test the impact of confounding factors (e.g. BMI) on the cardiac effects of candidate metabolites for AVS risk.

Perspectives: limitations and strengths of this study

The use of comprehensive metabolomic profiling in this thesis represents a pioneering approach in the study of AVS pathogenesis. Our data underline the power of metabolomics to quantitatively analyze variations in the concentration of a set of metabolites and test their possible involvement in AVS through association. They support the importance of combining multiple metabolomic tools to detect alterations in both urinary and blood metabolites in AVS. The different metabolomic approaches applied in different biological matrices contribute to improve our understanding of the biology of AVS and ultimately to determine therapeutic strategies to treat this disease. Even though comprehensive metabolomic analyses were performed in this thesis work and pointed to altered regulation of numerous metabolites in AVS patients, causal relationships between these metabolites and AVS cannot be inferred. It remains unclear if the altered metabolites are predictive of AVS or responsive to its development, to co-morbidities or to drug treatment (e.g. statins). Additional studies are required to investigate their direct or indirect contribution to AVS.

Candidate metabolites for AVS identified in this study in a population of relatively small size should be tested in larger cohorts to draw a complete picture of the metabolic differences between calcific AVS patients and controls. The inclusion of a larger cohort is essential and mandatory to generalize and validate our findings, and to translate these findings to clinical practices. Also, our findings may not be extrapolated to other populations. Therefore, the inclusion of different populations is essential. Hence, it was found that, for example, demographics with the Mediterranean diet rich with plant-based food have a reduced risk for cardiovascular disease and risk of cardiovascular risk factors (Guasch-Ferré *et al.*, 2017).

Experiments in *in vivo* and *in vitro* preclinical studies are also future areas of research to validate results obtained in humans and to investigate underlying cellular and molecular mechanisms. Preclinical systems allow monitoring of environmental conditions and investigations in standardized and controlled experimental settings in order to reduce interindividual variations. These models allow extensive analysis in tissues and cell systems at specific stages along the progression of the disease. In addition, these models elucidate mechanisms in specific tissues or cells contributing to the regulation of plasma and urine levels of AVS potential biomarkers. The use of metabolic profiling of biofluids and tissues in preclinical AVS models, along with metabolic profiling of biofluids in human clinical cohorts, may provide further information

about the use of the biomarkers identified in this study in early diagnosis and targeted treatment of AVS.

One of the strengths of our study is the detection of potential biomarkers for AVS, such as hippurate and benzoate, that are not known to participate in pathways already associated with cardiovascular diseases. Our findings suggest that metabolomics may identify a biofluid metabotype that characterizes AVS and thus shed light on targeted treatments. It offers new perspectives in the realm of diagnostic and therapeutic approaches to AVS. Our findings make an essential contribution to improve our understanding of the pathogenesis of the disease and to develop new pharmaceutical targets.

Chapter VI: Annex

VI.1. Data derived by MALDI/TOF-MS analysis of plasma samples

Annex Table 1 : All the peaks detected in plasma samples using MALDI-TOF/MS in the positive and negative ion modes. Data were derived by MALDI/TOF-MS analysis using different matrices of plasma samples from 46 patients and 46 controls. Peaks are presented with their mass to charge ratio (m/z); p-values are calculated from a volcano plot; Regulation gives information on up- or down-regulation of the features in AVS patients; CID fragments are obtained by CID (collision-induced dissociation) of the ions detected which helps in the ions' annotations; The ions are detected as adducts. Using the literature many ions were successfully assigned; a. Choline-H_2O; b. choline; c. Phosphocholine ion; d. 1,2-phosphodiester +Na from sodiated phosphatidylcholine (PC) or sphingomyelin (SM); e. Neutral loss of 141; f. Neutral loss of 183 Da from potassiated PC or SM; g. Neutral loss of 59 Da from sodiated PC or SM. GPC. Glycerophosphocholine; CPA. Cyclophosphatidic acid; LysoPA. Lysophosphatidic acid; LysoPC. Lysophosphatidylcholine; LysoPE. Lysophosphatidylethanolamine; LysoPC (ox). Oxidized-lysophosphatidylcholine; PC O-. Phosphatidylcholine plasmalogens; α-CHCA. alfa-cyano-4-hydroxycinnamic acid matrix; 2,5-DHB $CHCl_3$/MeOH/water. 2,5- Dihydroxybenzoic acid matrix dissolved in chloroform/methanol/water; DHB MeOH/water. DHB matrix dissolved in methanol diluted with water; 9-AA. 9-aminoacridine matrix

					CID fragments									
Matrix	**Ion mode**	**m/z**	**Regulation**	**p-value**	**a**	**b**	**c**	**d**	**e**	**f**	**g**	**Assignment**	**Adducts**	**Literature**
α-CHCA matrix	**Positive**													
		171.96	Up	0.87										
		184.02	Up	0.85	86.14									
		189.98	Down	0.88	86.14		184.07							
		195.01	Up	0.11										
		195.87	Up	0.94										
		211.98	Up	0.39										
		304.25	Up	0.15										
		326.35	Up	0.28			184.27		186.27					
		332.3	Down	0.83										
		334.7	Down	0.92										
		379.07	Up	0.63										
		380.07	Up	0.03										
		381.04	Down	0.48										
		485.35	Down	0.42	86.13		184.2			302.25				
		494.32	Down	0.99								LysoPC(16:1)	[M+H]+	
		496.33	Down	0.23		104.14	184.12					LysoPC(16:0)	[M+H]+	2,4,5,6,7,11
		497.33	Down	0.64										
		498.34	Down	0.86										
		518.32	Up	0.88							459.29	LysoPC(16:0)	[M+Na]+	2,4,6,9,11
		520.42	Up	0.72										
		521.46	Up	0.42										
		522.34	Down	0.60		104.13	184.1					lysoPC 18:1	[M+H]+	6,7,11
		524.32	Up	0.68										

		525.11	Up	0.16										
		534.29	Down	0.0005		104.13	184.12					LysoPC (ox 18:3)	[M+H]+	11
		544.34	Up	0.01		104.13	184.11					LysoPC 20:4	[M+H]+	3,7
		610.29	Up	0.93										
		611.29	Down	0.93										
		624.98	Down	0.44										
		626.26	Down	0.82										
		641.25	Down	0.60										
		642.25	Down	0.48										
		643.26	Down	0.55										
2,5-DHB matrix dissolved in CHCl3/MeOH/water	**Positive**	58.17	Up	0.69										
		85.99	Up	0.28										
		86.04	Up	0.24										
		104.06	Up	0.59										
		105.06	Down	0.30										
		183.9	Down	0.02	86.15									
		184.03	Down	0.02	86.14									
		185.04	Down	0.05										
		192.97	Down	0.55										
		194.85	Up	0.84	86.15		184.09							
		195.44	Down	0.40										
		196.09	Up	0.48			184.1							
		196.9	Up	0.93										
		201.96	Down	0.03										
		274.08	Down	0.72										
		298.33	Down	0.27										
		302.26	Up	0.77										

		304.26	Up	0.98										
		305.28	Up	0.72										
		317.64	Down	0.17										
		326.55	Up	0.92					186.28					
		327.36	Up	0.48										
		332.3	Up	0.79										
		333.31	Up	0.32										
		346.07	Up	0.71										
		346.74	Up	0.42										
		360.73	Up	0.70										
		362.01	Down	0.23			184.13							
		369.32	Down	0.35								Cholesterol	[M+H-H2O]+	1,2,9
		387.17	Down	0.16										
		409.15	Up	0.59										
		415.2	Up	0.72								CPA (16:0)	[M+Na]+	9
		425.13	Down	0.07										
		437.18	Down	0.57										
		438.18	Down	0.13										
		453.16	Down	0.002										
		453.82	Down	0.005										
		485.33	Down	0.38						302.25				
		486.35	Up	0.77										
		496.33	Down	0.80		104.14	184.12					LysoPC(16:0)	[M+H]+	2,4,5,6,7,11
		497.34	Down	0.81										
		499.76	Down	0.63										
		518.32	Down	1.00		104.13	184.11					LysoPC 18:3	[M+H]+	7
		520.2	Up	0.40										
		520.92	Up	0.32										

		522.35	Down	0.52		104.13	184.1					lysoPC 18:2	[M+H]+	6,7,11
		524.37	Down	0.65		104.14	184.12					LysoPC 18:1	[M+H]+	2,3,4,5,6,7,9,11
		525.37	Down	0.61										
		534.3	Down	0.0002		104.13	184.12					LysoPC (ox 18:3)	[M+H]+	11
		537.89	Up	0.79										
		539.22	Up	0.37										
		544.58	Up	0.58										
		546.36	Up	0.97		104.12	184.1					LysoPC 20:4	[M+H]+	3
		567.44	Up	0.67		104.13	184.1							
		568.5	Down	0.68		104.13	184.1					LysoPC 22:6	[M+H]+	7
		579.03	Up	0.50										
		599.39	Up	0.40										
		610.29	Up	0.17										
		625.28	Down	0.17										
		626.28	Down	0.12										
		641.26	Down	0.28										
		642.28	Down	0.31										
		643.28	Down	0.20										
		663.47	Up	0.48										
		685.45	Up	0.18	86.13	104.11	184.07							
		688.31	Up	0.77										
		701.79	Up	0.79			184.07							
		758.79	Up	0.46	86.14	104.13	184.09							
		759.82	Up	0.66										
		760.53	Down	0.09			184.1							
		761.6	Down	0.14										
		768.55	Up	0.61			184.19					PC O-36:4	[M+H]+	7
		780.57	Up	0.53								PC 34:2	[M+Na]+	1,5,6,9,11

		780.57	Up	0.53								PC 36:5	[M+H]+	3,7
		781.57	Up	0.48								SM 38:1	[M+Na]+	7
		782.59	Up	0.02	86.12		184.1					PC 36:4	[M+H]+	3,7,10
		782.59	Up	0.02	86.12		184.1					PC 36:4	[M+H]+	3,7,10
		783.57	Up	0.0006										
		784.6	Up	0.19								PC 36:3	[M+H]+	3,5,6,7,11
		785.6	Up	0.46										
		786.62	Up	0.28			184.11					PC 36:2	[M+H]+	1,5,6,7,11
		787.62	Up	0.81								SM(d18:1/22:0)	[M+H]+	10
		788.62	Up	0.72								PC 36:1	[M+H]+	5,7
		796.58	Down	0.11								PC (O-38:4)	[M+H]+	7
		796.58	Down	0.11								PC 34:2	[M+K]+	5
		806.59	Up	0.37								PC 36:3	[M+Na]+	1,4,5,6,9
		806.59	Up	0.37								PC 38:6	[M+H]+	3,7
		808.56	Up	0.03				147.01				PC 36:2	[M+Na]+	1,6,9
		808.56	Up	0.03	86.1		184.09					PC 38:5	[M+H]+	3,7
		810.56	Up	< 0.0001				147				PC 36:2	[M+Na]+	
		810.56	Up	< 0.0001	86.11		184.07					PC 38:5	[M+H]+	1,3,4,5,6,7
		811.43	Up	0.07										
		812.62	Up	0.07								PC 38:3	[M+H]+	6,7
		812.62	Up	0.07								p-PC 38:6	[M+Na]+	4,6
		882.59	Up	0.96								PC 42:7	[M+Na]+	
		950.6	Up	0.95								PC 46:1	[M+Na]+	
		952.5	Down	0.22										

2,5-DHB matrix dissolved in MeOH/Water	**Positive**	103.94	Down	0.09									
		104.07	Up	0.71									
		137.76	Down	0.001									
		154.79	Down	0.003									
		155.84	Down	0.01									
		183.89	Down	0.01	86.15								
		184.02	Down	0.76	86.14								
		194.12	Down	0.61	86.14		184.09						
		195.2	Down	0.96									
		196.05	Up	0.63			184.08						
		197.03	Down	0.07									
		201.91	Up	0.16									
		258.04	Up	0.60		104.14					GPC	[M+H]+	9
		274.29	Up	0.03									
		298.37	Down	0.001									
		302.58	Down	0.04									
		304.6	Up	0.55									
		305.28	Down	0.01									
		317.97	Down	0.06									
		319.75	Down	0.004									
		326.34	Up	0.08			184.27		186.27				
		327.34	Down	0.01									
		332.33	Up	0.37									
		333.31	Down	0.02									
		346.35	Down	0.07									
		360.82	Down	0.01									
		361.81	Down	0.01									
		369.33	Down	0.91							Cholesterol	[M+H-H2O]+	1,2,9

		370.34	Down	0.15										
		409.29	Down	0.07										
		437.55	Down	0.01										
		453.12	Down	0.002										
		485.29	Up	0.18										
		496.33	Down	0.18		104.14	184.12					LysoPC(16:0)	[M+H]+	2,4,5,6,7,11
		497.34	Down	0.29										
		498.34	Up	0.85										
		518.31	Up	0.32							459.29	LysoPC(16:0)	[M+Na]+	2,4,6,9,11
		519.32	Down	0.17										
		520.31	Down	0.98		104.13	184.11					lysoPC 18:2	[M+H]+	3,5,6,7,11
		520.99	Up	0.73										
		523.35	Down	0.10										
		524.35	Down	0.33		104.14	184.12					LysoPC 18:0	[M+H]+	2,3,4,5,6,7,9,11
		525.37	Up	0.69										
		534.29	Down	< 0.0001		104.13	184.12					LysoPC (ox 18:3)	[M+H]+	11
		541.63	Up	0.27										
		544.37	Up	0.001		104.13	184.11					LysoPC 20:5	[M+H]+	
		546.35	Up	0.89		104.12	184.1					LysoPC 20:3	[M+H]+	3
		567.68	Down	0.05										
		599.41	Down	0.05			184.21							
		610.3	Down	0.19										
		611.3	Down	0.01										
		623.55	Down	0.04										
		625.28	Down	0.03										
		626.28	Down	0.05										
		627.27	Down	0.02										
		641.26	Down	0.04										

		642.27	Down	0.03										
		643.28	Down	0.03										
		663.43	Down	0.78										
		685.45	Up	0.22	86.13	104.11	184.07							
		688.11	Down	0.10										
		703.05	Down	0.98										
		758.7	Down	0.99								PC 34:2	[M+H]+	1,5,6,7,10,11
		759.71	Up	0.15										
		760.59	Down	0.79										
		761.6	Down	0.50										
		768.55	Up	0.04			184.19							
		780.57	Up	0.14								PC 34:3	[M+Na]+	1,5,6,9,11
		780.57	Up	0.14								PC 36:5	[M+H]+	3,7
		781.58	Up	0.70								SM 38:1	[M+Na]+	7
		782.53	Up	0.0003				147				PC 34:1	[M+Na]+	1,5,6,9,11
		782.53	Up	0.0003				147				PC 34:1	[M+Na]+	1,5,6,9,11
		783.55	Up	0.01										
		784.57	Up	0.01								PC 36:3	[M+H]+	3,5,6,7,11
		785.6	Up	0.27										
		786.62	Down	0.25			184.11					PC 36:2	[M+H]+	1,5,6,7,11
		787.62	Down	0.40								SM(d18:1/22:0)	[M+H]+	10
		788.63	Down	0.97								PC 36:1	[M+H]+	5,7
		806.48	Up	0.02								PC 36:3	[M+Na]+	1,4,5,6,9
		806.48	Up	0.02								PC 38:6	[M+H]+	3,7
		808.56	Up	0.03				147.01				PC 36:2	[M+Na]+	1,6,9
		808.56	Up	0.03	86.1		184.09					PC 38:5	[M+H]+	3,7
		810.5	Up	0.01				147				PC 36:1	[M+Na]+	
		810.5	Up	0.01	86.11		184.07					PC 38:4	[M+H]+	1,3,4,5,6,7

		811.42	Up	0.22									
		850.56	Up	0.01			184.11				PC 40:9	[M+Na]+	
		882.59	Up	0.03							PC 42:7	[M+Na]+	
		991.71	Up	0.20									
		1165.79	Up	0.02									
9-AA matrix	**Negative**	61.92	Up	0.24									
		69	Up	0.09									
		78.9	Up	0.67									
		96.9	Up	0.89									
		97.12	Up	0.13									
		112.92	Up	0.81									
		113.21	Down	0.69									
		114.14	Up	0.81									
		152	Down	0.95									
		153	Down	0.68									
		154.02	Up	0.90									
		188.52	Down	0.76									
		193.42	Down	0.04									
		194.08	Down	0.23									
		195.09	Down	0.91									
		226.99	Down	0.50									
		248.98	Up	0.52									
		265.16	Down	0.15									
		273.07	Down	0.95									
		311.2	Down	0.74									
		325.23	Up	0.08									
		329.1	Down	0.005									
		353.04	Down	0.002									

		473.38	Up	0.87									
		474.4	Up	0.96									
		485.35	Down	0.36							LysoPA(22:4)	[M-H]-	8
α-CHCA matrix	**Negative**	144.03	Down	0.31									
		188.44	Down	0.19									
		189.04	Down	0.03									
		190.04	Up	0.32									
		333.12	Up	0.29									
		375.11	Down	0.76									
		399.11	Down	0.61									
2,5-DHB matrix dissolved in CHCl3/MeOH/water	**Negative**	152.16	Down	0.26									
		152.84	Up	0.11									
		153	Down	0.31									
		154.01	Up	0.99									
		307.07	Up	0.81									
		315.08	Down	0.99									
		328.07	Down	0.35									
		329.08	Down	0.26									
		330.08	Down	0.35									
		331	Up	0.68									
		345.06	Down	< 0.0001									
		360.02	Down	0.36									
		361.03	Down	0.72									
		498.1	Up	0.97							lysoPE(20:5)	[M-H]-	8
		499.11	Down	0.68									
		500.11	Up	0.98							lysoPE(20:4)	[M-H]-	8
		501.11	Up	0.54									

2,5-DHB matrix dissolved in MeOH/Water	**Negative**	152.07	Up	0.84										
		152.23	Up	0.23										
		152.99	Up	0.22										
		154.08	Up	0.14										
		289.1	Up	0.68										
		306.95	Up	0.65										
		314.95	Up	0.88										
		328.07	Up	0.04										
		329.08	Up	0.14										
		331.3	Up	0.22										
		345.16	Down	< 0.0001										
		360.04	Down	0.04										
		361.03	Down	0.03										
		498.09	Down	0.11								LysoPE(20:5)	[M-H]-	8
		499.1	Up	0.32										
		500.1	Up	0.85								LysoPE(20:4)	[M-H]-	8

1. Schiller et al., 2001 ; 2. Hidaka et al., 2007 ; 3. Guerrera et al., 2009; 4. Fuchs et al., 2010 ; 5. Zemski Berry et al., 2011 ; 6. Preianò et al., 2012 ; 7. Serna et al., 2015 ; 8. Wang et al., 2015; 9. Korte et al., 2016 ; 10. Tipthara and Thongboonkerd, 2016 ; 11. Milman et al., 2017

VI.2. Samples preparation, data acquisition and analysis

Metabolomics helps in discovering altered metabolic pathways and new gene functions. The advanced instruments, the statistical methods, and publicly available metabolic pathways and large metabolite database give advantage to metabolomics studies (Nagana Gowda and Raftery, 2013).

Figure S 4 : Sample preparation for Mass Spectrometry

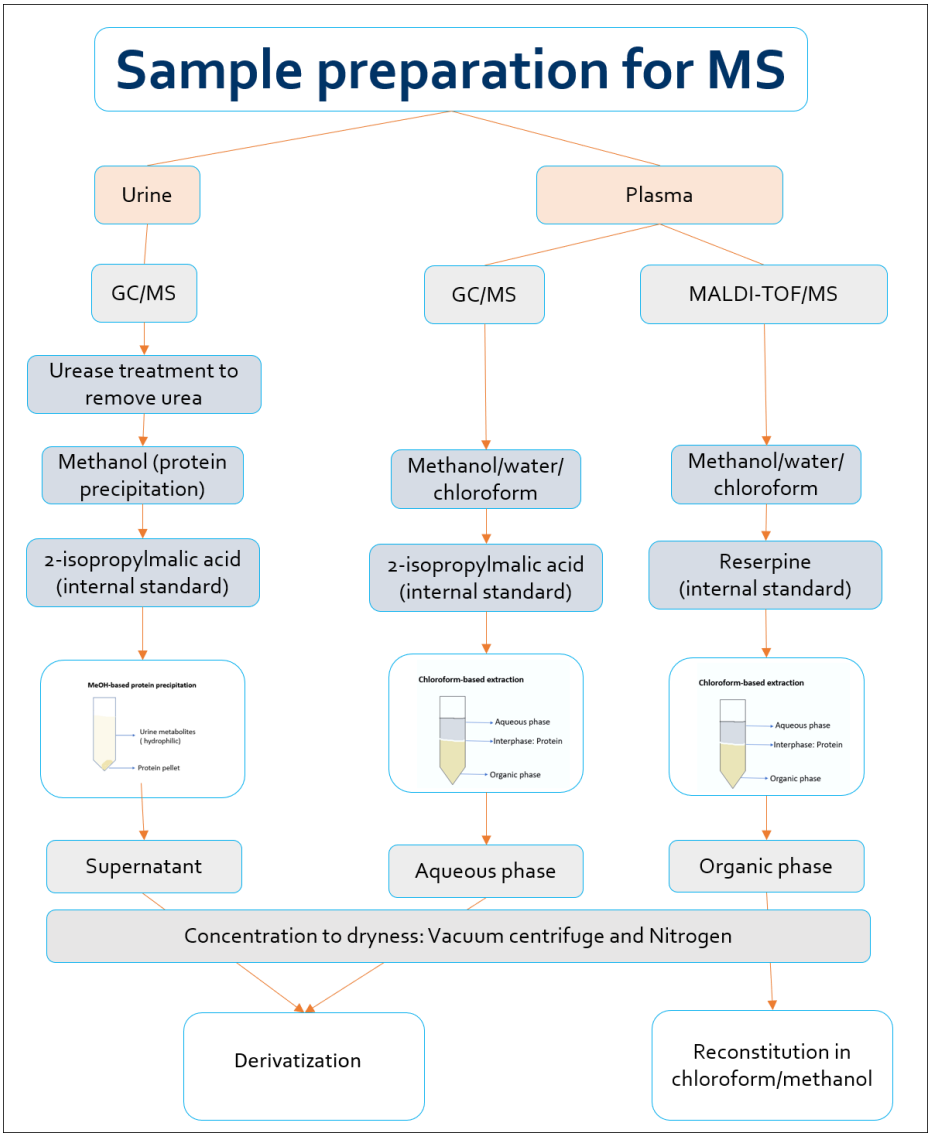

VI.2.1. Urine samples preparation for GC/MS data acquisition

When analyzing urine with gas chromatography mass spectrometry (GC/MS), urine samples should be thawed then centrifuged to remove any solids (Fanos *et al.*, 2014). Urease should be added to remove urea from urine (Fanos *et al.*, 2014), because it can affect the abundance of some metabolites (Bouatra *et al.*, 2013). Urine samples were prepared using a modified Cheng et al 2012 method (Cheng *et al.*, 2012) (**Figure S 4**). The 92 urine samples were extracted using 200 μL aliquot. After centrifugation at 12000 rpm for 10 minutes, a 50 μL of the supernatant was used, then 10 μL urease, 1 mg/mL in 75:25 water/glycerol from Canavalia ensiformis (Jack bean), was added in order to remove the high concentration of urea and the mixture was incubated at 37 ˚C for 30 minutes. The supernatant was spiked with 10 μL 2-isopropylmalic acid 1 mg/mL in HPLC water, an internal standard used for quality control and metabolites quantification. The low concentration of proteins was removed with 170 μL methanol followed with vortex for 30 seconds. 200 μL supernatant was transferred to clean 1.5 ml Eppendorf tubes after centrifugation for 5 min at 12000 rpm leaving a white pellet (protein precipitation). Extracts were concentrated to dryness with Vacuum Centrifuge and left at -80 °C until derivatization and analysis with GC/MS (Lee and Fiehn, 2008).

VI.2.2. Plasma samples preparation for GC/MS data acquisition

For GC/MS, plasma samples were extracted using Nishiumi et al 2010 method (Nishiumi *et al.*, 2010) (**Figure S 4**). Plasma samples were extracted using a ratio of 50:250 of plasma to solvent mixture. The solvent mixture includes an internal standard, 2-isopropylmalic acid 0.5 mg/mL in HPLC-grade water, which was mixed at a ratio 6:250 with the extraction solvent that contains methanol/water/chloroform 2.5:1:1. Then the solution was incubated for 30 min at 37 ˚C and centrifuged for 5 min at 16000 xg. 200 μL of the upper-hydrophilic-phase was collected and mixed with water. The solution was mixed and centrifuged, then the supernatant was collected, dried with vacuum centrifuged for 2 hours and stored at -80 °C.

VI.2.3. Derivatization for GC/MS data acquisition

When needed, the extract residue was derivatized with oximation followed with trimethylsilylation. Oximation reaction was performed after adding 80 μL methoxyamine hydrochloride 98% 15 mg/mL in pyridine, and incubation for 90 min at 30 ˚C. Trimethylsilylation was done after incubation with BSTFA (N,O-bis(trimethylsilyl)trifluoroacetamide) mixed with (1% TMCS (trimethylchlorosilane)) for 60 min at 70 ˚C. After a quick spin down, 130 μL was transferred to GC/MS glass vials with fused insert.

VI.2.4. Analysis with GC/MS

Urine and plasma samples were subjected to gas chromatography coupled with mass spectrometry GC/MS HP6890 equipped with a capillary column HP-5MS 5% phenyl methyl siloxane of 30 m nominal length, 250 µm nominal diameter and 0.25 µm nominal film thickness. 1 μL of the derivatized solution was injected under split mode with a ratio 3:1 using Helium gas. The gas flow was 2 mL/min. The initial temperature was 80˚C for 2 minutes then it was increased to 315˚at a rate 15˚C/min and held at 315 degrees for 15 minutes. The complete GC program duration was 32 minutes. The acquisition was in scan mode to broaden the search process. GC/MS raw chromatograms were exported in CDF format for data-preprocessing. CSV files were obtained which include peak retention time, peak height, peak Area, metabolites identification with NIST08 library. Metabolites annotation were manually checked with a similarity of more than 80 %.

Figure S 5: GC/MS chromatogram and fragmentation spectrum of the internal standard detected at RT 7.6 min

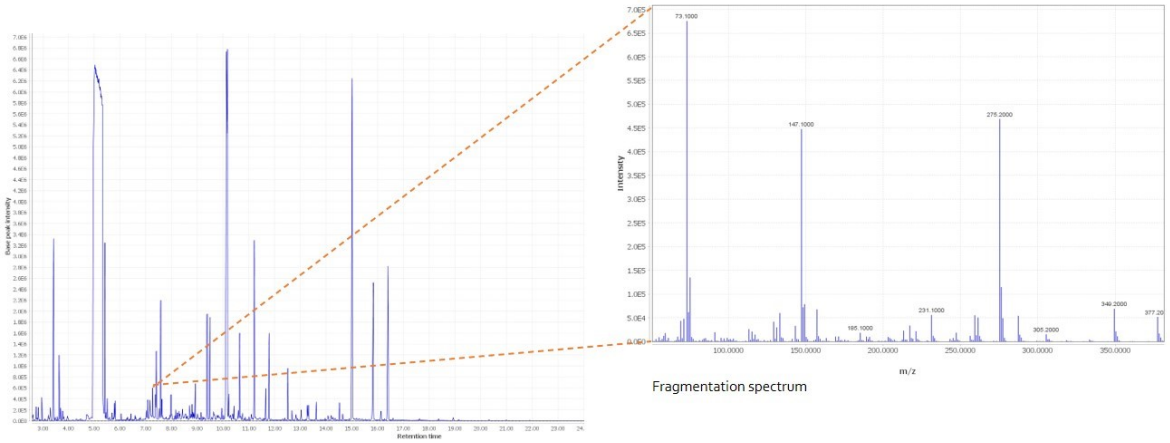

VI.2.5. GC/MS data pre-processing

GC/MS Raw data were preprocessed to generate a peak table which is a comprehensive table of all detected peaks characterized by a specific R.T. and the intensity of each peak across multiple samples from two/many sample groups (Coble and Fraga, 2014). In the present work, XCMS (v 3.6.1) tool in R statistical language (through Bioconductor v 1.30.4) was used for GC/MS data preprocessing where the retention times were aligned, and signal drift and batch effect were corrected (**Figure S 6**). XCMS uses CDF format as input, and as output it gives dataMatrix table. Using XCMS, (i) peak detection was performed thus the peak width parameter was set visually after assessment the chromatographic peaks belonging to the internal standard. The range of RT values was set between 450 and 460 seconds, the range of m/z was between 275 and 278 and the value of maximum expected deviation of values was set to 3 ppm. Then (ii) peak alignment was performed so that all RTs can be adjusted to match across all samples.

Figure S 6 : Raw GC/MS data pre-processing with XCMS

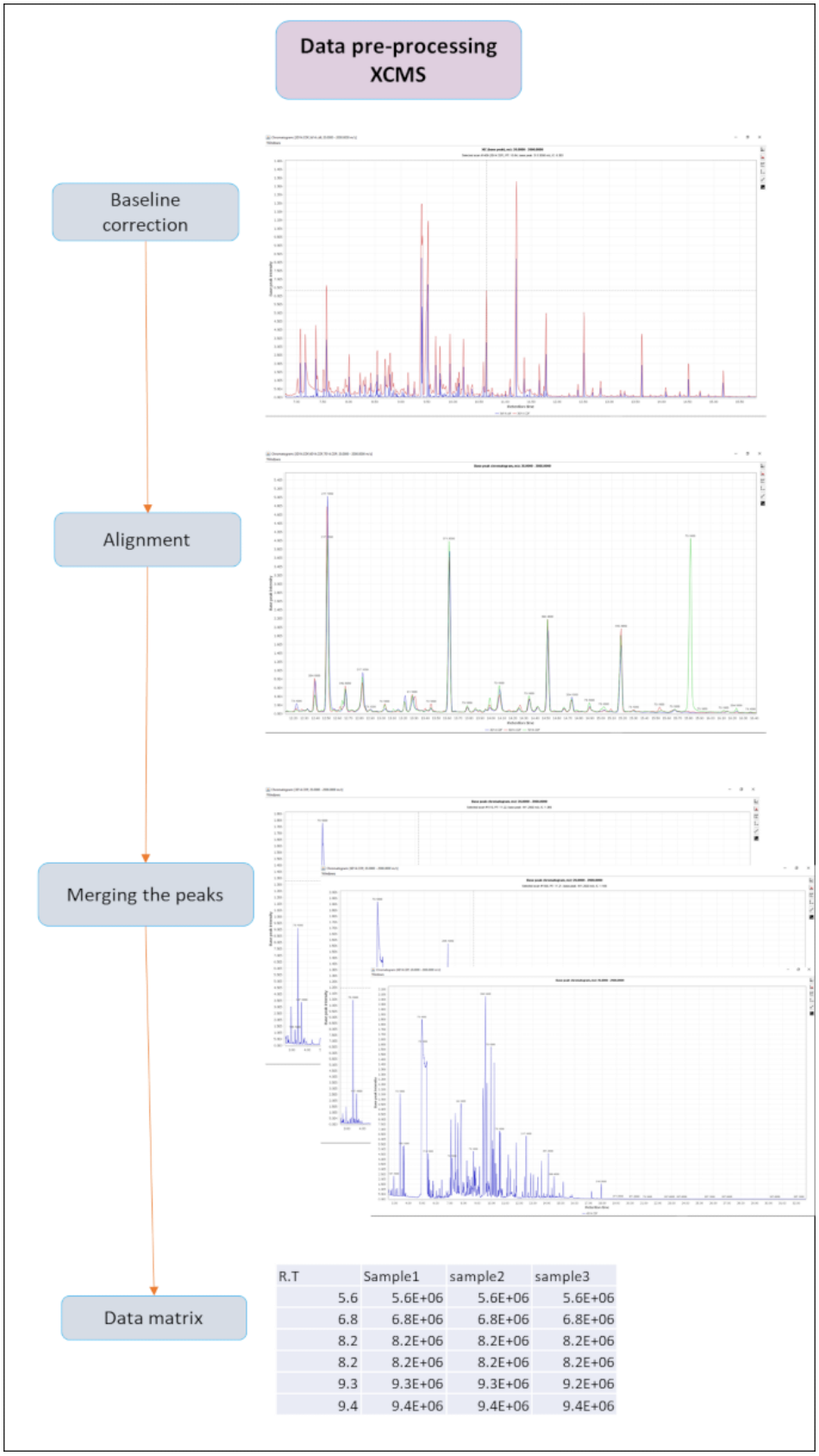

VI.2.6. Plasma samples preparation for MALDI-TOF/MS data acquisition

For MALDI-TOF/MS data acquisition, 92 plasma samples were extracted with Liquid-liquid extraction method following the Folch method (Lee *et al.*, 2014) using $CHCl_3$/MeOH/water 2:1:0.8 ratio (**Figure S 4**). 30 µL plasma sample was mixed with 225 µL MeOH and the mixture was vortexed for 10 sec. After that, the mixture was incubated for 1 hour in a shaker after adding 450 µL $CHCl_3$. Phase separation was induced by adding 187 µL MS-grade water. The lower organic phase was collected, dried with vacuum centrifuge, and stored at -80 ˚C until analysis. An internal standard was used to evaluate data acquisition with MALDI-TOF/MS. Reserpine 0.1 mg/mL in $CHCl_3$ was spiked in the extracted samples.

VI.2.7. Analysis with MALDI-TOF/MS

Lipid extracts were analyzed using MALDI-TOF/MS on a 4800 MALDI TOF/TOF Analyzer instrument operated by the 4000 Series Explorer software version 3.5.1 (Applied Biosystems, USA). For the calibration, peptide calibration standard mixture was used for calibration and testing MALDI-TOF/MS in a mass range between ~ 900 and 3700 Dalton. The mixture contains the following six standard peptides and their mono-isotopic masses: Des-Arg-Bradykinin (904.4681 Da), Angiotensin I (1296.6853 Da), glu1-fibrinopeptide (1570.6774 Da), ACTH (1-17 clip) (2093.0867 Da), ACTH (18-39 clip) (2465.1989 Da), and ACTH (7-38 clip) (3657.9294 Da). For plate calibration, 1 µL standard solution was mixed with 12 µL matrix A diluent (50:50 ACN/HPLC-grade water, 0.1 % TFA) and 12 µL matrix A (10 mg α-CHCA in 1 mL matrix A diluent). 0.8 µL standard was spotted onto 13 MALDI standard spots on a stainless-steel target plate (Opti-TOF TM 384 Well Insert, 123×81 mm RevA, Applied Biosystems, USA) and the spots were air-dried. Lipids were measured in the positive and negative ion modes using MALDI-TOF MS mode, then the product ions of lipids were measured using MALDI-TOF MS/MS. MS/MS acquisition was performed in Collision-induced dissociation (CID) mode.

VI.2.8. Sample spotting in MALDI-TOF/MS

The extracts were dissolved in Folch's solution, 28 µL $CHCl_3$/MeOH 2:1, spiked with 2 µL reserpine 0.1 mg/mL in $CHCl_3$. 0.8 µL of the mixture was spotted and dried in vacuum chamber. After that, 0.8 µL of matrix solution was added on top and the plate was immediately moved to the vacuum chamber. The vacuum chamber was used to avoid long-term exposure to air that may cause oxidization of unsaturated lipids (Schröter *et al.*, 2017). In the positive ion mode three matrices were used in order to cover as much as possible lipids. 10 mg 2,5-DHB matrix in 1 mL $CHCl_3$/MeOH/water 4:2:0.3; 10 mg 2,5-DHB matrix in 1 mL MeOH/water 70:30 0.1% TFA; 10 mg α-CHCA matrix in 1 mL MeOH/water 70:30 0.1% TFA; while 9-aminoacridine (9-AA) matrix (20 mg in 1 ml of 2:1 ratio $CHCl_3$ to MeOH) was used in the negative-ion mode. Moreover, matrices were spotted alone as controls, and were spiked with the internal standard used (reserpine) to facilitate peak alignment in data pre-processing. The plate was loaded into the mass spectrometer and the mass spectrum was acquired in the mass range 100 to 1,500 with a nitrogen N_2 laser at 337 nm.

VI.2.9. MALDI-TOF/MS Data pre-processing and processing

The mass assignment for a certain peak can be shifted, this can be due to the different settings to process the sample, spotting pattern, instrument temperature, laser power attenuation, and calibration constants. Before the availability of bioinformatics analysis, the analyses were performed visually, thus leading for human errors. Five-step data preprocessing can be applied, knowing that there are no standard procedures for cleaning the raw MS data: smoothing, baseline correction, peak identification, normalizing and peak alignment (Tong *et al.*, 2011). Therefore, MALDI raw data were extracted then the BioNumeric software was used for noise filtering, baseline correction, normalization, peak alignment and detection. As input, BioNumerics uses text format files that contain all the detected peaks and their intensities, and as output it gives a dataMatrix table with only the aligned peaks in columns and the samples in rows.

Univariate analysis using volcano plot was performed; Thus, the ions with the same relative abundance between the two groups will be plotted at the x-axis origin (log2 (1) =0) and the

metabolites that are relatively low or high in one group will be plotted in either to the left or to the left. Ions with significant p-values will be plotted in the upper part.

VI.2.10. Lipids identification

Lipid identification from the desorbed ions during MALDI-TOF/MS can be quite challenging. Since MALDI-TOF/MS spectrum shows only the assumption lipids' molecular weight plus or minus adducts $[M+H]^+$, $[M+Na]^+$, $[M+K]^+$, $[M-H]^-$. Sometimes the ion may be a fragment of a larger lipid after losing (OH) or (H_2O). Metabolites were assigned using existing databases, such as LIPID MALPS Lipidomics Gateway, HMDB and mMass software. LipidMAPS and HMDB use a list of peaks, while mMass software uses as input the raw data. In addition to that, MALDI-TOF MS/MS raw data were used for better identification. MALDI-TOF MS/MS raw data were exported in MzML format then MS Convert GUI software was used to convert the MzML data to MGF format. The MGF files were imported in NIST MS software to better identify lipids using the daughter peaks resulting from CID fragmentation of parent peaks. To confirm the identity of lipids, the metabolites were assigned on the basis of comparison with the literature.

VI.2.11. Sample preparation for 1H NMR, data acquisition and pre-processing

Urine samples were profiled using ^{1}H NMR spectroscopy. The samples were transferred to NMR tubes 3 mm. NMR spectra were acquired on a Bruker DRX 600 MHz spectrometer (Bruker Biospin Ltd) that operates at 600 MHz and 310 K. J-resolved (JRES) sequence experiment was performed as describes in Dona et al 2014 since it gives information on small molecular weight metabolites (Dona *et al.*, 2014).

^{1}H NMR spectra were imported in MATLAB. The calibration of the spectra was performed to the glucose alpha anomeric signal at δ 5.23 using an automated calibration script (Pearce *et al.*, 2008). Raw data were preprocessed to remove the spectral regions corresponding to water and urea. The spectra were normalized using probabilistic quotient normalization (PQN) to reduce systematic variations between samples such as sample dilution (Dieterle *et al.*, 2006). Peak alignment was performed using recursive segment-wise peak alignment (RSPA) (Veselkov *et al.*, 2009). The statistical recoupling of variables (SRV) algorithm was applied, in order to

reduce the high dimensionality of the dataset (Blaise *et al.*, 2009). Finally, Hippurate and other peaks were annotated (**Figure S 7**).

Figure S 7 : Data pre-processing of 1H NMR-based untargeted metabolomics data and Hippurate annotation

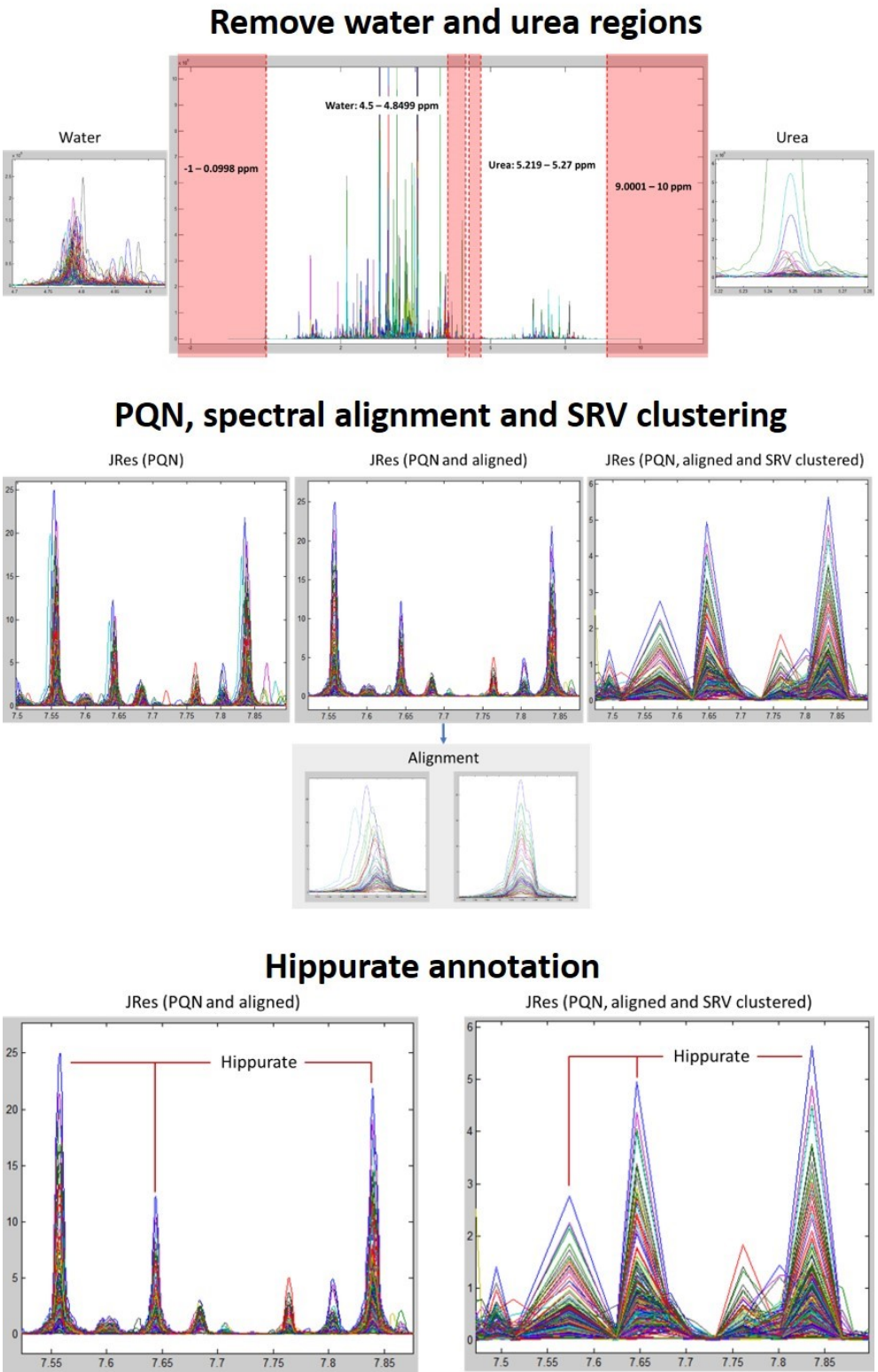

VI.2.12. Data processing

In this study, MetaboAnalyst tool (v 2.0.1) in R package was used for statistical analysis, where the uploaded table should be in comma separated values (.csv) format and samples can be in rows or columns, with class group (case/control) immediately following the sample IDs. Before data analysis, (1) a data integrity check is usually performed in MetaboAnalyst to make sure that all information is present in the data matrix. By default, the missing values will be replaced by a small value (imputation). (2) Data filtering was applied in order to identify and remove variables that are unlikely to be of use when modeling the data. (3) Data were normalized with 2 steps; each metabolite profile was normalized to the internal standard (2-isopropylmalic acid in GC/MS).

Univariate analysis using volcano plot was performed for selecting differentiating metabolites; thus, volcano plot has the power to show the combination between the fold-change (log 2(FC)) of the relative abundance of each metabolites between the 2 groups (cases/controls) and the statistical significance p-value of the ratio fold-change. The volcano plot represents on the y-axis the significance from t-test (-log10 (p-value)) and fold change on the x-axis. The metabolites with the same relative abundance between the two groups will be plotted at the x-axis origin (log2 (1) =0) and the metabolites that are relatively low or high in one group will be plotted in either to the left or to the left. Metabolites with significant p-values will be plotted in the upper part.

Multivariate analysis was also performed using PCA, PLS-DA and OPLS-DA. The 95% confidence regions are displayed by shaded ellipses. The PCA score plot which is related to samples (observation) was used to identify potential outliers. PLS-DA was performed and the Cross validation (CV) method was 10-fold CV, with Q^2 as measured performance (Barberini *et al.*, 2016). R^2 represents reliability of the model, and Q^2 represents the predictive capacity of the model (Jasbi *et al.*, 2019). Values of R^2 and Q^2 near 1 indicate perfect description and perfect predictability of the model respectively (Triba *et al.*, 2014). In general when R^2 and Q^2 are > 50%, they are considered satisfactory for metabolic experiment and can explain the model (Azizan, Ghani and Nawawi, 2015). Since PLS-DA tends to over fit data, the model needs to be validated to understand the significance of class discrimination. Therefore, a permutation test was performed (Barberini *et al.*, 2016). With permutation test a histogram showing the

distribution derived from the permuted samples can be obtained. In PLS-DA, a Variable Importance in Projection (VIP) can be obtained to identify which variables are responsible for the separation between cases and controls in PLS-DA model. The VIP cut-off value was set at 1 to identify potential biomarkers. OPLS-DA model was performed to find potential biomarkers for AVS. In OPLS-DA score plot, the x-axis (t[1]) represents the predictive variation among the classes and the y-axis (to[1]) represents the variation orthogonal to the class specific variation. To assess the significance of class discrimination, a permutation test was performed. The quality of the model is described by the R^2X or R^2Y and Q^2 values. R^2X or R^2Y indicates goodness of fit. Q^2 indicates predictability and it is used to as goodness-of-prediction parameter (Gao *et al.*, 2012). Metabolites selected with VIP value >1 were pre-screened as potential biomarkers. To decrease the rate of false positives in the selection, adjusted p-values (q-values) were calculated using Benjamini-Hochberg method and the threshold was set at 0.05 (Jasbi *et al.*, 2019).

VI.2.13. Regression analysis

Generalized linear models (GLMs) were used to determine which metabolomic peaks were associated with different sample metadata. After adjusting for age and sex, linear regression was used to assess the association of metabolite peaks with BMI, HDL- and LDL-cholesterol levels while logistic regression was used to assess the association of the metabolite peaks with AVS after adjusting for age, sex, BMI, hyperlipidemia and diabetes. R package was used to perform the statistical analyses and to calculate the statistical significance. The p-values obtained corresponded to the p-value of the peak in each model. These values were then corrected using the Benjamini-Hochberg method. Peaks were considered to be significant if their adjusted p-values were less 0.05.

VI.2.14. Biomarker analysis

ROC analysis for the model was developed using the Biomarker Analysis tool in MetaboAnalyst. Classical ROC curve analysis was performed to evaluate the performance of each significant metabolite as a potential biomarker. The ROC curve summarizes the sensitivity and specificity of that single feature to accurately classify data, which can then be used to compare the overall accuracy of different potential biomarkers. Classical univariate ROC curve analysis generates ROC curve to calculate AUC as well as their 95% confidence intervals. Area

under ROC curve (AUROC) for each metabolite was obtained along with T-test and log2(FC) values. Area under ROC curve (AUROC) is used to assess the utility of a biomarker. Therefore, when AUC (Area under the curve) is between 0.9 and 1 the biomarker is excellent; AUC between 0.8 and 0.9, the biomarker is good; AUC between 0.7 and 0.8, the biomarker utility is fair, AUC 0.6-0.7, the biomarker utility is poor; AUC between 0.5 and 0.6, the biomarker utility is fail (Xia *et al.*, 2013).

VI.2.15. Pathway analysis

The biochemical pathways (intracellular fluxes) of metabolites must be understood in order to be able to explain the alteration of metabolite levels. Based on the identified differential metabolites in plasma and urine, a metabolomics Pathway Analysis using the web-tool metaboAnalyst (https://www.metaboanalyst.ca/) based on KEGG human metabolic pathways was employed to find the most perturbed metabolic pathways related to AVS. We evaluated both a test for significantly altered metabolites in a pathway based on the hypergeometric tests and for the impact of the altered metabolites on the pathway function via alterations in important junction points of the pathway. Thus, to understand the functional impact of the alterations of plasma and urine metabolites, the metabolic pathways obtained were plotted according to the impact value and the most significant pathways according to the *P*-values from the hypergeometric test.

VI.2.16. In-Vivo preclinical validation

VI.2.16.1. Animal experiments

A group of 18 of six-week-old C57BL/6J male mice was fed control carbohydrate diet (CHD) (D 12450Ki, Research diets, NJ) (**Table S 1**) and a group of 18 mice was fed high fat (60% fat and sucrose) diet (HFD) (D12492i, Research diets, NJ) (**Table S 1**).

Table S 1 : Caloric information of high fat diet and carbohydrate diet

Carbohydrate diet	
Protein:	20 % Kcal
Fat:	10 % Kcal
Carbohydrate:	70 % Kcal
Energy density:	3.82 Kcal/g
High fat diet	
Protein:	20 % Kcal
Fat:	60 % Kcal
Carbohydrate:	20 % Kcal
Energy density:	5.21 Kcal/g

(From Research Diets Available at : https://researchdiets.com/formulas/D12492iD%2012450Ki,%20Research%20diets and https://researchdiets.com/formulas/D12492i)

The mice were maintained in specific pathogen free (SPF) condition on a 12h light/dark cycle. One week later mice were anaesthetized with isoflurane and osmotic minipumps (Alzet® model 2006, Charles River Lab France, l'Arbresle, France) filled with a solution of hippurate, benzoate or with saline (5.55mM in 0.9% NaCl) (Sigma Aldrich, St Quentin, France). Mice were separated into 6 groups; Two control groups of which CHD-fed and HFD-fed mice were exposed to saline. Four experimental groups in which CHD-fed and HFD-fed mice were exposed to either benzoate or hippurate. The minipumps were inserted subcutaneously on the dorsal left side (**Figure S 8**). Concentration of these metabolites was adjusted for a flow rate of 0.15mL/h. Body weight were measured at the end of the experiment. After six weeks of metabolite treatment, animals were killed by decapitation and organs were dissected and weighed. All procedures were authorized following review by the institutional ethic committee and carried out under national license condition (Ref 00486.02).

Figure S 8 : Experimental design illustration of the study of the effects of hippurate, benzoate and saline (control) subcutaneous administrated on mice fed either carbohydrate diet or high fat diet.

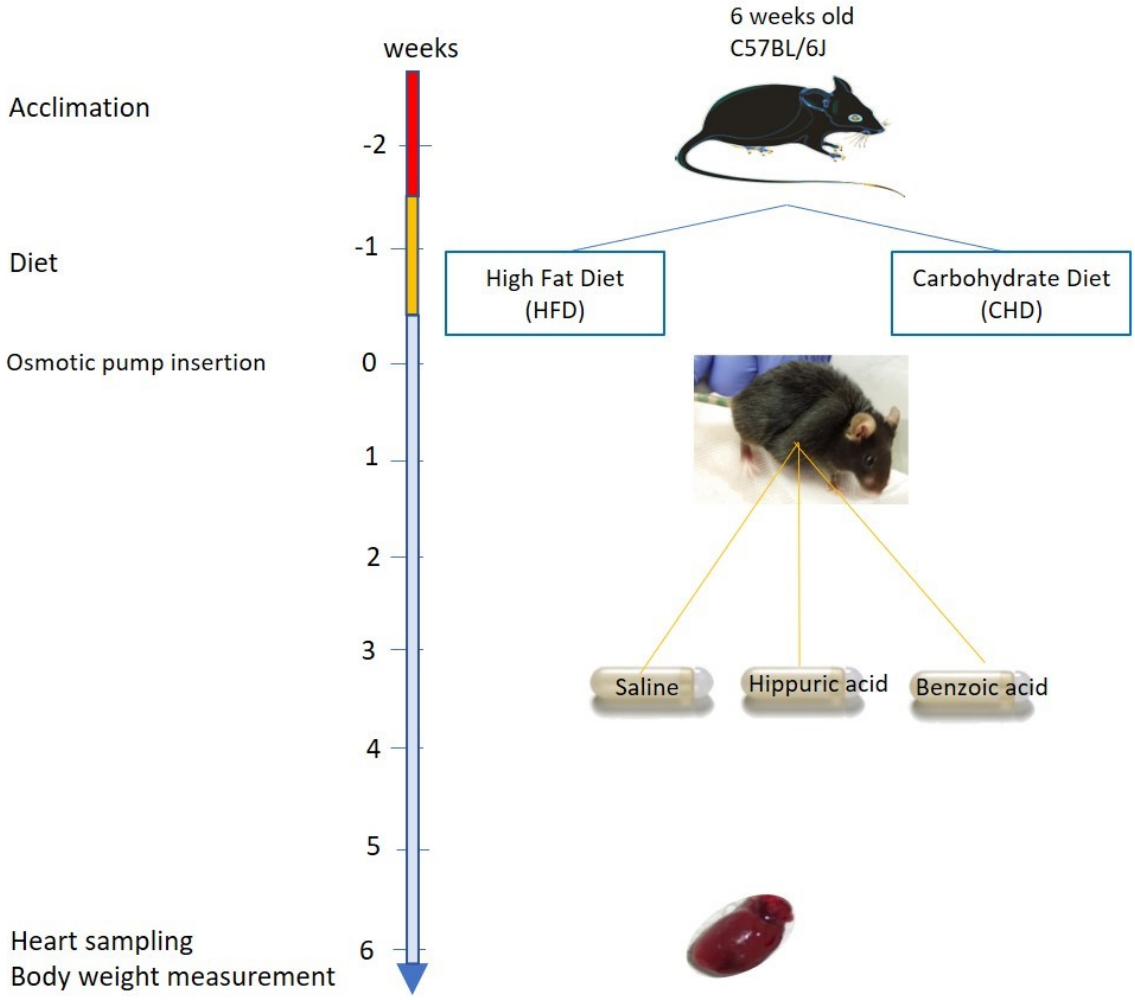

VI.2.16.2. RNA extraction

Heart RNA was extracted and quantified. Total RNA was isolated using RNeasy RNA Mini Kit (Qiagen, Courtaboeuf, France) (**Figure S 9**). Tissue samples from -80 degrees were lysed with Quiazol lysis reagent then homogenized with a Tissue Lyser. The lysate was then incubated with chloroform for phase separation, thus after centrifugation the upper aqueous phase that contain RNA was collected. Ethanol was added to the aqueous phase to provide ideal binding to the RNeasy Mini spin column. After that, the lysate was loaded to the column so that the RNA binds to the silica membrane while all contaminants were discarded in the flow-

through after centrifugation. To make sure that the RNA is not contaminated with DNA, DNase treatment for 15 min was applied on-column. Pure and concentrated RNA was finally eluted in 30 µl RNase-free water. The RNA samples were stored at -20 ˚C. The RNA quantity was obtained using a NanoDrop spectrophotometer.

Figure S 9 : RNA extraction from Heart mice tissues

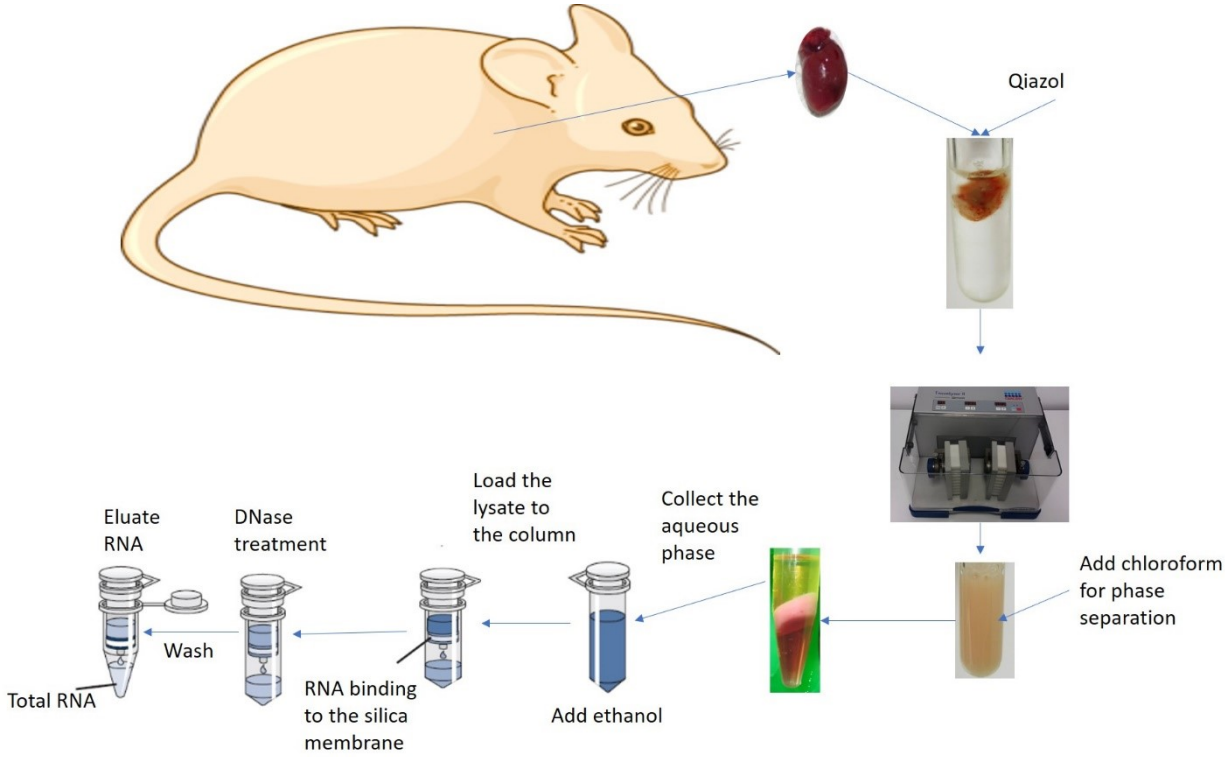

VI.2.16.3. RNA quality assessment

The quality of extracted RNA was assessed by electrophoresis on agarose gel run at 110V. For RNA staining, SYBR Safe DNA Gel Stain from Invitrogen was used for being less hazardous and alternative to ethidium bromide. The visualization was done under UV light. The quality of RNA was assessed based on the presence of rRNA (ribosomal RNA) bands at 23S and 16S (**Figure S 10**). Thus, intact RNA will have sharp rRNA bands 28S and 18S while the degraded RNA will appear as smear.

Figure S 10: Agarose gel electrophoresis of extracted RNA

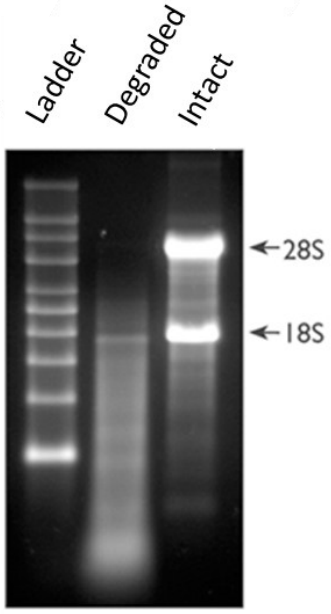

VI.2.16.4. Reverse transcription

Reverse transcription was performed using a M-MLV reverse transcriptase kit (ThermoFisher, Villebon, France). Reverse transcription is a process in which single-stranded mRNA is inversely transcribed into complementary DNA (cDNA). This was done using the M-MLV reverse transcriptase enzyme, random primers, dNTPs (deoxyribonucleotide) and DTT (Dithiothreitol) (**Figure S 11**). This reaction was performed using a 20 µL final volume with 500 ng RNA and it was carried out according to the following program: 10 mins at 25 °C, 50 mins at 37 °C and 15 minutes at 70 °C. The cDNA products were stored at -20 °C.

Figure S 11 : Reverse transcription of RNA into complementary DNA (cDNA)

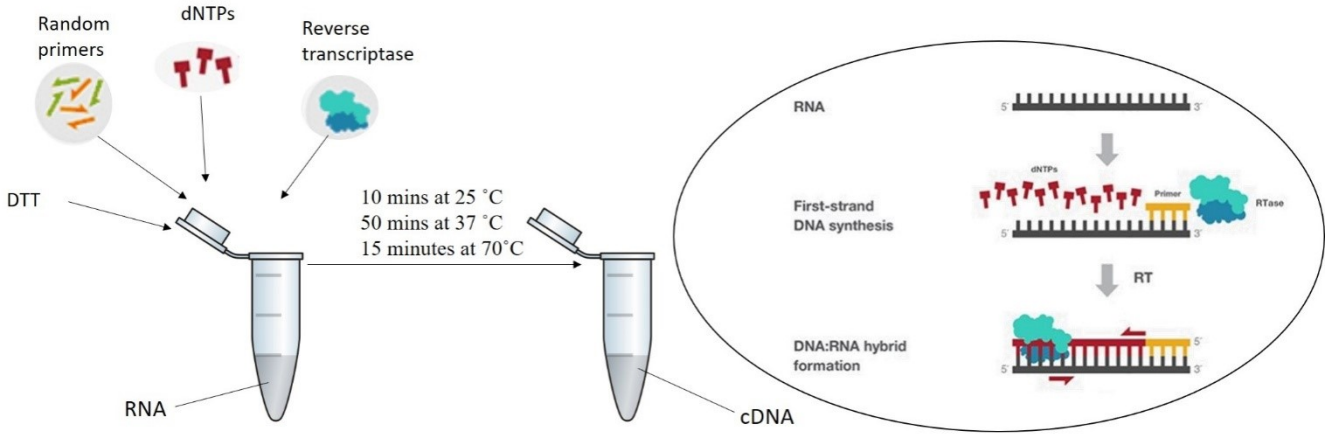

(Adapted from Reverse Transcription Applications - ThermoFisher. Available at : https://www.thermofisher.com/ae/en/home/life-science/cloning/cloning-learning-center/invitrogen-school-of-molecular-biology/rt-education/reverse-transcription-applications.html)

VI.2.16.5. Primer design for Quantitative RT-PCR

Two primers for each gene were designed and tested. Primers were designed using IDT (integrated DNA technologies) web-tool then validated for their specificity with Primer-BLAST (**Table S 2**).

Table S 2 : Oligonucleotides used in qPCR experiments in mice

Gene mouse	Forward	Reverse
PALMD-1	ACCGGCAGAAATCAGTCTATG	GTACTCTGTGGGCGATTTAGAG
PALMD-2	AGTCTATGCTGTTAGCTCCAATC	TCCTCTCTGAGGCTTGTCTTA
BMP2-1	AGTAGTTTCCAGCACCGAATTA	TTCACTAACCTGGTGTCCAATAG
BMP2-2	CATTTAGAGGAGAACCCAGGTG	AGTCACTAGCAATGGCCTTATC
IL6-1	CTTCCATCCAGTTGCCTTCT	CTCCGACTTGTGAAGTGGTATAG
NFκB-1	GGGATTTCGATTCCGCTATGT	GACCTGTGGGTAGGATTTCTTG
NFκB-2	GGATGACAGAGGCGTGTATTAG	CCTTCTCTCTGTCTGTGAGTTG
BMP6-1	CCAACTACTGTGATGGAGAGTG	GGACGTACTCGGGATTCATAAG
BMP6-2	CTCCAACATCGGCTCTGTAA	TCTCTGGGTTTCGGCTTTAG
IFNγ-1	AAATCCTGCAGAGCCAGATTAT	GCTGTTGCTGAAGAAGGTAGTA
IFNγ-2	GGCCATCAGCAACAACATAAG	GTTGACCTCAAACTTGGCAATAC
Cxcl9-1	GTTCGAGGAACCCTAGTGATAAG	GTTTGAGGTCTTTGAGGGATTTG
Cxcl9-2	GTGTCTCAGAGATGGTGCTAATG	TGAAATCCCATGGTCTCGAAAG
IL1β-1	GGTGTGTGACGTTCCCATTA	ATTGAGGTGGAGAGCTTTCAG
IL1β-2	GAGGACATGAGCACCTTCTTT	GCCTGTAGTGCAGTTGTCTAA

TNF-α	GGGGGCTTCCAGAACTC	GGGCTACAGGCTTGTCAC
MCP1	AGGTCCCTGTCATGCTTCTG	GCTGCTGGTGATCCTCTTGT
IL10	GGTTGCCAAGCCTTATCGGA	ACCTGCTCCACTGCCTTGCT
TBP	ACCCTTCACCAATGACTCCTATG	ATGACTGCAGCAAATCGCTTGG
HPRT	AAGCCTAAGATGAGCGCAAG	TTACTAGGCAGATGGCCACA

VI.2.16.6. Quantitative RT-PCR

Primers validation was performed with a standard curve for each gene, and the best primers were selected based on their efficiency which should be between 80 and 110 (80<E<110) (**Table S3**). Two housekeeping genes, TBP and HPRT, were tested to be used as reference for the relative quantification of target genes. Thus, TBP was chosen for having better Efficiency (**Table S3**).

Table S 3 : The efficiency of primers tested for qPCR. Standard curves were used to assess the reactions efficiencies and parameters (e.g., Slope). A good slope is between −3.9 and −3.0 which reflect an efficiency between 80 and 110%. Most of the targets have two specific primer pairs. The primer pairs *BMP2-1*, *BMP6-2*, *CXCL9-2*, *IL1β-2*, *NFκB-1*, *PALMD-2* have better efficiencies then the other primer pairs and were selected for qPCR experiments. *IL6* and *MCP1* have high efficiency % (>110%) but were selected for their C_t – threshold cycle (near 30) which indicate a moderate level of the targets in the samples. *IFNγ*, *TNFa* and *IL10* were not selected for their abnormal efficiency % (>>110% or <<80%). The housekeeping gene *TBP* was selected over HPRT for its better efficiency. S, Selected for qPCR experiments. NS, Not Selected for qPCR experiments. C_t, threshold cycle.

Target	Efficiency %	Slope	Selection
BMP2-1	100.592	-3.308	S
BMP2-2	91.297	-3.550	NS
BMP6-1	95.014	-3.447	NS
BMP6-2	101.126	-3.295	S
CXCL9-1	83.033	-3.809	NS
CXCL9-2	84.628	-3.755	S
TNF-α	9.669	-24.948	NS, E << 80%
IFNγ-1	168.433	-2.332	NS, Slope >-3.1 (E> 110%)

IFNγ-2	338.184	-1.558	NS, Slope >-3.1 (E> 110%)
IL10	1533.713	-0.824	NS, Slope >-3.1 (E> 110%)
IL1β-1	71.319	-4.277	NS, slope <-3.9 (E < 80%)
IL1β-2	96.099	-3.419	S
IL6	211.030	-2.029	S, Ct 32.2
MCP1	155.647	-2.453	S, Ct 30.9
NFκB-1	95.644	-3.431	S
NFκB-2	75.768	-4.083	NS
PALMD-1	95.970	-3.422	NS
PALMD-2	96.654	-3.405	S
HPRT	88.357	-3.637	NS
TBP	97.150	-3.392	S

Quantitative RT-PCR (qPCR) (**Figure S 12**) was performed using the Takyon™ Rox SYBR MasterMix dTTP Blue from Eurogentec. In qPCR reactions of 10 µL final volume, cDNA was mixed with the MasterMix, that contain SYBR Safe, Takyon DNA polymerase, dNTPs, $MgCl_2$, and with the forward and reverse oligonucleotides of the target gene. The qPCR cycling conditions were set as the following: a denaturation step at 95°C for 3 mins, then 40 cycles at 95 °C for 30 s and at 60 °C for 1 min (for primers annealing and extension step). Finally, a dissociation step at 95 °C for 15 s, 60 °C for 1 min and 65 °C for 15 s.

Figure S 12 : Real-time PCR with SYBR green. SYBR green dye is an intercalator that emits fluorescent signal when it binds to double stranded DNA.

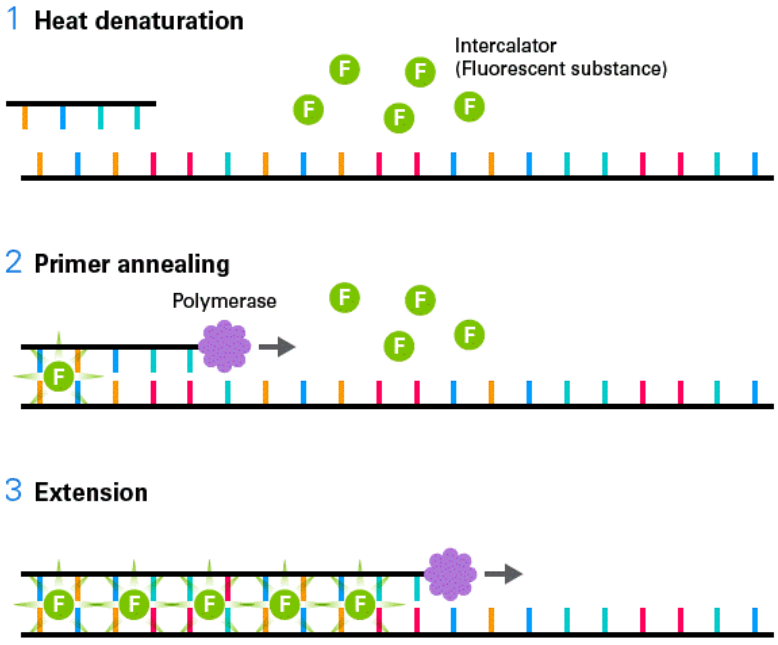

(From One-step RT-qPCR. Available at : https://www.takarabio.com/learning-centers/real-time-pcr/overview/one-step-rt-qpcr-kits)

VI.2.16.7. mRNA expression

In this work the gene expression was measured based on relative quantification that measures the difference in gene expression between two sample groups. The Pfaffl method of relative quantification was adopted to estimate the copy number of genes. Unlike the classic delta-delta Ct method which assumes primers efficiency are 100% (with each PCR cycle the amount of product will double), the Pfaffl takes into consideration the efficiency of each gene. In this method, in addition to the Ct values, primer efficiencies of all the genes are needed. This method can estimate the number of copies of genes and it requires the existence of control and a housekeeping gene of constant copy number, which allows the standardization of quantitative data. In this work, *TBP* gene was used as housekeeping gene (HKG).

The primers efficiency was converted following this equation "converted primer efficiency = ((Primer efficiency % / 100) +1)". Then the ΔCt of each gene was calculated as follows ΔCt = (Ct control samples - Ct treated sample). After that, the gene expression ratio was calculated using Pfaffl equation "gene expression ratio = $[(E_{\text{gene of interest}})^{\Delta Ct\ (\text{gene of interest})} / (E_{HKG})^{\Delta Ct\ (HKG)}]$". The results were compared to the control group and normalized to TBP gene. The data are

expressed as fold change. The control group is considered normal with a value of 1. Any value greater than 1 is considered overexpression and if the value is less than 1 is considered downregulated.

List of figures

Bibliography

Adams, D. H., Popma, J. J., Reardon, M. J., Yakubov, S. J., Coselli, J. S., Deeb, G. M., Gleason, T. G., Buchbinder, M., Hermiller, J., Kleiman, N. S., *et al.* (2014) 'Transcatheter Aortic-Valve Replacement with a Self-Expanding Prosthesis', *New England Journal of Medicine,* 370(19), pp. 1790-1798.

Afshar, M., Kamstrup Pia, R., Williams, K., Sniderman Allan, D., Nordestgaard Børge, G. and Thanassoulis, G. (2016) 'Estimating the Population Impact of Lp(a) Lowering on the Incidence of Myocardial Infarction and Aortic Stenosis—Brief Report', *Arteriosclerosis, Thrombosis, and Vascular Biology,* 36(12), pp. 2421-2423.

Aguado, B. A., Schuetze, K. B., Grim, J. C., Walker, C. J., Cox, A. C., Ceccato, T. L., Tan, A.-C., Sucharov, C. C., Leinwand, L. A., Taylor, M. R. G., *et al.* (2019) 'Transcatheter aortic valve replacements alter circulating serum factors to mediate myofibroblast deactivation', *Science Translational Medicine,* 11(509), pp. eaav3233.

Aksoy, O., Cam, A., Goel, S. S., Houghtaling, P. L., Williams, S., Ruiz-Rodriguez, E., Menon, V., Kapadia, S. R., Tuzcu, E. M., Blackstone, E. H. and Griffin, B. P. (2012) 'Do Bisphosphonates Slow the Progression of Aortic Stenosis?', *Journal of the American College of Cardiology,* 59(16), pp. 1452-1459.

Andreu, N., Escarceller, M., Feather, S., Devriendt, K., Wolf, A. S., Estivill, X. and Sumoy, L. (2001) 'PALML, a novel paralemmin-related gene mapping on human chromosome 1p21', *Gene,* 278(1), pp. 33-40.

Anwar, S., Bhandari, U., Panda, B. P., Dubey, K., Khan, W. and Ahmad, S. (2018) 'Trigonelline inhibits intestinal microbial metabolism of choline and its associated cardiovascular risk', *Journal of Pharmaceutical and Biomedical Analysis,* 159, pp. 100-112.

Argulian, E., Windecker, S. and Messerli, F. H. (2017) 'Misconceptions and Facts About Aortic Stenosis', *The American Journal of Medicine,* 130(4), pp. 398-402.

Arsenault, B. J., Boekholdt, S. M., Dubé, M.-P., Rhéaume, É., Wareham, N. J., Khaw, K.-T., Sandhu, M. S. and Tardif, J.-C. (2014) 'Lipoprotein(a) Levels, Genotype, and Incident Aortic Valve Stenosis: A Prospective Mendelian Randomization Study and Replication in a Case–Control Cohort', *Circulation: Cardiovascular Genetics,* 7(3), pp. 304-310.

Awan, Z., Alrasadi, K., Francis, G. A., Hegele, R. A., McPherson, R., Frohlich, J., Valenti, D., de Varennes, B., Marcil, M., Gagne, C., Genest, J. and Couture, P. (2008) 'Vascular calcifications in homozygote familial hypercholesterolemia', *Arteriosclerosis, Thrombosis, and Vascular Biology,* 28(4), pp. 777-785.

Awan, Z., Denis, M., Bailey, D., Giaid, A., Prat, A., Goltzman, D., Seidah, N. G. and Genest, J. (2011) 'The LDLR deficient mouse as a model for aortic calcification and quantification by micro-computed tomography', *Atherosclerosis,* 219(2), pp. 455-462.

Azizan, K. A., Ghani, N. H. A. and Nawawi, M. F. (2015) 'GC-MS based metabolomics and multivariate statistical analysis of Wedelia trilobata extracts for the identification of potential phytochemical properties', *Plant OMICS,* 8(6), pp. 537-543.

Barberini, L., Noto, A., Saba, L., Palmas, F., Fanos, V., Dessì, A., Zavattoni, M., Fattuoni, C. and Mussap, M. (2016) 'Multivariate data validation for investigating primary HCMV infection in pregnancy', *Data in Brief,* 9, pp. 220-230.

Bashir, M., Harky, A., Bleetman, D., Adams, B., Roberts, N., Balmforth, D., Yap, J., Lall, K., Shipolini, A., Oo, A. and Uppal, R. (2017) 'Aortic Valve Replacement: Are We Spoiled for Choice?', *Seminars in Thoracic and Cardiovascular Surgery,* 29(3), pp. 265-272.

Baumgartner, H., Hung, J., Bermejo, J., Chambers, J. B., Evangelista, A., Griffin, B. P., Iung, B., Otto, C. M., Pellikka, P. A. and Quiñones, M. (2009) 'Echocardiographic Assessment of Valve Stenosis: EAE/ASE Recommendations for Clinical Practice', *Journal of the American Society of Echocardiography,* 22(1), pp. 1-23.

Berry, K. A. Z., Hankin, J. A., Barkley, R. M., Spraggins, J. M., Caprioli, R. M. and Murphy, R. C. (2011) 'MALDI imaging of lipid biochemistry in tissues by mass spectrometry', *Chemical reviews,* 111(10), pp. 6491-6512.

Bhinderwala, F., Wase, N., DiRusso, C. and Powers, R. (2018) 'Combining Mass Spectrometry and NMR Improves Metabolite Detection and Annotation', *Journal of Proteome Research,* 17(11), pp. 4017-4022.

Blaise, B. J., Shintu, L., Elena, B., Emsley, L., Dumas, M.-E. and Toulhoat, P. (2009) 'Statistical Recoupling Prior to Significance Testing in Nuclear Magnetic Resonance Based Metabonomics', *Analytical Chemistry,* 81(15), pp. 6242-6251.

Boateng, S. and Sanborn, T. (2013) 'Acute myocardial infarction', *Disease-a-Month,* 59(3), pp. 83-96.

Bouatra, S., Aziat, F., Mandal, R., Guo, A. C., Wilson, M. R., Knox, C., Bjorndahl, T. C., Krishnamurthy, R., Saleem, F., Liu, P., Dame, Z. T., Poelzer, J., Huynh, J., Yallou, F. S., Psychogios, N., Dong, E., Bogumil, R., Roehring, C. and Wishart, D. S. (2013) 'The Human Urine Metabolome', *PLOS ONE,* 8(9), pp. e73076.

Bouchareb, R., Mahmut, A., Nsaibia Mohamed, J., Boulanger, M.-C., Dahou, A., Lépine, J.-L., Laflamme, M.-H., Hadji, F., Couture, C., Trahan, S., *et al.* (2015) 'Autotaxin Derived From Lipoprotein(a) and Valve Interstitial Cells Promotes Inflammation and Mineralization of the Aortic Valve', *Circulation,* 132(8), pp. 677-690.

Buchholz, A., Hurlebaus, J., Wandrey, C. and Takors, R. (2002) 'Metabolomics: quantification of intracellular metabolite dynamics', *Biomol Eng,* 19(1), pp. 5-15.

Bujak, R., Struck-Lewicka, W., Markuszewski, M. J. and Kaliszan, R. (2015) 'Metabolomics for laboratory diagnostics', *Journal of Pharmaceutical and Biomedical Analysis,* 113, pp. 108-120.

Cai, Z., Li, F., Gong, W., Liu, W., Duan, Q., Chen, C., Ni, L., Xia, Y., Cianflone, K., Dong, N. and Wang Dao, W. (2013) 'Endoplasmic Reticulum Stress Participates in Aortic Valve

Calcification in Hypercholesterolemic Animals', *Arteriosclerosis, Thrombosis, and Vascular Biology,* 33(10), pp. 2345-2354.

Cairns, B. J., Coffey, S., Travis, R. C., Prendergast, B., Green, J., Engert, J. C., Lathrop, M., Thanassoulis, G. and Clarke, R. (2017) 'A Replicated, Genome-Wide Significant Association of Aortic Stenosis With a Genetic Variant for Lipoprotein(a)', *Circulation,* 135(12), pp. 1181-1183.

Capoulade, R., Chan, K. L., Yeang, C., Mathieu, P., Bossé, Y., Dumesnil, J. G., Tam, J. W., Teo, K. K., Mahmut, A., Yang, X., *et al.* (2015) 'Oxidized Phospholipids, Lipoprotein(a), and Progression of Calcific Aortic Valve Stenosis', *Journal of the American College of Cardiology,* 66(11), pp. 1236-1246.

Carabello, B. A. and Paulus, W. J. (2009) 'Aortic stenosis', *Lancet,* 373(9667), pp. 956-66.

Catalano, M., Lin, D., Cassiere, H., Kohn, N., Rutkin, B., Maurer, G., Berg, J. A., Jahn, J., Esposito, R., Hartman, A. and Yu, P.-J. (2019) 'Incidence of Acute Kidney Injury in Patients with Chronic Renal Insufficiency: Transcatheter versus Surgical Aortic Valve Replacement', *Journal of Interventional Cardiology,* 2019, pp. e9780415.

Chan, K. L., Teo, K., Dumesnil, J. G., Ni, A., Tam, J. and Investigators, A. (2010) 'Effect of Lipid lowering with rosuvastatin on progression of aortic stenosis: results of the aortic stenosis progression observation: measuring effects of rosuvastatin (ASTRONOMER) trial', *Circulation,* 121(2), pp. 306-314.

Chang, P. P., Wruck, L. M., Shahar, E., Rossi, J. S., Loehr, L. R., Russell, S. D., Agarwal, S. K., Konety, S. H., Rodriguez, C. J. and Rosamond, W. D. (2018) 'Trends in Hospitalizations and Survival of Acute Decompensated Heart Failure in Four US Communities (2005–2014)', *Circulation,* 138(1), pp. 12-24.

Chen, H. Y., Cairns, B. J., Small, A. M., Burr, H. A., Ambikkumar, A., Martinsson, A., Thériault, S., Munter, H. M., Steffen, B., Zhang, R., *et al.* (2020) 'Association of FADS1/2 Locus Variants and Polyunsaturated Fatty Acids With Aortic Stenosis', *JAMA Cardiology*.

Chen, Z. and Kim, J. (2016) 'Urinary proteomics and metabolomics studies to monitor bladder health and urological diseases', *BMC urology,* 16, pp. 11-11.

Cheng, Y., Xie, G., Chen, T., Qiu, Y., Zou, X., Zheng, M., Tan, B., Feng, B., Dong, T., He, P., Zhao, L., Zhao, A., Xu, L. X., Zhang, Y. and Jia, W. (2012) 'Distinct Urinary Metabolic Profile of Human Colorectal Cancer', *Journal of Proteome Research,* 11(2), pp. 1354-1363.

Coble, J. B. and Fraga, C. G. (2014) 'Comparative evaluation of preprocessing freeware on chromatography/mass spectrometry data for signature discovery', *Journal of Chromatography A,* 1358, pp. 155-164.

Coffey, S., Cox, B. and Williams, M. J. A. (2014) 'The Prevalence, Incidence, Progression, and Risks of Aortic Valve Sclerosis: A Systematic Review and Meta-Analysis', *Journal of the American College of Cardiology,* 63(25, Part A), pp. 2852-2861.

Cowell, S. J., Newby, D. E., Prescott, R. J., Bloomfield, P., Reid, J., Northridge, D. B. and Boon, N. A. (2005) 'A Randomized Trial of Intensive Lipid-Lowering Therapy in Calcific Aortic Stenosis', *New England Journal of Medicine,* 352(23), pp. 2389-2397.

Czarny, M. J. and Resar, J. R. (2014) 'Diagnosis and Management of Valvular Aortic Stenosis', *Clinical Medicine Insights: Cardiology,* 8s1, pp. CMC.S15716.

Dashzeveg, N., Taira, N., Lu, Z. G., Kimura, J. and Yoshida, K. (2014) 'Palmdelphin, a novel target of p53 with Ser46 phosphorylation, controls cell death in response to DNA damage', *Cell Death & Disease,* 5(5), pp. e1221.

Deidda, M., Piras, C., Dessalvi, C. C., Locci, E., Barberini, L., Torri, F., Ascedu, F., Atzori, L. and Mercuro, G. (2015) 'Metabolomic approach to profile functional and metabolic changes in heart failure', *Journal of Translational Medicine,* 13(1), pp. 297.

Dharmarajan, K., Foster, J., Coylewright, M., Green, P., Vavalle, J. P., Faheem, O., Huang, P.-H., Krishnaswamy, A., Thourani, V. H., McCoy, L. A. and Wang, T. Y. (2017) 'The medically managed patient with severe symptomatic aortic stenosis in the TAVR era: Patient characteristics, reasons for medical management, and quality of shared decision making at heart valve treatment centers', *PLOS ONE,* 12(4), pp. e0175926.

Dieterle, F., Ross, A., Schlotterbeck, G. and Senn, H. (2006) 'Probabilistic Quotient Normalization as Robust Method to Account for Dilution of Complex Biological Mixtures. Application in 1H NMR Metabonomics', *Analytical Chemistry,* 78(13), pp. 4281-4290.

Dona, A. C., Jiménez, B., Schäfer, H., Humpfer, E., Spraul, M., Lewis, M. R., Pearce, J. T. M., Holmes, E., Lindon, J. C. and Nicholson, J. K. (2014) 'Precision High-Throughput Proton NMR Spectroscopy of Human Urine, Serum, and Plasma for Large-Scale Metabolic Phenotyping', *Analytical Chemistry,* 86(19), pp. 9887-9894.

Dumesnil, J. G. and Pibarot, P. (2013) 'The Obesity Paradox in Aortic Stenosis: To Be or Not To Be∗', *Journal of the American College of Cardiology,* 62(18), pp. 1691-1693.

Dunn, W. B., Lin, W., Broadhurst, D., Begley, P., Brown, M., Zelena, E., Vaughan, A. A., Halsall, A., Harding, N., Knowles, J. D., *et al.* (2015) 'Molecular phenotyping of a UK population: defining the human serum metabolome', *Metabolomics,* 11, pp. 9-26.

Dweck, M. R., Boon, N. A. and Newby, D. E. (2012) 'Calcific Aortic Stenosis: A Disease of the Valve and the Myocardium', *Journal of the American College of Cardiology,* 60(19), pp. 1854-1863.

Eleid Mackram, F., Nishimura Rick, A., Sorajja, P. and Borlaug Barry, A. (2013) 'Systemic Hypertension in Low-Gradient Severe Aortic Stenosis With Preserved Ejection Fraction', *Circulation,* 128(12), pp. 1349-1353.

Elmariah, S., Farrell, L. A., Daher, M., Shi, X., Keyes, M. J., Cain, C. H., Pomerantsev, E., Vlahakes, G. J., Inglessis, I., Passeri, J. J., *et al.* (2016) 'Metabolite Profiles Predict Acute Kidney Injury and Mortality in Patients Undergoing Transcatheter Aortic Valve Replacement', *Journal of the American Heart Association,* 5(3), pp. e002712-e002712.

Emdin, C. A., Khera, A. V., Natarajan, P., Klarin, D., Won, H.-H., Peloso, G. M., Stitziel, N. O., Nomura, A., Zekavat, S. M., Bick, A. G., *et al.* (2016) 'Phenotypic Characterization of Genetically Lowered Human Lipoprotein(a) Levels', *Journal of the American College of Cardiology,* 68(25), pp. 2761-2772.

Eveborn, G. W., Schirmer, H., Heggelund, G., Lunde, P. and Rasmussen, K. (2013) 'The evolving epidemiology of valvular aortic stenosis. The Tromsø Study', *Heart,* 99(6), pp. 396-400.

Fanos, V., Caboni, P., Corsello, G., Stronati, M., Gazzolo, D., Noto, A., Lussu, M., Dessì, A., Giuffrè, M., Lacerenza, S., *et al.* (2014) 'Urinary 1H-NMR and GC-MS metabolomics predicts early and late onset neonatal sepsis', *Early Human Development,* 90, pp. S78-S83.

Fernandez Esmerats, J., Villa-Roel, N., Kumar, S., Gu, L., Salim, M. T., Ohh, M., Taylor, W. R., Nerem, R. M., Yoganathan, A. P. and Jo, H. (2019) 'Disturbed Flow Increases UBE2C (Ubiquitin E2 Ligase C) via Loss of miR-483-3p, Inducing Aortic Valve Calcification by the pVHL (von Hippel-Lindau Protein) and HIF-1α (Hypoxia-Inducible Factor-1α) Pathway in Endothelial Cells', *Arteriosclerosis, Thrombosis, and Vascular Biology,* 39(3), pp. 467-481.

Fuchs, B., Süss, R. and Schiller, J. (2010) *An update of MALDI-TOF mass spectrometry in lipid research.*

Gao, X., Chen, W., Li, R., Wang, M., Chen, C., Zeng, R. and Deng, Y. (2012) 'Systematic variations associated with renal disease uncovered by parallel metabolomics of urine and serum', *BMC Systems Biology,* 6(Suppl 1), pp. S14.

Garg, V., Muth, A. N., Ransom, J. F., Schluterman, M. K., Barnes, R., King, I. N., Grossfeld, P. D. and Srivastava, D. (2005) 'Mutations in NOTCH1 cause aortic valve disease', *Nature,* 437(7056), pp. 270-274.

Gałąska, R., Kulawiak-Gałąska, D., Chmara, M., Chlebus, K., Studniarek, M., Fijałkowski, M., Wasąg, B., Rynkiewicz, A. and Gruchała, M. (2018) 'Aortic valve calcium score in hypercholesterolemic patients with and without low-density lipoprotein receptor gene mutation', *PLoS ONE,* 13(12).

Gebhard, C., Maafi, F., Stähli, B. E., Bonnefoy, A., Gebhard, C. E., Nachar, W., de Oliveira Moraes, A. B., Mecteau, M., Mihalache-Avram, T., *et al.* (2018) 'Beneficial Effects of High-Density Lipoproteins on Acquired von Willebrand Syndrome in Aortic Valve Stenosis', *Thrombosis and Haemostasis,* 118(2), pp. 288-297.

Glader, C. A., Birgander, L. S., Söderberg, S., Ildgruben, H. P., Saikku, P., Waldenström, A. and Dahlén, G. H. (2003) 'Lipoprotein(a), Chlamydia pneumoniae, leptin and tissue plasminogen activator as risk markers for valvular aortic stenosis', *European Heart Journal,* 24(2), pp. 198-208.

Goemann, I. M., Londero, T. M. and Dora, J. M. (2015) 'PCSK9 Inhibitors and Cardiovascular Events', *The New England Journal of Medicine,* 373(8), pp. 773-774.

Gordon, T., Castelli, W. P., Hjortland, M. C., Kannel, W. B. and Dawber, T. R. (1977) 'High density lipoprotein as a protective factor against coronary heart disease: The Framingham study', *The American Journal of Medicine,* 62(5), pp. 707-714.

Guasch‐Ferré, M., Hu, F. B., Ruiz‐Canela, M., Bulló, M., Toledo, E., Wang, D. D., Corella, D., Gómez‐Gracia, E., Fiol, M., Estruch, R., *et al.* (2017) 'Plasma Metabolites From Choline Pathway and Risk of Cardiovascular Disease in the PREDIMED (Prevention With Mediterranean Diet) Study', *Journal of the American Heart Association: Cardiovascular and Cerebrovascular Disease,* 6(11).

Haeusler Karl, G., Laufs, U. and Endres, M. (2011) 'Chronic Heart Failure and Ischemic Stroke', *Stroke,* 42(10), pp. 2977-2982.

He, M., Chen, Z., Martin, M., Zhang, J., Sangwung, P., Woo, B., Tremoulet, A. H., Shimizu, C., Jain, M. K., Burns, J. C. and Shyy, J. Y. J. (2017) 'miR-483 Targeting of CTGF Suppresses Endothelial-to-Mesenchymal Transition: Therapeutic Implications in Kawasaki Disease', *Circulation Research,* 120(2), pp. 354-365.

Helas, S., Goettsch, C., Schoppet, M., Zeitz, U., Hempel, U., Morawietz, H., Kostenuik, P. J., Erben, R. G. and Hofbauer, L. C. (2009) 'Inhibition of Receptor Activator of NF-κB Ligand by Denosumab Attenuates Vascular Calcium Deposition in Mice', *The American Journal of Pathology,* 175(2), pp. 473-478.

Helgadottir, A., Thorleifsson, G., Gretarsdottir, S., Stefansson, O. A., Tragante, V., Thorolfsdottir, R. B., Jonsdottir, I., Bjornsson, T., Steinthorsdottir, V., Verweij, N., *et al.* (2018) 'Genome-wide analysis yields new loci associating with aortic valve stenosis', *Nature Communications,* 9(1).

Helske, S., Lindstedt, K. A., Laine, M., Mäyränpää, M., Werkkala, K., Lommi, J., Turto, H., Kupari, M. and Kovanen, P. T. (2004) 'Induction of local angiotensin II-producing systems in stenotic aortic valves', *Journal of the American College of Cardiology,* 44(9), pp. 1859-1866.

Hidaka, H., Hanyu, N., Sugano, M., Kawasaki, K., Yamauchi, K. and Katsuyama, T. (2007) 'Analysis of Human Serum Lipoprotein Lipid Composition Using MALDI-TOF Mass Spectrometry', *Annals of Clinical & Laboratory Science,* 37(3), pp. 213-221.

Ho, Y.-P. and Huang, P.-C. (2002) 'A novel structural analysis of glycerophosphocholines as TFA/K(+) adducts by electrospray ionization ion trap tandem mass spectrometry', *Rapid communications in mass spectrometry: RCM,* 16(16), pp. 1582-1589.

Hoffman, J. D., Yanckello, L. M., Chlipala, G., Hammond, T. C., McCulloch, S. D., Parikh, I., Sun, S., Morganti, J. M., Green, S. J. and Lin, A.-L. (2019) 'Dietary inulin alters the gut microbiome, enhances systemic metabolism and reduces neuroinflammation in an APOE4 mouse model', *PLoS ONE,* 14(8).

Hofmann, B., Yakobus, Y., Indrasari, M., Nass, N., Santos, A. N., Kraus, F. B., Silber, R.-E. and Simm, A. (2014) 'RAGE influences the development of aortic valve stenosis in mice on a high fat diet', *Experimental Gerontology,* 59, pp. 13-20.

Hu, F. B., Stampfer, M. J., Manson, J. E., Ascherio, A., Colditz, G. A., Speizer, F. E., Hennekens, C. H. and Willett, W. C. (1999) 'Dietary saturated fats and their food sources in relation to the risk of coronary heart disease in women', *The American Journal of Clinical Nutrition,* 70(6), pp. 1001-1008.

Hyder, J. A., Allison, M. A., Criqui, M. H. and Wright, C. M. (2007) 'Association between Systemic Calcified Atherosclerosis and Bone Density', *Calcified Tissue International,* 80(5), pp. 301-306.

Ilavenil, S., Kim, D. H., Jeong, Y.-I., Arasu, M. V., Vijayakumar, M., Prabhu, P. N., Srigopalram, S. and Choi, K. C. (2015) 'Trigonelline protects the cardiocyte from hydrogen peroxide induced apoptosis in H9c2 cells', *Asian Pacific Journal of Tropical Medicine,* 8(4), pp. 263-268.

Jasbi, P., Wang, D., Cheng, S. L., Fei, Q., Cui, J. Y., Liu, L., Wei, Y., Raftery, D. and Gu, H. (2019) 'Breast cancer detection using targeted plasma metabolomics', *Journal of Chromatography B,* 1105, pp. 26-37.

Johnson, M. and Rajamannan, N. (2006) 'Diseases of Wnt signaling', *Reviews in endocrine & metabolic disorders,* 7, pp. 41-9.

Joseph, J., Naqvi, S. Y., Giri, J. and Goldberg, S. (2016) *Aortic Stenosis: Pathophysiology, Diagnosis, and Therapy.*

K, S. (2014) 'Metabolic profiling in diabetes', *The Journal of Endocrinology,* 221(3), pp. R75-85.

Kaltoft, M., Langsted, A. and Nordestgaard, B. G. (2020) 'Obesity as a Causal Risk Factor for Aortic Valve Stenosis', *Journal of the American College of Cardiology,* 75(2), pp. 163-176.

Kamstrup, P. R., Hung, M. Y., Witztum, J. L., Tsimikas, S. and Nordestgaard, B. G. (2017) 'Oxidized Phospholipids and Risk of Calcific Aortic Valve Disease: The Copenhagen General Population Study', *Arteriosclerosis, Thrombosis, and Vascular Biology,* 37(8), pp. 1570-1578.

Kamstrup, P. R., Tybjærg-Hansen, A. and Nordestgaard, B. G. (2014) 'Elevated Lipoprotein(a) and Risk of Aortic Valve Stenosis in the General Population', *Journal of the American College of Cardiology,* 63(5), pp. 470-477.

Kapoor, R., Ladak, S. and Gomase, V. (2009) *MALDI-TOF based Metabolomic approach.*

Kay, H. H., Zhu, S. and Tsoi, S. (2007) 'Hypoxia and Lactate Production in Trophoblast Cells', *Placenta,* 28(8), pp. 854-860.

Khot, U. N., Novaro, G. M., Popović, Z. B., Mills, R. M., Thomas, J. D., Tuzcu, E. M., Hammer, D., Nissen, S. E. and Francis, G. S. (2003) 'Nitroprusside in Critically Ill Patients with Left Ventricular Dysfunction and Aortic Stenosis', *New England Journal of Medicine,* 348(18), pp. 1756-1763.

Kranzhöfer, R., Schmidt, J., Pfeiffer Carolein, A. H., Hagl, S., Libby, P. and Kübler, W. (1999) 'Angiotensin Induces Inflammatory Activation of Human Vascular Smooth Muscle Cells', *Arteriosclerosis, Thrombosis, and Vascular Biology,* 19(7), pp. 1623-1629.

Krau, N.-C., Lünstedt, N.-S., Freitag‐Wolf, S., Brehm, D., Petzina, R., Lutter, G., Bramlage, P., Dempfle, A., Frey, N. and Frank, D. (2015) 'Elevated growth differentiation factor 15 levels predict outcome in patients undergoing transcatheter aortic valve implantation', *European Journal of Heart Failure,* 17(9), pp. 945-955.

Kurtz, C. E. and Otto, C. M. (2010) 'Aortic stenosis: clinical aspects of diagnosis and management, with 10 illustrative case reports from a 25-year experience', *Medicine,* 89(6), pp. 349-379.

Lancellotti, P. (2012) 'Grading aortic stenosis severity when the flow modifies the gradientvalve area correlation', *Cardiovascular Diagnosis and Therapy,* 2(1), pp. 6-9.

Larsson, S. C., Wolk, A., Håkansson, N. and Bäck, M. (2017) 'Overall and abdominal obesity and incident aortic valve stenosis: two prospective cohort studies', *European Heart Journal,* 38(28), pp. 2192-2197.

Lee, D. Y. and Fiehn, O. (2008) 'High quality metabolomic data for Chlamydomonas reinhardtii', *Plant Methods,* 4(1), pp. 7.

Lee, D. Y., Kind, T., Yoon, Y.-R., Fiehn, O. and Liu, K.-H. (2014) 'Comparative evaluation of extraction methods for simultaneous mass-spectrometric analysis of complex lipids and primary metabolites from human blood plasma', *Analytical and Bioanalytical Chemistry,* 406(28), pp. 7275-7286.

Lei, Y., Sinha, A., Nosoudi, N., Grover, A. and Vyavahare, N. (2014) 'Hydroxyapatite and calcified elastin induce osteoblast-like differentiation in rat aortic smooth muscle cells', *Experimental Cell Research,* 323(1), pp. 198-208.

Leibundgut, G., Scipione, C., Yin, H., Schneider, M., Boffa, M. B., Green, S., Yang, X., Dennis, E., Witztum, J. L., Koschinsky, M. L. and Tsimikas, S. (2013) 'Determinants of binding of oxidized phospholipids on apolipoprotein (a) and lipoprotein (a)', *Journal of lipid research,* 54(10), pp. 2815-2830.

Leon, M. B., Smith, C. R., Mack, M., Miller, D. C., Moses, J. W., Svensson, L. G., Tuzcu, E. M., Webb, J. G., Fontana, G. P., Makkar, R. R., *et al.* (2010) 'Transcatheter Aortic-Valve Implantation for Aortic Stenosis in Patients Who Cannot Undergo Surgery', *New England Journal of Medicine,* 363(17), pp. 1597-1607.

Lewis, G. D., Wei, R., Liu, E., Yang, E., Shi, X., Martinovic, M., Farrell, L., Asnani, A., Cyrille, M., Ramanathan, A., *et al.* (2008) 'Metabolite profiling of blood from individuals undergoing planned myocardial infarction reveals early markers of myocardial injury', *The Journal of Clinical Investigation,* 118(10), pp. 3503-3512.

Lindman, B. R., Clavel, M.-A., Mathieu, P., Iung, B., Lancellotti, P., Otto, C. M. and Pibarot, P. (2016) 'Calcific aortic stenosis', *Nature Reviews. Disease Primers,* 2, pp. 16006.

Lindroos, M., Kupari, M., Valvanne, J., Strandberg, T., HeikkilÄ, J. and TlLvis, R. (1994) 'Factors associated with calcific aortic valve degeneration in the elderly', *European Heart Journal,* 15(7), pp. 865-870.

Linefsky, J. P., O'Brien, K. D., Katz, R., de Boer, I. H., Barasch, E., Jenny, N. S., Siscovick, D. S. and Kestenbaum, B. (2011) 'Association of serum phosphate levels with aortic valve sclerosis and annular calcification: the cardiovascular health study', *Journal of the American College of Cardiology,* 58(3), pp. 291-297.

Liu, A. C., Joag, V. R. and Gotlieb, A. I. (2007) 'The emerging role of valve interstitial cell phenotypes in regulating heart valve pathobiology', *The American journal of pathology,* 171(5), pp. 1407-1418.

Ljungberg, J., Janiec, M., Bergdahl, I. A., Holmgren, A., Hultdin, J., Johansson, B., Näslund, U., Siegbahn, A., Fall, T. and Söderberg, S. (2018) 'Proteomic Biomarkers for Incident Aortic Stenosis Requiring Valvular Replacement', *Circulation,* 138(6), pp. 590-599.

Mahmut, A., Boulanger, M.-C., El Husseini, D., Fournier, D., Bouchareb, R., Després, J.-P., Pibarot, P., Bossé, Y. and Mathieu, P. (2014) 'Elevated Expression of Lipoprotein-Associated Phospholipase A2 in Calcific Aortic Valve Disease: Implications for Valve Mineralization', *Journal of the American College of Cardiology,* 63(5), pp. 460-469.

Marquis-Gravel, G., Redfors, B., Leon, M. B. and Généreux, P. (2016) 'Medical Treatment of Aortic Stenosis', *Circulation,* 134(22), pp. 1766-1784.

Mathieu, J. and Ruohola-Baker, H. (2017) 'Metabolic remodeling during the loss and acquisition of pluripotency', *Development,* 144(4), pp. 541-551.

Mathieu, P., Arsenault, B. J., Boulanger, M.-C., Bossé, Y. and Koschinsky, M. L. (2017) 'Pathobiology of Lp(a) in calcific aortic valve disease', *Expert Review of Cardiovascular Therapy,* 15(10), pp. 797-807.

McLaughlin, M. A. and Fuster, V. (1995) 'The three mechanisms for coronary artery disease progression: insights into future management', *The Mount Sinai Journal of Medicine, New York,* 62(4), pp. 265-274.

Messika-Zeitoun, D., Bielak, L. F., Peyser, P. A., Sheedy, P. F., Turner, S. T., Nkomo, V. T., Breen, J. F., Maalouf, J., Scott, C., Tajik, A. J. and Enriquez-Sarano, M. (2007) 'Aortic valve calcification: determinants and progression in the population', *Arteriosclerosis, Thrombosis, and Vascular Biology,* 27(3), pp. 642-648.

Milman, B. L., Lugovkina, N. V. and Zhurkovich, I. K. (2017) 'Phospholipid Composition of Human Blood Plasma as Detected by Matrix-Assisted Laser Desorption/Ionization Mass Spectrometry: New Observations', *Journal of Analytical Chemistry,* 72(14), pp. 1411-1418.

Misfeld, M. and Sievers, H.-H. (2007) 'Heart valve macro- and microstructure', *Philosophical Transactions of the Royal Society B: Biological Sciences,* 362(1484), pp. 1421-1436.

Monteiro, M. S., Carvalho, M., Bastos, M. L. and Pinho, P. G. d. (2013) 'Metabolomics Analysis for Biomarker Discovery: Advances and Challenges', *Current Medicinal Chemistry,* 20(2), pp. 257-271.

Monteiro, M. S., Carvalho, M. and Pinho, M. L. B. a. P. G. d. (2012) 'Metabolomics Analysis for Biomarker Discovery: Advances and Challenges', *Current Medicinal Chemistry*.

Mori, K., Ishida, T., Yasuda, T., Hasokawa, M., Monguchi, T., Sasaki, M., Kondo, K., Nakajima, H., Shinohara, M., Shinke, T., *et al.* (2015) 'Serum Trans-Fatty Acid Concentration Is Elevated in Young Patients With Coronary Artery Disease in Japan', *Circulation Journal,* 79(9), pp. 2017-2025.

Mourino-Alvarez, L., Baldan-Martin, M., Sastre-Oliva, T., Martin-Lorenzo, M., Maroto, A. S., Corbacho-Alonso, N., Rincon, R., Martin-Rojas, T., Lopez-Almodovar, L. F., Alvarez-Llamas, G., *et al.* (2018) 'A comprehensive study of calcific aortic stenosis: from rabbit to human samples', *Disease Models & Mechanisms,* 11(6), pp. dmm033423.

Murphy, R. C., Hankin, J. A. and Barkley, R. M. (2009) 'Imaging of lipid species by MALDI mass spectrometry', *Journal of Lipid Research,* 50(Suppl), pp. S317-S322.

Nagana Gowda, G. A. and Raftery, D. (2013) 'Biomarker Discovery and Translation in Metabolomics', *Current Metabolomics,* 1(3), pp. 227-240.

Nagana Gowda, G. A., Zhang, S., Gu, H., Asiago, V., Shanaiah, N. and Raftery, D. (2008) 'Metabolomics-Based Methods for Early Disease Diagnostics: A Review', *Expert review of molecular diagnostics,* 8(5), pp. 617-633.

Nazarzadeh, M., Pinho-Gomes, A.-C., Bidel, Z., Dehghan, A., Canoy, D., Hassaine, A., Ayala Solares, J. R., Salimi-Khorshidi, G., Smith, G. D., Otto, C. M. and Rahimi, K. (2020) 'Plasma lipids and risk of aortic valve stenosis: a Mendelian randomization study', *European Heart Journal*.

Nichols, M., Townsend, N., Scarborough, P. and Rayner, M. (2013) 'Cardiovascular disease in Europe: epidemiological update', *European Heart Journal,* 34(39), pp. 3028-3034.

Nie, Y., Chen, H., Guo, C., Yuan, Z., Zhou, X., Zhang, Y., Zhang, X., Mo, D. and Chen, Y. (2017) 'Palmdelphin promotes myoblast differentiation and muscle regeneration', *Scientific Reports,* 7, pp. 41608.

Nishimura, R. A., Otto, C. M., Bonow, R. O., Carabello, B. A., Erwin, J. P., Guyton, R. A., O'Gara, P. T., Ruiz, C. E., Skubas, N. J., Sorajja, P., Sundt, T. M. and Thomas, J. D. (2014) '2014 AHA/ACC Guideline for the Management of Patients With Valvular Heart Disease: A Report of the American College of Cardiology/American Heart Association Task Force on Practice Guidelines', *Journal of the American College of Cardiology,* 63(22), pp. e57-e185.

Nishiumi, S., Shinohara, M., Ikeda, A., Yoshie, T., Hatano, N., Kakuyama, S., Mizuno, S., Sanuki, T., Kutsumi, H., Fukusaki, E., Azuma, T., Takenawa, T. and Yoshida, M. (2010) *Serum metabolomics as a novel diagnostic approach for pancreatic cancer.*

Nkomo, V. T., Gardin, J. M., Skelton, T. N., Gottdiener, J. S., Scott, C. G. and Enriquez-Sarano, M. (2006) 'Burden of valvular heart diseases: a population-based study', *Lancet,* 368(9540), pp. 1005-11.

Novaro Gian, M., Sachar, R., Pearce Gregory, L., Sprecher Dennis, L. and Griffin Brian, P. (2003) 'Association Between Apolipoprotein E Alleles and Calcific Valvular Heart Disease', *Circulation,* 108(15), pp. 1804-1808.

Oakman, C., Tenori, L., Biganzoli, L., Santarpia, L., Cappadona, S., Luchinat, C. and Di Leo, A. (2011) 'Uncovering the metabolomic fingerprint of breast cancer', *The International Journal of Biochemistry & Cell Biology,* 43(7), pp. 1010-1020.

Otto, C. M. (2008) 'Calcific Aortic Stenosis — Time to Look More Closely at the Valve', *New England Journal of Medicine,* 359(13), pp. 1395-1398.

Otto, C. M., Lind, B. K., Kitzman, D. W., Gersh, B. J. and Siscovick, D. S. (1999) 'Association of aortic-valve sclerosis with cardiovascular mortality and morbidity in the elderly', *The New England Journal of Medicine,* 341(3), pp. 142-147.

Otto, C. M. and Prendergast, B. (2014) 'Aortic-valve stenosis--from patients at risk to severe valve obstruction', *N Engl J Med,* 371(8), pp. 744-56.

Ozkan, A., Kapadia, S., Tuzcu, M. and Marwick, T. H. (2011) 'Assessment of left ventricular function in aortic stenosis', *Nature Reviews. Cardiology,* 8(9), pp. 494-501.

O'Brien Kevin, D., Reichenbach Dennis, D., Marcovina Santica, M., Kuusisto, J., Alpers Charles, E. and Otto Catherine, M. (1996) 'Apolipoproteins B, (a), and E Accumulate in the Morphologically Early Lesion of 'Degenerative' Valvular Aortic Stenosis', *Arteriosclerosis, Thrombosis, and Vascular Biology,* 16(4), pp. 523-532.

Park, S. J., Kim, S. H., Choi, H. S., Rhee, Y. and Lim, S.-K. (2009) 'Fibroblast growth factor 2-induced cytoplasmic asparaginyl-tRNA synthetase promotes survival of osteoblasts by regulating anti-apoptotic PI3K/Akt signaling', *Bone,* 45(5), pp. 994-1003.

Patel, A. and Kirtane, A. J. (2016) 'Aortic Valve Stenosis', *JAMA Cardiol,* 1(5), pp. 623.

Patti, G. J., Yanes, O. and Siuzdak, G. (2012) 'Innovation: Metabolomics: the apogee of the omics trilogy', *Nature reviews. Molecular cell biology,* 13(4), pp. 263-269.

Pawade, T. A., Newby, D. E. and Dweck, M. R. (2015) 'Calcification in Aortic Stenosis: The Skeleton Key', *Journal of the American College of Cardiology,* 66(5), pp. 561-577.

Pearce, J. T. M., Athersuch, T. J., Ebbels, T. M. D., Lindon, J. C., Nicholson, J. K. and Keun, H. C. (2008) 'Robust Algorithms for Automated Chemical Shift Calibration of 1D 1H NMR Spectra of Blood Serum', *Analytical Chemistry,* 80(18), pp. 7158-7162.

Perk, J., De Backer, G., Gohlke, H., Graham, I., Reiner, Z., Verschuren, M., Albus, C., Benlian, P., Boysen, G., Cifkova, R., *et al.* (2012) 'European Guidelines on cardiovascular disease prevention in clinical practice (version 2012): The Fifth Joint Task Force of the European Society of Cardiology and Other Societies on Cardiovascular Disease Prevention in Clinical Practice (constituted by representatives of nine societies and by invited experts) * Developed with the special contribution of the European Association for Cardiovascular Prevention & Rehabilitation (EACPR)', *European Heart Journal,* 33(13), pp. 1635-1701.

Popma, J. J., Adams, D. H., Reardon, M. J., Yakubov, S. J., Kleiman, N. S., Heimansohn, D., Hermiller, J., Hughes, G. C., Harrison, J. K., Coselli, J., *et al.* (2014) 'Transcatheter Aortic Valve Replacement Using a Self-Expanding Bioprosthesis in Patients With Severe Aortic Stenosis at Extreme Risk for Surgery', *Journal of the American College of Cardiology,* 63(19), pp. 1972-1981.

Raghow, R. (2016) 'An 'Omics' Perspective on Cardiomyopathies and Heart Failure', *Trends in Molecular Medicine,* 22(9), pp. 813-827.

Ren, S., Hinzman, A. A., Kang, E. L., Szczesniak, R. D. and Lu, L. J. (2015) 'Computational and statistical analysis of metabolomics data', *Metabolomics,* 11(6), pp. 1492-1513.

Rhee, E. P. and Gerszten, R. E. (2012) 'Metabolomics and Cardiovascular Biomarker Discovery', *Clinical Chemistry,* 58(1), pp. 139.

Rossebø, A. B., Pedersen, T. R., Boman, K., Brudi, P., Chambers, J. B., Egstrup, K., Gerdts, E., Gohlke-Bärwolf, C., Holme, I., Kesäniemi, Y. A., *et al.* (2008) 'Intensive Lipid Lowering with Simvastatin and Ezetimibe in Aortic Stenosis', *New England Journal of Medicine,* 359(13), pp. 1343-1356.

Rossignol, F., Solares, M., Balanza, E., Coudert, J. and Clottes, E. (2003) 'Expression of lactate dehydrogenase A and B genes in different tissues of rats adapted to chronic hypobaric hypoxia', *Journal of Cellular Biochemistry,* 89(1), pp. 67-79.

Roth, G. A., Mensah, G. A., Johnson, C. O., Addolorato, G., Ammirati, E., Baddour, L. M., Barengo, N. C., Beaton, A. Z., Benjamin, E. J., Benziger, C. P., *et al.* (2020) 'Global Burden of Cardiovascular Diseases and Risk Factors, 1990–2019: Update From the GBD 2019 Study', *Journal of the American College of Cardiology,* 76(25), pp. 2982-3021.

Sana, T., Waddell, K. and Fischer, S. (2008) *A sample extraction and chromatographic strategy for increasing LC/MS detection coverage of the erythrocyte metabolome.*

Schlotter, F., Halu, A., Goto, S., Blaser, M. C., Body, S. C., Lee, L. H., Higashi, H., DeLaughter, D. M., Hutcheson, J. D., Vyas, P., *et al.* (2018) 'Spatiotemporal Multi-Omics Mapping Generates a Molecular Atlas of the Aortic Valve and Reveals Networks Driving Disease', *Circulation,* 138(4), pp. 377-393.

Schröter, J., Popkova, Y., Süß, R. and Schiller, J. (2017) 'Combined Use of MALDI-TOF Mass Spectrometry and 31P NMR Spectroscopy for Analysis of Phospholipids', in Bhattacharya, S.K. (ed.) *Lipidomics: Methods and Protocols Methods in Molecular Biology*. New York, NY: Springer New York, pp. 107-122.

Ser, Z., Liu, X., Tang, N. N. and Locasale, J. W. (2015) 'Extraction parameters for metabolomics from cultured cells', *Analytical Biochemistry,* 475(Supplement C), pp. 22-28.

Serna, J., García-Seisdedos, D., Alcázar, A., Lasunción, M. Á., Busto, R. and Pastor, Ó. (2015) 'Quantitative lipidomic analysis of plasma and plasma lipoproteins using MALDI-TOF mass spectrometry', *Chemistry and Physics of Lipids,* 189, pp. 7-18.

Shaffer, F., McCraty, R. and Zerr, C. L. (2014) 'A healthy heart is not a metronome: an integrative review of the heart's anatomy and heart rate variability', *Frontiers in Psychology,* 5, pp. 1040.

Shah, S. H., Bain, J. R., Muehlbauer, M. J., Stevens, R. D., Crosslin, D. R., Haynes, C., Dungan, J., Newby, L. K., Hauser, E. R., Ginsburg, G. S., *et al.* (2010) 'Association of a Peripheral Blood Metabolic Profile With Coronary Artery Disease and Risk of Subsequent Cardiovascular Events', *Circulation: Cardiovascular Genetics,* 3(2), pp. 207-214.

Sherwood, M. W. and Kiefer, T. L. (2017) 'Challenges in Aortic Valve Stenosis: Low-Flow States Diagnosis, Management, and a Review of the Current Literature', *Curr Cardiol Rep,* 19(12), pp. 130.

Shipton, B. and Wahba, H. (2001) 'Valvular heart disease: review and update', *Am Fam Physician,* 63(11), pp. 2201-8.

Shroff, R., Rulíšek, L., Doubský, J. and Svatoš, A. (2009) 'Acid–base-driven matrix-assisted mass spectrometry for targeted metabolomics', *Proceedings of the National Academy of Sciences,* 106(25), pp. 10092-10096.

Siu, S. C. and Silversides, C. K. (2010) 'Bicuspid Aortic Valve Disease', *Journal of the American College of Cardiology,* 55(25), pp. 2789-2800.

Smith, C. R., Leon, M. B., Mack, M. J., Miller, D. C., Moses, J. W., Svensson, L. G., Tuzcu, E. M., Webb, J. G., Fontana, G. P., Makkar, R. R., *et al.* (2011) 'Transcatheter versus Surgical Aortic-Valve Replacement in High-Risk Patients', *New England Journal of Medicine,* 364(23), pp. 2187-2198.

Stewart, B. F., Siscovick, D., Lind, B., Gardin, J., S. Gottdiener, J., E. Smith, V., W. Kitzman, D. and M. Otto, C. (1997) *Clinical Factors Associated With Calcific Aortic Valve Disease.*

Suhre, K. and Gieger, C. (2012) 'Genetic variation in metabolic phenotypes: study designs and applications', *Nature Reviews Genetics,* 13(11), pp. 759-769.

Suhre, K., Raffler, J. and Kastenmüller, G. (2016) 'Biochemical insights from population studies with genetics and metabolomics', *Archives of Biochemistry and Biophysics,* 589, pp. 168-176.

Surendran, A., Edel, A., Chandran, M., Bogaert, P., Hassan-Tash, P., Kumar Asokan, A., Hiebert, B., Solati, Z., Sandhawalia, S., Raabe, M., *et al.* (2020) 'Metabolomic Signature of Human Aortic Valve Stenosis', *JACC: Basic to Translational Science,* 5(12), pp. 1163-1177.

Sádaba, J. R., Martínez-Martínez, E., Arrieta, V., Álvarez, V., Fernández-Celis, A., Ibarrola, J., Melero, A., Rossignol, P., Cachofeiro, V. and López-Andrés, N. (2016) 'Role for Galectin-3 in Calcific Aortic Valve Stenosis', *Journal of the American Heart Association,* 5(11).

Tao, T., He, T., Wang, X. and Liu, X. (2019) 'Metabolic Profiling Analysis of Patients With Coronary Heart Disease Undergoing Xuefu Zhuyu Decoction Treatment', *Frontiers in Pharmacology,* 10.

Tellis, C. C. and Tselepis, A. D. (2009) 'The role of lipoprotein-associated phospholipase A2 in atherosclerosis may depend on its lipoprotein carrier in plasma', *Biochimica et Biophysica Acta (BBA) - Molecular and Cell Biology of Lipids,* 1791(5), pp. 327-338.

Teo, K. K., Corsi, D. J., Tam, J. W., Dumesnil, J. G. and Chan, K. L. (2011) 'Lipid Lowering on Progression of Mild to Moderate Aortic Stenosis: Meta-analysis of the Randomized Placebo-Controlled Clinical Trials on 2344 Patients', *Canadian Journal of Cardiology,* 27(6), pp. 800-808.

Teul, J., Rupérez, F. J., Garcia, A., Vaysse, J., Balayssac, S., Gilard, V., Malet-Martino, M., Martin-Ventura, J. L., Blanco-Colio, L. M., Tuñón, J., Egido, J. and Barbas, C. (2009) 'Improving Metabolite Knowledge in Stable Atherosclerosis Patients by Association and Correlation of GC-MS and 1H NMR Fingerprints', *Journal of Proteome Research,* 8(12), pp. 5580-5589.

Thanassoulis, G., Campbell, C. Y., Owens, D. S., Smith, J. G., Smith, A. V., Peloso, G. M., Kerr, K. F., Pechlivanis, S., Budoff, M. J., Harris, T. B., *et al.* (2013) 'Genetic Associations with Valvular Calcification and Aortic Stenosis', *New England Journal of Medicine,* 368(6), pp. 503-512.

Thanassoulis, G., Massaro, J. M., Cury, R., Manders, E., Benjamin, E. J., Vasan, R. S., Cupple, L. A., Hoffmann, U., O'Donnell, C. J. and Kathiresan, S. (2010) 'Associations of Long-Term and Early Adult Atherosclerosis Risk Factors With Aortic and Mitral Valve Calcium', *Journal of the American College of Cardiology,* 55(22), pp. 2491-2498.

Thériault, S., Gaudreault, N., Lamontagne, M., Rosa, M., Boulanger, M.-C., Messika-Zeitoun, D., Clavel, M.-A., Capoulade, R., Dagenais, F., Pibarot, P., Mathieu, P. and Bossé, Y. (2018) 'A transcriptome-wide association study identifies PALMD as a susceptibility gene for calcific aortic valve stenosis', *Nature Communications,* 9(1).

Tong, D. L., Boocock, D. J., Coveney, C., Saif, J., Gomez, S. G., Querol, S., Rees, R. and Ball, G. R. (2011) 'A simpler method of preprocessing MALDI-TOF MS data for differential biomarker analysis: stem cell and melanoma cancer studies', *Clinical Proteomics,* 8(1), pp. 14.

Townsend, N., Nichols, M., Scarborough, P. and Rayner, M. (2015) 'Cardiovascular disease in Europe — epidemiological update 2015', *European Heart Journal,* 36(40), pp. 2696-2705.

Townsend, N., Wilson, L., Bhatnagar, P., Wickramasinghe, K., Rayner, M. and Nichols, M. (2016) 'Cardiovascular disease in Europe: epidemiological update 2016', *European Heart Journal,* 37(42), pp. 3232-3245.

Trenkwalder, T., Nelson, C. P., Musameh, M. D., Mordi, I. R., Kessler, T., Pellegrini, C., Debiec, R., Rheude, T., Lazovic, V., Zeng, L., *et al.* (2019) 'Effects of the coronary artery disease associated LPA and 9p21 loci on risk of aortic valve stenosis', *International Journal of Cardiology,* 276, pp. 212-217.

Triba, M. N., Moyec, L. L., Amathieu, R., Goossens, C., Bouchemal, N., Nahon, P., Rutledge, D. N. and Savarin, P. (2014) 'PLS/OPLS models in metabolomics: the impact of permutation of dataset rows on the K-fold cross-validation quality parameters', *Molecular BioSystems,* 11(1), pp. 13-19.

Troisi, J., Sarno, L., Landolfi, A., Scala, G., Martinelli, P., Venturella, R., Di Cello, A., Zullo, F. and Guida, M. (2018) 'Metabolomic Signature of Endometrial Cancer', *Journal of Proteome Research,* 17(2), pp. 804-812.

Vallejo, M., García, A., Tuñón, J., García-Martínez, D., Angulo, S., Martin-Ventura, J. L., Blanco-Colio, L. M., Almeida, P., Egido, J. and Barbas, C. (2009) 'Plasma fingerprinting with GC-MS in acute coronary syndrome', *Analytical and Bioanalytical Chemistry,* 394(6), pp. 1517-1524.

Varbo, A., Benn, M., Smith, G. D., Timpson, N. J., Tybjaerg-Hansen, A. and Nordestgaard, B. G. (2015) 'Remnant cholesterol, low-density lipoprotein cholesterol, and blood pressure as mediators from obesity to ischemic heart disease', *Circulation Research,* 116(4), pp. 665-673.

Veselkov, K. A., Lindon, J. C., Ebbels, T. M. D., Crockford, D., Volynkin, V. V., Holmes, E., Davies, D. B. and Nicholson, J. K. (2009) 'Recursive Segment-Wise Peak Alignment of

Biological 1H NMR Spectra for Improved Metabolic Biomarker Recovery', *Analytical Chemistry,* 81(1), pp. 56-66.

Viney, N. J., van Capelleveen, J. C., Geary, R. S., Xia, S., Tami, J. A., Yu, R. Z., Marcovina, S. M., Hughes, S. G., Graham, M. J., Crooke, R. M., *et al.* (2016) 'Antisense oligonucleotides targeting apolipoprotein(a) in people with raised lipoprotein(a): two randomised, double-blind, placebo-controlled, dose-ranging trials', *The Lancet,* 388(10057), pp. 2239-2253.

von zur Muhlen, C., Schiffer, E., Zuerbig, P., Kellmann, M., Brasse, M., Meert, N., Vanholder, R. C., Dominiczak, A. F., Chen, Y. C., Mischak, H., Bode, C. and Peter, K. (2009) 'Evaluation of Urine Proteome Pattern Analysis for Its Potential To Reflect Coronary Artery Atherosclerosis in Symptomatic Patients', *Journal of Proteome Research,* 8(1), pp. 335-345.

Wang, Y., Sun, W., Zheng, J., Xu, C., Wang, X., Li, T., Tang, Y. and Li, Z. (2018) 'Urinary metabonomic study of patients with acute coronary syndrome using UPLC-QTOF/MS', *Journal of Chromatography B,* 1100-1101, pp. 122-130.

Wilson, P. W., D'Agostino, R. B., Levy, D., Belanger, A. M., Silbershatz, H. and Kannel, W. B. (1998) 'Prediction of coronary heart disease using risk factor categories', *Circulation,* 97(18), pp. 1837-1847.

Xia, J., Broadhurst, D. I., Wilson, M. and Wishart, D. S. (2013) 'Translational biomarker discovery in clinical metabolomics: an introductory tutorial', *Metabolomics,* 9(2), pp. 280-299.

Yahagi, K., Torii, S., Ladich, E., Kutys, R., Romero, M. E., Mori, H., Kolodgie, F. D., Popma, J. J., Virmani, R. and Finn, A. V. (2018) 'Pathology of self-expanding transcatheter aortic valves: Findings from the CoreValve US pivotal trials', *Catheterization and Cardiovascular Interventions: Official Journal of the Society for Cardiac Angiography & Interventions,* 91(5), pp. 947-955.

Yan, A. T., Koh, M., Chan, K. K., Guo, H., Alter, D. A., Austin, P. C., Tu, J. V., Wijeysundera, H. C. and Ko, D. T. (2017) 'Association Between Cardiovascular Risk Factors and Aortic Stenosis: The CANHEART Aortic Stenosis Study', *Journal of the American College of Cardiology,* 69(12), pp. 1523-1532.

Yang, K. and Han, X. (2016) 'Lipidomics: Techniques, Applications, and Outcomes Related to Biomedical Sciences', *Trends in biochemical sciences,* 41(11), pp. 954-969.

Yap, I. K. S., Brown, I. J., Chan, Q., Wijeyesekera, A., Garcia-Perez, I., Bictash, M., Loo, R. L., Chadeau-Hyam, M., Ebbels, T., De Iorio, M., *et al.* (2010) 'Metabolome-Wide Association Study Identifies Multiple Biomarkers that Discriminate North and South Chinese Populations at Differing Risks of Cardiovascular Disease: INTERMAP Study', *Journal of proteome research,* 9(12), pp. 6647-6654.

Yoon, M. A., Jeong, T. S., Park, D. S., Xu, M. Z., Oh, H. W., Song, K. B., Lee, W. S. and Park, H. Y. (2006) 'Antioxidant effects of quinoline alkaloids and 2,4-di-tert-butylphenol isolated from Scolopendra subspinipes', *Biol Pharm Bull,* 29(4), pp. 735-9.

Yoshinari, O., Sato, H. and Igarashi, K. (2009) 'Anti-Diabetic Effects of Pumpkin and Its Components, Trigonelline and Nicotinic Acid, on Goto-Kakizaki Rats', *Bioscience, Biotechnology, and Biochemistry,* 73(5), pp. 1033-1041.

Yu, B., Khan, K., Hamid, Q., Mardini, A., Siddique, A., Aguilar-Gonzalez, L. P., Makhoul, G., Alaws, H., Genest, J., Thanassoulis, G., Cecere, R. and Schwertani, A. (2018) 'Pathological significance of lipoprotein(a) in aortic valve stenosis', *Atherosclerosis,* 272, pp. 168-174.

Yutzey, K. E., Demer, L. L., Body, S. C., Huggins, G. S., Towler, D. A., Giachelli, C. M., Hofmann-Bowman, M. A., Mortlock, D. P., Rogers, M. B., Sadeghi, M. M. and Aikawa, E. (2014) 'Calcific aortic valve disease: A consensus summary from the Alliance of Investigators on Calcific Aortic Valve Disease', *Arteriosclerosis, thrombosis, and vascular biology,* 34(11), pp. 2387-2393.

Zeng, Q., Song, R., Fullerton, D. A., Ao, L., Zhai, Y., Li, S., Ballak, D. B., Cleveland, J. C., Reece, T. B., McKinsey, T. A., Xu, D., Dinarello, C. A. and Meng, X. (2017) 'Interleukin-37 suppresses the osteogenic responses of human aortic valve interstitial cells in vitro and alleviates valve lesions in mice', *Proceedings of the National Academy of Sciences,* 114(7), pp. 1631-1636.

Zhang, A., Sun, H., Yan, G., Wang, P. and Wang, X. (2015) 'Metabolomics for Biomarker Discovery: Moving to the Clinic', *BioMed Research International,* 2015, pp. 1-6.

Zhang, A. H., Sun, H., Wu, X. and Wang, X.-J. (2012) *Urine metabolomics.*

Zschörnig, O., Richter, V., Rassoul, F., Süß, R., Arnold, K. and Schiller, J. (2006) 'Analysis of Human Blood Plasma by MALDI ‐ TOF MS−Evaluation of Critical Parameters', *Analytical Letters,* 39(6), pp. 1101-1113.